

# The Bright SHARC Survey: The Selection Function and its Impact on the Cluster X-ray Luminosity Function

C. Adami

*IGRAP-laboratoire d'Astronomie Spatiale, Traverse du siphon, 13012 Marseille, France  
 Department of Physics and Astronomy, Northwestern University, Dearborn Observatory, 2131  
 Sheridan, 60208-2900 Evanston, USA*

`adami@lilith.astro.nwu.edu`

M.P. Ulmer

*Department of Physics and Astronomy, Northwestern University, Dearborn Observatory, 2131  
 Sheridan, 60208-2900 Evanston, USA*

`ulmer@curie.astro.nwu.edu`

A.K. Romer

*Department of Physics, Carnegie Mellon University, 5000 Forbes Avenue, Pittsburgh, PA 15213,  
 USA*

`romer@cmu.edu`

R.C. Nichol

*Department of Physics, Carnegie Mellon University, 5000 Forbes Avenue, Pittsburgh, PA 15213,  
 USA*

`nichol@cmu.edu`

B.P. Holden

*Department of Astronomy and Astrophysics, University of Chicago, 5640 S. Ellis Avenue,  
 Chicago, IL 60637, USA*

`holden@tokyo-rose.uchicago.edu`

R.A. Pildis

*Department of Physics and Astronomy, Northwestern University, Dearborn Observatory, 2131  
 Sheridan, 60208-2900 Evanston, USA*

## ABSTRACT

We present the results of a comprehensive set of simulations designed to quantify the selection function of the Bright SHARC survey (Romer et al. 2000a) for distant clusters. The statistical significance of the simulations relied on the creation of many thousands of artificial clusters with redshifts and luminosities in the range  $0.25 < z < 0.95$  and  $0.5 < L_X < 10 \times 10^{44}$  erg s $^{-1}$  (0.5–2.0 keV). We created 1 standard and 19 varied distribution functions, each of which assumed a different set of cluster, cosmological and operational parameters. The parameters we varied included the values of  $\Omega_0$ ,  $\Omega_\Lambda$ ,  $\beta$ , core radius ( $r_c$ ) and ellipticity ( $e$ ). We also investigated how non-standard surface brightness profiles (i.e the Navarro, Frenk & White 1997, NFW, model); cooling flows; and the ROSAT pointing target, influence the selection function in the Bright SHARC survey. For our standard set we adopted the parameters used during the derivation of the Bright SHARC Cluster X-ray Luminosity Function (CXLF, Nichol et al. 1999, N99), i.e.  $\Omega_0 = 1$ ,  $\Omega_\Lambda=0$  and an isothermal  $\beta$  model with  $\beta=0.67$ ,  $r_c=250$  kpc and  $e = 0.15$ . We found that certain parameters have a dramatic effect on our ability to detect clusters, e.g. the presence of a NFW profile or a strong cooling flow profile, or the value of  $r_c$  and  $\beta$ . Other parameters had very little effect, e.g. the type of ROSAT target and the cluster ellipticity. At distant redshift ( $z > 0.8$ ), elliptical clusters are significantly easier to detect than spherical ones in the Bright SHARC survey. We show also that all the tested parameters have only a small influence on the computed luminosity of the clusters (*recovered luminosity* in the text) except the presence of a strong cooling flow. We conclude that the CXLF presented in N99 is robust (under the assumption of standard parameters), but stress the importance of cluster follow-up, by *Chandra* and XMM, in order to better constrain the morphology of the distant clusters found in the Bright SHARC and other surveys.

*Subject headings:* galaxies: clusters: general — cosmology: observations — cosmology: large-scale structure of Universe — X-rays: general

## 1. Introduction

Numerous authors have demonstrated that the observed evolution of clusters of galaxies can place a strong constraint on the present day value of the matter density of the Universe,  $\rho_0/\rho_c=\Omega_m$  (see Gunn & Gott 1972; Press & Schechter 1974; Lacey & Cole 1993; Oukbir & Blanchard 1992 & 1997; Richstone, Loeb & Turner 1992). In recent years, there has been considerable interest in constraining  $\Omega_m$  using the observed abundance of clusters as a function of redshift (see Viana & Liddle 1996 & 1999; Henry et al. 1997; Bahcall, Fan & Cen 1997; Sadat et al. 1998; Reichart et al. 1999; Borgani et al. 1999). The effect of  $\Omega_0$  ( $=\Omega_m$  if  $\Omega_\Lambda=0$ ) on cluster abundances is very large. For example, the space density of high redshift ( $z > 0.3$ ), massive ( $T > 6$  KeV) clusters in an  $\Omega_m = 0.3$  universe is 100 times greater than that in an  $\Omega_m = 1$  universe (e.g. Viana & Liddle 1996, Oukbir & Blanchard 1992, Oukbir & Blanchard 1997, Romer et al. 2000b). Unfortunately,

the various studies performed to date have produced a wide range of results, from  $\Omega_m = 0.3 \pm 0.1$  (Bahcall et al. 1997) to  $\Omega_m = 0.96^{+0.36}_{-0.32}$  (Reichart et al. 1999). This observed dispersion in  $\Omega_m$  is most likely due to the fact that the cluster surveys currently available do not sample a large enough volume to include sufficient numbers of distant and massive clusters. Nevertheless, it is still important to quantify the uncertainties that are applicable to the data in hand. This allows us not only better to understand the uncertainties in using the ROSAT database, but this also provides insight as how to proceed in the future.

In this paper, we discuss the selection function of one of the ROSAT archival surveys for distant clusters; namely, the Bright Serendipitous High-redshift Archival ROSAT Cluster (Bright SHARC) survey. The cluster catalog resulting from the Bright SHARC survey has been presented elsewhere (Romer et al. 2000a, R00 hereafter) as was the initial determination of the Bright SHARC Cluster X-ray Luminosity Function (CXLF; Nichol et al. 1999, N99 hereafter). Here we describe the results of a full set of simulations designed to determine the ability of the Bright SHARC survey to detect clusters of different morphologies, luminosities and redshifts under different cosmological and observational conditions. Earlier works such as that of Rosati et al. (1995) or Vikhlinin et al. (1998) set the standards of this kind of work, however, we have performed these simulations in a much more detailed way and have examined the effects of different cosmologies and cluster profiles on the completeness of the Bright SHARC survey.

An outline of the paper is as follows: Section 2 gives an overview of the Bright SHARC survey and details the techniques used to perform the selection function simulations. Section 3 gives the results of the simulations. Section 4 describes how the areal coverage of the survey was determined. Section 5 describes CXLF's derived from our selection function simulations. In section 6 we present a discussion of the results and our conclusions are in section 7.

Throughout we keep  $H_0$  fixed at  $50 \text{ km s}^{-1} \text{ Mpc}^{-1}$  but  $\Omega_m$ ,  $\Omega_\Lambda (= \Lambda c^2 / 3H_0)$  and  $\Omega_0$  are varied.

## 2. The data and the Simulation Techniques

### 2.1. Survey Overview

The Bright SHARC survey has been described in detail in R00, but we review the salient points here. The survey was comprised of 460 ROSAT PSPC pointings. The pointings all had exposure times greater than 10 ks and lie at Galactic latitudes greater than  $b = |20^\circ|$ . The 460 pointings were directed towards nine different categories of targets; 1) normal stars (18 pointings), 2) white dwarfs (55 pointings), 3) cataclysmic variables (37 pointings), 4) neutron stars and black holes (8 pointings), 5) supernova remnants (1 pointing), 6) normal galaxies (75 pointings), 7) AGN (150 pointings), 8) clusters of galaxies (71 pointings) and 9) other possible sources of diffuse X-ray emission (45 pointings). Each pointing has a unique six digit identification number, with the first digit being set by the target category, e.g. pointing 600005 which was directed towards the galaxy

NGC 720. (For a full listing of identification numbers and pointing targets, see Appendix A of R00.) The Bright SHARC survey took advantage of the fact that the pointing targets covered only a small fraction of the total field of view of the PSPC detector, leaving the rest of the field of view (FOV) available for serendipitous cluster detections. FOV of the ROSAT PSPC extends to a radius of  $\simeq 1^\circ$ , but in the Bright SHARC survey, we chose to use only an annular region bounded by radii of 2.'5 and 22.'4. (Beyond 22.'4 the point spread function degrades rapidly which makes detections of the extended emission from clusters increasingly difficult.)

Each of the 460 pointings was run through a pipeline processing which identified the extended sources in each field. In total 374 extended sources were catalogued (see Appendix E of R00). These 374 sources met the following three criteria; they were detected at a signal-to-noise ratio of 8 or higher, they were more than  $3\sigma$  (wavelet defined, see R00) extended and had filling factors<sup>1</sup> of less than  $f = 1.3$ . The Bright SHARC survey is comprised of the brightest 94 of these 374 extended sources. These 94 all have count rates in excess of 0.01163 counts s<sup>-1</sup>. Optical identifications have been secured for all but 3 of the Bright SHARC sources, resulting in a sample of 37 clusters ( $0.3 < z < 0.83$ : 12 clusters).

Relevant to this paper is the method by which cluster luminosities are derived in R00 (we refer to this as the “R00 luminosity method” hereafter): Once a source was identified as a cluster, and its redshift measured, its total count rate was determined. This was done by laying down a metric aperture which encircles 80% of the flux from an isothermal  $\beta$  profile:

$$I(r) = \frac{I_0}{[1 + (r/r_c)^2]^{3\beta-1/2}} , \quad (1)$$

at redshift  $z$ , where  $I$  is the surface brightness at radius  $r$ . In R00 the slope and core radius were set to  $\beta = 0.67$  and  $r_c = 250$  kpc respectively. The effect of the ROSAT PSPC point spread function was taken into account by convolving with the appropriate off-axis PSPC PSF. The count rate measured inside the 80% aperture was scaled to a total value by dividing by 0.8. The total count rates were then converted into an unabsorbed flux and a rest frame luminosity in the 0.5–2.0 keV band pass using conversion factors determined using the XSPEC (Arnaud 1996) package.

Also relevant to this paper is the fact that the Bright SHARC count rate threshold (0.01163 counts s<sup>-1</sup>) was applied before the total derived count rates (see above) were known. Instead, it was applied to the wavelet count rate which is, on average, a factor of 2.1 times smaller than the total derived count rate. (Wavelet count rates were not determined in metric apertures but within source boundaries defined by the automated wavelet transform detection software, see R00 §3.)

We have included in the Bright SHARC survey PSPC pointings that contain extended on-axis targets *e.g.* supernova remnants (1 pointing), clusters of galaxies (71 pointings) and other sources of diffuse X-ray emission (45 pointings in class 9). The supernova remnants pose no threat to the Bright SHARC search as only one such pointing was included. Clusters and other sources of diffuse

---

<sup>1</sup>The filling factor is a simple shape parameter designed to filter out obviously blended sources, see R00 §3.

emission may cause some obscuration. However, when we simulated these pointing types separately (see §3.7), we found that our success rate was not significantly different from the other pointing types. For the cluster pointings included in the Bright SHARC there is an additional concern regarding the cluster–cluster correlation function. We discuss this problem in Section 3.7 but note here that Romer et al. 2000 examined this problem in detail for the Bright SHARC and concluded that at most 2 Bright SHARC clusters were possibly associated with the on-axis targeted cluster. Both of these “serendipitous” detections were not used in our analyses *e.g.* N99. Finally, we note that other authors have shown that concerns about cluster–cluster correlations are unimportant in the construction of large serendipitous surveys of X-ray clusters (cf Ebeling et al. 1998).

## 2.2. Details of the Simulation Process

The simulation procedure is quite complex and we describe it below in detail, but, in essence, the basic concept is straightforward. We have created thousands of artificial clusters with a range of different parameters, placed these clusters at different positions in ROSAT PSPC pointings and then ran the modified pointings through the Bright SHARC survey pipeline processing. We used these simulations to tell us how sensitive the survey is to each type of artificial cluster and also to evaluate the completeness of the SHARC survey as a function of X-ray luminosity, shape and cosmology.

In Table 1, we outline 20 different simulation runs (see §2.2.1 for more details). For each of these runs we selected a random set of pointings from the 460 that comprise the Bright SHARC survey. In runs 1 through 12, 200 pointings were selected. In runs 13 through 20 - where we concentrated on specific pointing types - between 35 and 150 pointings were selected. Into each pointing we placed an artificial cluster of a certain redshift and luminosity. The pointings were then processed to determine the percentage of times that our pipeline flagged an artificial cluster as an extended source. The process was repeated so that a full range of cluster redshifts and luminosities could be tested. Fifteen different redshifts ( $0.25 < z < 0.95$  with  $\delta z=0.05$ ) and six different luminosities ( $L_{44} = 1.0, 2.0, 3.5, 5.0, 7.5$  and  $10.0$ ) were used ( $L_{44}$  is in units of  $1 \times 10^{44}$  erg s $^{-1}$  in the 0.5–2.0 keV bandpass). Thus the total number of artificial clusters analyzed in each of the first 12 simulation runs was  $200 \times 15 \times 6 = 18000$  (more than 300000 artificial clusters in total when we include runs 13 through 20).

To be flagged as an extended source and to be associated with a cluster, the artificial clusters had to have a detection centroid not more than 5 pixels (1. $'25$ ) from the input centroid and also had to meet the three criteria described above (*i.e.*  $S/N > 8\sigma$ ,  $> 3\sigma$  extended,  $f < 1.3$ ).

In order to test how the survey sensitivity varied with off-axis angle, the artificial clusters in each run were divided among four non-overlapping annuli: 9 to 28, 28 to 53, 53 to 78 and 78 to 103 ( $\sim 15''$ ) pixels respectively. The exact positions of the artificial clusters within these annuli were selected at random.

The artificial clusters were generated as follows: First we calculated the expected ROSAT PSPC count rate from a cluster with a certain redshift and total luminosity using the R00 luminosity method in reverse. The Penn (1999) formulae for luminosity distance was used when  $\Omega_\Lambda$  was non zero, e.g for run 3. Second, the count rate was converted into a number of counts using the correct exposure time for the chosen position on the field of view and by assuming a Poisson distribution in the number of counts (to take into account the shot-noise in the photon statistic). Third, the counts were distributed over a model surface brightness profile (with a random rotational orientation) which had been convolved with the appropriate off-axis point spread function. Fourth, the surface brightness image was divided up into  $15'' \times 15''$  pixels and distributed so that there were only integer numbers of counts per pixel. Therefore, the total image was scaled so that it was in the same units (counts  $s^{-1}$  arcmin $^{-2}$ ) as the pointing into which it had been placed.

We have used the L-T relation of Arnaud & Evrard (1999) to assign a temperature and hence a K-correction to each simulated cluster. The K-corrections are small ( $\leq 15\%$ ) for clusters temperatures in the range of those we have detected ([1;9]keV, see Table 2 of R00).

The point spread convolution performed on the model surface brightness profiles differed from that used in R00. In R00, the Nichol et al. (1997) empirical fit to the off-axis PSF degradation was used. The Nichol et al. (1997) PSF was symmetric whereas, in reality, the PSF is not symmetric. The asymmetry was important to take into account in our simulations which included the ellipticity of the cluster profile. Here, we used, therefore, composite images of the PSF generated by co-adding high signal to noise ( $S/N > 15\sigma$ ) images of point sources. The individual point source images were accumulated in 5 pixel wide annuli. The artificial clusters were convolved with the composite PSF image with the closest mean off-axis angle (the mean distance between an artificial cluster and the selected PSF:  $37''$ ).

### 2.2.1. Description of the Twenty Simulation Runs

In Table 1 we summarize the parameters used during each of the 20 different simulation runs. Column 1 gives the run number, column 2 the surface brightness model, column 4 the cluster ellipticity, column 5 the core radius, column 6  $\beta$ , column 7  $\Omega_m$ , column 8  $\Omega_\Lambda$ , column 10 the number of pointings used and column 9 the type of pointing used. We describe each of the 20 runs in more detail below.

- Run 1: This run used a standard set of parameters and acted as the benchmark against which the other simulations were compared. The parameters chosen for this run match closely those in the R00 luminosity method, i.e.  $\Omega_m = \Omega_0 = 1$ , ( $\Omega_\Lambda = 0$ ) and an isothermal  $\beta$  profile (equation 1.) with  $\beta = 0.67$  and  $r_c = 250$  kpc. In a slight departure from R00, a small ellipticity (ellipticity:  $e = 0.15$ ) was introduced into each cluster profile. This value is typical for an ensemble average of clusters and is in agreement with the work of Wang & Ulmer (1997). This was the mean X-ray ellipticity they found for 10 distant ( $0.17 \leq z \leq 0.54$ )

rich clusters of galaxies.

- Runs 2 and 3: In these runs we examined the effect of the assumed values of  $\Omega_0$  and  $\Omega_\Lambda$  on our selection function. In run 2, an open model was used ( $\Omega_m=0.1$ ,  $\Omega_\Lambda=0$ ). In run 3 a flat model with a positive cosmological constant was used ( $\Omega_m=0.4$ ,  $\Lambda=0.6$ ),  $\Omega_0=1$ .
- Runs 4 and 5: In these runs we examined the effect of varying the cluster ellipticity. We used values of  $e = 0$  and  $e = 0.3$  in runs 4 and 5 respectively.
- Runs 6, 7 and 8: In these runs we examined how different surface brightness models affected cluster detectability. Numerical simulations, for example by Navarro, Frenk and White (1997, NFW hereafter), have shown that dark matter profiles are more peaked at the cluster center than are isothermal  $\beta$  profiles. In run 6 we used a slightly modified version of the NFW profile whereby we added a strong cusp to the central surface brightness to an isothermal  $\beta$ -model with  $\beta=0.67$  and  $r_c=250$  kpc (see Adami et al. 1998 for more details). In run 7 and 8 we examined the effect of cooling flows. For this we add a Gaussian (FWHM=400 kpc) which contains 10% of the total luminosity and a Gaussian (FWHM=200 kpc) which contains 50% of the total luminosity to a standard isothermal  $\beta$ -model ( $\beta=0.67$ ,  $r_c=250$  kpc). The runs 7 and 8 profiles mimicked, respectively, the moderate and strong cooling flow surface brightness profiles given in Peres et al. (1998).
- Runs 9 and 10: In these runs we examined the effect of varying the value of the slope parameter  $\beta$ . We used values of  $\beta = 0.55$  and  $\beta = 0.75$  in runs 9 and 10 respectively.
- Runs 11 and 12: In these runs we examined the effect of varying the core radius in the isothermal  $\beta$  profile. We used core radius values of  $r_c = 100$  kpc and 400 kpc in runs 11 and 12 respectively.
- Runs 13 to 20: In these runs we examined how the pointing target affects cluster visibility. As stated in §2.1, the 460 Bright SHARC pointings have nine different types of pointing targets. Of these nine, six types were represented more than 35 times. In runs 13 to 20 we ran simulations on a single pointing type (or on a single class of pointing types: point sources versus diffuse sources). Run 13 was comprised of 55 type-2 pointings (white dwarves), run 14 of 37 type-3 pointings (cataclysmic variables), run 15 of 75 type-6 pointings (normal galaxies), run 16 of 150 type-7 pointings (AGN), run 17 of 71 type-8 pointings (clusters), run 18 of 45 type-9 pointings (diffuse X-ray sources), run 19 of the types 1+2+3+4 (point sources) and run 20 of the types 5+6+7+8+9 (extended sources).

### 3. The Results

This section describes the results presented in the Tables 3 and 4 and Figures 1 to 11. We show only the figures describing the results for run 1 (i.e. the standard parameter set) and those from subsequent runs which showed a significant departure from run 1.

### 3.1. Results with the Standard Set of Parameters

#### 3.1.1. Detection efficiencies and recovered luminosity

We present the results from run 1 in Figures 1, 2 and 3 and Tables 3 and 4. Figures 1 and 2 use grey scale shading to illustrate the numerical results presented in Table 3. Similarly, Figure 3 illustrates the results in Table 4. Each figure is comprised of 9 disks. Each disk represents a different redshift ( $z=0.25$  to  $z=0.95$  in  $z = 0.1$  increments) and is divided into 6 sectors, with each sector representing a different luminosity ( $L_{44}=1, 2, 3.5, 5, 7.5, 10$  respectively). Each sector is further subdivided into 4 rings to represent the 4 off-axis annuli used in the simulations. These shaded areas represent the average detection efficiency or the recovered luminosity (see below).

Figure 1 illustrates the percentage of artificial clusters that were detected as extended sources when no count rate limit was imposed (the *total detection efficiency* hereafter). Figure 2 illustrates the corresponding percentages when the Bright SHARC count rate limit of  $0.01163 \text{ counts s}^{-1}$  is imposed (the *Bright SHARC detection efficiency* hereafter). As expected, the efficiency drops off when a count rate threshold is imposed. It is apparent from both Figure 1 and Figure 2 that the efficiency falls off with decreasing luminosity and increasing redshift. Figure 3 illustrates the percentage of the input luminosity recovered by the R00 luminosity method (when we used the Bright SHARC simulations with the count rate cut: *recovered luminosity* hereafter). If the R00 method were essentially perfect, then we would have expected to recover close to 100% of the input luminosity everytime we detected an artificial cluster as an extended source.

#### 3.1.2. Uncertainties of detection efficiencies and recovered luminosity

In order to estimate the significance level of the statements discussed below we have estimated the uncertainties for the detection efficiencies and recovered luminosities (see also Tables 3 and 4) in run 1. These uncertainties are the statistical dispersion of the computed percentages based on performing the simulations 50 times for the standard parameter set per given luminosity, redshift and location in the pointings.

We summarize the results as follow: for the *total detection efficiency*, the mean uncertainty is  $9\pm 5\%$ . For the *Bright SHARC detection efficiency*, the mean uncertainty is  $6\pm 4\%$ . For the *recovered luminosity*, the mean uncertainty is  $8\pm 6\%$ . If we limit the analysis to the fourth bin of the ROSAT pointings, the previous mean uncertainties are, respectively,  $11\pm 5\%$ ,  $10\pm 5\%$  and  $11\pm 10\%$ . These values are slightly higher due to the degraded PSF. The standard errors on the uncertainty are, however, not very large whatever the detection efficiency: they all have amplitudes similar to the mean uncertainty itself.

For redshifts lower than  $\sim 0.6$  and luminosities greater than  $3.5\times 10^{44}$ , our detection efficiency versus luminosity (cf. Figs. 1 and 2) depends on the annulus, *i.e.* our detection efficiency is almost constant for the outer annulus but increases from 40 to 100% for the 3 inner annuli. According to

the error bars, this trend may be significant (near the  $3\sigma$  level) and is probably due to the larger PSF at large off-axis angles. A small number of SHARC point sources were probably classified as extended, thus slightly boosting ( $\sim 5\%$ ) the number of initial extended sources. This is a negligible effect on our results.

### 3.1.3. Results

We have used the results of the run 1 simulations to determine the lowest detection efficiency level which can be safely used to define a selection function. We have done this by determining the rate of spurious extended sources detections, i.e. the number of cases where an extended X-ray source, lying close to the position of an artificial cluster, is falsely associated with that cluster (the probability that this extended source is a real cluster is low based on the number of pointings: 460 and the number of detected clusters in R00: 37). To this end, we have carried out an additional simulation set for run 1 with  $L_{44} = 0.5$ . This luminosity is so low that it produces a flux that is well below our detection limit for  $z > 0.30$ . So, if any of the  $L_{44} = 0.5$  clusters were "detected" as extended sources, then those detections would most likely be spurious. The mean detection efficiency for  $L_{44} = 0.5$  artificial clusters is, therefore, a measure of the source confusion in the SHARC survey. Not surprisingly, we detected very few of the 200  $L_{44} = 0.5$  artificial clusters we created; we measured a mean *Bright SHARC detection efficiency* for them of only 1% and a maximum *Bright SHARC detection efficiency* of less than 5% (this value is consistent with the uncertainties estimated in 3.1.2). Given this confusion level, we adopted for the simulations a lower limit to the acceptable efficiency level of 15% when making comparisons between run 1 and runs 2-20 (see Figures 4 to 11). This limit ensures that there are at least 3 times more true detections of extended sources than false detections (detections of point-like sources classified as extended).

By comparing Figures 2 and 3, it is clear that the *recovered luminosity* is close to 100% where the *Bright SHARC detection efficiency* was greater than 15%. Averaging over all regions where the *Bright SHARC detection efficiency* was greater than 15%, we measured a mean *recovered luminosity* of  $99 \pm 8\%$ . The *recovered luminosity* was found to vary with position on the field of view: the mean *recovered luminosities* in the 4 annuli studied were  $96 \pm 13\%$ ,  $94 \pm 10\%$ ,  $94 \pm 8\%$  and  $111 \pm 3\%$  respectively. We attribute the  $111 \pm 3\%$  result to the fact that the PSF is so large in the outer annulus, that it increased the chance of flux contamination by point sources. The R00 luminosity method used model parameters that are very close to those used here to generate the artificial clusters except that in run 1 the simulated clusters are not exactly circular ( $e = 0.15$ ).

We have also used the results from simulation run 1 to determine the number of times artificial clusters were not detected for reasons other than because they were too faint or not sufficiently extended. These reasons included cases where the SHARC detection pipeline measured an artificial cluster centroid which was more than  $1.^{\circ}25$  from the input centroid, or cases where the cluster was placed almost exactly on top of a bright point source (so that the resulting blended source is not flagged as extended, see R00 for the definition of a blended source). We have estimated the

number of times these situations arise by assuming our pipeline should detect 100% of all  $L_{44} = 10.0$  artificial clusters in the lowest redshift bin ( $z = 0.25$ ) in the first, second and third radial annuli. We excluded the fourth annulus from our test because of the degraded PSF which can cause some of these clusters to be missed for reasons other than confusion or false positioning. We detected 97% of these clusters. We conclude therefore that  $\sim 3\%$  of all clusters went undetected from the SHARC survey for these technical reasons. This is a negligible effect compared to the statistical uncertainties of our results.

In summary, we have shown, using simulation run 1, how the *Bright SHARC detection efficiency* falls off with decreasing luminosity and increasing redshift. We have also demonstrated that above efficiency levels of 15%, we can be confident than significantly less than 1/3 of the detections in the simulations are spurious (i.e. non extended sources that were detected as extended). Above the 15% efficiency level, we found that the R00 methodology accurately recovers the input luminosities of the clusters. Finally, we demonstrated that only a small percentage of the simulated clusters ( $\sim 3\%$ ) were not detected for technical reasons, such as bad centroid fitting or bright source confusion.

In the following subsections we discuss the results of the other 19 simulation runs by making comparisons with the results from run 1. In Figures 4 to 11, we present the percentage difference between the run 1 and the run  $n$  *Bright SHARC detection efficiency* (or *total detection efficiency*) as a function of off-axis angle for a subset of the luminosity ( $L_{44}=2.0, 5.0 \& 10.0$ ) and redshift ( $z=0.25, 0.35, 0.45, 0.55, 0.65, 0.75, 0.9$ ) values simulated in each run (the complete results for all the redshifts are given in the tables). A positive percentage means that the efficiency of detection was higher in run 1 than it was in run  $n$ , and vice versa. The percentage differences were only calculated for those luminosity and redshift combinations where the run 1 detection efficiency is greater than 15%. Regions of parameter space where the run 1 detection efficiency is  $< 15\%$  are indicated on Figures 4 to 11 by crosses on the 0% line.

In this section, and throughout this article, we have only discussed simulations of extended sources with profiles similar to galaxy clusters. However, there are other sources of extended X-ray emission – *e.g.* supernova remnants, galaxies, low luminosity nearby galaxies, groups and fossil groups *etc.* – and this explains the discrepancy between our  $\geq 85\%$  rate of extended sources being clusters (the other  $\leq 15\%$  being blends of too faint to detect on their own clusters with real ROSAT sources) in our simulations versus only  $\sim 40\%$  of the Bright SHARC extended sources being real clusters (see R00). In other words, our simulations only tell us how often a cluster of a given luminosity and redshift would have made it into the Bright SHARC; the simulations can not tell us how often we would have found other X-ray extended sources.

### 3.2. Effect of the Cosmological Parameters

We tested the effect of the underlying cosmological models on our ability to detect clusters by comparing the results of run 1 with the results of runs 2 ( $\Omega_m=0.1$ ,  $\Omega_\Lambda=0$ ) and 3 ( $\Omega_m=0.4$ ,  $\Lambda=0.6$ ). For both the alternative cosmologies tested, we found lower values of the *total* and *Bright SHARC detection efficiency* (the latter are shown in Figure 4). This was because, for the same redshift and total luminosity, a low  $\Omega_m$  produced clusters which were larger in angular extent than did a high  $\Omega_m = 1$ . Despite their increased angular extent, clusters in a low  $\Omega_m$  Universe are harder to detect than their counterparts in a  $\Omega_m = 1$  Universe because their surface brightness (and hence contrast against the X-ray background) is diminished.

For those artificial clusters detected in runs 2 and 3 we find their *recovered luminosities* to be similar to those measured in run 1. The mean percentage difference between the *recovered luminosities* in run 1 and run 2 was  $3\pm18\%$ . This difference was  $7\pm30\%$  when compared runs 1 and 3. The standard errors associated with these two mean percentages are somewhat large, but we did not detect any systematic trends with the redshift and/or the luminosity.

In summary, if we assume lower values of  $\Omega_0$  (for a flat or an open Universe), the luminosity estimates are as good, on average, as when we assume  $\Omega_0=1$  ( $\Omega_\Lambda = 0$ ). However, changing the value of  $\Omega_0$  and  $\Omega_\Lambda$  has a marked effect on the detection efficiency of the survey, especially for high redshift and/or low luminosity clusters. We show in Section 5 that this effect has, however, only a small influence on the derived Cluster X-ray Luminosity Function because of the distribution of the Bright SHARC real clusters in the  $(z, L_{44})$  space.

### 3.3. Effect of the ellipticity

We have investigated the effect of cluster ellipticity on the detection efficiency of the survey by comparing the results from run 1 ( $e = 0.15$ ) to those from runs 4 ( $e = 0.0$ ) and 5 ( $e = 0.3$ ). For a fixed cosmology, an elliptical cluster will have a higher central surface brightness than a circular cluster of the same luminosity in proportion of the surface difference induced by the ellipticity (if the image is contracted along the minor axis). In doing this, we kept the core radius constant along the major axis: we contracted the image along the minor axis. Instead, we could have elongated the image along the major axis to make clusters elliptical. However, doing this would lead to a lower surface brightness cluster. Such clusters would be similar to our low- $\beta$  and our large core radius models. Elliptical clusters which have longer than normal major axes would, therefore, not be preferentially detected at high redshift. If the majority of high redshift clusters were found to have extended major axes, then we could conclude that the detection of mostly elliptical clusters at high redshifts is not a selection effect.

As shown in Figure 5, the *total detection efficiency* is very similar for the three runs except at the very luminous, very high redshift end, where it appears that increased ellipticity leads

to increased detectability. We find no similar systematic trend in the *Bright SHARC detection efficiency* and so do not plot those results. We attribute this to the fact that very few clusters with  $z > 0.75$  met the Bright SHARC count rate threshold and, since the effect of ellipticity on the *total detection efficiency* is only seen in the  $z = 0.9$  bin, then there would be very little, if any, corresponding effect on the *Bright SHARC detection efficiency*.

We find no systematic trend in the *recovered luminosity* with ellipticity. The mean percentage difference in *recovered luminosity* is  $1 \pm 22\%$  between runs 1 and 4 and  $2 \pm 30\%$  between runs 1 and 5. This is good, since it shows that the R00 luminosity method, which assumes a single ellipticity of  $e = 0$ , did not introduce a systematic bias into the measured Bright SHARC cluster luminosities.

In summary, ellipticity has minimal effect on the *recovered luminosity* and on the *Bright SHARC detection efficiency*. However, we do find a significant trend for increased *total detection efficiency* with ellipticity at very high redshifts. We attribute the lack of a similar trend in the *Bright SHARC detection efficiency* to the insensitivity of the Bright SHARC survey at very high redshifts, i.e. where the ellipticity effect becomes important. We have not examined with these simulations the effect of cluster orientation (prolate or oblate) on detection efficiency.

### 3.4. Effect of the Central Surface Brightness Model

Here we examine how the adopted surface brightness model for the artificial clusters affects their detectability. In run 1 a simple isothermal  $\beta$ -profile was used. We contrast this with a pseudo-NFW profile in run 6 and with a pseudo cooling flow profile in runs 7 and 8. Both the NFW profile and the cooling flow profiles are more peaked than the isothermal  $\beta$ -profile, and hence, they have higher central surface brightnesses. From figure 6 it can be seen that the detection efficiency for a moderate cooling flow (run 7) was similar to that for run 1 and there are no clear trends with redshift or luminosity. In other words, the presence of a moderate cooling flow does not have a significant impact on the detectability of a cluster. By contrast, the strong cooling flows (run 8: Fig. 7) and the NFW profile clusters simulated in run 6 were significantly (up to two times) easier to detect than the equivalent isothermal  $\beta$ -profile clusters. We attribute this to the surface brightness in the cluster core being significantly higher than for a  $\beta$ -profile.

We found the *recovered luminosities* from runs 6 and 7 to be very similar to those from run 1. The mean percentage difference in *recovered luminosity* is  $2 \pm 17\%$  between runs 1 and 6 and  $2 \pm 16\%$  between runs 1 and 7. This demonstrates that the R00 methodology, which assumes all clusters have isothermal  $\beta$ -profiles, provides a valid approximation for the run 6 and 7.

The *recovered luminosities* from run 8 are, however, underestimated by  $27 \pm 7\%$ . Based on the uncertainty, this trend seems to be significant (Fig. 6b). Assuming that the R00 methodology is able to recover a valid luminosity for  $\beta$ -like profiles, we can infer that the difference comes mainly from the cooling-flow profile itself. If the Gaussian model peak of the cooling-flow is relatively bright compared to the  $\beta$ -profile (200 kpc in this case), the R00 methodology fails to recover the

entire luminosity due to the normalization technique which assumed a standard  $\beta$ -profile.

However, the percentages of clusters exhibiting strong cooling flows in the Bright SHARC redshift range is probably low. Assuming, for example, a central cooling-time between 1 and 2 Gyears (e.g. Peres et al. 1998), most of the known cooling-flows in clusters at  $z \sim 0.1$  have been initiated only at redshifts lower than  $z \sim 0.3$  ( $q_0 \leq 0.5$ ). It is, therefore, very likely that we only have a small percentage of cooling-flow clusters (or at least with moderate cooling flows) in the redshift range of our simulations and in the Bright SHARC. This is confirmed by the fact that there are not many clusters detected at redshift higher than 0.3 with known cooling-flows (e.g. 3C 295: Henry & Henriksen 1986) whereas the X-ray detection of such clusters should be easier, theoretically, than for the non-cooling-flow clusters.

### 3.5. Effect of $\beta$

In runs 9 and 10 we examined the effects of  $\beta$  on the detectability of clusters with isothermal  $\beta$ -profiles. In run 9 we use a value of  $\beta=0.55$ , whereas, in run 10, we use  $\beta=0.75$ . We compared the results from these runs against those from run 1 ( $\beta=0.67$ ) in Figure 9. From Figure 9 it is clear that clusters with higher  $\beta$  values are easier to detect (this trend is seen in both the *total* and the *Bright SHARC detection efficiency*). This can be explained by the fact that higher  $\beta$  values result in more concentrated, and hence higher surface brightness, clusters.

Lowering the value of  $\beta$  to  $\beta=0.55$  was found to have a significant effect on value of the *recovered luminosity* (see Figure 10). Where the detection is easy (low redshift + high luminosity), the *recovered luminosity* estimate is the same whatever the value of  $\beta$ . Where the detection is more difficult, however, the *recovered luminosity* of the  $\beta=0.55$  tends to be low. There are two reasons for this. First the detection efficiency for  $\beta=0.55$  clusters is significantly lower than that of  $\beta=0.67$  clusters (see Figure 9). So that, even when the run 1 detection efficiency is above our minimum threshold of 15%, the run 9 efficiency can be much lower. (In other words well into the regime where most of the detections are spurious.) Second the R00 luminosity method, which assumes all clusters have  $\beta=0.67$ , breaks down when  $\beta < 0.67$ . If the true  $\beta$  value is smaller than  $\beta=0.67$ , this aperture will encircle less than 80% of the actual flux, which can lead to a significant underestimate of the total luminosity. In principle, R00 could have corrected for the  $\beta$  effect by fitting the cluster profiles and then deriving a flux, but the low number of counts available in the ROSAT PSPC images made such an approach impractical. We found that the fitted  $\beta$  value was so poorly constrained as to lead to best fit values that could easily be very far away from the true value.

### 3.6. Effect of the Core Radius

In runs 11 and 12 we examined the effects of the size of the core radius ( $r_c$ ) on the detectability of clusters. In run 11 we adopted  $r_c = 100$  kpc and, in run 12, we adopted  $r_c = 400$  kpc. We compared the results from these runs with those from run 1 ( $r_c = 250$  kpc) in Figure 11. The effect of  $r_c$  turns out to be more complex than the effect of  $\beta$ . The *Bright SHARC detection efficiencies* for the  $r_c = 100$  kpc clusters was consistently lower than that of  $r_c = 250$  kpc clusters, with the effect being most pronounced at lower luminosities. By contrast, the  $r_c = 400$  kpc clusters could be either easier or harder to detect than the  $r_c = 250$  kpc clusters, depending on the redshift and luminosity. They were easier to detect in the low redshift  $L_{44} = 2.0$  and the intermediate redshift  $L_{44} = 5.0$  bins, but harder to detect in the  $L_{44} = 10.0$  and low redshift  $L_{44} = 5.0$  bins. This demonstrates the competing effects of surface brightness and extent: Clusters with higher surface brightnesses were easier for the wavelet pipeline to detect, but those with small angular sizes were less likely to be flagged as extended sources.

We found no significant difference in the *recovered luminosity* between run 11 ( $r_c=400$  kpc) and run 1 ( $r_c=250$  kpc). By comparison, we found a small, but systematic, enhancement in the *recovered luminosity* for run 11 ( $r_c=100$  kpc) compared to run 1 ( $r_c=250$  kpc). The enhancement was at the  $\simeq 10\%$  level and resulted from the fact that the R00 luminosity method will over estimate the true luminosity if the true core radius is smaller than the assumed value of  $r_c=250$  kpc. Similar enhancements were found when R00 compared the Bright SHARC luminosities to those derived by Vikhlinin et al. (1998) for the 11 clusters they had in common. (Vikhlinin et al. 1998 used the best fit value of  $r_c$  to compute cluster luminosities and, in the majority of cases, their  $r_c$  values were smaller than 250 kpc.)

### 3.7. Effect of Target Type

In section 2.1 we mentioned that the original targets of the 460 Bright SHARC pointings are divided into 9 different categories. It is reasonable to ask whether the target category has any influence on the sensitivity of a particular pointing to cluster detection. For example, pointings with targets that reside in regions of high local hydrogen column density would tend to have decreased sensitivity or diffuse extended sources can produce obscurations.

Therefore, in runs 13 to 20, we have investigated the effect of target type. In each of these runs we placed artificial clusters into pointings of only one type. We compared the results from these runs with those from run 1 (which used pointings with a random selection of targets). We find very little variation in the detection efficiency between runs 13 to 20 and run 1. For both the *total* and the *Bright SHARC detection efficiency*, we measured a mean variation of only  $2 \pm 5\%$ . The *recovered luminosities* were also very similar with a mean value of 4% without any detectable systematic trends with redshift and/or luminosity. In order to investigate possible statistical bias due to the small number of pointings in each of the six previous classes, we also merged all the

pointing classes into two sub-classes: point sources (run 19) and extended sources (run 20). We found that the detection efficiencies of these runs were similar to run 1, and we conclude that the difference between using all kinds of point sources (run 19) and diffuse sources (run 20) was negligible, as we found very little difference between runs 19, 20 and 1. The *recovered luminosities* were also very similar, with a mean variation of less than 5%. We can safely conclude, therefore, that the target type has no influence on the sensitivity of a particular pointing to serendipitous cluster detections.

We have not investigated, however, the influence of the cluster-cluster correlation function in any of our simulations. Clusters are known to be clustered (e.g. Romer et al. 1994), meaning that pointings with cluster targets will include, on average, a larger number of serendipitous cluster detections (see also Ebeling et al. 1998 for a discussion of this point). For example, R00 highlighted two Bright SHARC clusters that are most probably associated with the pointing target. The fact that we have ignored cluster correlations in our simulations is not a concern, however, since these two clusters were excluded from the Bright SHARC CXLF analyses (N99 and §5) because they were at low redshift.

#### 4. Areal Coverage

To be able to compute an CXLF, we need, in addition to the results of our simulations, an estimate of the area covered by the Bright SHARC survey. R00 calculated the maximum areal coverage of the survey to be 179 deg<sup>2</sup>. However, the R00 calculation did not include an uncertainty estimate or a quantification of how the areal coverage falls off with cluster flux. We have corrected for those shortcomings here.

The effective areal coverage of the survey is a complex function of the cluster flux, the cluster extent and the background level. This is because clusters need to meet a signal to noise threshold and an extent criterion to be included in the Bright SHARC cluster candidate list. So, we have computed the areal coverage as a function of flux for each of the 460 pointings individually. Since the background level and PSF varies across the FOV, we need to break up each pointing into several regions to ensure an accurate calculation. We chose to break the FOV up into the same 4 annuli as we used in the simulations. We determined a mean noise level ( $\bar{N}$ ) for an annulus by examining the  $S/N$  values of *all* the extended sources with a  $S/N > 2$  (we chose this low signal to noise threshold <sup>2</sup> to ensure we had more than 3 detections for each annulus) detected in that annulus (when doing this, we did not set a minimum count rate threshold breaking, only for this purpose, our  $S/N$  criterion for Bright SHARC). We computed  $\bar{N}$  as (with  $n$  the number of sources detected in a given annulus):

$$\overline{(S/N)} = \sum [S_i/N_i]/n$$

---

<sup>2</sup>This measure of the  $\bar{N}$  by using  $S/N > 2$  does not reflect the  $S/N$  of 8 used for our detection criterion.

$$\bar{S} = \sum [S_i/n]$$

$$\bar{N} = S/(S/N)$$

From  $\bar{N}$  we estimate the lowest signal ( $S_{min}$ ) that would yield a  $S/\bar{N} > 8$  detection of an extended source in that annulus. For signals greater or equal to  $S_{min}$ , the whole<sup>3</sup> area of the annulus can be added to the total areal coverage of the survey. (For signals less than  $S_{min}$ , none of the area is added.) Thus, we build up an areal coverage of the whole survey, as a function of  $S$ , by summing over each annulus in each of the 460 pointings. It is clear that for very bright sources, all annuli in all pointings will contribute. Thus this method yields a maximum areal coverage which is, as expected, identical to the value calculated in R00 ( $179 \text{ deg}^2$ ). But, as the signal decreases, more and more of the annuli drop out of the calculation and the areal coverage falls to zero. These effects are illustrated in Figure 12, where we have converted signal (i.e. count rate) into flux using the conversion tables devised for R00.

Also shown in Figure 12 is our estimate of the uncertainty in the areal coverage (dotted lines). We calculated this uncertainty by examining the distribution of  $S/N$  values for the extended sources in each annulus. For the solid line on Figure 12 we used  $\bar{N}$  to determine  $S_{min}$ . For the upper (lower) dotted line we used an estimate of  $\bar{N} + \delta N$  ( $\bar{N} - \delta N$ ). The number of extended sources per annulus was usually too small to determine a reliable standard deviation on  $\bar{N}$ . We, therefore, chose to set  $\bar{N} + \delta N$  to be equal to  $N_{max}$  (the maximum noise level for that annulus) and  $\bar{N} - \delta N$  to be equal to  $N_{min}$ . We determined that this method provided a good estimate of the 1 sigma errors on the areal coverage. We did this as follows. Based on detected extended sources, we calculated the lowest and the highest noise level for each pointing (without splitting the pointings in 4 annuli). The range of areal coverage versus flux thus derived for each pointing is so large as to effectively assure us that the true value of areal coverage versus flux level lies within this range. We then compared this with the more precise uncertainty estimate we derived, based on dividing the field of view of each pointing into 4 parts as described above. To estimate the statistical significance (sigma level) to assign to this uncertainty derived from the 4 annuli approach, we compared the area covered between the dotted curves in Figure 12 (the area covered by the uncertainties when we split each pointing in four annuli) with the area covered by the maximum possible deviation to the areal coverage (computed without splitting the pointings in 4 annuli). This ratio is 0.61 which is close enough to  $1\sigma$  that we take the dotted curves as delineating the  $1\sigma$  range in the discussion that follows.

As can be seen in Figure 12, as the flux limit is lower, the uncertainty of the areal coverage gets larger. This is because at decreasing flux levels, the fluctuations due to counting statistics become relatively larger, and because the effective coverage decreases rapidly with the flux level. In Figure 12 we show with the thick solid vertical line, the flux at which the  $1\sigma$  uncertainty in

---

<sup>3</sup>After excluding pixels which overlapped with other pointings and/or with the shadow of the X-ray mirror support, see R00 §4.

the areal coverage is 10%. As can be seen from the thin vertical lines (Bright SHARC clusters), all the Bright SHARC clusters were detected at fluxes where the areal coverage error was < 10%. The lowest flux cluster used in N99 (thin solid line) has an associated areal coverage uncertainty of only 5%. Therefore, we can safely neglect the effect of such uncertainties when determining the Bright SHARC CXLF. However, surveys that go to much lower flux levels (e.g. Burke et al. 1997, Vikhlinin et al. 1998, Rosati et al. 1998, Ebeling et al. 1999) may need to be concerned about uncertainties in their areal coverage at low fluxes.

## 5. Influence of the Different Sets of Parameters on the CXLF

N99 used a preliminary set of selection function simulations to derive the Bright SHARC CXLF. This preliminary set used the same parameters as run 1, i.e. an isothermal  $\beta$  profile with  $\beta = 0.67$ ,  $r_c = 250$  kpc,  $e = 0.15$ ,  $\Omega_0 = 1$  and  $\Omega_\Lambda = 0$ , but covered a smaller range of redshifts and luminosities. Here we redetermine the Bright SHARC CXLF using the results of run 1 in order to test the robustness of the N99 results. We also investigate how the CXLF changes when we use selection functions derived from the results of runs 2 to 12. We note that we have detected a systematic trend affecting the accuracy of the Bright SHARC cluster luminosity measurements only when we use a low value of the slope  $\beta$  or strong cooling flow profiles (which are not, however, very likely at high redshift). None of the other tested parameters have a systematic effect. This means that our luminosity measurements are not very dependent of the parameters tested in this work.

We have used the same  $1/V_a$  methodology as N99 (adapted where necessary for different cosmological models) to determine the Bright SHARC CXLF.  $V_a$  is defined as the available sampled volume for any given cluster in the survey and can be computed for a cluster of luminosity  $L_x$  using

$$V_a = \int_{z_{low}}^{z_{high}} \Omega(L_x, z) V(z) dz, \quad (2)$$

where  $z_{low}$  and  $z_{high}$  are the lower and upper bounds of the redshift shell of interest,  $V(z)$  is the volume per unit solid angle for that redshift shell and  $\Omega(L_x, z)$  is the effective area of the Bright SHARC survey. This effective area was calculated by multiplying the areal coverage of the survey at the corresponding ROSAT flux by the appropriate *Bright SHARC detection efficiency*. The detection efficiency is a function of the cluster redshift and luminosity (see Table 3). The effective area is also (see Figure 13 for an illustration of how  $\Omega(L_x, z)$  varies with  $L_x$  and  $z$ ). Very bright clusters (e.g.  $L_{44}=10.0$  clusters at  $z = 0.25$ ) will have an effective area equal to the maximum areal coverage of the survey (i.e.  $179 \text{ deg}^2$ ). Whereas very faint clusters will have an effective area that approaches zero. The effective area was calculated for each of the 4 annuli separately and then co-added, since the detection efficiency is also a function of off-axis angle (see Table 3). The maximum areal coverage of the inner annulus was  $9.7 \text{ deg}^2$ ,  $47 \text{ deg}^2$  for the second annulus,  $94.3$

$\text{deg}^2$  for the third annulus and  $28 \text{ deg}^2$  for the outer annulus.

In order to compare with the earlier calculations of N99, we show in Figure 13 the effective area computed for the standard set of parameters. The results are similar to the preliminary simulations presented in N99 except for the high luminosity and high redshift clusters, where we now find a lower effective area than thought. This is primarily due to the increased precision of the simulations presented herein. The main consequence of this change is in the statistical significance of any proposed deficit of high luminosity, high redshift clusters (see N99). We have repeated the analysis of N99 and find that at  $L_x > 5 \times 10^{44}$ , and in the redshift range  $0.3 < z < 0.7$ , we would expect to have detected about 2 clusters (using the De Grandi et al. 1999 or Ebeling et al. 1997 luminosity function) in the Bright SHARC using the effective area curves presented in Figure 13.

In N99, the CXLF was calculated using the 12 Bright SHARC clusters with  $z > 0.3$ . In this study we used a slightly lower redshift limit ( $z > 0.285$ ) to increase the number of clusters in the sample. We list the detection efficiencies (as well as the redshift, luminosity and off-axis angle) for the 15  $z > 0.285$  Bright SHARC clusters in Table 2, of which we used 13 (see below). Because the simulations covered only discrete values of  $L_x$  and  $z$ , we had to use linear interpolation to estimate the detection efficiency for these clusters. It can be seen from Table 2 that the detection efficiency can vary dramatically with the run number. We did not include clusters for which the mean (over all runs 1 to 11) *Bright SHARC detection efficiency* was less than 5%. We, therefore, excluded two clusters (RXJ1334 and RXJ1308 which were both used in N99) from our list of fifteen. The remaining thirteen clusters are divided into 4 luminosity bins (see Fig. 12 and 13). These bins contained 4, 5, 3 and 1 clusters respectively. The redshift ranges for these bins were slightly different from N99; for bins 1,2 and 3 we used  $0.285 \leq z \leq 0.7$  (compared to  $0.3 \leq z \leq 0.7$ ) and for bin 4 we used  $0.285 \leq z \leq 1.0$  (compared to  $0.3 \leq z \leq 1.0$ ).

Table 2, upon which our XCLF's (Figures 14 and 15) were based, has 5 clusters below the 15% level (3 clusters we used; the two lowest efficiency clusters were not used). These "low efficiency" clusters are not spurious as they have been optically verified. The uncertainty of the efficiency of detection of these clusters is indeed higher than the other clusters we used and we have factored this into the calculation of the CXLF error bars.

The results are shown in Figures 14 and 15. In these figures, we have overplotted the local CXLF computed by de Grandi et al. (1999) and Ebeling et al. (1997). In Figure 14, we also plotted the N99 CXLF and its uncertainty envelope. The error bars (plotted only on the run 1 points to avoid crowding) in Figures 14 and 15 are the quadratic sum of the *Bright SHARC detection efficiency* uncertainty and of the Poisson statistical uncertainty due to the small number of clusters in each bin.

Figure 14 shows the results of our CXLF calculations using the runs 1 to 3 detection efficiencies. The first point to note is that the run 1 CXLF (open circles) is consistent with the results of N99. This demonstrates the robustness of the N99 result (under the assumption of standard parameters). In the last luminosity bin we derived a slightly higher number density of clusters compared to N99.

This is because our run 1 simulation yielded a lower *Bright SHARC detection efficiency* in this bin than did the simulations used by N99. (When the detection efficiency is lower, the effective area – and hence volume – is smaller which pushes up the number density.) The second point to note from Figure 14 is that the value of  $\Omega_0$  and  $\Omega_\Lambda$  have a small effect on the CXLF, not discernable in a log-log plot. We do see a small systematic offset between the  $\Omega_0 = 1$  and  $\Omega_0 < 1$  points (because the detection efficiencies in runs 2 and 3 were lower than those in run 1), but this offset is smaller than the 1 sigma uncertainties.

In Figure 15 we present 4 separate sets of CXLF results, comparing the run 1 number densities to those derived from runs 4 through 12. We see, from the lower left panel, that ellipticity has a very small effect on the CXLF. However, in the other 3 panels we see some quite dramatic effects when we change the core radius (lower right panel), the value of  $\beta$  (upper left panel) and surface brightness profile (upper right panel: we have only plotted the results using moderate cooling flows and NFW profiles). When clusters are more diffuse (e.g. if  $\beta$  is smaller or  $r_c$  is larger than our canonical values), the detection efficiency declines (see §3.5 and §3.6) hence the cluster number density goes up. By contrast, when the clusters become more concentrated (e.g. if we use a NFW profile or a strong cooling flow instead of an isothermal  $\beta$  model), then detection efficiency goes up (see §3.4) and the number density goes down.

In summary, we have shown that the N99 CXLF is robust, under the assumption of standard parameters, despite the fact that it was derived using a less sophisticated set of selection function simulations than run 1. We find that the CXLF is not very sensitive to the values of certain parameters,  $\Omega_0$ ,  $\Omega_\Lambda$  and ellipticity. Other parameters have a more significant effect on the CXLF; these are the values of  $\beta$  and  $r_c$  and the shape of the cluster surface brightness profile. If all clusters had NFW profiles, for example, then the N99 CXLF will significantly over estimate the number density of high redshift clusters (since it was derived using a selection function that assumed isothermal  $\beta$  profiles). Alternatively, if all clusters had large core radii, then the N99 CXLF will significantly under estimate the number density of clusters (since it was derived using a selection function that assumed  $r_c = 250$  kpc).

## 6. Discussion

The evolution of the CXLF with redshift, especially at the bright (i.e. high mass) end, provides - in principle - strong constraints on the value of  $\Omega_m$  (see §1). If we see, for example, a much lower number density of high luminosity clusters at high redshift, as opposed to the number density at low redshift, then we have strong support for a high  $\Omega_m$  Universe (and vice versa) because  $\Omega_\Lambda$  has little effect on the evolution of the CXLF out to at least  $z \sim 1$  (e.g. Holder et al. 2000). However, since the existing cluster samples only contain very small numbers of distant and luminous clusters, our ability to constrain  $\Omega_m$  crucially depends on our ability to define the volume in which those clusters were detected. For example, the Bright SHARC has only one cluster in the highest luminosity bin (RXJ0152). If we over (under) estimate the volume in which this cluster was detected then our

number density will be too low (high) and our inferred value of  $\Omega_0$  too high (low).

In section 5 we attempted to determine the sensitivity of the Bright SHARC CXLF to the assumptions that were incorporated into the selection function simulations. We have shown that the initial choice of cosmological parameters has only a small influence on the CXLF. This result is fundamental because it means that, whatever cosmology is assumed when measuring the CXLF, we will still be able to probe CXLF evolution, and thus constrain the value of  $\Omega_m$ . The same cannot be said for the assumed surface brightness model; if all clusters follow NFW profiles or have strong cooling flows, we will significantly over-estimate the high  $z$  cluster number density (and thus drive  $\Omega_m$  down). By contrast, if we underestimate the value of  $r_c$ , or overestimate the value of  $\beta$ , we will significantly underestimate the high  $z$  cluster number density (and thus drive  $\Omega_m$  up).

Despite the fact that we have found cluster ellipticity to have minimal effect on our CXLF, we draw attention to the fact that, at high redshift, highly elliptical clusters are easier to detect than circular ones in our simulations. This may offer a partial explanation as to why the only  $z > 0.8$  X-ray cluster detected in the Bright SHARC survey (RXJ0152) is highly elliptical with a complex and elongated morphology (we missed probably the faint  $z > 0.8$  more regular clusters). We note also that Ebeling et al. (1999) claimed that high levels of substructure can also lead to decrease the probability of detection.

With the X-ray data currently available we are not able to quantify just how much the various selection function assumptions might bias an  $\Omega_m$  measurement. This is because we are not able to determine the distribution of  $r_c$  and  $\beta$  values for the Bright SHARC clusters, or determine what fraction of those clusters are better fit with NFW profiles than with isothermal  $\beta$  profiles (see also Durret et al. 1994). To address this, we have begun a program to study cluster morphologies (and temperature profiles) with the new X-ray satellites XMM and *Chandra*. The follow-up of known clusters, such as those in the EMSS or Bright SHARC samples, will be one of major contributions of XMM and *Chandra* to cosmology. Both satellites have smaller fields of view than did ROSAT and so do not lend themselves well to serendipitous, or dedicated, cluster surveys. The catalogs derived from the ROSAT archive (see also Ebeling et al. 2000) will remain the pre-eminent source of high redshift X-ray clusters for some time to come. The recent work by Romer et al. (2000b) has demonstrated that in 5-10 years, XMM will have covered sufficient area to sufficient depth to allow new cluster catalogs to be created. These new catalogs will contain more high redshift, high luminosity clusters than the ROSAT and EMSS samples and so will provide much better constraints on  $\Omega_m$ . These catalogs will require detailed simulations in order to determine their selection function. The work presented herein provides important guidelines as to how those simulations should be carried out.

Previously, several other groups (e.g. Vikhlinin et al. 1998, Burke et al. 1997, Scharf et al. 1997 or Rosati et al. 1995) have simulated selection functions in order to measure their CXLF's. Their methods were generally the same as those in this paper. All the morphological parameters tested here were, however, not included, preventing them from showing the dependence of the

selection function with the X-ray morphology of the clusters. In a future work we plan to apply our results to the faint SHARC sample (including the Southern SHARC by Burke et al. 1997) and to derive the limits to the evolution of the CXLF based on the uncertainties we have determined.

## 7. Summary and Conclusions

The areal coverage of serendipitous surveys, such as SHARC is, as we have shown here, poorly determined at faint flux limits. For the Bright SHARC CXLF we have demonstrated that all the clusters in this sample are bright enough that the error in the areal coverage is  $\sim 5\%$ . The uncertainty of the completeness of the survey then, becomes important when the areal coverage uncertainty is so small.

We have carried out a detailed set of simulations in order to probe the effects of certain assumptions about distant clusters and the geometry of the Universe on the completeness of the Bright SHARC survey. These assumptions have ramifications for the Cluster X-ray Luminosity Function (CXLF) derived for the SHARC survey and, ultimately, for the value of the matter density ( $\Omega_m$ ) derived from CXLF evolution. Under the assumption of a standard set of morphological parameters, we find that the Bright SHARC CXLF as determined by N99 (using a less sophisticated set of selection function simulations) is robust. The new Bright SHARC CXLF presented in Figure 14 agrees (within the 1 sigma envelope) with earlier estimates of the SHARC CXLF (Nichol et al. 1997, N99, Burke et al. 1997) and shows no statistical evidence for strong evolution at any luminosity out to  $z=0.7$ . At present, we are unable to make any definitive statement about a possible deficit of high redshift, high luminosity clusters in the Bright SHARC (see N99) since we are still hampered by a combination of small number statistics, uncertainties in the local CXLF, incompleteness in our optical and X-ray follow-up as well as the systematic uncertainties in the Bright SHARC selection due to the unknown surface brightness profiles of distant clusters.

We find that certain assumptions have little effect on the detection efficiency of the survey: the target of the X-ray pointing, the moderate ( $e \leq 0.3$ ) ellipticity of the cluster or the presence of moderate cooling flows. None of these assumptions has a significant impact on our ability to measure cluster luminosities using the simple method adopted in R00. Other assumptions, specifically those associated with the cluster X-ray morphology (e.g. sharply peaked surface brightness profile or high ellipticity), can have a significant impact on cluster detectability (and the inferred completeness of the survey) and the derived CXLF. We have shown, then, that even with an increased number of detected clusters, the results based on attempting to measure CXLF evolution to constrain  $\Omega_m$  will remain highly uncertain. Follow-up studies by *Chandra* and XMM that measure the X-ray morphology of distant clusters will, therefore, play a key role in the measurement of  $\Omega_m$ .

CA thanks the staff of the Dearborn Observatory for hospitality during his postdoctoral fellowship. The authors thank the Institut Gassendi pour la Recherche Astronomique en Provence for

numerical support. The authors thank the referee Harald Ebeling for detailed comments which have lead to a greatly improved paper. This project was funded in part by NASA grants NAG5-2432 and NAG5-6548.

## REFERENCES

- Adami, C., Mazure, A., Katgert, P., & Biviano, A. 1998, A&A, 336, 63
- Arnaud, K.A. 1996, ASP Conf. Series, 101, 17
- Arnaud, M., & Evrard, A.E. 1999, MNRAS, 305, 631
- Bahcall, N.A., Fan, X., & Cen, R. 1997, ApJ, 485, L53
- Borgani, S., Rosati, P., Tozzi, P., & Norman, C. 1999, ApJ, 517, 40
- Burke, D.J., Collins, C.A., Sharples, R.M., Romer, A.K., Holden, B.P., & Nichol, R.C. 1997, ApJ, 488, L83
- Durret, F., Gerbal, D., Lachieze-Rey, M., Lima-Neto, G., & Sadat , R. 1994, A&A, 287, 733
- Ebeling, H., Edge, A., & Henry, J.P. 2000, Large-Scale Structure in the X-ray Universe, Plionis & Georgantopoulos (eds), atlantisciences, p39
- Ebeling, H., Jones, L.R., Perlman, E., Scharf, C., Horner, D., Wegner, G., Malkan, M., Fairley, B., & Mullis, C.R. 2000, ApJ, 534, 133
- Ebeling, H., Edge, A.C., Bohringer, H., Allen, S.W., Crawford, C.S., Fabian, A.C., Voges, W., & Huchra, J.P. 1998, MNRAS, 301, 881
- Ebeling, H., Edge, A.C., Fabian, A.C., Allen, S.W., Crawford, C.S. , & Bohringer, H. 1997, ApJ, 479, L101
- de Grandi, S., Bohringer, H., Guzzo, L., Molendi, S., Chincarini, G. , Collins, C., Cruddace, R., Neumann, D., Schindler, S., Schuecker, P., & Voges, W. 1999, ApJ, in press
- Gunn, J.E., & Gott, J.R. 1972, ApJ, 176, 1
- Henry, J.P., Gioia, I.M., Mullis, C.R., Clowe, D.I., Luppino, G.A., Böhringer, H., Briel, U.G., Voges, W., & Huchra, J.P. 1997, AJ, 114, 1293
- Henry, J.P., & Henriksen, M.J. 1986, ApJ, 301, 689
- Holder, G.P., Mohr, J.J., Carlstrom, J.E., Evrard, A.E., & Leitch, E.M. 2000, ApJ submitted
- Lacey, C., & Cole, S. 1993, MNRAS, 262, 627
- Navarro, J.F., Frenk, C.S., & White, S.D.M. 1997, ApJ, 490, 493
- Nichol, R.C., Romer, A.K., Holden, B.P., Ulmer, M.P., Pildis, R.A., Adami, C., Merrelli, A.J., Burke, D.J., & Collins, C.A. 1999, ApJ let, 521, L21: N99

- Nichol, R.C., Holden, B.P., Romer, A.K., Ulmer, M.P., Burke, D.J., & Collins, C.A., 1997, ApJ, 481, 644
- Oukbir, J., & Blanchard, A. 1997, A&A, 317, 1
- Oukbir, J., & Blanchard, A. 1992, A&A, 262, L21
- Pen, U. 1999, ApJS, 120, 49
- Peres, C.B., Fabian, A.C., Edge, A.C., et al. 1998, MNRAS, 298, 416
- Press, W.H., & Schechter, P. 1974, ApJ, 187, 425
- Reichart, D.E., Nichol, R.C., Castander, F.J., Burke, D.J., Romer, A.K., Holden, B.P., Collins, C.A., & Ulmer, M.P. 1999, ApJ, 518, 521
- Richstone, D., Loeb, A., & Turner, E.L. 1992, ApJ, 393, 477
- Romer, A.K., Viana, P., Liddle, A., & Mann, R.G. 2000b, ApJ, in preparation
- Romer, A.K., Nichol, R.C., Holden, B.P., Ulmer M.P., Pildis, R.A., Merrelli, A.J., Adami, C., Burke, D.J., Collins, C.A., Metevier, A.J., Kron, R., & Commons, K. 2000a, ApJS in press: R00
- Romer, A.K., Collins, C.A., Böhringer, H., Cruddace, R.G., Ebeling, H., MacGillivray, H.G., & Voges, W. 1994, Nature, 372, 75
- Rosati, P., Della Ceca, R., Norman, C., & Giacconi, R. 1998, ApJ, 492, 21
- Rosati, P., Della Ceca, R., Burg, R., Norman, C., & Giacconi, R. 1995, ApJ, 445, L11
- Sadat, R. 1998, ApSS, 261, 331
- Scharf, C.A., Jones, L.R., Ebeling, H., Perlman, E., Malkan, M., & Wegner, G. 1997, ApJ, 477, 79
- Viana, P.T.P., & Liddle, A.R. 1999, MNRAS, 303, 535
- Viana, P.T.P., & Liddle, A.R. 1996, MNRAS, 281, 323
- Vikhlinin, A., McNamara, B.R., Forman, W., Jones, C., Quintana, H., & Hornstrup, A. 1998, ApJ, 502, 558
- Wang, Q.D., & Ulmer, M.P. 1997, MNRAS, 292, 920

Fig. 1.— *total detection efficiency* (see text for the definition) for run 1 (standard parameter set). Each disk represents the results for a different redshift bin (we note that not all redshifts used in the simulations are represented). We have split each disk into 4 radial bins and 6 sectors, each of the 24 regions represents the results from a different luminosity ( $L_{44} = 1, 2, 3.5, 5, 7.5, 10$ ) and off-axis annulus combination. The uncertainties on the detection levels are  $9 \pm 5\%$ , therefore, less than the color variation of the color bar between 0 and 20%.

Fig. 2.— As Fig. 1, but for the *Bright SHARC detection efficiency* (see text for definition) instead of the *total detection efficiency*. The uncertainties on the detection levels are  $9 \pm 5\%$ , therefore, less than the color variation of the color bar between 0 and 20%.

Fig. 3.— As Fig. 1, but here grayscale levels show the *recovered luminosity* (see text for definition). The uncertainties on the *recovered luminosity* are  $8 \pm 6\%$ , therefore, less than the color variation of the color bar between 25 and 55%.

Fig. 4.— Percentage difference (inner y-axes) between the *Bright SHARC detection efficiency* for run 1 ( $\Omega_0=1, \Omega_\Lambda=0$ ) and run 2 ( $\Omega_0=0.1, \Omega_\Lambda=0$ , circles) and run 3 ( $\Omega_0 = 0.4, \Lambda=0.6$ , filled squares). The outer x and y-axes give the cluster redshift and luminosity respectively. The inner x-axes are the distances from the ROSAT PSPC pointing center in (15'') pixels. The crosses depict redshift and luminosity combinations where the detection efficiency for run 1 was  $< 15\%$ . The  $1-\sigma$  error bars are only plotted on the circles. The error bars are approximatively the same size for the squares as for the open circles and are not shown for the squares in the figures.

Fig. 5.— As Fig. 4, but here we test the effects of ellipticity on the *total detection efficiency*. The circles represent the percentage difference between run 1 ( $e = 0.15$ ) and run 5 ( $e = 0.3$ ), whereas the filled squares represent the percentage difference between run 1 and run 4 ( $e = 0$ ). The  $1-\sigma$  error bars are only plotted on the circles.

Fig. 6.— As Fig. 4, but here we test the effects of surface brightness profile on the *Bright SHARC detection efficiency*. The circles represent the detection difference between run 1 (isothermal  $\beta$  profiles) and run 7 (moderate cooling flow profiles), whereas the filled squares represent the percentage difference between run 1 and run 6 (NFW profiles). The  $1-\sigma$  error bars are only plotted on the circles.

Fig. 7.— As Fig. 6. Circles represent the *Bright SHARC detection efficiency* percentage difference between run 1 (isothermal  $\beta$  profiles) and run 8 (strong cooling flow profiles), whereas the filled squares represent the percentage difference between run 1 and run 6 (NFW profiles). The  $1-\sigma$  error bars are only plotted on the circles.

Fig. 8.— Percentage difference (inner y-axes) between the *Bright SHARC recovered luminosity* for run 1 ( $\beta=0.67$ ) and run 8 (strong cooling-flow profile) and for run 1 ( $\beta=0.67$ ) and run 6 (NFW profile, squares). The  $1-\sigma$  error bars are only plotted on the circles.

Fig. 9.— As Fig. 4, but here we test the effects of varying  $\beta$  on the *Bright SHARC detection efficiency*. The circles represent the percentage difference between run 1 ( $\beta=0.67$ ) and run 9 ( $\beta=0.55$ ), whereas the filled squares represent the percentage difference between run 1 and run 10 ( $\beta=0.75$ ). The  $1-\sigma$  error bars are only plotted on the circles.

Fig. 10.— Percentage difference (inner y-axes) between the *Bright SHARC recovered luminosity* for run 1 ( $\beta=0.67$ ) and run 9 ( $\beta=0.55$ , circles) and for run 1 ( $\beta=0.67$ ) and run 10 ( $\beta=0.75$ , squares). The  $1-\sigma$  error bars are only plotted on the circles.

Fig. 11.— As Fig. 4, but here we test the effects of varying the core radius on the *Bright SHARC detection efficiency*. The circles represent the percentage difference between run 1 ( $r_c=250$  kpc) and run 12 ( $r_c=400$  kpc), whereas the filled squares represent the percentage difference between run 1 and run 11 ( $r_c=100$  kpc). The  $1-\sigma$  error bars are only plotted on the circles.

Fig. 12.— The solid curve shows how the Bright SHARC areal coverage varies with extended source flux (where  $f_{-13}$  is the 0.5-2.0 keV flux in units of  $10^{-13}$  erg s $^{-1}$  cm $^{-2}$ ) or count rate. The two dotted curves depict the estimated  $1-\sigma$  errors. The thick vertical solid line is drawn where the  $1-\sigma$  errors are  $\pm 10\%$ . The fluxes of each of the 13 Bright SHARC distant clusters ( $z \geq 0.285$ ) are plotted as thin vertical lines. The faintest cluster is depicted by the thin vertical solid line (here the error is  $\pm 5\%$ ).

Fig. 13.— Effective area of the Bright sample as a function of cluster luminosity and redshift. The six curves represent the six different input luminosities (in units of  $10^{44}$  ergs.s $^{-1}$ ).

Fig. 14.— The Bright SHARC CXLF as a function of assumed cosmological model. The x-axis gives the log of the cluster luminosity (erg s $^{-1}$ ) in the [0.5-2.0 keV] band. The y-axis gives the log of cluster number density in units of Mpc $^{-3}$  ( $10^{44}$  erg s $^{-1}$ ) $^{-1}$ . The error bars are shown for the run 1 ( $\Omega_0=1$ ) points (circles). We plot also the error envelope from N99 (two dashed lines). The two solid lines are the envelope of the local CXLF from De Grandi et al. (1999) and Ebeling et al. (1997).

Fig. 15.— The Bright SHARC CXLF as a function of cluster morphology: (lower left) ellipticity ; (lower right) core radius ; (upper left) slope  $\beta$  ; (upper right) surface brightness profile. The x-axis gives the log of the cluster luminosity (erg s $^{-1}$ ) in the [0.5-2.0 keV] band. The y-axis gives the log of cluster number density in units of Mpc $^{-3}$  ( $10^{44}$  erg s $^{-1}$ ) $^{-1}$ . The error bars are shown for the run 1 points (circles). The two solid lines are the envelope of the local CXLF from De Grandi et al. (1999) and Ebeling et al. (1997).

Table 1. The parameters used for each of the 16 different simulation runs: run number, surface brightness profile, ellipticity, core radius, profile slope,  $\Omega_0$ ,  $\Lambda$ , number of pointings and pointing type.

run	profile	$e$	$r_c$ (kpc)	$\beta$	$\Omega_m$	$\Lambda$	ptg. type
1	Isothermal	0.15	250	0.67	1.	0.	all
2	Isothermal	0.15	250	0.67	0.1	0.	all
3	Isothermal	0.15	250	0.67	0.4	0.6	all
4	Isothermal	0.	250	0.67	1.	0.	all
5	Isothermal	0.30	250	0.67	1.	0.	all
6	NFW	0.15	250	0.67	1.	0.	all
7	moderate cool. flow	0.15	250	0.67	1.	0.	all
8	strong cool. flow	0.15	250	0.67	1.	0.	all
9	Isothermal	0.15	250	0.55	1.	0.	all
10	Isothermal	0.15	250	0.75	1.	0.	all
11	Isothermal	0.15	100	0.67	1.	0.	all
12	Isothermal	0.15	400	0.67	1.	0.	all
13	Isothermal	0.15	250	0.67	1.	0.	type 2
14	Isothermal	0.15	250	0.67	1.	0.	type 3
15	Isothermal	0.15	250	0.67	1.	0.	type 6
16	Isothermal	0.15	250	0.67	1.	0.	type 7
17	Isothermal	0.15	250	0.67	1.	0.	type 8
18	Isothermal	0.15	250	0.67	1.	0.	type 9
19	Isothermal	0.15	250	0.67	1.	0.	point sources
20	Isothermal	0.15	250	0.67	1.	0.	diffuse sources

Table 2. Percentage of *Bright SHARC detection efficiency* for the 15 Bright SHARC clusters (noted Cl.) with  $z > 0.285$  for the run 1 to 12. The redshift z, luminosity  $L_{44}$  and Offaxis angle (in pixels) are from R00. The two clusters labelled by a “\*” have been discarded from the CXLF analysis because their mean *Bright SHARC detection efficiency*, over simulation runs 1 to 12, was lower than 5%. We note than when an individual success rate (one of the numbers in this table) was less than 5%, we have used the value 5% (see text §3.1) as the efficiency to compute the CXLF’s.

Cl.	z	$L_{44}$	Off	1	2	3	4	5	6	7	8	9	11	12
0152	0.83	8.26	57	11.5	4.5	5.9	15.2	7.4	12.6	14.4	73.1	15.7	4.1	26.6
0221	0.45	2.87	74	25.9	10.2	8.7	21.6	8.1	19.2	22.9	63.3	20.2	0.6	38.3
0256	0.36	4.16	84	62.9	61.0	60.0	25.9	34.0	59.6	62.8	75.4	56.2	20.7	61.5
0318	0.37	3.28	43	70.4	62.2	55.7	60.2	34.2	71.8	70.8	88.9	66.0	2.7	85.4
0426	0.38	3.20	23	46.3	41.9	41.0	25.4	22.3	47.0	48.9	69.4	38.1	4.2	53.6
1120	0.60	5.01	48	19.6	3.5	3.1	19.0	3.2	13.6	13.9	89.7	15.6	0.7	30.2
1211	0.34	1.59	62	14.4	7.5	6.5	28.0	3.2	15.3	13.5	54.1	15.5	0.2	30.8
1241	0.39	3.10	77	45.8	36.2	34.7	32.1	19.3	45.5	46.0	71.6	37.3	2.1	57.4
1308*	0.33	0.96	45	0.5	0.9	0.7	5.7	0.5	0.5	0.7	38.0	0.3	0.5	6.5
1311	0.43	1.92	74	7.9	1.9	1.0	7.2	1.6	5.7	4.0	47.3	4.0	0.1	12.1
1334*	0.62	3.46	70	1.2	0.4	0.2	5.3	0.7	1.5	2.1	35.0	2.4	0.1	5.8
1418	0.29	2.76	30	72.9	66.3	61.6	86.1	32.5	72.4	68.6	81.8	66.5	8.7	84.9
1701	0.45	3.49	13	18.7	7.7	1.1	42.1	6.8	19.3	16.4	79.6	22.2	0.1	4.9
2237	0.30	1.35	88	26.8	18.5	13.8	17.9	3.5	18.4	23.8	57.0	19.2	0.7	39.4
2258	0.29	2.06	52	63.6	53.0	44.6	79.4	13.8	62.3	59.8	73.4	51.3	2.2	77.5

Table 3. Detection efficiency percentages for run 1 (standard parameter set)

total detection efficiency <sup>a</sup>							Bright SHARC detection efficiency <sup>a</sup>						
z	$L_{44}$	1 <sup>st</sup>	2 <sup>nd</sup>	3 <sup>rd</sup>	4 <sup>th</sup>	z	$L_{44}$	1 <sup>st</sup>	2 <sup>nd</sup>	3 <sup>rd</sup>	4 <sup>th</sup>		
0.25	1.0	40±11	42±12	30±17	25±8	0.25	1.0	2± 5	7±13	7±11	17±9		
0.30	1.0	27±7	33±16	28±18	20±19	0.30	1.0	0±2	1±7	2±12	13±12		
0.35	1.0	12±10	16±10	17±7	5±9	0.35	1.0	0±3	0±5	0±2	0±4		
0.40	1.0	4±13	14±17	5±7	5±6	0.40	1.0	0±2	1±2	0±2	2±4		
0.45	1.0	3±7	5±11	3±8	1±6	0.45	1.0	0±2	0±2	0±2	0±4		
0.25	2.0	74±9	72±9	73±13	56±7	0.25	2.0	73±9	72±9	73±13	56±17		
0.30	2.0	68±12	76±11	58±11	54±8	0.30	2.0	49±14	68±12	51±11	54±8		
0.35	2.0	60±12	71±8	42±21	40±11	0.35	2.0	14±12	23±11	16±20	36±11		
0.40	2.0	45±11	46±9	45±15	33±12	0.40	2.0	4±6	2±4	11±8	21±12		
0.45	2.0	31±13	44±11	26±13	18±11	0.45	2.0	0±3	3±5	3±3	7±9		
0.25	3.5	81±9	90±3	78±8	58±17	0.25	3.5	81±9	90±3	78±8	58±17		
0.30	3.5	76±5	85±7	75±5	64±15	0.30	3.5	76±5	85±7	75±5	64±15		
0.35	3.5	77±5	86±9	72±6	53±9	0.35	3.5	73±5	86±9	72±6	53±9		
0.40	3.5	77±11	79±6	69±6	43±14	0.40	3.5	56±12	75±6	65±6	43±14		
0.45	3.5	68±14	75±11	67±10	48±15	0.45	3.5	19±12	38±12	40±12	45±15		
0.25	5.0	90±6	96±3	89±3	69±14	0.25	5.0	90±6	96±3	89±3	69±14		
0.30	5.0	91±6	88±4	85±3	71±18	0.30	5.0	91±6	88±4	85±3	71±18		
0.35	5.0	90±5	89±1	85±8	66±14	0.35	5.0	89±5	89±1	85±8	66±14		
0.40	5.0	86±5	92±3	79±4	54±9	0.40	5.0	85±5	92±3	78±4	54±9		
0.45	5.0	88±4	87±5	81±9	54±9	0.45	5.0	81±4	87±5	81±9	54±9		
0.25	7.5	97±4	100±1	95±4	60±10	0.25	7.5	97±4	100±1	95±4	60±10		
0.30	7.5	90±4	96±1	98±1	64±18	0.30	7.5	90± 4	96±1	98±1	64±18		
0.35	7.5	87±3	99±3	94±3	60±12	0.35	7.5	87±3	99±3	94±3	60±12		
0.40	7.5	91±4	96±4	93±4	55±12	0.40	7.5	91±4	96±4	93±4	55±12		
0.45	7.5	88±7	95±4	83±4	55±13	0.45	7.5	86±7	95±4	83±4	55±13		
0.25	10.0	93±1	98±1	98±1	68±16	0.25	10.0	93±1	98±1	98±1	68±16		
0.30	10.0	94±3	99±1	97±3	65±12	0.30	10.0	94±3	99±1	97±3	65±12		
0.35	10.0	94±1	98±1	99±6	67±17	0.35	10.0	94±1	98±1	99±6	67±17		
0.40	10.0	99±6	98±1	96±6	56±14	0.40	10.0	100±6	98±1	96±6	56±14		
0.45	10.0	93±4	98±4	92±4	60±18	0.45	10.0	93±4	98±4	92±4	60±18		
0.50	10.0	93±3	96±6	92±5	52±8	0.50	10.0	93±3	96±6	92±5	52±8		
0.55	10.0	94±8	94±1	87±6	59±9	0.55	10.0	94±8	94±1	87±6	59±9		
0.60	10.0	94±5	94±4	83±13	59±17	0.60	10.0	94±5	94±4	83±13	59±17		
0.65	10.0	89±8	91±6	85±15	46±17	0.65	10.0	87±8	90±6	84±15	46±17		
0.70	10.0	85±9	92±8	79±21	52±15	0.70	10.0	72±9	90±8	78±21	52±15		
0.50	7.5	90±4	96±3	95±10	62±20	0.50	7.5	90±4	96±3	95±10	62±20		
0.55	7.5	84±5	92±4	88±11	53±10	0.55	7.5	79±5	92±4	88±11	53±10		
0.60	7.5	87±10	93±7	77±12	59±12	0.60	7.5	67±9	89±7	74±12	59±12		
0.65	7.5	80±5	84±10	65±15	46±8	0.65	7.5	30±8	51±11	39±13	46±8		

Table 3—Continued

total detection efficiency <sup>a</sup>							Bright SHARC detection efficiency <sup>a</sup>						
z	$L_{44}$	1 <sup>st</sup>	2 <sup>nd</sup>	3 <sup>rd</sup>	4 <sup>th</sup>	z	$L_{44}$	1 <sup>st</sup>	2 <sup>nd</sup>	3 <sup>rd</sup>	4 <sup>th</sup>		
0.50	5.0	77±4	79±5	84±6	55±13	0.50	5.0	49±7	71±5	75±4	54±13		
0.55	5.0	74±15	83±8	60±12	38±16	0.55	5.0	17±8	40±16	29±13	38±14		
0.60	5.0	57±12	72±12	64±11	48±12	0.60	5.0	8±6	20±6	18±9	41±12		
0.65	5.0	46±14	58±14	38±11	27±16	0.65	5.0	3±7	5±4	7±6	20±15		
0.70	5.0	43±13	42±11	34±11	21±11	0.70	5.0	0±5	5±4	3±5	9±8		
0.50	3.5	68±14	61±8	53±20	37±12	0.50	3.5	14±12	12±11	12±8	33±12		
0.55	3.5	45±14	55±15	32±26	36±13	0.55	3.5	3±6	6±8	5±6	19±12		
0.60	3.5	29±14	48±12	32±11	17±9	0.60	3.5	0±7	6±6	0±6	4±5		
0.65	3.5	26±17	28±12	18±16	12±9	0.65	3.5	1±4	1±5	2±1	1±4		
0.70	3.5	19±14	25±12	11±9	8±8	0.70	3.5	0±4	0±3	0±4	0±1		
0.50	2.0	15±16	24±25	12±18	11±14	0.50	2.0	1±1	1±3	1±6	1±4		
0.55	2.0	15±13	13±13	15±9	6±5	0.55	2.0	1±3	0±1	1±3	0±1		
0.60	2.0	11±9	12±17	3±13	5±9	0.60	2.0	1±1	0±1	0±1	1±1		
0.65	2.0	6±12	5±9	3±7	1±9	0.65	2.0	0±1	0±1	0±4	0±1		
0.70	2.0	7±6	1±9	3±8	2±0	0.70	2.0	0±1	0±1	0±1	1±1		
0.50	1.0	6±6	2±7	1±7	2±6	0.50	1.0	0±1	0±1	0±1	0±3		
0.55	1.0	2±6	5±6	0±7	1±5	0.55	1.0	0±1	0±1	0±1	1±1		
0.60	1.0	0±4	2±6	0±3	0±3	0.60	1.0	0±1	0±3	0±1	0±1		
0.65	1.0	1±5	2±7	1±4	2±3	0.65	1.0	0±1	0±1	0±1	1±1		
0.70	1.0	1±6	0±5	0±4	0±1	0.70	1.0	0±1	0±1	0±3	0±1		
0.75	1.0	2±6	0±1	0±1	0±12	0.75	1.0	2±6	0±1	0±1	0±12		
0.80	1.0	0±3	1±1	1±1	0±9	0.80	1.0	0±3	1±1	0±1	0±9		
0.85	1.0	0±6	0±3	0±1	1±10	0.85	1.0	0±6	0±3	0±1	0±10		
0.90	1.0	0±4	0±1	1±1	0±8	0.90	1.0	0±4	0±1	0±1	0±8		
0.95	1.0	0±5	0±1	0±3	0±10	0.95	1.0	0±5	0±1	0±3	0±10		
0.75	2.0	3±3	1±3	1±1	1±8	0.75	2.0	0±3	0±3	0±1	0±8		
0.80	2.0	4±6	1±3	0±1	1±13	0.80	2.0	1±6	1±3	0±1	0±13		
0.85	2.0	1±1	1±3	1±1	1±15	0.85	2.0	0±1	0±3	0±1	0±15		
0.90	2.0	2±4	0±1	0±1	0±10	0.90	2.0	0±4	0±1	0±1	0±10		
0.95	2.0	1±4	1±3	0±1	1±10	0.95	2.0	1±4	0±3	0±1	1±10		
0.75	3.5	11±1	19±1	14±1	5±11	0.75	3.5	0±1	1±1	1±1	0±11		
0.80	3.5	7±1	10±1	6±1	4±16	0.80	3.5	0±1	0±1	0±1	0±16		
0.85	3.5	10±3	7±1	2±1	1±11	0.85	3.5	0±3	1±1	0±1	0±11		
0.90	3.5	5±3	5±1	1±1	1±14	0.90	3.5	0±3	0±1	0±1	0±14		
0.95	3.5	3±1	1±1	3±1	0±9	0.95	3.5	1±1	0±1	0±1	0±9		
0.75	5.0	19±1	41±1	25±1	17±14	0.75	5.0	0±1	0±1	3±1	1±14		
0.80	5.0	19±1	13±1	18±1	12±18	0.80	5.0	1±1	0±1	0±1	3±18		
0.85	5.0	6±1	11±1	5±1	2±9	0.85	5.0	1±1	2±1	1±1	0±9		
0.90	5.0	5±1	6±3	4±1	1±11	0.90	5.0	0±1	0±3	0±1	0±11		
0.95	5.0	4±1	5±1	2±1	0±8	0.95	5.0	0±1	0±1	0±1	0±8		

Table 3—Continued

total detection efficiency <sup>a</sup>						Bright SHARC detection efficiency <sup>a</sup>					
z	$L_{44}$	1 <sup>st</sup>	2 <sup>nd</sup>	3 <sup>rd</sup>	4 <sup>th</sup>	z	$L_{44}$	1 <sup>st</sup>	2 <sup>nd</sup>	3 <sup>rd</sup>	4 <sup>th</sup>
0.75	7.5	69±4	69±1	60±1	36±18	0.75	7.5	11±4	11±1	10±1	31±18
0.80	7.5	48±3	59±1	41±1	34±13	0.80	7.5	4±3	4±1	3±1	14±13
0.85	7.5	27±3	40±1	23±1	21±14	0.85	7.5	2±3	2±1	0±1	4±14
0.90	7.5	21±4	22±1	16±1	7±10	0.90	7.5	0±4	0±1	1±1	2±10
0.95	7.5	7±3	13±1	11±3	3±13	0.95	7.5	0±3	0±1	2±3	0±13
0.75	10.0	81±4	85±4	74±4	41±3	0.75	10.0	34±5	68±5	51±5	41±4
0.80	10.0	57±4	75±4	61±4	52±3	0.80	10.0	12±5	13 ±5	20±5	50±4
0.85	10.0	51±4	60±4	41±4	24±3	0.85	10.0	3±5	6±5	4±5	14±3
0.90	10.0	38±4	44±4	25±4	19±3	0.90	10.0	1±5	3±5	2±5	10±4
0.95	10.0	15±4	24±4	17±4	9±3	0.95	10.0	0±5	4±5	1±5	1±3

<sup>a</sup>The percentage *total detection efficiency* (left columns) and the *Bright SHARC detection efficiency* (right columns). The columns 1 and 7 give the cluster redshift, columns 2 and 8 the cluster luminosities, columns 3 and 9 the percentage detection efficiency in the inner annulus, columns 4 and 10 the percentage detection efficiency in the second annulus, etc.

Table 4. Recovered luminosity percentages for run 1 (standard parameter set)

total sample <sup>a</sup>							Bright SHARC sample <sup>a</sup>						
z	$L_{44}$	$1^{st}$	$2^{nd}$	$3^{rd}$	$4^{th}$	z	$L_{44}$	$1^{st}$	$2^{nd}$	$3^{rd}$	$4^{th}$		
0.25	1.0	109±23	100±22	104±8	115±24	0.25	1.0	130±8	125±8	110±8	119±24		
0.30	1.0	108±27	94±20	102±26	124±13	0.30	1.0	0	173±8	176±8	132±8		
0.35	1.0	112±36	107±14	106±25	116±13	0.35	1.0	0	0	0	0		
0.40	1.0	141±83	121±23	130±13	184±13	0.40	1.0	0	200±8	0	999		
0.45	1.0	90±16	149±19	156±13	128±13	0.45	1.0	0	0	0	0		
0.25	2.0	106±13	103±4	102±11	116±6	0.25	2.0	106±13	103±4	102±11	116±6		
0.30	2.0	97±16	94±13	99±9	116±11	0.30	2.0	99±16	96±13	99±9	116±11		
0.35	2.0	99±22	95±14	97±20	109±10	0.35	2.0	124±28	107±4	105±8	111±10		
0.40	2.0	95±30	86±20	97±20	119±13	0.40	2.0	123±8	112±8	120±8	126±14		
0.45	2.0	100±15	97±17	100±17	127±7	0.45	2.0	0	184±18	192±18	148±18		
0.25	3.5	104±6	101±3	101±13	115±13	0.25	3.5	104±6	101±3	101±13	115±13		
0.30	3.5	98±6	96±6	97±8	117±8	0.30	3.5	98±6	96±6	97±8	117±8		
0.35	3.5	94±9	92±10	92±10	112±17	0.35	3.5	94±9	92±10	92±10	112±17		
0.40	3.5	92±9	89±10	89±9	111±12	0.40	3.5	93±9	90±10	89±9	111±12		
0.45	3.5	91±13	87±9	90±7	113±13	0.45	3.5	99±13	92±9	96±7	115±18		
0.25	5.0	104±4	100±4	102±3	116±5	0.25	5.0	104±4	100±4	102±3	116±5		
0.30	5.0	98±4	96±5	96±4	114±4	0.30	5.0	98±4	96±5	96±4	114±5		
0.35	5.0	96±10	93±4	92±6	113±14	0.35	5.0	95±10	93±4	92±6	113±14		
0.40	5.0	93±6	88±7	90±8	113±17	0.40	5.0	93±6	88±7	90±8	113±17		
0.45	5.0	92±12	87±7	87±6	112±16	0.45	5.0	92±12	87±7	87±6	112±16		
0.25	7.5	104±2	101±4	101±2	118±8	0.25	7.5	104±2	101±4	101±2	118±8		
0.30	7.5	97±3	95±4	97±2	115±3	0.30	7.5	97±3	95±4	97±2	115±3		
0.35	7.5	94±2	92±4	92±3	112±4	0.35	7.5	94±2	92±4	92±3	112±4		
0.40	7.5	92±5	89±9	89±5	109±5	0.40	7.5	92±5	89±9	89±5	109±5		
0.45	7.5	88±3	88±5	87±4	112±2	0.45	7.5	88±3	88±5	87±4	112±2		
0.25	10.0	99±3	100±2	101±2	115±4	0.25	10.0	99±3	100±2	101±2	115±4		
0.30	10.0	95±5	98±1	97±5	113±3	0.30	10.0	95±5	98±1	97±5	113±3		
0.35	10.0	91±3	91±3	92±5	113±2	0.35	10.0	91±2	91±3	92±5	113±2		
0.40	10.0	88±6	89±3	89±2	112±2	0.40	10.0	88±6	89±3	89±2	112±2		
0.45	10.0	87±2	88±3	89±5	113±4	0.45	10.0	87±2	88±3	89±5	113±4		
0.50	10.0	85±6	87±4	85±5	110±3	0.50	10.0	85±6	87±4	85±5	110±3		
0.55	10.0	82±4	95±6	84±5	111±13	0.55	10.0	82±4	95±6	84±5	111±8		
0.60	10.0	84±9	82±12	84±9	112±12	0.60	10.0	84±9	82±13	84±9	112±12		
0.65	10.0	81±6	84±5	82±3	109±20	0.65	10.0	81±6	84±5	82±3	109±20		
0.70	10.0	81±5	82±5	84±12	110±18	0.70	10.0	82±5	82±5	84±12	110±18		
0.50	7.5	86±10	87±7	85±9	111±9	0.50	7.5	86±10	87±7	85±9	111±9		
0.55	7.5	83±7	83±4	85±16	113±19	0.55	7.5	83±7	83±4	85±16	113±19		
0.60	7.5	83±12	83±17	84±6	109±13	0.60	7.5	82±12	83±17	84±6	109±8		
0.65	7.5	82±3	83±21	83±20	112±9	0.65	7.5	91±3	87±21	87±24	112±9		

Table 4—Continued

total sample <sup>a</sup>							Bright SHARC sample <sup>a</sup>						
z	$L_{44}$	$1^{st}$	$2^{nd}$	$3^{rd}$	$4^{th}$	z	$L_{44}$	$1^{st}$	$2^{nd}$	$3^{rd}$	$4^{th}$		
0.50	5.0	88±9	86±13	85±5	114±8	0.50	5.0	91±10	88±13	86±5	114±7		
0.55	5.0	88±8	86±9	86±20	117±2	0.55	5.0	110±6	94±9	95±24	117±2		
0.60	5.0	90±2	89±6	86±12	118±13	0.60	5.0	137±10	106±8	98±7	120±8		
0.65	5.0	87±15	86±11	89±8	118±4	0.65	5.0	109±8	122±8	108±8	125±4		
0.70	5.0	88±19	97±14	85±41	111±20	0.70	5.0	0	148±8	121±8	121±17		
0.50	3.5	93±13	84±27	87±8	116±16	0.50	3.5	118±1	96±8	104±8	118±17		
0.55	3.5	91±20	88±21	93±5	116±8	0.55	3.5	153±8	112±5	129±8	124±7		
0.60	3.5	91±20	92±17	87±12	117±38	0.60	3.5	0	140±8	0	146±8		
0.65	3.5	95±2	94±13	104±17	115±13	0.65	3.5	181±8	173±8	148±8	149±8		
0.70	3.5	96±5	102±13	95±46	120±13	0.70	3.5	0	0	0	0		
0.50	2.0	108±12	99±15	103±40	125±13	0.50	2.0	168±8	999	150±8	999		
0.55	2.0	113±19	102±12	113±12	132±13	0.55	2.0	153±8	0	200±8	0		
0.60	2.0	165±13	135±13	100±13	171±13	0.60	2.0	999	0	0	999		
0.65	2.0	101±13	126±13	169±13	173±13	0.65	2.0	0	0	0	0		
0.70	2.0	146±13	143±13	151±13	198±13	0.70	2.0	0	0	0	999		
0.50	1.0	191±13	172±13	82±13	168±13	0.50	1.0	0	0	0	0		
0.55	1.0	136±13	137±13	0	999	0.55	1.0	0	0	0	999		
0.60	1.0	0	999	0	0	0.60	1.0	0	0	0	0		
0.65	1.0	999	189±13	999	999	0.65	1.0	0	0	0	999		
0.70	1.0	999	0	0	0	0.70	1.0	0	0	0	0		
0.75	1.0	999	0	0	0	0.75	1.0	999	0	0	0		
0.80	1.0	0	999	999	0	0.80	1.0	0	999	0	0		
0.85	1.0	0	0	0	999	0.85	1.0	0	0	0	0		
0.90	1.0	0	0	999	0	0.90	1.0	0	0	0	0		
0.95	1.0	0	0	0	0	0.95	1.0	0	0	0	0		
0.75	2.0	999	83±13	86±13	146±13	0.75	2.0	0	0	0	0		
0.80	2.0	999	999	0	999	0.80	2.0	999	999	0	0		
0.85	2.0	114±13	999	999	999	0.85	2.0	0	0	0	0		
0.90	2.0	999	0	0	0	0.90	2.0	0	0	0	0		
0.95	2.0	999	999	0	999	0.95	2.0	999	0	0	999		
0.75	3.5	106±13	109±13	124±13	116±13	0.75	3.5	0	999	999	0		
0.80	3.5	107±13	108±13	147±13	120±13	0.80	3.5	0	0	0	0		
0.85	3.5	155±13	999	91±13	999	0.85	3.5	0	999	0	0		
0.90	3.5	168±13	156±13	137±13	999	0.90	3.5	0	0	0	0		
0.95	3.5	999	142±13	163±13	0	0.95	3.5	999	0	0	0		
0.75	5.0	93±21	89±18	91±13	109±13	0.75	5.0	0	0	153±8	134±8		
0.80	5.0	107±13	92±34	117±13	141±13	0.80	5.0	141	0	0	176±8		
0.85	5.0	140±13	118±13	999	167±13	0.85	5.0	999	196±8	999	0		
0.90	5.0	130±13	99±13	140±13	106±13	0.90	5.0	0	0	0	0		
0.95	5.0	170±13	157±13	159±13	0	0.95	5.0	0	0	0	0		

Table 4—Continued

total sample <sup>a</sup>						Bright SHARC sample <sup>a</sup>					
z	$L_{44}$	$1^{st}$	$2^{nd}$	$3^{rd}$	$4^{th}$	z	$L_{44}$	$1^{st}$	$2^{nd}$	$3^{rd}$	$4^{th}$
0.75	7.5	83±13	82±20	82±13	112±42	0.75	7.5	104±8	101±8	102±8	113±8
0.80	7.5	86±13	85±34	97±13	115±17	0.80	7.5	124±8	153±8	999	125±8
0.85	7.5	109±13	91±20	83±12	114±13	0.85	7.5	999	153±8	0	135±8
0.90	7.5	104±13	88±13	96±13	165±13	0.90	7.5	0	0	168±8	999
0.95	7.5	116±13	112±13	149±13	98±13	0.95	7.5	0	0	999	0
0.75	10.0	81±16	81±8	81±10	110±6	0.75	10.0	90±8	83±8	84±3	110±7
0.80	10.0	81±12	84±36	86±4	112±27	0.80	10.0	97±8	106±8	104±8	113±43
0.85	10.0	82±13	87±17	87±27	116±13	0.85	10.0	152±8	137±8	113±8	123±8
0.90	10.0	85±48	85±7	93±16	124±13	0.90	10.0	151±8	149±8	194±8	136±8
0.95	10.0	91±13	107±13	105±13	111±13	0.95	10.0	0	173±8	185±8	121±8

<sup>a</sup>The *recovered luminosity* (in percent) when no count rate limit is imposed (left columns) and when the Bright SHARC count rate limit is imposed (right columns). The columns 1 and 7 give the cluster redshift, columns 2 and 8 the cluster luminosities, columns 3 and 9 the percentage detection efficiency in the inner annulus, columns 4 and 10 the percentage detection efficiency in the second annulus, etc. Incidences of 999 indicate places where we recovered more than 200% of the input luminosity, i.e. spurious detections.

Table 5. Detection efficiency percentage for the NFW set of parameters

<i>total detection efficiency</i>						<i>Bright SHARC detection efficiency</i>					
<i>z</i>	<i>L</i> <sub>44</sub>	1st <sup>a</sup>	2nd <sup>a</sup>	3rd <sup>a</sup>	4th <sup>a</sup>	<i>z</i>	<i>L</i> <sub>44</sub>	1st <sup>a</sup>	2nd <sup>a</sup>	3rd <sup>a</sup>	4th <sup>a</sup>
0.25	1.0	52	56	45	46	0.25	1.0	52	56	45	46
0.30	1.0	54	48	39	54	0.30	1.0	53	48	39	54
0.35	1.0	47	42	37	41	0.35	1.0	24	33	30	41
0.40	1.0	34	27	30	22	0.40	1.0	3	5	7	14
0.45	1.0	13	20	11	11	0.45	1.0	2	2	0	1
0.25	2.0	60	78	67	62	0.25	2.0	60	78	67	62
0.30	2.0	70	77	68	65	0.30	2.0	70	77	68	65
0.35	2.0	67	70	69	55	0.35	2.0	66	70	69	55
0.40	2.0	60	66	54	63	0.40	2.0	58	66	54	63
0.45	2.0	47	65	52	47	0.45	2.0	24	58	47	46
0.25	3.5	82	97	90	75	0.25	3.5	82	97	90	75
0.30	3.5	85	92	88	76	0.30	3.5	85	92	88	76
0.35	3.5	90	95	90	65	0.35	3.5	90	95	90	65
0.40	3.5	90	91	82	69	0.40	3.5	90	91	82	69
0.45	3.5	80	88	80	67	0.45	3.5	80	88	80	67
0.25	5.0	89	98	97	75	0.25	5.0	89	98	97	75
0.30	5.0	96	98	99	74	0.30	5.0	96	98	99	74
0.35	5.0	90	97	97	72	0.35	5.0	90	97	97	72
0.40	5.0	100	98	98	75	0.40	5.0	100	98	98	75
0.45	5.0	92	96	97	72	0.45	5.0	92	96	97	72
0.25	7.5	96	98	96	79	0.25	7.5	89	98	97	75
0.30	7.5	98	100	97	72	0.30	7.5	96	98	99	74
0.35	7.5	96	100	100	72	0.35	7.5	90	97	97	72
0.40	7.5	95	99	98	79	0.40	7.5	100	98	98	75
0.45	7.5	96	98	95	72	0.45	7.5	92	96	97	72
0.25	10.0	91	98	99	72	0.25	10.0	91	98	99	72
0.30	10.0	99	100	100	76	0.30	10.0	99	100	100	76
0.35	10.0	96	100	99	72	0.35	10.0	96	100	99	72
0.40	10.0	95	100	99	73	0.40	10.0	95	100	99	73
0.45	10.0	96	99	100	69	0.45	10.0	96	99	100	69
0.50	10.0	99	97	99	72	0.50	10.0	99	97	99	72
0.55	10.0	97	100	99	78	0.55	10.0	97	100	99	78
0.60	10.0	89	100	100	73	0.60	10.0	89	100	100	73
0.65	10.0	90	98	93	67	0.65	10.0	90	98	93	67
0.70	10.0	92	95	90	66	0.70	10.0	92	95	90	66
0.50	7.5	95	98	97	65	0.50	7.5	95	98	97	65
0.55	7.5	92	98	94	65	0.55	7.5	92	98	94	65
0.60	7.5	87	94	95	73	0.60	7.5	87	94	95	73
0.65	7.5	82	90	88	76	0.65	7.5	82	90	88	76

Table 5—Continued

total detection efficiency							Bright SHARC detection efficiency						
z	$L_{44}$	1st <sup>a</sup>	2nd <sup>a</sup>	3rd <sup>a</sup>	4th <sup>a</sup>	z	$L_{44}$	1st <sup>a</sup>	2nd <sup>a</sup>	3rd <sup>a</sup>	4th <sup>a</sup>		
0.50	5.0	90	92	91	68	0.50	5.0	90	92	91	68		
0.55	5.0	84	96	88	66	0.55	5.0	84	96	88	66		
0.60	5.0	81	90	89	66	0.60	5.0	80	90	89	66		
0.65	5.0	77	83	75	68	0.65	5.0	73	83	75	68		
0.70	5.0	81	73	73	60	0.70	5.0	65	72	72	60		
0.50	3.5	78	85	70	55	0.50	3.5	77	85	70	55		
0.55	3.5	67	74	62	59	0.55	3.5	53	73	61	59		
0.60	3.5	61	68	56	43	0.60	3.5	23	43	51	43		
0.65	3.5	47	59	42	30	0.65	3.5	8	16	17	24		
0.70	3.5	34	56	37	28	0.70	3.5	4	8	3	16		
0.50	2.0	45	55	27	35	0.50	2.0	8	17	7	28		
0.55	2.0	21	31	19	19	0.55	2.0	1	3	2	9		
0.60	2.0	11	16	10	9	0.60	2.0	0	1	0	4		
0.65	2.0	9	10	5	6	0.65	2.0	0	1	0	1		
0.70	2.0	5	5	3	1	0.70	2.0	0	0	0	0		
0.50	1.0	6	7	4	5	0.50	1.0	1	0	0	0		
0.55	1.0	3	6	1	2	0.55	1.0	0	2	0	1		
0.60	1.0	2	2	0	0	0.60	1.0	0	0	0	0		
0.65	1.0	2	2	0	1	0.65	1.0	0	0	0	1		
0.70	1.0	0	1	0	0	0.70	1.0	0	1	0	0		
0.75	1.0	4	2	1	0	0.75	1.0	1	0	0	0		
0.80	1.0	1	1	0	0	0.80	1.0	0	0	0	0		
0.85	1.0	0	1	0	0	0.85	1.0	0	0	0	0		
0.90	1.0	1	1	0	1	0.90	1.0	0	1	0	0		
0.95	1.0	0	1	1	0	0.95	1.0	0	0	0	0		
0.75	2.0	1	0	2	1	0.75	2.0	0	0	0	0		
0.80	2.0	2	1	0	0	0.80	2.0	0	0	0	0		
0.85	2.0	2	2	0	0	0.85	2.0	0	0	0	0		
0.90	2.0	1	2	0	0	0.90	2.0	0	0	0	0		
0.95	2.0	2	1	0	1	0.95	2.0	0	0	0	1		
0.75	3.5	26	40	21	14	0.75	3.5	1	1	2	4		
0.80	3.5	22	24	13	12	0.80	3.5	2	0	1	1		
0.85	3.5	7	21	7	11	0.85	3.5	0	1	0	3		
0.90	3.5	12	9	5	3	0.90	3.5	2	0	0	0		
0.95	3.5	11	10	6	2	0.95	3.5	1	0	0	0		
0.75	5.0	62	77	48	44	0.75	5.0	23	53	35	44		
0.80	5.0	60	62	50	48	0.80	5.0	13	25	23	46		
0.85	5.0	40	49	49	28	0.85	5.0	4	5	12	18		
0.90	5.0	41	43	25	28	0.90	5.0	1	12	3	18		
0.95	5.0	35	39	21	18	0.95	5.0	1	2	6	4		

Table 5—Continued

total detection efficiency						Bright SHARC detection efficiency					
z	$L_{44}$	1st <sup>a</sup>	2nd <sup>a</sup>	3rd <sup>a</sup>	4th <sup>a</sup>	z	$L_{44}$	1st <sup>a</sup>	2nd <sup>a</sup>	3rd <sup>a</sup>	4th <sup>a</sup>
0.75	7.5	77	78	78	57	0.75	7.5	70	78	78	57
0.80	7.5	71	81	66	53	0.80	7.5	64	81	65	52
0.85	7.5	66	75	67	50	0.85	7.5	38	60	56	49
0.90	7.5	65	67	59	37	0.90	7.5	24	42	37	35
0.95	7.5	50	57	50	51	0.95	7.5	7	28	16	47
0.75	10.0	91	95	92	63	0.75	10.0	90	95	92	63
0.80	10.0	89	90	83	57	0.80	10.0	89	90	83	57
0.85	10.0	84	87	83	57	0.85	10.0	83	87	83	57
0.90	10.0	88	86	74	47	0.90	10.0	84	86	74	47
0.95	10.0	80	82	73	55	0.95	10.0	69	81	73	55

Table 6. Recovered luminosity percentage for the NFW set of parameters

total sample							Bright SHARC sample						
z	$L_{44}$	1st <sup>a</sup>	2nd <sup>a</sup>	3rd <sup>a</sup>	4th <sup>a</sup>	z	$L_{44}$	1st <sup>a</sup>	2nd <sup>a</sup>	3rd <sup>a</sup>	4th <sup>a</sup>		
0.25	1.0	102	101	100	113	0.25	1.0	102	101	100	113		
0.30	1.0	95	96	98	110	0.30	1.0	95	96	98	110		
0.35	1.0	96	93	96	108	0.35	1.0	96	96	96	108		
0.40	1.0	94	99	91	109	0.40	1.0	98	130	107	113		
0.45	1.0	123	102	93	110	0.45	1.0	168	168	0	125		
0.25	2.0	99	100	100	110	0.25	2.0	99	100	100	110		
0.30	2.0	95	95	96	111	0.30	2.0	95	95	96	111		
0.35	2.0	94	92	92	114	0.35	2.0	93	92	92	114		
0.40	2.0	91	88	90	109	0.40	2.0	90	88	90	109		
0.45	2.0	88	87	86	106	0.45	2.0	93	88	87	107		
0.25	3.5	95	96	96	108	0.25	3.5	95	96	96	108		
0.30	3.5	94	94	95	111	0.30	3.5	94	94	95	111		
0.35	3.5	92	91	91	109	0.35	3.5	92	91	91	109		
0.40	3.5	89	88	88	108	0.40	3.5	89	88	88	108		
0.45	3.5	86	87	87	108	0.45	3.5	86	87	87	108		
0.25	5.0	87	90	94	109	0.25	5.0	87	90	94	109		
0.30	5.0	91	93	93	110	0.30	5.0	91	93	93	110		
0.35	5.0	90	91	91	109	0.35	5.0	90	91	91	109		
0.40	5.0	87	88	88	106	0.40	5.0	87	88	88	106		
0.45	5.0	86	87	86	107	0.45	5.0	86	87	86	107		
0.25	7.5	92	94	95	999	0.25	7.5	92	94	95	999		
0.30	7.5	84	88	90	110	0.30	7.5	84	88	90	110		
0.35	7.5	88	90	90	107	0.35	7.5	88	90	90	107		
0.40	7.5	87	88	88	108	0.40	7.5	87	88	88	108		
0.45	7.5	84	86	85	107	0.45	7.5	84	86	85	107		
0.25	10.0	999	999	999	999	0.25	10.0	999	999	999	999		
0.30	10.0	80	82	85	105	0.30	10.0	80	82	85	105		
0.35	10.0	83	85	87	107	0.35	10.0	83	85	87	107		
0.40	10.0	83	86	86	106	0.40	10.0	83	86	86	106		
0.45	10.0	84	85	85	108	0.45	10.0	84	85	85	108		
0.50	10.0	84	84	83	107	0.50	10.0	84	84	83	107		
0.55	10.0	81	83	82	108	0.55	10.0	81	83	82	108		
0.60	10.0	81	82	81	106	0.60	10.0	81	82	81	106		
0.65	10.0	79	81	80	108	0.65	10.0	79	81	80	108		
0.70	10.0	79	82	80	107	0.70	10.0	79	82	80	107		
0.50	7.5	83	85	83	108	0.50	7.5	83	85	83	108		
0.55	7.5	82	83	84	108	0.55	7.5	82	83	84	108		
0.60	7.5	82	85	83	106	0.60	7.5	82	85	83	106		
0.65	7.5	80	82	83	107	0.65	7.5	80	82	83	107		

Table 6—Continued

total sample							Bright SHARC sample						
z	$L_{44}$	1st <sup>a</sup>	2nd <sup>a</sup>	3rd <sup>a</sup>	4th <sup>a</sup>	z	$L_{44}$	1st <sup>a</sup>	2nd <sup>a</sup>	3rd <sup>a</sup>	4th <sup>a</sup>		
0.50	5.0	84	84	84	108	0.50	5.0	84	84	84	108		
0.55	5.0	81	85	83	109	0.55	5.0	81	85	83	109		
0.60	5.0	84	83	82	108	0.60	5.0	83	83	82	108		
0.65	5.0	81	83	85	108	0.65	5.0	81	83	85	108		
0.70	5.0	80	82	82	104	0.70	5.0	81	82	82	104		
0.50	3.5	85	86	84	106	0.50	3.5	85	86	84	106		
0.55	3.5	85	86	83	110	0.55	3.5	85	87	83	110		
0.60	3.5	83	82	83	111	0.60	3.5	89	87	83	111		
0.65	3.5	84	85	86	112	0.65	3.5	100	103	95	117		
0.70	3.5	90	89	84	111	0.70	3.5	160	112	86	120		
0.50	2.0	91	87	85	110	0.50	2.0	118	98	96	115		
0.55	2.0	91	87	96	118	0.55	2.0	137	105	123	132		
0.60	2.0	92	88	95	146	0.60	2.0	0	111	0	193		
0.65	2.0	111	121	89	137	0.65	2.0	0	999	0	189		
0.70	2.0	100	124	102	118	0.70	2.0	0	0	0	0		
0.50	1.0	999	106	126	133	0.50	1.0	999	0	0	0		
0.55	1.0	114	999	999	176	0.55	1.0	0	999	0	999		
0.60	1.0	999	178	0	0	0.60	1.0	0	0	0	0		
0.65	1.0	174	99	0	999	0.65	1.0	0	0	0	999		
0.70	1.0	0	999	0	0	0.70	1.0	0	999	0	0		
0.75	1.0	999	999	90	0	0.75	1.0	999	0	0	0		
0.80	1.0	120	999	0	0	0.80	1.0	0	0	0	0		
0.85	1.0	0	999	0	0	0.85	1.0	0	0	0	0		
0.90	1.0	999	999	0	999	0.90	1.0	0	999	0	0		
0.95	1.0	0	999	999	0	0.95	1.0	0	0	0	0		
0.75	2.0	147	0	153	145	0.75	2.0	0	0	0	0		
0.80	2.0	999	142	0	0	0.80	2.0	0	0	0	0		
0.85	2.0	171	146	0	0	0.85	2.0	0	0	0	0		
0.90	2.0	999	999	0	0	0.90	2.0	0	0	0	0		
0.95	2.0	999	999	0	999	0.95	2.0	0	0	0	0	999	
0.75	3.5	98	89	91	111	0.75	3.5	999	999	117	133		
0.80	3.5	110	83	97	116	0.80	3.5	999	0	185	100		
0.85	3.5	86	92	95	143	0.85	3.5	0	100	0	179		
0.90	3.5	166	101	102	146	0.90	3.5	999	0	0	0		
0.95	3.5	166	113	106	123	0.95	3.5	999	0	0	0		
0.75	5.0	80	84	82	107	0.75	5.0	89	88	85	107		
0.80	5.0	82	83	83	108	0.80	5.0	94	93	94	108		
0.85	5.0	87	82	84	116	0.85	5.0	156	102	99	125		
0.90	5.0	82	91	81	115	0.90	5.0	103	114	102	123		
0.95	5.0	91	84	100	113	0.95	5.0	999	160	142	183		

Table 6—Continued

total sample						Bright SHARC sample					
z	$L_{44}$	1st <sup>a</sup>	2nd <sup>a</sup>	3rd <sup>a</sup>	4th <sup>a</sup>	z	$L_{44}$	1st <sup>a</sup>	2nd <sup>a</sup>	3rd <sup>a</sup>	4th <sup>a</sup>
0.75	7.5	80	82	79	107	0.75	7.5	80	82	79	107
0.80	7.5	77	81	83	107	0.80	7.5	78	81	83	108
0.85	7.5	77	83	79	110	0.85	7.5	82	85	80	110
0.90	7.5	78	83	79	111	0.90	7.5	87	88	83	112
0.95	7.5	80	84	83	109	0.95	7.5	103	94	97	110
0.75	10.0	78	81	80	105	0.75	10.0	78	81	80	105
0.80	10.0	78	83	80	106	0.80	10.0	78	83	80	106
0.85	10.0	78	83	79	109	0.85	10.0	78	83	79	109
0.90	10.0	78	81	79	104	0.90	10.0	78	81	79	104
0.95	10.0	78	81	81	108	0.95	10.0	79	81	81	108

Table 7. Detection efficiency percentage for the  $\Omega_0=0.1$  set of parameters

total detection efficiency						Bright SHARC detection efficiency					
z	$L_{44}$	1st <sup>a</sup>	2nd <sup>a</sup>	3rd <sup>a</sup>	4th <sup>a</sup>	z	$L_{44}$	1st <sup>a</sup>	2nd <sup>a</sup>	3rd <sup>a</sup>	4th <sup>a</sup>
0.25	1.0	29	39	32	14	0.25	1.0	4	6	9	10
0.30	1.0	19	20	14	8	0.30	1.0	0	1	1	1
0.35	1.0	9	13	5	6	0.35	1.0	1	1	0	0
0.40	1.0	7	4	1	2	0.40	1.0	0	0	0	0
0.45	1.0	2	1	1	0.45	1.0	0	0	0	0	0
0.25	2.0	72	76	56	59	0.25	2.0	67	75	56	58
0.30	2.0	64	72	55	54	0.30	2.0	17	53	41	51
0.35	2.0	44	53	43	30	0.35	2.0	3	4	5	18
0.40	2.0	36	40	26	19	0.40	2.0	0	4	2	8
0.45	2.0	10	24	12	7	0.45	2.0	0	1	1	0
0.25	3.5	82	94	77	60	0.25	3.5	82	94	77	60
0.30	3.5	83	87	83	65	0.30	3.5	83	87	83	65
0.35	3.5	81	89	75	54	0.35	3.5	69	89	75	53
0.40	3.5	75	75	63	47	0.40	3.5	29	51	40	46
0.45	3.5	59	69	60	35	0.45	3.5	8	12	10	31
0.25	5.0	93	97	95	70	0.25	5.0	93	97	95	70
0.30	5.0	90	95	89	55	0.30	5.0	90	95	89	55
0.35	5.0	92	92	91	58	0.35	5.0	91	92	91	58
0.40	5.0	89	91	91	53	0.40	5.0	85	91	91	53
0.45	5.0	80	88	77	37	0.45	5.0	40	81	70	37
0.25	7.5	94	98	97	73	0.25	7.5	94	98	97	73
0.30	7.5	97	100	95	58	0.30	7.5	97	100	95	58
0.35	7.5	95	94	94	60	0.35	7.5	95	94	94	60
0.40	7.5	95	94	94	58	0.40	7.5	95	94	94	58
0.45	7.5	92	94	87	49	0.45	7.5	92	94	87	49
0.25	10.0	99	98	97	66	0.25	10.0	99	98	97	66
0.30	10.0	96	99	98	56	0.30	10.0	96	99	98	56
0.35	10.0	98	97	98	58	0.35	10.0	98	97	98	58
0.40	10.0	95	99	96	46	0.40	10.0	95	99	96	46
0.45	10.0	93	97	97	51	0.45	10.0	93	97	97	51
0.50	10.0	91	97	90	50	0.50	10.0	91	97	90	50
0.55	10.0	94	92	92	48	0.55	10.0	92	92	92	48
0.60	10.0	89	95	88	48	0.60	10.0	79	95	88	48
0.65	10.0	88	88	80	41	0.65	10.0	34	70	53	40
0.70	10.0	79	87	81	34	0.70	10.0	14	30	27	33
0.50	7.5	87	96	93	51	0.50	7.5	76	96	93	51
0.55	7.5	82	94	85	43	0.55	7.5	51	80	65	43
0.60	7.5	75	78	73	30	0.60	7.5	18	40	31	30
0.65	7.5	59	76	56	27	0.65	7.5	9	11	14	22

Table 7—Continued

total detection efficiency							Bright SHARC detection efficiency						
z	$L_{44}$	1st <sup>a</sup>	2nd <sup>a</sup>	3rd <sup>a</sup>	4th <sup>a</sup>	z	$L_{44}$	1st <sup>a</sup>	2nd <sup>a</sup>	3rd <sup>a</sup>	4th <sup>a</sup>		
0.50	5.0	70	80	70	34	0.50	5.0	16	36	29	32		
0.55	5.0	58	60	45	30	0.55	5.0	8	6	7	20		
0.60	5.0	39	52	39	24	0.60	5.0	6	2	6	11		
0.65	5.0	31	37	26	15	0.65	5.0	0	0	1	4		
0.70	5.0	22	29	12	6	0.70	5.0	0	0	0	0		
0.50	3.5	45	55	39	24	0.50	3.5	4	4	4	10		
0.55	3.5	30	35	19	24	0.55	3.5	2	0	0	11		
0.60	3.5	17	22	14	10	0.60	3.5	1	0	0	2		
0.65	3.5	7	16	8	10	0.65	3.5	1	2	0	2		
0.70	3.5	10	9	4	5	0.70	3.5	0	0	0	1		
0.50	2.0	15	14	9	9	0.50	2.0	0	0	1	3		
0.55	2.0	8	8	6	2	0.55	2.0	0	1	1	0		
0.60	2.0	6	8	3	3	0.60	2.0	1	0	1	0		
0.65	2.0	4	4	0	0	0.65	2.0	0	0	0	0		
0.70	2.0	2	4	2	1	0.70	2.0	0	0	0	0		
0.50	1.0	0	0	1	0	0.50	1.0	0	0	0	0		
0.55	1.0	4	0	0	0	0.55	1.0	0	0	0	0		
0.60	1.0	1	2	0	0	0.60	1.0	0	0	0	0		
0.65	1.0	0	1	0	0	0.65	1.0	0	0	0	0		
0.70	1.0	0	1	1	0	0.70	1.0	0	0	0	0		
0.75	1.0	1	1	0	0	0.75	1.0	0	0	0	0		
0.80	1.0	2	1	0	0	0.80	1.0	0	0	0	0		
0.85	1.0	2	2	0	1	0.85	1.0	0	0	0	0		
0.90	1.0	0	0	0	0	0.90	1.0	0	0	0	0		
0.95	1.0	1	1	1	1	0.95	1.0	0	0	0	0		
0.75	2.0	2	1	1	1	0.75	2.0	0	0	0	0		
0.80	2.0	2	1	0	0	0.80	2.0	0	0	0	0		
0.85	2.0	2	1	0	0	0.85	2.0	0	0	0	0		
0.90	2.0	2	1	1	0	0.90	2.0	0	0	1	0		
0.95	2.0	1	2	0	0	0.95	2.0	0	0	0	0		
0.75	3.5	8	7	3	4	0.75	3.5	0	3	0	0		
0.80	3.5	6	1	3	0	0.80	3.5	0	0	0	0		
0.85	3.5	5	5	1	0	0.85	3.5	0	0	0	0		
0.90	3.5	5	4	5	0	0.90	3.5	0	0	1	0		
0.95	3.5	2	3	2	0	0.95	3.5	0	0	1	0		
0.75	5.0	13	16	10	8	0.75	5.0	0	0	1	1		
0.80	5.0	14	18	9	6	0.80	5.0	1	1	1	0		
0.85	5.0	7	12	4	1	0.85	5.0	0	1	0	0		
0.90	5.0	7	6	3	0	0.90	5.0	0	0	0	0		
0.95	5.0	4	4	3	3	0.95	5.0	1	0	0	1		

Table 7—Continued

total detection efficiency						Bright SHARC detection efficiency					
z	$L_{44}$	1st <sup>a</sup>	2nd <sup>a</sup>	3rd <sup>a</sup>	4th <sup>a</sup>	z	$L_{44}$	1st <sup>a</sup>	2nd <sup>a</sup>	3rd <sup>a</sup>	4th <sup>a</sup>
0.75	7.5	41	54	38	30	0.75	7.5	1	2	1	10
0.80	7.5	35	42	23	21	0.80	7.5	1	0	3	1
0.85	7.5	22	32	20	15	0.85	7.5	0	1	1	2
0.90	7.5	17	27	10	8	0.90	7.5	2	1	0	2
0.95	7.5	11	20	8	7	0.95	7.5	0	1	1	0
0.75	10.0	82	77	64	37	0.75	10.0	8	10	8	28
0.80	10.0	56	74	48	23	0.80	10.0	9	6	2	11
0.85	10.0	54	52	40	25	0.85	10.0	2	3	1	12
0.90	10.0	40	47	35	24	0.90	10.0	1	2	2	5
0.95	10.0	28	41	18	11	0.95	10.0	2	3	1	0

Table 8. Recovered luminosity percentage for the  $\Omega_0=0.1$  set of parameters

total sample						Bright SHARC sample					
z	$L_{44}$	1st <sup>a</sup>	2nd <sup>a</sup>	3rd <sup>a</sup>	4th <sup>a</sup>	z	$L_{44}$	1st <sup>a</sup>	2nd <sup>a</sup>	3rd <sup>a</sup>	4th <sup>a</sup>
0.25	1.0	109	105	108	118	0.25	1.0	147	141	125	119
0.30	1.0	111	95	105	105	0.30	1.0	0	140	127	139
0.35	1.0	133	111	107	124	0.35	1.0	141	999	0	0
0.40	1.0	138	119	64	99	0.40	1.0	0	0	0	0
0.45	1.0	75	81	192	99	0.45	1.0	0	0	0	0
0.25	2.0	103	99	100	113	0.25	2.0	103	99	100	113
0.30	2.0	95	94	93	114	0.30	2.0	98	98	96	116
0.35	2.0	90	90	88	116	0.35	2.0	107	146	106	121
0.40	2.0	94	96	90	122	0.40	2.0	0	171	159	151
0.45	2.0	101	108	108	115	0.45	2.0	0	175	118	0
0.25	3.5	102	98	98	114	0.25	3.5	102	98	98	114
0.30	3.5	95	93	92	111	0.30	3.5	95	93	92	111
0.35	3.5	91	89	89	112	0.35	3.5	90	89	89	113
0.40	3.5	87	88	86	109	0.40	3.5	92	91	92	110
0.45	3.5	86	88	85	116	0.45	3.5	116	114	106	118
0.25	5.0	100	98	98	115	0.25	5.0	100	98	98	115
0.30	5.0	93	93	93	112	0.30	5.0	93	93	93	112
0.35	5.0	90	88	88	111	0.35	5.0	90	88	88	111
0.40	5.0	85	86	85	110	0.40	5.0	85	86	85	110
0.45	5.0	85	88	85	112	0.45	5.0	89	89	86	112
0.25	7.5	99	98	99	113	0.25	7.5	99	98	99	113
0.30	7.5	95	93	92	113	0.30	7.5	95	93	92	113
0.35	7.5	90	87	89	112	0.35	7.5	90	87	89	112
0.40	7.5	87	86	86	110	0.40	7.5	87	86	86	110
0.45	7.5	84	83	82	110	0.45	7.5	84	83	82	110
0.25	10.0	98	98	99	113	0.25	10.0	98	98	99	113
0.30	10.0	92	92	92	113	0.30	10.0	92	92	92	113
0.35	10.0	87	89	90	113	0.35	10.0	87	89	90	113
0.40	10.0	86	86	85	111	0.40	10.0	86	86	85	111
0.45	10.0	82	85	83	114	0.45	10.0	82	85	83	114
0.50	10.0	80	82	81	110	0.50	10.0	80	82	81	110
0.55	10.0	77	80	80	112	0.55	10.0	77	80	80	112
0.60	10.0	78	79	80	115	0.60	10.0	79	79	80	115
0.65	10.0	77	78	77	112	0.65	10.0	86	80	80	113
0.70	10.0	79	80	79	109	0.70	10.0	112	93	91	109
0.50	7.5	80	81	81	108	0.50	7.5	80	81	81	108
0.55	7.5	80	79	78	112	0.55	7.5	85	81	80	112
0.60	7.5	77	83	82	114	0.60	7.5	89	90	93	114
0.65	7.5	79	80	80	109	0.65	7.5	113	105	94	112

Table 8—Continued

total sample							Bright SHARC sample						
z	$L_{44}$	1st <sup>a</sup>	2nd <sup>a</sup>	3rd <sup>a</sup>	4th <sup>a</sup>	z	$L_{44}$	1st <sup>a</sup>	2nd <sup>a</sup>	3rd <sup>a</sup>	4th <sup>a</sup>		
0.50	5.0	85	85	83	114	0.50	5.0	107	95	95	115		
0.55	5.0	84	84	80	106	0.55	5.0	124	109	100	112		
0.60	5.0	90	83	89	117	0.60	5.0	152	123	135	140		
0.65	5.0	91	84	92	125	0.65	5.0	0	0	149	162		
0.70	5.0	83	86	85	127	0.70	5.0	0	0	0	0		
0.50	3.5	88	86	92	122	0.50	3.5	120	114	131	139		
0.55	3.5	87	88	92	133	0.55	3.5	170	0	0	154		
0.60	3.5	113	89	88	151	0.60	3.5	999	0	0	999		
0.65	3.5	161	119	110	146	0.65	3.5	999	999	0	999		
0.70	3.5	113	126	116	143	0.70	3.5	0	0	0	999		
0.50	2.0	112	108	116	146	0.50	2.0	0	0	999	999		
0.55	2.0	116	142	174	189	0.55	2.0	0	999	999	0		
0.60	2.0	999	160	999	148	0.60	2.0	999	0	999	0		
0.65	2.0	161	176	0	0	0.65	2.0	0	0	0	0		
0.70	2.0	999	999	133	87	0.70	2.0	0	0	0	0		
0.50	1.0	0	0	999	0	0.50	1.0	0	0	0	0		
0.55	1.0	999	0	0	0	0.55	1.0	0	0	0	0		
0.60	1.0	999	999	0	0	0.60	1.0	0	0	0	0		
0.65	1.0	0	999	0	0	0.65	1.0	0	0	0	0		
0.70	1.0	0	999	999	0	0.70	1.0	0	0	0	0		
0.75	1.0	999	999	0	0	0.75	1.0	0	0	0	0		
0.80	1.0	999	999	0	0	0.80	1.0	0	0	0	0		
0.85	1.0	999	999	0	999	0.85	1.0	0	0	0	0		
0.90	1.0	0	0	0	0	0.90	1.0	0	0	0	0		
0.95	1.0	999	999	999	999	0.95	1.0	0	0	0	0		
0.75	2.0	166	108	999	999	0.75	2.0	0	0	0	0		
0.80	2.0	123	161	0	0	0.80	2.0	0	0	0	0		
0.85	2.0	999	999	0	0	0.85	2.0	0	0	0	0		
0.90	2.0	999	999	999	0	0.90	2.0	0	0	999	0		
0.95	2.0	999	999	0	0	0.95	2.0	0	0	0	0		
0.75	3.5	121	999	172	157	0.75	3.5	0	999	0	0		
0.80	3.5	124	146	183	0	0.80	3.5	0	0	0	0		
0.85	3.5	164	152	104	0	0.85	3.5	0	0	0	0		
0.90	3.5	161	173	999	0	0.90	3.5	0	0	999	0		
0.95	3.5	999	152	999	0	0.95	3.5	0	0	999	0		
0.75	5.0	97	92	107	130	0.75	5.0	0	0	999	999		
0.80	5.0	116	136	153	178	0.80	5.0	999	999	999	0		
0.85	5.0	121	144	118	101	0.85	5.0	0	999	0	0		
0.90	5.0	160	149	126	0	0.90	5.0	0	0	0	0		
0.95	5.0	174	186	999	174	0.95	5.0	999	0	0	999		

Table 8—Continued

total sample							Bright SHARC sample						
z	$L_{44}$	1st <sup>a</sup>	2nd <sup>a</sup>	3rd <sup>a</sup>	4th <sup>a</sup>	z	$L_{44}$	1st <sup>a</sup>	2nd <sup>a</sup>	3rd <sup>a</sup>	4th <sup>a</sup>		
0.75	7.5	78	84	79	122	0.75	7.5	106	144	108	142		
0.80	7.5	88	85	104	119	0.80	7.5	195	0	999	163		
0.85	7.5	86	91	96	135	0.85	7.5	0	191	150	174		
0.90	7.5	110	101	93	124	0.90	7.5	999	190	0	183		
0.95	7.5	109	99	133	141	0.95	7.5	0	999	999	0		
0.75	10.0	78	79	78	114	0.75	10.0	130	101	101	118		
0.80	10.0	80	81	77	111	0.80	10.0	110	134	99	118		
0.85	10.0	79	85	85	125	0.85	10.0	116	157	141	145		
0.90	10.0	79	85	88	114	0.90	10.0	196	194	144	145		
0.95	10.0	91	97	78	114	0.95	10.0	192	999	150	0		

Table 9. Detection efficiency percentage for the  $\Omega_0=0.4 + \Lambda=0.6$  set of parameters

total detection efficiency						Bright SHARC detection efficiency					
z	$L_{44}$	1st <sup>a</sup>	2nd <sup>a</sup>	3rd <sup>a</sup>	4th <sup>a</sup>	z	$L_{44}$	1st <sup>a</sup>	2nd <sup>a</sup>	3rd <sup>a</sup>	4th <sup>a</sup>
0.25	1.0	39	41	38	30	0.25	1.0	4	4	7	17
0.30	1.0	21	26	13	9	0.30	1.0	0	2	0	0
0.35	1.0	10	10	9	9	0.35	1.0	0	0	0	1
0.40	1.0	7	7	1	2	0.40	1.0	0	2	0	1
0.45	1.0	3	2	2	1	0.45	1.0	0	0	0	0
0.25	2.0	75	78	60	53	0.25	2.0	67	78	57	53
0.30	2.0	63	73	54	40	0.30	2.0	23	40	30	39
0.35	2.0	49	51	46	37	0.35	2.0	2	4	6	23
0.40	2.0	29	37	13	14	0.40	2.0	1	2	0	6
0.45	2.0	15	20	12	5	0.45	2.0	0	1	0	1
0.25	3.5	81	93	76	61	0.25	3.5	81	93	76	61
0.30	3.5	74	85	82	57	0.30	3.5	70	85	82	57
0.35	3.5	71	88	70	56	0.35	3.5	55	86	67	56
0.40	3.5	74	80	75	43	0.40	3.5	27	36	40	43
0.45	3.5	53	65	45	25	0.45	3.5	1	6	11	22
0.25	5.0	85	94	90	64	0.25	5.0	85	94	90	64
0.30	5.0	91	96	90	55	0.30	5.0	91	96	90	55
0.35	5.0	88	89	87	59	0.35	5.0	88	89	87	59
0.40	5.0	90	90	87	45	0.40	5.0	86	89	87	45
0.45	5.0	80	85	69	47	0.45	5.0	33	61	50	47
0.25	7.5	97	98	95	62	0.25	7.5	97	98	95	62
0.30	7.5	98	96	94	59	0.30	7.5	98	96	94	59
0.35	7.5	94	93	94	52	0.35	7.5	94	93	94	52
0.40	7.5	87	93	94	55	0.40	7.5	87	93	94	55
0.45	7.5	89	95	89	37	0.45	7.5	89	95	89	37
0.25	10.0	97	98	100	65	0.25	10.0	97	98	100	65
0.30	10.0	98	100	99	49	0.30	10.0	98	100	99	49
0.35	10.0	97	100	98	58	0.35	10.0	97	100	98	58
0.40	10.0	91	98	97	55	0.40	10.0	91	98	97	55
0.45	10.0	90	97	99	57	0.45	10.0	90	97	99	57
0.50	10.0	93	95	96	45	0.50	10.0	93	95	96	45
0.55	10.0	91	93	86	47	0.55	10.0	88	93	86	47
0.60	10.0	89	87	88	42	0.60	10.0	69	85	82	41
0.65	10.0	82	91	73	41	0.65	10.0	24	52	47	38
0.70	10.0	68	82	75	41	0.70	10.0	14	25	32	39
0.50	7.5	86	87	85	44	0.50	7.5	80	87	85	44
0.55	7.5	84	82	67	38	0.55	7.5	44	64	53	38
0.60	7.5	69	88	69	44	0.60	7.5	11	37	31	41
0.65	7.5	66	67	57	27	0.65	7.5	9	8	12	25

Table 9—Continued

total detection efficiency							Bright SHARC detection efficiency						
z	$L_{44}$	1st <sup>a</sup>	2nd <sup>a</sup>	3rd <sup>a</sup>	4th <sup>a</sup>	z	$L_{44}$	1st <sup>a</sup>	2nd <sup>a</sup>	3rd <sup>a</sup>	4th <sup>a</sup>		
0.50	5.0	72	78	67	43	0.50	5.0	15	19	26	39		
0.55	5.0	60	70	49	24	0.55	5.0	5	8	9	15		
0.60	5.0	47	54	38	22	0.60	5.0	3	2	5	9		
0.65	5.0	24	33	19	11	0.65	5.0	1	0	0	5		
0.70	5.0	21	24	19	11	0.70	5.0	1	0	2	1		
0.50	3.5	34	44	30	23	0.50	3.5	2	4	2	5		
0.55	3.5	31	30	23	12	0.55	3.5	1	0	3	2		
0.60	3.5	28	23	12	3	0.60	3.5	2	2	0	1		
0.65	3.5	13	16	6	1	0.65	3.5	0	1	0	1		
0.70	3.5	11	6	7	1	0.70	3.5	1	0	1	0		
0.50	2.0	7	11	4	3	0.50	2.0	0	1	0	0		
0.55	2.0	6	10	4	0	0.55	2.0	0	0	0	0		
0.60	2.0	3	0	4	2	0.60	2.0	0	0	0	0		
0.65	2.0	2	2	4	1	0.65	2.0	0	0	0	0		
0.70	2.0	2	3	2	1	0.70	2.0	1	0	0	1		
0.50	1.0	0	4	0	1	0.50	1.0	0	0	0	1		
0.55	1.0	1	0	0	2	0.55	1.0	0	0	0	0		
0.60	1.0	1	0	0	1	0.60	1.0	0	0	0	0		
0.65	1.0	2	1	0	1	0.65	1.0	0	1	0	1		
0.70	1.0	1	1	2	0	0.70	1.0	0	0	1	0		
0.75	1.0	1	1	0	0	0.75	1.0	1	0	0	0		
0.80	1.0	1	0	0	0	0.80	1.0	0	0	0	0		
0.85	1.0	0	1	0	0	0.85	1.0	0	0	0	0		
0.90	1.0	0	1	1	0	0.90	1.0	0	0	0	0		
0.95	1.0	0	1	1	0	0.95	1.0	0	0	0	0		
0.75	2.0	2	1	0	1	0.75	2.0	0	0	0	0		
0.80	2.0	1	1	1	0	0.80	2.0	0	0	0	0		
0.85	2.0	2	2	1	0	0.85	2.0	0	1	0	0		
0.90	2.0	1	1	0	1	0.90	2.0	0	0	0	1		
0.95	2.0	2	0	1	0	0.95	2.0	0	0	0	0		
0.75	3.5	12	5	6	0	0.75	3.5	1	0	1	0		
0.80	3.5	4	4	2	0	0.80	3.5	1	0	0	0		
0.85	3.5	6	5	0	1	0.85	3.5	1	0	0	0		
0.90	3.5	1	3	1	0	0.90	3.5	1	0	0	0		
0.95	3.5	1	4	2	0	0.95	3.5	0	0	0	0		
0.75	5.0	16	14	12	6	0.75	5.0	0	0	0	1		
0.80	5.0	10	13	6	7	0.80	5.0	0	1	2	2		
0.85	5.0	11	6	6	6	0.85	5.0	1	0	0	0		
0.90	5.0	6	10	3	2	0.90	5.0	0	1	0	0		
0.95	5.0	4	8	0	0	0.95	5.0	1	0	0	0		

Table 9—Continued

total detection efficiency						Bright SHARC detection efficiency					
z	$L_{44}$	1st <sup>a</sup>	2nd <sup>a</sup>	3rd <sup>a</sup>	4th <sup>a</sup>	z	$L_{44}$	1st <sup>a</sup>	2nd <sup>a</sup>	3rd <sup>a</sup>	4th <sup>a</sup>
0.75	7.5	25	42	29	13	0.75	7.5	1	1	4	5
0.80	7.5	21	29	16	10	0.80	7.5	1	3	2	1
0.85	7.5	13	17	4	5	0.85	7.5	0	0	0	0
0.90	7.5	13	15	6	6	0.90	7.5	1	1	1	1
0.95	7.5	10	6	4	1	0.95	7.5	0	0	1	0
0.75	10.0	68	75	51	23	0.75	10.0	7	10	9	19
0.80	10.0	55	54	36	24	0.80	10.0	3	8	4	13
0.85	10.0	39	51	33	17	0.85	10.0	5	5	3	4
0.90	10.0	28	44	32	13	0.90	10.0	2	4	5	4
0.95	10.0	22	29	20	8	0.95	10.0	0	3	1	1

Table 10. Recovered luminosity percentage for the  $\Omega_0=0.4 + \Lambda=0.6$  set of parameters

total sample							Bright SHARC sample						
z	$L_{44}$	1st <sup>a</sup>	2nd <sup>a</sup>	3rd <sup>a</sup>	4th <sup>a</sup>	z	$L_{44}$	1st <sup>a</sup>	2nd <sup>a</sup>	3rd <sup>a</sup>	4th <sup>a</sup>		
0.25	1.0	120	106	106	117	0.25	1.0	166	145	132	126		
0.30	1.0	110	111	101	123	0.30	1.0	0	167	0	0		
0.35	1.0	126	133	139	137	0.35	1.0	0	0	0	999		
0.40	1.0	163	999	121	999	0.40	1.0	0	999	0	999		
0.45	1.0	999	156	999	999	0.45	1.0	0	0	0	0		
0.25	2.0	109	104	102	118	0.25	2.0	107	104	102	118		
0.30	2.0	106	96	97	114	0.30	2.0	118	101	103	114		
0.35	2.0	98	95	99	117	0.35	2.0	143	146	142	118		
0.40	2.0	96	96	96	135	0.40	2.0	149	145	0	156		
0.45	2.0	106	103	95	127	0.45	2.0	0	171	0	116		
0.25	3.5	107	101	103	118	0.25	3.5	107	101	103	118		
0.30	3.5	103	95	96	116	0.30	3.5	102	95	96	116		
0.35	3.5	99	91	93	114	0.35	3.5	100	91	94	114		
0.40	3.5	108	91	93	119	0.40	3.5	139	98	99	119		
0.45	3.5	96	90	93	121	0.45	3.5	134	118	104	123		
0.25	5.0	104	101	102	117	0.25	5.0	104	101	102	117		
0.30	5.0	100	96	96	115	0.30	5.0	100	96	96	115		
0.35	5.0	94	92	92	113	0.35	5.0	94	92	92	113		
0.40	5.0	93	88	93	112	0.40	5.0	92	88	93	112		
0.45	5.0	91	88	91	116	0.45	5.0	103	90	95	116		
0.25	7.5	102	102	101	117	0.25	7.5	102	102	101	117		
0.30	7.5	98	96	97	117	0.30	7.5	98	96	97	117		
0.35	7.5	93	93	93	114	0.35	7.5	93	93	93	114		
0.40	7.5	90	91	90	115	0.40	7.5	90	91	90	115		
0.45	7.5	88	88	87	115	0.45	7.5	88	88	87	115		
0.25	10.0	103	102	102	116	0.25	10.0	103	102	102	116		
0.30	10.0	96	96	97	116	0.30	10.0	96	96	97	116		
0.35	10.0	95	92	92	115	0.35	10.0	95	92	92	115		
0.40	10.0	91	90	90	116	0.40	10.0	91	90	90	116		
0.45	10.0	93	88	88	116	0.45	10.0	93	88	88	116		
0.50	10.0	86	86	87	113	0.50	10.0	86	86	87	113		
0.55	10.0	85	90	84	112	0.55	10.0	85	90	84	112		
0.60	10.0	88	85	87	119	0.60	10.0	90	85	88	120		
0.65	10.0	81	86	84	112	0.65	10.0	91	92	89	113		
0.70	10.0	88	85	86	113	0.70	10.0	115	96	95	114		
0.50	7.5	86	86	86	112	0.50	7.5	86	86	86	112		
0.55	7.5	87	85	88	116	0.55	7.5	89	88	91	116		
0.60	7.5	86	87	89	119	0.60	7.5	111	98	96	121		
0.65	7.5	91	85	88	117	0.65	7.5	132	107	112	119		

Table 10—Continued

total sample							Bright SHARC sample						
z	$L_{44}$	1st <sup>a</sup>	2nd <sup>a</sup>	3rd <sup>a</sup>	4th <sup>a</sup>	z	$L_{44}$	1st <sup>a</sup>	2nd <sup>a</sup>	3rd <sup>a</sup>	4th <sup>a</sup>		
0.50	5.0	88	89	90	114	0.50	5.0	110	104	104	115		
0.55	5.0	91	89	91	115	0.55	5.0	151	120	122	123		
0.60	5.0	91	87	96	119	0.60	5.0	168	134	156	129		
0.65	5.0	90	89	93	150	0.65	5.0	139	0	0	183		
0.70	5.0	103	93	116	138	0.70	5.0	999	0	193	999		
0.50	3.5	100	92	93	112	0.50	3.5	143	139	147	126		
0.55	3.5	101	86	114	123	0.55	3.5	107	0	999	197		
0.60	3.5	98	94	102	134	0.60	3.5	171	151	0	185		
0.65	3.5	100	117	113	999	0.65	3.5	0	999	0	999		
0.70	3.5	145	105	159	999	0.70	3.5	999	0	999	0		
0.50	2.0	120	124	117	123	0.50	2.0	0	999	0	0		
0.55	2.0	147	143	131	0	0.55	2.0	0	0	0	0		
0.60	2.0	145	0	200	999	0.60	2.0	0	0	0	0		
0.65	2.0	999	176	999	999	0.65	2.0	0	0	0	0		
0.70	2.0	999	999	999	999	0.70	2.0	999	0	0	999		
0.50	1.0	0	145	0	999	0.50	1.0	0	0	0	0	999	
0.55	1.0	999	0	0	999	0.55	1.0	0	0	0	0	0	
0.60	1.0	999	0	0	999	0.60	1.0	0	0	0	0	0	
0.65	1.0	999	999	0	999	0.65	1.0	0	999	0	0	999	
0.70	1.0	999	999	999	0	0.70	1.0	0	0	0	999	0	
0.75	1.0	999	999	0	0	0.75	1.0	999	0	0	0	0	
0.80	1.0	999	0	0	0	0.80	1.0	0	0	0	0	0	
0.85	1.0	0	999	0	0	0.85	1.0	0	0	0	0	0	
0.90	1.0	0	999	999	0	0.90	1.0	0	0	0	0	0	
0.95	1.0	0	999	999	0	0.95	1.0	0	0	0	0	0	
0.75	2.0	999	140	0	999	0.75	2.0	0	0	0	0	0	
0.80	2.0	999	999	145	0	0.80	2.0	0	0	0	0	0	
0.85	2.0	999	999	999	0	0.85	2.0	0	999	0	0	0	
0.90	2.0	999	172	0	999	0.90	2.0	0	0	0	0	999	
0.95	2.0	999	0	999	0	0.95	2.0	0	0	0	0	0	
0.75	3.5	999	111	999	0	0.75	3.5	999	0	0	999	0	
0.80	3.5	999	136	161	0	0.80	3.5	999	0	0	0	0	
0.85	3.5	999	188	0	999	0.85	3.5	999	0	0	0	0	
0.90	3.5	999	155	999	0	0.90	3.5	999	0	0	0	0	
0.95	3.5	999	999	999	0	0.95	3.5	0	0	0	0	0	
0.75	5.0	110	95	109	175	0.75	5.0	0	0	0	0	999	
0.80	5.0	116	116	160	999	0.80	5.0	0	999	999	999	999	
0.85	5.0	999	100	154	159	0.85	5.0	999	0	0	0	0	
0.90	5.0	999	128	132	999	0.90	5.0	0	166	0	0	0	
0.95	5.0	178	150	0	0	0.95	5.0	999	0	0	0	0	

Table 10—Continued

total sample						Bright SHARC sample					
z	$L_{44}$	1st <sup>a</sup>	2nd <sup>a</sup>	3rd <sup>a</sup>	4th <sup>a</sup>	z	$L_{44}$	1st <sup>a</sup>	2nd <sup>a</sup>	3rd <sup>a</sup>	4th <sup>a</sup>
0.75	7.5	95	89	95	126	0.75	7.5	179	152	144	142
0.80	7.5	94	110	96	116	0.80	7.5	168	999	185	184
0.85	7.5	91	98	88	115	0.85	7.5	0	0	0	0
0.90	7.5	119	106	120	150	0.90	7.5	999	163	196	999
0.95	7.5	106	95	132	113	0.95	7.5	0	0	999	0
0.75	10.0	85	89	87	119	0.75	10.0	119	127	106	122
0.80	10.0	87	88	88	122	0.80	10.0	116	122	111	128
0.85	10.0	95	89	88	105	0.85	10.0	174	131	162	110
0.90	10.0	90	93	99	129	0.90	10.0	149	154	142	153
0.95	10.0	90	116	101	127	0.95	10.0	0	999	171	187

Table 11. Detection efficiency percentage for the moderate cooling-flow-like set of parameters

total detection efficiency						Bright SHARC detection efficiency					
z	$L_{44}$	1st <sup>a</sup>	2nd <sup>a</sup>	3rd <sup>a</sup>	4th <sup>a</sup>	z	$L_{44}$	1st <sup>a</sup>	2nd <sup>a</sup>	3rd <sup>a</sup>	4th <sup>a</sup>
0.25	1.0	31	48	24	34	0.25	1.0	1	8	12	25
0.30	1.0	13	28	9	12	0.30	1.0	0	1	0	8
0.35	1.0	8	9	7	3	0.35	1.0	0	0	0	1
0.40	1.0	4	5	3	4	0.40	1.0	0	0	0	1
0.45	1.0	2	4	1	1	0.45	1.0	0	0	0	0
0.25	2.0	79	60	50	47	0.25	2.0	74	60	50	47
0.30	2.0	57	57	51	41	0.30	2.0	36	52	45	40
0.35	2.0	49	53	40	30	0.35	2.0	8	22	21	27
0.40	2.0	42	43	30	21	0.40	2.0	7	5	6	12
0.45	2.0	26	26	17	12	0.45	2.0	0	3	1	3
0.25	3.5	83	86	74	54	0.25	3.5	83	86	74	54
0.30	3.5	81	84	70	54	0.30	3.5	79	84	70	54
0.35	3.5	74	79	59	44	0.35	3.5	71	79	59	44
0.40	3.5	75	77	55	37	0.40	3.5	59	75	53	37
0.45	3.5	63	60	52	44	0.45	3.5	23	32	30	41
0.25	5.0	94	97	91	64	0.25	5.0	94	97	91	64
0.30	5.0	95	93	89	60	0.30	5.0	95	93	89	60
0.35	5.0	89	84	79	61	0.35	5.0	89	84	79	61
0.40	5.0	89	88	83	51	0.40	5.0	88	88	83	51
0.45	5.0	80	89	71	44	0.45	5.0	68	88	71	44
0.25	7.5	96	99	93	58	0.25	7.5	96	99	93	58
0.30	7.5	97	99	96	52	0.30	7.5	97	99	96	52
0.35	7.5	94	97	94	55	0.35	7.5	94	97	94	55
0.40	7.5	94	94	96	58	0.40	7.5	94	94	96	58
0.45	7.5	93	93	87	49	0.45	7.5	93	93	87	49
0.25	10.0	98	100	100	65	0.25	10.0	98	100	100	65
0.30	10.0	100	99	98	61	0.30	10.0	100	99	98	61
0.35	10.0	97	94	91	59	0.35	10.0	97	94	91	59
0.40	10.0	94	95	96	54	0.40	10.0	94	95	96	54
0.45	10.0	92	96	97	45	0.45	10.0	92	96	97	45
0.50	10.0	94	97	92	53	0.50	10.0	94	97	92	53
0.55	10.0	92	97	88	43	0.55	10.0	92	97	88	43
0.60	10.0	94	94	83	55	0.60	10.0	94	94	83	55
0.65	10.0	84	84	79	56	0.65	10.0	82	84	78	56
0.70	10.0	89	91	72	46	0.70	10.0	72	87	70	46
0.50	7.5	91	88	86	60	0.50	7.5	89	88	86	60
0.55	7.5	86	88	74	49	0.55	7.5	84	88	74	49
0.60	7.5	78	85	75	53	0.60	7.5	58	83	75	53
0.65	7.5	79	79	72	42	0.65	7.5	29	59	40	42

Table 11—Continued

total detection efficiency							Bright SHARC detection efficiency						
z	$L_{44}$	1st <sup>a</sup>	2nd <sup>a</sup>	3rd <sup>a</sup>	4th <sup>a</sup>	z	$L_{44}$	1st <sup>a</sup>	2nd <sup>a</sup>	3rd <sup>a</sup>	4th <sup>a</sup>		
0.50	5.0	72	81	67	45	0.50	5.0	41	79	62	44		
0.55	5.0	70	78	55	45	0.55	5.0	15	33	24	42		
0.60	5.0	58	64	59	24	0.60	5.0	8	17	12	20		
0.65	5.0	49	53	44	33	0.65	5.0	5	8	6	21		
0.70	5.0	38	44	32	22	0.70	5.0	1	2	3	8		
0.50	3.5	54	64	48	23	0.50	3.5	10	13	15	18		
0.55	3.5	33	49	39	23	0.55	3.5	2	4	8	15		
0.60	3.5	25	38	19	20	0.60	3.5	0	3	3	5		
0.65	3.5	21	31	11	12	0.65	3.5	1	1	0	5		
0.70	3.5	16	23	5	7	0.70	3.5	0	0	1	3		
0.50	2.0	12	18	11	5	0.50	2.0	0	1	1	0		
0.55	2.0	7	12	6	3	0.55	2.0	0	1	1	2		
0.60	2.0	4	4	2	1	0.60	2.0	1	0	1	0		
0.65	2.0	1	2	1	0	0.65	2.0	0	0	0	0		
0.70	2.0	5	2	0	1	0.70	2.0	0	0	0	1		
0.50	1.0	2	3	0	1	0.50	1.0	1	0	0	0		
0.55	1.0	3	0	0	2	0.55	1.0	1	0	0	0		
0.60	1.0	2	0	1	0	0.60	1.0	0	0	0	0		
0.65	1.0	2	0	1	2	0.65	1.0	1	0	0	0		
0.70	1.0	1	0	0	0	0.70	1.0	0	0	0	0		
0.75	1.0	3	0	1	0	0.75	1.0	0	0	1	0		
0.80	1.0	1	0	1	0	0.80	1.0	0	0	0	0		
0.85	1.0	1	2	0	0	0.85	1.0	0	0	0	0		
0.90	1.0	1	1	0	0	0.90	1.0	0	0	0	0		
0.95	1.0	2	0	0	0	0.95	1.0	0	0	0	0		
0.75	2.0	0	2	2	0	0.75	2.0	0	1	0	0		
0.80	2.0	2	2	1	0	0.80	2.0	0	0	0	0		
0.85	2.0	1	1	0	0	0.85	2.0	0	0	0	0		
0.90	2.0	1	1	1	0	0.90	2.0	0	0	0	0		
0.95	2.0	1	0	1	0	0.95	2.0	0	0	0	0		
0.75	3.5	11	8	5	3	0.75	3.5	0	1	2	1		
0.80	3.5	7	7	1	1	0.80	3.5	0	1	0	1		
0.85	3.5	4	1	3	2	0.85	3.5	1	0	0	1		
0.90	3.5	5	3	2	0	0.90	3.5	0	0	0	0		
0.95	3.5	2	2	1	0	0.95	3.5	0	1	0	0		
0.75	5.0	27	35	19	21	0.75	5.0	0	2	2	5		
0.80	5.0	26	30	8	9	0.80	5.0	0	2	0	0		
0.85	5.0	15	15	11	6	0.85	5.0	0	1	1	0		
0.90	5.0	8	8	9	4	0.90	5.0	0	1	2	0		
0.95	5.0	5	9	3	3	0.95	5.0	0	0	0	1		

Table 11—Continued

total detection efficiency						Bright SHARC detection efficiency					
z	$L_{44}$	1st <sup>a</sup>	2nd <sup>a</sup>	3rd <sup>a</sup>	4th <sup>a</sup>	z	$L_{44}$	1st <sup>a</sup>	2nd <sup>a</sup>	3rd <sup>a</sup>	4th <sup>a</sup>
0.75	7.5	70	78	52	32	0.75	7.5	8	16	12	24
0.80	7.5	56	64	38	28	0.80	7.5	8	7	9	19
0.85	7.5	49	52	41	23	0.85	7.5	5	3	3	9
0.90	7.5	35	46	28	20	0.90	7.5	2	3	4	7
0.95	7.5	28	32	24	16	0.95	7.5	3	0	2	3
0.75	10.0	73	82	64	44	0.75	10.0	34	66	55	43
0.80	10.0	68	77	59	46	0.80	10.0	18	43	29	45
0.85	10.0	58	70	59	37	0.85	10.0	9	18	24	35
0.90	10.0	59	66	45	28	0.90	10.0	6	9	7	23
0.95	10.0	49	45	40	33	0.95	10.0	3	3	5	24

Table 12. Recovered luminosity percentage for the moderate cooling-flow-like set of parameters

total sample						Bright SHARC sample					
z	$L_{44}$	1st <sup>a</sup>	2nd <sup>a</sup>	3rd <sup>a</sup>	4th <sup>a</sup>	z	$L_{44}$	1st <sup>a</sup>	2nd <sup>a</sup>	3rd <sup>a</sup>	4th <sup>a</sup>
0.25	1.0	105	99	105	111	0.25	1.0	123	119	112	117
0.30	1.0	111	95	108	146	0.30	1.0	0	116	0	161
0.35	1.0	170	119	98	145	0.35	1.0	0	0	0	186
0.40	1.0	107	124	106	153	0.40	1.0	0	0	0	999
0.45	1.0	999	159	131	124	0.45	1.0	0	0	0	0
0.25	2.0	106	103	100	113	0.25	2.0	106	103	100	113
0.30	2.0	103	97	99	112	0.30	2.0	101	98	100	112
0.35	2.0	96	92	95	116	0.35	2.0	115	100	101	117
0.40	2.0	106	91	93	115	0.40	2.0	153	130	112	119
0.45	2.0	92	96	101	118	0.45	2.0	0	150	132	166
0.25	3.5	107	100	102	113	0.25	3.5	107	100	102	113
0.30	3.5	103	95	96	111	0.30	3.5	102	95	96	111
0.35	3.5	99	92	96	114	0.35	3.5	98	92	96	114
0.40	3.5	97	88	92	112	0.40	3.5	98	88	93	112
0.45	3.5	97	88	88	110	0.45	3.5	111	94	92	112
0.25	5.0	103	101	101	113	0.25	5.0	103	101	101	113
0.30	5.0	98	96	98	110	0.30	5.0	98	96	98	110
0.35	5.0	96	92	92	113	0.35	5.0	96	92	92	113
0.40	5.0	92	90	89	112	0.40	5.0	92	90	89	112
0.45	5.0	89	87	88	110	0.45	5.0	89	87	88	110
0.25	7.5	102	101	102	114	0.25	7.5	102	101	102	114
0.30	7.5	97	95	95	114	0.30	7.5	97	95	95	114
0.35	7.5	92	92	94	112	0.35	7.5	92	92	94	112
0.40	7.5	91	89	90	113	0.40	7.5	91	89	90	113
0.45	7.5	89	88	87	109	0.45	7.5	89	88	87	109
0.25	10.0	101	101	101	115	0.25	10.0	101	101	101	115
0.30	10.0	95	95	96	113	0.30	10.0	95	95	96	113
0.35	10.0	92	91	92	109	0.35	10.0	92	91	92	109
0.40	10.0	88	89	89	111	0.40	10.0	88	89	89	111
0.45	10.0	87	87	87	111	0.45	10.0	87	87	87	111
0.50	10.0	88	86	87	109	0.50	10.0	88	86	87	109
0.55	10.0	84	84	85	109	0.55	10.0	84	84	85	109
0.60	10.0	84	83	83	114	0.60	10.0	84	83	83	114
0.65	10.0	84	84	79	111	0.65	10.0	84	84	79	111
0.70	10.0	82	83	90	109	0.70	10.0	83	83	91	109
0.50	7.5	86	85	84	111	0.50	7.5	86	85	84	111
0.55	7.5	82	88	86	112	0.55	7.5	82	88	86	112
0.60	7.5	82	84	85	114	0.60	7.5	84	84	85	114
0.65	7.5	81	82	80	113	0.65	7.5	87	84	86	113

Table 12—Continued

total sample							Bright SHARC sample						
z	$L_{44}$	1st <sup>a</sup>	2nd <sup>a</sup>	3rd <sup>a</sup>	4th <sup>a</sup>	z	$L_{44}$	1st <sup>a</sup>	2nd <sup>a</sup>	3rd <sup>a</sup>	4th <sup>a</sup>		
0.50	5.0	91	86	84	112	0.50	5.0	94	86	84	112		
0.55	5.0	87	86	85	111	0.55	5.0	102	97	92	112		
0.60	5.0	86	86	84	114	0.60	5.0	109	101	107	116		
0.65	5.0	87	91	84	113	0.65	5.0	117	115	107	117		
0.70	5.0	86	86	88	120	0.70	5.0	128	133	118	143		
0.50	3.5	88	90	90	111	0.50	3.5	108	106	104	116		
0.55	3.5	86	89	90	125	0.55	3.5	119	126	117	130		
0.60	3.5	90	92	93	122	0.60	3.5	0	140	130	158		
0.65	3.5	91	102	94	164	0.65	3.5	146	160	0	999		
0.70	3.5	95	103	117	156	0.70	3.5	0	0	999	999		
0.50	2.0	119	107	104	98	0.50	2.0	0	151	165	0		
0.55	2.0	115	131	140	999	0.55	2.0	0	999	999	999		
0.60	2.0	999	97	999	160	0.60	2.0	999	0	999	0		
0.65	2.0	999	136	143	0	0.65	2.0	0	0	0	0		
0.70	2.0	148	175	0	999	0.70	2.0	0	0	0	0	999	
0.50	1.0	999	184	0	999	0.50	1.0	999	0	0	0		
0.55	1.0	999	0	0	999	0.55	1.0	999	0	0	0		
0.60	1.0	999	0	999	0	0.60	1.0	0	0	0	0		
0.65	1.0	999	0	999	999	0.65	1.0	999	0	0	0		
0.70	1.0	999	0	0	0	0.70	1.0	0	0	0	0		
0.75	1.0	999	0	999	0	0.75	1.0	0	0	0	999		
0.80	1.0	999	0	999	0	0.80	1.0	0	0	0	0		
0.85	1.0	999	999	0	0	0.85	1.0	0	0	0	0		
0.90	1.0	999	999	0	0	0.90	1.0	0	0	0	0		
0.95	1.0	999	0	0	0	0.95	1.0	0	0	0	0		
0.75	2.0	0	999	999	0	0.75	2.0	0	999	0	0		
0.80	2.0	193	999	162	0	0.80	2.0	0	0	0	0		
0.85	2.0	999	999	0	0	0.85	2.0	0	0	0	0		
0.90	2.0	999	150	999	0	0.90	2.0	0	0	0	0		
0.95	2.0	999	0	999	0	0.95	2.0	0	0	0	0		
0.75	3.5	111	126	150	168	0.75	3.5	0	999	999	999		
0.80	3.5	128	130	149	999	0.80	3.5	0	999	0	999		
0.85	3.5	999	144	125	999	0.85	3.5	999	0	0	999		
0.90	3.5	139	152	133	0	0.90	3.5	0	0	0	0		
0.95	3.5	153	999	999	0	0.95	3.5	0	999	0	0		
0.75	5.0	104	97	99	128	0.75	5.0	0	161	160	186		
0.80	5.0	99	98	104	111	0.80	5.0	0	169	0	0		
0.85	5.0	103	102	111	128	0.85	5.0	0	150	999	0		
0.90	5.0	123	127	137	144	0.90	5.0	0	999	999	0		
0.95	5.0	135	94	149	182	0.95	5.0	0	0	0	999		

Table 12—Continued

total sample							Bright SHARC sample				
z	$L_{44}$	1st <sup>a</sup>	2nd <sup>a</sup>	3rd <sup>a</sup>	4th <sup>a</sup>	z	$L_{44}$	1st <sup>a</sup>	2nd <sup>a</sup>	3rd <sup>a</sup>	4th <sup>a</sup>
0.75	7.5	82	87	83	114	0.75	7.5	103	109	101	118
0.80	7.5	87	82	87	118	0.80	7.5	140	104	109	124
0.85	7.5	94	88	84	117	0.85	7.5	164	129	124	135
0.90	7.5	90	87	98	134	0.90	7.5	148	132	183	167
0.95	7.5	103	94	113	124	0.95	7.5	999	0	999	158
0.75	10.0	80	83	82	111	0.75	10.0	84	85	83	111
0.80	10.0	81	83	80	110	0.80	10.0	94	90	86	110
0.85	10.0	83	82	86	117	0.85	10.0	118	97	100	118
0.90	10.0	87	82	83	108	0.90	10.0	130	106	108	111
0.95	10.0	84	85	93	115	0.95	10.0	125	124	199	119

Table 13. Detection efficiency percentage for the major cooling-flow-like set of parameters

<i>total detection efficiency</i>						<i>Bright SHARC detection efficiency</i>					
<i>z</i>	<i>L</i> <sub>44</sub>	1st <sup>a</sup>	2nd <sup>a</sup>	3rd <sup>a</sup>	4th <sup>a</sup>	<i>z</i>	<i>L</i> <sub>44</sub>	1st <sup>a</sup>	2nd <sup>a</sup>	3rd <sup>a</sup>	4th <sup>a</sup>
0.25	1.0	64	63	51	52	0.25	1.0	64	63	51	52
0.30	1.0	41	38	28	45	0.30	1.0	40	38	28	45
0.35	1.0	8	15	9	14	0.35	1.0	0	5	2	14
0.40	1.0	83	57	60	52	0.40	1.0	49	33	35	43
0.45	1.0	35	33	23	23	0.45	1.0	23	13	11	12
0.25	2.0	62	80	68	63	0.25	2.0	62	80	68	63
0.30	2.0	48	63	53	50	0.30	2.0	48	63	53	50
0.35	2.0	100	100	100	97	0.35	2.0	100	100	100	97
0.40	2.0	100	93	80	90	0.40	2.0	99	93	80	90
0.45	2.0	62	75	61	56	0.45	2.0	36	68	56	54
0.25	3.5	75	89	86	70	0.25	3.5	75	89	86	70
0.30	3.5	53	72	68	55	0.30	3.5	53	72	68	55
0.35	3.5	100	100	100	100	0.35	3.5	100	100	100	100
0.40	3.5	100	100	100	89	0.40	3.5	100	100	100	89
0.45	3.5	87	94	85	71	0.45	3.5	87	94	85	71
0.25	5.0	72	83	83	63	0.25	5.0	72	83	83	63
0.30	5.0	100	100	100	100	0.30	5.0	100	100	100	100
0.35	5.0	100	100	100	100	0.35	5.0	100	100	100	100
0.40	5.0	100	100	100	89	0.40	5.0	100	100	100	89
0.45	5.0	88	91	91	69	0.45	5.0	88	91	91	69
0.25	7.5	67	77	77	60	0.25	7.5	61	77	77	56
0.30	7.5	100	100	100	100	0.30	7.5	100	100	100	100
0.35	7.5	100	100	100	95	0.35	7.5	100	100	100	95
0.40	7.5	96	98	98	86	0.40	7.5	96	98	98	82
0.45	7.5	80	85	85	62	0.45	7.5	79	85	85	62
0.25	10.0	53	71	71	45	0.25	10.0	53	71	71	45
0.30	10.0	100	100	100	100	0.30	10.0	100	100	100	100
0.35	10.0	100	100	100	88	0.35	10.0	100	100	100	88
0.40	10.0	90	93	93	72	0.40	10.0	90	93	93	72
0.45	10.0	70	79	79	52	0.45	10.0	70	79	79	52
0.50	10.0	100	100	100	100	0.50	10.0	100	100	100	100
0.55	10.0	100	100	100	100	0.55	10.0	100	100	100	100
0.60	10.0	98	99	99	82	0.60	10.0	98	99	99	82
0.65	10.0	80	87	87	59	0.65	10.0	80	87	87	59
0.70	10.0	57	73	68	41	0.70	10.0	57	73	68	41
0.50	7.5	100	100	100	99	0.50	7.5	100	100	100	99
0.55	7.5	100	100	100	82	0.55	7.5	100	100	100	82
0.60	7.5	91	95	95	75	0.60	7.5	91	95	95	75
0.65	7.5	61	77	75	62	0.65	7.5	61	77	75	62

Table 13—Continued

total detection efficiency							Bright SHARC detection efficiency						
z	$L_{44}$	1st <sup>a</sup>	2nd <sup>a</sup>	3rd <sup>a</sup>	4th <sup>a</sup>	z	$L_{44}$	1st <sup>a</sup>	2nd <sup>a</sup>	3rd <sup>a</sup>	4th <sup>a</sup>		
0.50	5.0	100	100	100	95	0.50	5.0	100	100	100	95		
0.55	5.0	100	100	100	76	0.55	5.0	100	100	100	76		
0.60	5.0	74	86	85	60	0.60	5.0	73	86	85	60		
0.65	5.0	44	62	53	46	0.65	5.0	40	62	53	46		
0.70	5.0	100	100	100	95	0.70	5.0	100	100	100	95		
0.50	3.5	100	100	90	74	0.50	3.5	100	100	90	74		
0.55	3.5	73	78	65	62	0.55	3.5	57	77	64	62		
0.60	3.5	41	55	42	28	0.60	3.5	0	28	36	28		
0.65	3.5	100	100	85	72	0.65	3.5	73	56	58	65		
0.70	3.5	76	84	63	53	0.70	3.5	43	31	26	40		
0.50	2.0	63	67	36	45	0.50	2.0	22	25	14	37		
0.55	2.0	11	24	11	11	0.55	2.0	0	0	0	0		
0.60	2.0	0	0	0	0	0.60	2.0	0	0	0	0		
0.65	2.0	63	43	37	38	0.65	2.0	53	33	32	33		
0.70	2.0	33	21	19	16	0.70	2.0	28	15	15	15		
0.50	1.0	9	7	3	4	0.50	1.0	4	0	0	0		
0.55	1.0	0	0	0	0	0.55	1.0	0	0	0	0		
0.60	1.0	0	0	0	0	0.60	1.0	0	0	0	0		
0.65	1.0	44	27	25	26	0.65	1.0	42	25	25	26		
0.70	1.0	17	9	8	8	0.70	1.0	17	9	8	8		
0.75	1.0	0	0	0	0	0.75	1.0	0	0	0	0		
0.80	1.0	0	0	0	0	0.80	1.0	0	0	0	0		
0.85	1.0	56	35	34	34	0.85	1.0	56	34	34	34		
0.90	1.0	32	19	18	19	0.90	1.0	31	19	18	18		
0.95	1.0	6	2	2	1	0.95	1.0	6	1	1	1		
0.75	2.0	0	0	0	0	0.75	2.0	0	0	0	0		
0.80	2.0	0	0	0	0	0.80	2.0	0	0	0	0		
0.85	2.0	48	29	27	27	0.85	2.0	46	27	27	27		
0.90	2.0	22	13	11	11	0.90	2.0	20	11	11	11		
0.95	2.0	0	0	0	0	0.95	2.0	0	0	0	0		
0.75	3.5	0	22	1	0	0.75	3.5	0	0	0	0		
0.80	3.5	84	63	51	50	0.80	3.5	62	36	38	38		
0.85	3.5	43	43	28	32	0.85	3.5	35	21	20	23		
0.90	3.5	23	13	9	7	0.90	3.5	12	4	4	4		
0.95	3.5	0	0	0	0	0.95	3.5	0	0	0	0		
0.75	5.0	28	55	24	19	0.75	5.0	0	29	9	19		
0.80	5.0	100	98	84	82	0.80	5.0	63	57	55	80		
0.85	5.0	68	67	67	44	0.85	5.0	28	18	26	33		
0.90	5.0	44	44	24	27	0.90	5.0	0	10	0	16		
0.95	5.0	12	23	3	0	0.95	5.0	0	0	0	0		

Table 13—Continued

total detection efficiency						Bright SHARC detection efficiency					
z	$L_{44}$	1st <sup>a</sup>	2nd <sup>a</sup>	3rd <sup>a</sup>	4th <sup>a</sup>	z	$L_{44}$	1st <sup>a</sup>	2nd <sup>a</sup>	3rd <sup>a</sup>	4th <sup>a</sup>
0.75	7.5	100	100	100	100	0.75	7.5	100	100	100	100
0.80	7.5	100	100	95	81	0.80	7.5	100	100	94	79
0.85	7.5	86	88	80	61	0.85	7.5	55	72	67	60
0.90	7.5	60	63	54	30	0.90	7.5	14	36	30	28
0.95	7.5	18	36	28	29	0.95	7.5	0	4	0	25
0.75	10.0	100	100	100	100	0.75	10.0	100	100	100	100
0.80	10.0	100	100	100	78	0.80	10.0	100	100	100	78
0.85	10.0	95	95	90	62	0.85	10.0	94	95	90	62
0.90	10.0	74	77	64	34	0.90	10.0	70	77	64	34
0.95	10.0	40	56	46	27	0.95	10.0	28	55	46	27

Table 14. Recovered luminosity percentage for the major cooling-flow-like set of parameters

total sample							Bright SHARC sample						
z	$L_{44}$	1st <sup>a</sup>	2nd <sup>a</sup>	3rd <sup>a</sup>	4th <sup>a</sup>	z	$L_{44}$	1st <sup>a</sup>	2nd <sup>a</sup>	3rd <sup>a</sup>	4th <sup>a</sup>		
0.25	1.0	78	76	76	86	0.25	1.0	78	76	76	86		
0.30	1.0	72	74	74	83	0.30	1.0	72	74	74	83		
0.35	1.0	72	71	73	81	0.35	1.0	72	73	73	81		
0.40	1.0	72	75	69	84	0.40	1.0	75	99	80	87		
0.45	1.0	94	77	72	84	0.45	1.0	128	127	1	96		
0.25	2.0	75	77	77	84	0.25	2.0	75	77	77	84		
0.30	2.0	72	73	73	84	0.30	2.0	72	73	73	84		
0.35	2.0	72	70	69	86	0.35	2.0	72	70	69	86		
0.40	2.0	69	67	67	84	0.40	2.0	69	67	67	84		
0.45	2.0	67	66	66	81	0.45	2.0	71	66	67	82		
0.25	3.5	72	74	73	82	0.25	3.5	72	74	73	82		
0.30	3.5	71	72	72	84	0.30	3.5	71	72	72	84		
0.35	3.5	71	69	69	84	0.35	3.5	71	69	69	84		
0.40	3.5	68	66	68	83	0.40	3.5	68	66	68	83		
0.45	3.5	65	68	67	82	0.45	3.5	65	68	67	82		
0.25	5.0	66	69	72	83	0.25	5.0	66	69	72	83		
0.30	5.0	70	71	71	83	0.30	5.0	70	71	71	83		
0.35	5.0	69	69	69	84	0.35	5.0	69	69	69	84		
0.40	5.0	66	66	68	81	0.40	5.0	66	66	68	81		
0.45	5.0	65	67	66	81	0.45	5.0	65	67	66	81		
0.25	7.5	69	72	72	999	0.25	7.5	69	72	72	999		
0.30	7.5	65	67	68	83	0.30	7.5	65	67	68	83		
0.35	7.5	68	68	67	82	0.35	7.5	68	68	67	82		
0.40	7.5	66	66	68	82	0.40	7.5	66	66	68	82		
0.45	7.5	64	66	65	81	0.45	7.5	64	66	65	81		
0.25	10.0	999	999	999	999	0.25	10.0	999	999	999	999		
0.30	10.0	62	62	64	81	0.30	10.0	62	62	64	81		
0.35	10.0	63	64	67	82	0.35	10.0	63	64	67	82		
0.40	10.0	63	66	66	81	0.40	10.0	63	66	66	81		
0.45	10.0	63	65	65	82	0.45	10.0	63	65	65	82		
0.50	10.0	65	64	63	81	0.50	10.0	65	64	63	81		
0.55	10.0	62	63	62	83	0.55	10.0	62	63	62	83		
0.60	10.0	62	62	62	81	0.60	10.0	62	62	62	81		
0.65	10.0	60	63	61	82	0.65	10.0	60	63	61	82		
0.70	10.0	59	63	61	80	0.70	10.0	59	63	61	80		
0.50	7.5	64	65	63	83	0.50	7.5	64	65	63	83		
0.55	7.5	63	62	65	83	0.55	7.5	63	62	65	83		
0.60	7.5	62	65	63	81	0.60	7.5	62	65	63	81		
0.65	7.5	60	63	63	81	0.65	7.5	60	63	63	81		

Table 14—Continued

total sample							Bright SHARC sample						
z	$L_{44}$	1st <sup>a</sup>	2nd <sup>a</sup>	3rd <sup>a</sup>	4th <sup>a</sup>	z	$L_{44}$	1st <sup>a</sup>	2nd <sup>a</sup>	3rd <sup>a</sup>	4th <sup>a</sup>		
0.50	5.0	64	64	63	83	0.50	5.0	64	64	63	83		
0.55	5.0	62	64	64	83	0.55	5.0	62	64	64	83		
0.60	5.0	63	64	63	82	0.60	5.0	63	64	63	82		
0.65	5.0	61	64	65	81	0.65	5.0	61	64	65	81		
0.70	5.0	62	62	62	80	0.70	5.0	63	62	62	80		
0.50	3.5	65	65	65	81	0.50	3.5	65	65	65	81		
0.55	3.5	64	67	64	84	0.55	3.5	64	67	64	84		
0.60	3.5	63	63	63	84	0.60	3.5	67	67	64	84		
0.65	3.5	65	65	65	84	0.65	3.5	77	78	72	88		
0.70	3.5	69	67	63	85	0.70	3.5	122	85	64	92		
0.50	2.0	70	65	66	84	0.50	2.0	90	74	74	88		
0.55	2.0	69	67	73	90	0.55	2.0	104	80	94	100		
0.60	2.0	70	67	72	110	0.60	2.0	0	85	0	146		
0.65	2.0	85	92	67	103	0.65	2.0	1	193	0	143		
0.70	2.0	76	94	76	90	0.70	2.0	0	0	0	0		
0.50	1.0	999	80	96	101	0.50	1.0	999	0	0	0		
0.55	1.0	86	999	164	134	0.55	1.0	0	999	0	191		
0.60	1.0	154	136	0	0	0.60	1.0	0	0	0	0		
0.65	1.0	133	75	0	999	0.65	1.0	0	0	0	999		
0.70	1.0	0	999	1	0	0.70	1.0	0	999	1	0		
0.75	1.0	999	999	69	0	0.75	1.0	999	1	0	0		
0.80	1.0	91	999	0	0	0.80	1.0	0	0	0	0		
0.85	1.0	1	171	0	0	0.85	1.0	1	0	0	0		
0.90	1.0	168	999	0	999	0.90	1.0	0	999	0	0		
0.95	1.0	0	999	999	0	0.95	1.0	0	0	0	0		
0.75	2.0	111	0	116	110	0.75	2.0	0	0	0	0		
0.80	2.0	173	108	0	0	0.80	2.0	0	0	0	0		
0.85	2.0	131	111	0	1	0.85	2.0	0	0	0	1		
0.90	2.0	999	194	1	0	0.90	2.0	0	0	1	0		
0.95	2.0	177	999	0	999	0.95	2.0	0	1	0	999		
0.75	3.5	74	68	69	84	0.75	3.5	999	175	89	100		
0.80	3.5	85	63	73	87	0.80	3.5	999	0	140	75		
0.85	3.5	66	69	71	110	0.85	3.5	0	76	0	137		
0.90	3.5	126	76	79	111	0.90	3.5	999	0	0	0		
0.95	3.5	126	87	81	93	0.95	3.5	999	0	0	0		
0.75	5.0	60	64	62	81	0.75	5.0	67	67	65	81		
0.80	5.0	63	63	63	83	0.80	5.0	72	71	71	83		
0.85	5.0	66	61	65	89	0.85	5.0	119	77	76	95		
0.90	5.0	62	70	62	88	0.90	5.0	78	88	78	93		
0.95	5.0	69	65	76	86	0.95	5.0	999	122	108	139		

Table 14—Continued

total sample						Bright SHARC sample					
z	$L_{44}$	1st <sup>a</sup>	2nd <sup>a</sup>	3rd <sup>a</sup>	4th <sup>a</sup>	z	$L_{44}$	1st <sup>a</sup>	2nd <sup>a</sup>	3rd <sup>a</sup>	4th <sup>a</sup>
0.75	7.5	62	63	60	81	0.75	7.5	62	63	60	81
0.80	7.5	59	61	62	82	0.80	7.5	60	61	63	83
0.85	7.5	59	62	61	84	0.85	7.5	62	64	62	84
0.90	7.5	59	64	61	85	0.90	7.5	66	68	63	85
0.95	7.5	60	64	63	82	0.95	7.5	78	72	74	83
0.75	10.0	60	62	60	79	0.75	10.0	60	62	60	79
0.80	10.0	60	62	60	82	0.80	10.0	60	62	60	82
0.85	10.0	59	62	61	83	0.85	10.0	59	62	61	83
0.90	10.0	58	62	60	79	0.90	10.0	59	62	60	79
0.95	10.0	58	62	62	81	0.95	10.0	59	62	62	81

Table 15. Detection efficiency percentage for the  $\beta=0.55$  set of parameters

<i>total detection efficiency</i>						<i>Bright SHARC detection efficiency</i>					
<i>z</i>	<i>L</i> <sub>44</sub>	1st <sup>a</sup>	2nd <sup>a</sup>	3rd <sup>a</sup>	4th <sup>a</sup>	<i>z</i>	<i>L</i> <sub>44</sub>	1st <sup>a</sup>	2nd <sup>a</sup>	3rd <sup>a</sup>	4th <sup>a</sup>
0.25	1.0	2	5	1	2	0.25	1.0	0	2	0	0
0.30	1.0	2	0	1	1	0.30	1.0	0	0	0	0
0.35	1.0	0	3	2	0	0.35	1.0	0	1	0	0
0.40	1.0	0	0	0	0	0.40	1.0	0	0	0	0
0.45	1.0	0	1	0	0	0.45	1.0	0	0	0	0
0.25	2.0	9	17	8	15	0.25	2.0	1	4	0	8
0.30	2.0	10	11	8	5	0.30	2.0	0	2	1	2
0.35	2.0	3	9	2	4	0.35	2.0	0	0	0	2
0.40	2.0	2	4	4	2	0.40	2.0	1	0	0	0
0.45	2.0	2	1	2	1	0.45	2.0	0	0	0	0
0.25	3.5	39	45	24	30	0.25	3.5	25	43	23	30
0.30	3.5	36	31	20	25	0.30	3.5	10	11	13	25
0.35	3.5	26	33	17	20	0.35	3.5	3	4	4	12
0.40	3.5	15	29	16	9	0.40	3.5	0	2	1	2
0.45	3.5	9	12	7	7	0.45	3.5	0	0	1	1
0.25	5.0	37	56	38	41	0.25	5.0	36	56	38	41
0.30	5.0	45	50	41	40	0.30	5.0	38	48	41	40
0.35	5.0	40	41	35	45	0.35	5.0	19	22	21	38
0.40	5.0	42	45	23	28	0.40	5.0	7	8	7	21
0.45	5.0	31	29	26	16	0.45	5.0	3	4	1	6
0.25	7.5	46	58	44	47	0.25	7.5	46	58	44	47
0.30	7.5	50	66	49	52	0.30	7.5	50	66	49	52
0.35	7.5	51	59	49	50	0.35	7.5	45	57	49	50
0.40	7.5	55	57	43	57	0.40	7.5	30	54	42	56
0.45	7.5	50	57	38	41	0.45	7.5	19	34	23	37
0.25	10.0	55	68	59	52	0.25	10.0	55	68	59	52
0.30	10.0	63	74	62	61	0.30	10.0	63	74	62	61
0.35	10.0	70	72	63	59	0.35	10.0	70	72	63	59
0.40	10.0	70	75	69	63	0.40	10.0	70	75	69	63
0.45	10.0	66	75	62	50	0.45	10.0	56	73	62	50
0.50	10.0	72	70	57	41	0.50	10.0	31	53	41	41
0.55	10.0	54	58	44	41	0.55	10.0	8	13	15	37
0.60	10.0	53	53	40	37	0.60	10.0	4	8	11	21
0.65	10.0	35	33	27	31	0.65	10.0	2	2	4	13
0.70	10.0	35	33	26	20	0.70	10.0	2	1	4	6
0.50	7.5	33	48	27	34	0.50	7.5	3	15	7	27
0.55	7.5	31	38	25	28	0.55	7.5	1	3	7	22
0.60	7.5	25	28	17	12	0.60	7.5	1	1	4	4
0.65	7.5	16	18	7	9	0.65	7.5	1	3	1	1

Table 15—Continued

total detection efficiency							Bright SHARC detection efficiency						
z	$L_{44}$	1st <sup>a</sup>	2nd <sup>a</sup>	3rd <sup>a</sup>	4th <sup>a</sup>	z	$L_{44}$	1st <sup>a</sup>	2nd <sup>a</sup>	3rd <sup>a</sup>	4th <sup>a</sup>		
0.50	5.0	16	23	9	14	0.50	5.0	0	0	0	0	4	
0.55	5.0	7	13	9	3	0.55	5.0	0	0	1	1		
0.60	5.0	13	10	7	5	0.60	5.0	3	1	0	0		
0.65	5.0	4	3	5	2	0.65	5.0	1	0	0	0		
0.70	5.0	2	5	1	4	0.70	5.0	0	1	0	1		
0.50	3.5	7	10	3	5	0.50	3.5	0	2	1	2		
0.55	3.5	3	2	1	1	0.55	3.5	0	0	0	0		
0.60	3.5	1	2	1	1	0.60	3.5	0	1	0	0		
0.65	3.5	1	2	0	1	0.65	3.5	0	0	0	1		
0.70	3.5	2	2	0	2	0.70	3.5	0	0	0	0		
0.50	2.0	1	1	0	0	0.50	2.0	1	0	0	0		
0.55	2.0	2	1	0	0	0.55	2.0	0	0	0	0		
0.60	2.0	2	0	1	1	0.60	2.0	0	0	0	0		
0.65	2.0	4	1	1	0	0.65	2.0	2	0	0	0		
0.70	2.0	3	1	1	0	0.70	2.0	1	0	0	0		
0.50	1.0	1	1	0	1	0.50	1.0	0	0	0	0		
0.55	1.0	0	1	2	0	0.55	1.0	0	1	0	0		
0.60	1.0	1	0	1	0	0.60	1.0	0	0	0	0		
0.65	1.0	3	2	0	0	0.65	1.0	1	0	0	0		
0.70	1.0	0	0	0	0	0.70	1.0	0	0	0	0		
0.75	1.0	0	0	1	0	0.75	1.0	0	0	0	0		
0.80	1.0	1	2	1	0	0.80	1.0	0	0	1	0		
0.85	1.0	0	0	0	1	0.85	1.0	0	0	0	0		
0.90	1.0	0	1	0	1	0.90	1.0	0	0	0	0		
0.95	1.0	1	0	1	1	0.95	1.0	0	0	0	0		
0.75	2.0	1	0	1	0	0.75	2.0	1	0	0	0		
0.80	2.0	0	1	0	0	0.80	2.0	0	0	0	0		
0.85	2.0	1	1	0	0	0.85	2.0	0	1	0	0		
0.90	2.0	1	0	1	0	0.90	2.0	1	0	0	0		
0.95	2.0	1	0	0	0	0.95	2.0	1	0	0	0		
0.75	3.5	2	2	1	0	0.75	3.5	0	0	0	0		
0.80	3.5	3	3	1	1	0.80	3.5	0	1	0	0		
0.85	3.5	1	0	1	0	0.85	3.5	0	0	0	0		
0.90	3.5	2	2	0	1	0.90	3.5	0	1	0	0		
0.95	3.5	0	2	1	0	0.95	3.5	0	0	0	0		
0.75	5.0	1	5	3	1	0.75	5.0	1	1	1	0		
0.80	5.0	2	2	2	1	0.80	5.0	0	0	0	0		
0.85	5.0	3	0	2	0	0.85	5.0	0	0	0	0		
0.90	5.0	1	1	1	0	0.90	5.0	0	0	0	0		
0.95	5.0	2	3	2	0	0.95	5.0	0	0	1	0		

Table 15—Continued

total detection efficiency						Bright SHARC detection efficiency					
z	$L_{44}$	1st <sup>a</sup>	2nd <sup>a</sup>	3rd <sup>a</sup>	4th <sup>a</sup>	z	$L_{44}$	1st <sup>a</sup>	2nd <sup>a</sup>	3rd <sup>a</sup>	4th <sup>a</sup>
0.75	7.5	7	4	4	0	0.75	7.5	0	0	0	0
0.80	7.5	5	6	6	4	0.80	7.5	0	1	0	1
0.85	7.5	4	5	3	1	0.85	7.5	0	0	0	1
0.90	7.5	6	4	2	3	0.90	7.5	0	0	0	0
0.95	7.5	2	4	0	4	0.95	7.5	0	0	0	2
0.75	10.0	24	22	17	8	0.75	10.0	4	2	2	0
0.80	10.0	15	17	8	11	0.80	10.0	0	1	0	3
0.85	10.0	7	8	3	4	0.85	10.0	0	0	0	1
0.90	10.0	11	7	0	1	0.90	10.0	1	1	0	0
0.95	10.0	4	6	6	1	0.95	10.0	1	1	1	0

Table 16. Recovered luminosity percentage for the  $\beta=0.55$  set of parameters

total sample							Bright SHARC sample						
z	$L_{44}$	1st <sup>a</sup>	2nd <sup>a</sup>	3rd <sup>a</sup>	4th <sup>a</sup>	z	$L_{44}$	1st <sup>a</sup>	2nd <sup>a</sup>	3rd <sup>a</sup>	4th <sup>a</sup>		
0.25	1.0	999	999	122	154	0.25	1.0	0	999	0	0	0	
0.30	1.0	999	0	104	999	0.30	1.0	0	0	0	0	0	
0.35	1.0	0	999	999	0	0.35	1.0	0	999	0	0	0	
0.40	1.0	0	0	0	0	0.40	1.0	0	0	0	0	0	
0.45	1.0	0	999	0	0	0.45	1.0	0	0	0	0	0	
0.25	2.0	114	102	106	112	0.25	2.0	999	114	0	0	123	
0.30	2.0	106	114	108	126	0.30	2.0	0	178	118	156		
0.35	2.0	110	102	148	161	0.35	2.0	0	0	0	0	999	
0.40	2.0	999	124	129	109	0.40	2.0	999	0	0	0	0	
0.45	2.0	152	93	166	165	0.45	2.0	0	0	0	0	0	
0.25	3.5	108	100	100	111	0.25	3.5	107	101	100	100	111	
0.30	3.5	103	97	97	113	0.30	3.5	113	108	100	100	113	
0.35	3.5	102	97	99	115	0.35	3.5	128	121	125	125	120	
0.40	3.5	98	99	106	119	0.40	3.5	0	181	172	129		
0.45	3.5	87	91	166	123	0.45	3.5	0	0	999	0	155	
0.25	5.0	105	101	101	114	0.25	5.0	105	101	101	101	114	
0.30	5.0	99	92	97	111	0.30	5.0	99	93	97	97	111	
0.35	5.0	98	88	96	110	0.35	5.0	103	94	102	102	112	
0.40	5.0	94	92	93	116	0.40	5.0	118	119	104	104	120	
0.45	5.0	95	88	95	118	0.45	5.0	143	99	125	125	142	
0.25	7.5	104	99	101	113	0.25	7.5	104	99	101	101	113	
0.30	7.5	99	94	94	113	0.30	7.5	99	94	94	94	113	
0.35	7.5	93	89	93	111	0.35	7.5	93	90	93	93	111	
0.40	7.5	88	90	89	109	0.40	7.5	93	91	90	90	110	
0.45	7.5	92	87	89	104	0.45	7.5	103	92	96	96	106	
0.25	10.0	101	100	101	112	0.25	10.0	101	100	101	101	112	
0.30	10.0	95	95	96	110	0.30	10.0	95	95	96	96	110	
0.35	10.0	93	91	92	111	0.35	10.0	93	91	92	92	111	
0.40	10.0	88	88	90	108	0.40	10.0	88	88	90	90	108	
0.45	10.0	88	85	88	111	0.45	10.0	89	85	88	88	111	
0.50	10.0	88	85	85	110	0.50	10.0	95	86	88	88	110	
0.55	10.0	86	84	84	112	0.55	10.0	105	96	94	94	113	
0.60	10.0	87	86	90	110	0.60	10.0	121	112	106	106	117	
0.65	10.0	91	86	91	111	0.65	10.0	158	119	142	142	121	
0.70	10.0	94	88	99	113	0.70	10.0	157	187	153	153	124	
0.50	7.5	123	90	87	111	0.50	7.5	999	107	100	100	117	
0.55	7.5	87	102	96	126	0.55	7.5	128	999	124	124	131	
0.60	7.5	95	84	98	129	0.60	7.5	999	149	133	133	161	
0.65	7.5	107	122	97	120	0.65	7.5	999	136	169			

Table 16—Continued

total sample							Bright SHARC sample						
z	$L_{44}$	1st <sup>a</sup>	2nd <sup>a</sup>	3rd <sup>a</sup>	4th <sup>a</sup>	z	$L_{44}$	1st <sup>a</sup>	2nd <sup>a</sup>	3rd <sup>a</sup>	4th <sup>a</sup>		
0.50	5.0	94	93	96	139	0.50	5.0	0	0	0	0	999	
0.55	5.0	86	95	118	130	0.55	5.0	0	0	0	140	136	
0.60	5.0	168	127	126	121	0.60	5.0	999	999	0	0	0	
0.65	5.0	144	115	124	130	0.65	5.0	999	0	0	0	0	
0.70	5.0	129	195	155	183	0.70	5.0	0	999	0	0	999	
0.50	3.5	138	136	150	176	0.50	3.5	0	999	999	999	999	
0.55	3.5	183	141	163	115	0.55	3.5	0	0	0	0	0	
0.60	3.5	139	999	148	174	0.60	3.5	0	999	0	0	0	
0.65	3.5	182	159	0	999	0.65	3.5	0	0	0	0	999	
0.70	3.5	141	115	0	999	0.70	3.5	0	0	0	0	0	
0.50	2.0	999	999	0	0	0.50	2.0	999	0	0	0	0	
0.55	2.0	999	195	0	0	0.55	2.0	0	0	0	0	0	
0.60	2.0	999	0	999	999	0.60	2.0	0	0	0	0	0	
0.65	2.0	999	999	81	0	0.65	2.0	999	0	0	0	0	
0.70	2.0	999	146	999	0	0.70	2.0	999	0	0	0	0	
0.50	1.0	999	999	0	999	0.50	1.0	0	0	0	0	0	
0.55	1.0	0	999	999	0	0.55	1.0	0	999	0	0	0	
0.60	1.0	999	0	999	0	0.60	1.0	0	0	0	0	0	
0.65	1.0	999	999	0	0	0.65	1.0	999	0	0	0	0	
0.70	1.0	0	0	0	0	0.70	1.0	0	0	0	0	0	
0.75	1.0	0	0	999	0	0.75	1.0	0	0	0	0	0	
0.80	1.0	999	999	999	0	0.80	1.0	0	0	0	999	0	
0.85	1.0	0	0	0	999	0.85	1.0	0	0	0	0	0	
0.90	1.0	0	999	0	999	0.90	1.0	0	0	0	0	0	
0.95	1.0	999	0	999	999	0.95	1.0	0	0	0	0	0	
0.75	2.0	999	0	999	0	0.75	2.0	999	0	0	0	0	
0.80	2.0	0	999	0	0	0.80	2.0	0	0	0	0	0	
0.85	2.0	149	999	0	0	0.85	2.0	0	999	0	0	0	
0.90	2.0	999	0	999	0	0.90	2.0	999	0	0	0	0	
0.95	2.0	999	0	0	0	0.95	2.0	999	0	0	0	0	
0.75	3.5	179	188	999	0	0.75	3.5	0	0	0	0	0	
0.80	3.5	999	999	999	999	0.80	3.5	0	999	0	0	0	
0.85	3.5	999	0	165	0	0.85	3.5	0	0	0	0	0	
0.90	3.5	191	999	0	999	0.90	3.5	0	999	0	0	0	
0.95	3.5	0	999	153	0	0.95	3.5	0	0	0	0	0	
0.75	5.0	999	166	999	155	0.75	5.0	999	999	999	999	0	
0.80	5.0	168	160	999	999	0.80	5.0	0	0	0	0	0	
0.85	5.0	151	0	162	0	0.85	5.0	0	0	0	0	0	
0.90	5.0	999	999	999	0	0.90	5.0	0	0	0	0	0	
0.95	5.0	999	999	999	0	0.95	5.0	0	0	999	0	0	

Table 16—Continued

total sample						Bright SHARC sample					
z	$L_{44}$	1st <sup>a</sup>	2nd <sup>a</sup>	3rd <sup>a</sup>	4th <sup>a</sup>	z	$L_{44}$	1st <sup>a</sup>	2nd <sup>a</sup>	3rd <sup>a</sup>	4th <sup>a</sup>
0.75	7.5	92	93	116	0	0.75	7.5	0	0	0	0
0.80	7.5	107	127	128	162	0.80	7.5	0	999	0	999
0.85	7.5	172	106	171	999	0.85	7.5	0	0	0	999
0.90	7.5	152	159	158	191	0.90	7.5	0	0	0	0
0.95	7.5	94	106	0	999	0.95	7.5	0	0	0	999
0.75	10.0	119	105	94	113	0.75	10.0	999	187	131	0
0.80	10.0	97	90	85	135	0.80	10.0	0	103	0	171
0.85	10.0	114	110	96	174	0.85	10.0	0	0	0	999
0.90	10.0	160	122	0	999	0.90	10.0	999	184	0	0
0.95	10.0	999	138	999	115	0.95	10.0	999	999	999	0

Table 17. Detection efficiency percentage for the  $\beta=0.75$  set of parameters

total detection efficiency						Bright SHARC detection efficiency					
z	$L_{44}$	1st <sup>a</sup>	2nd <sup>a</sup>	3rd <sup>a</sup>	4th <sup>a</sup>	z	$L_{44}$	1st <sup>a</sup>	2nd <sup>a</sup>	3rd <sup>a</sup>	4th <sup>a</sup>
0.25	1.0	77	83	62	42	0.25	1.0	25	57	39	40
0.30	1.0	56	72	43	36	0.30	1.0	3	12	10	31
0.35	1.0	31	54	33	14	0.35	1.0	1	3	3	5
0.40	1.0	26	31	9	11	0.40	1.0	0	4	0	1
0.45	1.0	18	15	8	2	0.45	1.0	0	1	1	0
0.25	2.0	79	91	79	48	0.25	2.0	79	91	79	48
0.30	2.0	70	80	68	57	0.30	2.0	65	80	68	57
0.35	2.0	69	82	64	36	0.35	2.0	25	50	43	35
0.40	2.0	58	72	60	43	0.40	2.0	4	18	11	39
0.45	2.0	45	62	39	32	0.45	2.0	2	9	3	16
0.25	3.5	93	96	89	56	0.25	3.5	93	96	89	56
0.30	3.5	87	96	89	59	0.30	3.5	87	96	89	59
0.35	3.5	92	96	83	50	0.35	3.5	89	96	83	50
0.40	3.5	83	94	87	50	0.40	3.5	76	94	86	50
0.45	3.5	85	86	81	48	0.45	3.5	51	77	68	47
0.25	5.0	94	98	95	50	0.25	5.0	94	98	95	50
0.30	5.0	94	98	97	61	0.30	5.0	94	98	97	61
0.35	5.0	94	99	93	55	0.35	5.0	94	99	93	55
0.40	5.0	92	98	92	54	0.40	5.0	92	98	92	54
0.45	5.0	97	95	90	50	0.45	5.0	96	95	90	50
0.25	7.5	94	100	99	63	0.25	7.5	94	100	99	63
0.30	7.5	97	99	98	65	0.30	7.5	97	99	98	65
0.35	7.5	97	97	97	43	0.35	7.5	97	97	97	43
0.40	7.5	93	100	97	41	0.40	7.5	93	100	97	41
0.45	7.5	94	97	98	53	0.45	7.5	94	97	98	53
0.25	10.0	95	100	100	59	0.25	10.0	95	100	100	59
0.30	10.0	98	99	99	51	0.30	10.0	98	99	99	51
0.35	10.0	97	99	100	55	0.35	10.0	97	99	100	55
0.40	10.0	96	100	98	47	0.40	10.0	96	100	98	47
0.45	10.0	96	99	99	48	0.45	10.0	96	99	99	48
0.50	10.0	96	100	98	43	0.50	10.0	96	100	98	43
0.55	10.0	96	98	94	47	0.55	10.0	96	98	94	47
0.60	10.0	93	97	93	39	0.60	10.0	93	97	93	39
0.65	10.0	92	95	93	44	0.65	10.0	92	95	93	44
0.70	10.0	92	94	86	47	0.70	10.0	91	94	85	47
0.50	7.5	96	98	95	47	0.50	7.5	96	98	95	47
0.55	7.5	96	93	95	53	0.55	7.5	96	93	95	53
0.60	7.5	87	93	92	45	0.60	7.5	85	93	92	45
0.65	7.5	88	92	84	46	0.65	7.5	71	92	84	45

Table 17—Continued

total detection efficiency							Bright SHARC detection efficiency						
z	$L_{44}$	1st <sup>a</sup>	2nd <sup>a</sup>	3rd <sup>a</sup>	4th <sup>a</sup>	z	$L_{44}$	1st <sup>a</sup>	2nd <sup>a</sup>	3rd <sup>a</sup>	4th <sup>a</sup>		
0.50	5.0	83	93	84	47	0.50	5.0	80	93	84	46		
0.55	5.0	86	91	78	54	0.55	5.0	47	71	59	53		
0.60	5.0	65	82	70	38	0.60	5.0	16	32	26	37		
0.65	5.0	68	79	66	37	0.65	5.0	4	21	12	31		
0.70	5.0	55	68	60	28	0.70	5.0	5	6	6	18		
0.50	3.5	70	88	66	43	0.50	3.5	15	45	32	42		
0.55	3.5	65	68	51	31	0.55	3.5	5	8	10	24		
0.60	3.5	50	70	42	28	0.60	3.5	3	6	5	15		
0.65	3.5	41	49	37	21	0.65	3.5	0	4	4	5		
0.70	3.5	33	44	24	16	0.70	3.5	1	0	1	0		
0.50	2.0	27	35	29	14	0.50	2.0	2	4	4	1		
0.55	2.0	19	24	19	12	0.55	2.0	2	2	1	1		
0.60	2.0	11	12	5	8	0.60	2.0	0	0	0	3		
0.65	2.0	9	6	6	1	0.65	2.0	0	1	0	0		
0.70	2.0	5	7	5	3	0.70	2.0	0	0	1	1		
0.50	1.0	5	7	2	2	0.50	1.0	0	0	0	0		
0.55	1.0	2	5	6	4	0.55	1.0	0	0	0	0		
0.60	1.0	2	2	5	0	0.60	1.0	0	0	0	0		
0.65	1.0	7	2	0	0	0.65	1.0	0	0	0	0		
0.70	1.0	2	5	0	2	0.70	1.0	0	0	0	0		
0.75	1.0	2	8	1	1	0.75	1.0	0	0	0	1		
0.80	1.0	0	2	0	0	0.80	1.0	0	0	0	0		
0.85	1.0	0	0	1	0	0.85	1.0	0	0	0	0		
0.90	1.0	1	0	1	0	0.90	1.0	0	0	0	0		
0.95	1.0	1	4	0	0	0.95	1.0	0	0	0	0		
0.75	2.0	7	9	5	2	0.75	2.0	0	0	1	0		
0.80	2.0	5	6	5	1	0.80	2.0	0	1	0	1		
0.85	2.0	3	7	3	1	0.85	2.0	0	0	0	1		
0.90	2.0	1	3	1	0	0.90	2.0	0	0	1	0		
0.95	2.0	2	2	2	0	0.95	2.0	0	0	1	0		
0.75	3.5	27	38	21	7	0.75	3.5	2	2	1	1		
0.80	3.5	22	22	16	9	0.80	3.5	1	0	0	0		
0.85	3.5	19	21	14	7	0.85	3.5	0	1	0	0		
0.90	3.5	13	22	8	3	0.90	3.5	2	3	2	0		
0.95	3.5	5	12	5	4	0.95	3.5	0	1	0	0		
0.75	5.0	40	40	20	17	0.75	5.0	0	0	4	6		
0.80	5.0	34	57	25	15	0.80	5.0	0	0	0	0		
0.85	5.0	28	41	13	13	0.85	5.0	0	4	4	0		
0.90	5.0	13	13	19	3	0.90	5.0	0	0	0	3		
0.95	5.0	9	11	16	6	0.95	5.0	0	0	0	3		

Table 17—Continued

total detection efficiency						Bright SHARC detection efficiency					
z	$L_{44}$	1st <sup>a</sup>	2nd <sup>a</sup>	3rd <sup>a</sup>	4th <sup>a</sup>	z	$L_{44}$	1st <sup>a</sup>	2nd <sup>a</sup>	3rd <sup>a</sup>	4th <sup>a</sup>
0.75	7.5	75	85	76	41	0.75	7.5	16	36	35	41
0.80	7.5	73	75	58	36	0.80	7.5	6	21	8	34
0.85	7.5	58	65	53	31	0.85	7.5	8	9	9	21
0.90	7.5	50	65	41	26	0.90	7.5	4	6	4	17
0.95	7.5	35	45	29	17	0.95	7.5	0	1	3	4
0.75	10.0	90	94	82	29	0.75	10.0	75	92	81	28
0.80	10.0	81	88	75	51	0.80	10.0	44	80	60	50
0.85	10.0	83	93	75	48	0.85	10.0	29	45	39	47
0.90	10.0	75	91	75	37	0.90	10.0	10	21	18	36
0.95	10.0	63	77	59	31	0.95	10.0	6	11	9	26

Table 18. Recovered luminosity percentage for the  $\beta=0.75$  set of parameters

total sample							Bright SHARC sample						
z	$L_{44}$	1st <sup>a</sup>	2nd <sup>a</sup>	3rd <sup>a</sup>	4th <sup>a</sup>	z	$L_{44}$	1st <sup>a</sup>	2nd <sup>a</sup>	3rd <sup>a</sup>	4th <sup>a</sup>		
0.25	1.0	109	101	104	116	0.25	1.0	120	104	110	117		
0.30	1.0	103	102	99	123	0.30	1.0	151	124	121	125		
0.35	1.0	111	103	102	136	0.35	1.0	999	147	161	151		
0.40	1.0	99	108	103	126	0.40	1.0	0	188	0	999		
0.45	1.0	118	120	113	178	0.45	1.0	0	999	999	0		
0.25	2.0	108	104	104	116	0.25	2.0	108	104	104	116		
0.30	2.0	102	95	95	116	0.30	2.0	100	95	95	116		
0.35	2.0	97	95	94	111	0.35	2.0	107	99	97	111		
0.40	2.0	94	90	102	116	0.40	2.0	113	105	170	117		
0.45	2.0	101	97	100	125	0.45	2.0	178	149	150	142		
0.25	3.5	105	102	103	117	0.25	3.5	105	102	103	117		
0.30	3.5	99	96	97	113	0.30	3.5	99	96	97	113		
0.35	3.5	95	93	91	117	0.35	3.5	95	93	91	117		
0.40	3.5	91	90	92	113	0.40	3.5	90	90	92	113		
0.45	3.5	90	89	89	114	0.45	3.5	92	90	91	115		
0.25	5.0	102	101	101	116	0.25	5.0	102	101	101	116		
0.30	5.0	96	97	97	116	0.30	5.0	96	97	97	116		
0.35	5.0	92	93	92	115	0.35	5.0	92	93	92	115		
0.40	5.0	90	90	90	112	0.40	5.0	90	90	90	112		
0.45	5.0	89	88	89	114	0.45	5.0	89	88	89	114		
0.25	7.5	102	101	102	115	0.25	7.5	102	101	102	115		
0.30	7.5	97	96	97	116	0.30	7.5	97	96	97	116		
0.35	7.5	92	93	93	116	0.35	7.5	92	93	93	116		
0.40	7.5	90	90	89	116	0.40	7.5	90	90	89	116		
0.45	7.5	87	88	88	113	0.45	7.5	87	88	88	113		
0.25	10.0	101	101	102	117	0.25	10.0	101	101	102	117		
0.30	10.0	96	96	98	116	0.30	10.0	96	96	98	116		
0.35	10.0	92	93	93	115	0.35	10.0	92	93	93	115		
0.40	10.0	89	90	89	114	0.40	10.0	89	90	89	114		
0.45	10.0	86	87	89	111	0.45	10.0	86	87	89	111		
0.50	10.0	86	86	85	112	0.50	10.0	86	86	85	112		
0.55	10.0	82	84	84	114	0.55	10.0	82	84	84	114		
0.60	10.0	82	84	82	114	0.60	10.0	82	84	82	114		
0.65	10.0	82	83	82	111	0.65	10.0	82	83	82	111		
0.70	10.0	82	80	82	110	0.70	10.0	82	80	82	110		
0.50	7.5	88	85	86	111	0.50	7.5	88	85	86	111		
0.55	7.5	85	85	84	112	0.55	7.5	85	85	84	112		
0.60	7.5	83	83	84	113	0.60	7.5	83	83	84	113		
0.65	7.5	81	85	83	119	0.65	7.5	82	85	83	120		

Table 18—Continued

total sample							Bright SHARC sample						
z	$L_{44}$	1st <sup>a</sup>	2nd <sup>a</sup>	3rd <sup>a</sup>	4th <sup>a</sup>	z	$L_{44}$	1st <sup>a</sup>	2nd <sup>a</sup>	3rd <sup>a</sup>	4th <sup>a</sup>		
0.50	5.0	88	87	87	114	0.50	5.0	88	87	87	115		
0.55	5.0	85	86	85	117	0.55	5.0	90	88	87	118		
0.60	5.0	86	84	85	112	0.60	5.0	99	92	92	112		
0.65	5.0	84	88	85	121	0.65	5.0	111	110	107	126		
0.70	5.0	89	87	86	115	0.70	5.0	135	137	120	119		
0.50	3.5	87	90	88	114	0.50	3.5	97	96	96	113		
0.55	3.5	86	91	87	114	0.55	3.5	113	150	103	116		
0.60	3.5	89	91	89	117	0.60	3.5	135	142	135	124		
0.65	3.5	90	89	95	117	0.65	3.5	0	137	151	154		
0.70	3.5	89	91	96	117	0.70	3.5	164	0	148	0		
0.50	2.0	101	98	104	112	0.50	2.0	152	194	165	116		
0.55	2.0	107	94	108	126	0.55	2.0	189	177	999	999		
0.60	2.0	116	101	100	185	0.60	2.0	0	0	0	999		
0.65	2.0	146	150	134	197	0.65	2.0	0	999	0	0		
0.70	2.0	165	150	188	166	0.70	2.0	0	0	999	999		
0.50	1.0	105	96	85	130	0.50	1.0	0	0	0	0		
0.55	1.0	999	156	141	999	0.55	1.0	0	0	0	0		
0.60	1.0	74	159	999	0	0.60	1.0	0	0	0	0		
0.65	1.0	999	159	0	0	0.65	1.0	0	0	0	0		
0.70	1.0	999	177	0	136	0.70	1.0	0	0	0	0		
0.75	1.0	999	999	999	999	0.75	1.0	0	0	0	999		
0.80	1.0	0	999	0	0	0.80	1.0	0	0	0	0		
0.85	1.0	0	0	106	0	0.85	1.0	0	0	0	0		
0.90	1.0	999	0	112	0	0.90	1.0	0	0	0	0		
0.95	1.0	999	999	0	0	0.95	1.0	0	0	0	0		
0.75	2.0	93	118	172	159	0.75	2.0	0	0	999	0		
0.80	2.0	178	183	143	999	0.80	2.0	0	999	0	999		
0.85	2.0	97	144	153	999	0.85	2.0	0	0	0	999		
0.90	2.0	156	184	999	0	0.90	2.0	0	0	999	0		
0.95	2.0	100	147	999	0	0.95	2.0	0	0	999	0		
0.75	3.5	98	102	110	141	0.75	3.5	174	171	199	165		
0.80	3.5	97	97	107	142	0.80	3.5	169	0	0	0		
0.85	3.5	124	108	124	146	0.85	3.5	0	999	0	0		
0.90	3.5	999	140	155	156	0.90	3.5	999	999	999	0		
0.95	3.5	156	123	133	166	0.95	3.5	0	999	0	0		
0.75	5.0	90	83	99	107	0.75	5.0	0	0	130	104		
0.80	5.0	89	85	84	123	0.80	5.0	0	0	0	0		
0.85	5.0	110	96	105	132	0.85	5.0	0	122	180	0		
0.90	5.0	91	78	91	999	0.90	5.0	0	0	0	999		
0.95	5.0	80	91	95	999	0.95	5.0	0	0	0	999		

Table 18—Continued

total sample						Bright SHARC sample					
z	$L_{44}$	1st <sup>a</sup>	2nd <sup>a</sup>	3rd <sup>a</sup>	4th <sup>a</sup>	z	$L_{44}$	1st <sup>a</sup>	2nd <sup>a</sup>	3rd <sup>a</sup>	4th <sup>a</sup>
0.75	7.5	84	86	84	113	0.75	7.5	99	97	94	113
0.80	7.5	81	85	82	121	0.80	7.5	100	103	101	123
0.85	7.5	86	84	85	114	0.85	7.5	115	115	113	117
0.90	7.5	83	88	85	128	0.90	7.5	121	137	119	140
0.95	7.5	80	85	95	114	0.95	7.5	0	182	175	131
0.75	10.0	87	85	82	115	0.75	10.0	90	86	83	116
0.80	10.0	80	84	83	115	0.80	10.0	86	86	87	116
0.85	10.0	82	83	82	115	0.85	10.0	90	90	88	116
0.90	10.0	79	83	80	117	0.90	10.0	95	97	91	118
0.95	10.0	79	83	82	122	0.95	10.0	101	108	107	123

Table 19. Detection efficiency percentage for the  $c_r=100$  kpc set of parameters

<i>total detection efficiency</i>						<i>Bright SHARC detection efficiency</i>					
<i>z</i>	$L_{44}$	1st <sup>a</sup>	2nd <sup>a</sup>	3rd <sup>a</sup>	4th <sup>a</sup>	<i>z</i>	$L_{44}$	1st <sup>a</sup>	2nd <sup>a</sup>	3rd <sup>a</sup>	4th <sup>a</sup>
0.25	1.0	77	89	71	21	0.25	1.0	25	41	35	21
0.30	1.0	69	72	48	17	0.30	1.0	8	12	9	10
0.35	1.0	35	47	21	12	0.35	1.0	2	2	1	2
0.40	1.0	22	26	20	7	0.40	1.0	0	0	0	1
0.45	1.0	6	6	8	3	0.45	1.0	0	0	0	0
0.25	2.0	91	97	82	22	0.25	2.0	91	97	82	22
0.30	2.0	80	85	66	29	0.30	2.0	80	85	66	29
0.35	2.0	73	71	58	21	0.35	2.0	32	53	38	21
0.40	2.0	59	54	49	29	0.40	2.0	7	9	6	26
0.45	2.0	55	50	41	11	0.45	2.0	3	4	2	8
0.25	3.5	90	97	93	26	0.25	3.5	90	97	93	26
0.30	3.5	85	85	76	21	0.30	3.5	85	85	76	21
0.35	3.5	70	73	63	16	0.35	3.5	70	73	63	16
0.40	3.5	64	54	56	15	0.40	3.5	64	54	56	15
0.45	3.5	68	56	50	20	0.45	3.5	44	53	42	20
0.25	5.0	96	99	95	26	0.25	5.0	96	99	95	26
0.30	5.0	93	89	76	21	0.30	5.0	93	89	76	21
0.35	5.0	60	67	49	16	0.35	5.0	60	67	49	16
0.40	5.0	50	61	38	26	0.40	5.0	50	61	38	26
0.45	5.0	60	46	51	17	0.45	5.0	60	46	51	17
0.25	7.5	98	100	97	33	0.25	7.5	98	100	97	33
0.30	7.5	88	96	79	21	0.30	7.5	88	96	79	21
0.35	7.5	67	64	60	15	0.35	7.5	67	64	60	15
0.40	7.5	54	42	36	15	0.40	7.5	54	42	36	15
0.45	7.5	56	47	37	13	0.45	7.5	56	47	37	13
0.25	10.0	97	100	97	32	0.25	10.0	97	100	97	32
0.30	10.0	91	97	76	28	0.30	10.0	91	97	76	28
0.35	10.0	65	73	61	16	0.35	10.0	65	73	61	16
0.40	10.0	39	30	40	19	0.40	10.0	39	30	40	19
0.45	10.0	45	25	34	11	0.45	10.0	45	25	34	11
0.50	10.0	49	35	37	9	0.50	10.0	32	16	26	13
0.55	10.0	45	33	31	13	0.55	10.0	31	18	22	12
0.60	10.0	42	37	42	8	0.60	10.0	37	17	27	9
0.65	10.0	41	45	33	13	0.65	10.0	41	25	30	14
0.70	10.0	49	37	35	12	0.70	10.0	32	26	33	7
0.50	7.5	50	32	30	12	0.50	7.5	50	32	30	12
0.55	7.5	44	30	31	13	0.55	7.5	44	30	31	13
0.60	7.5	46	33	36	14	0.60	7.5	46	33	36	14
0.65	7.5	42	29	42	17	0.65	7.5	38	29	40	17

Table 19—Continued

total detection efficiency							Bright SHARC detection efficiency						
z	$L_{44}$	1st <sup>a</sup>	2nd <sup>a</sup>	3rd <sup>a</sup>	4th <sup>a</sup>	z	$L_{44}$	1st <sup>a</sup>	2nd <sup>a</sup>	3rd <sup>a</sup>	4th <sup>a</sup>		
0.50	5.0	51	49	29	9	0.50	5.0	50	49	29	9		
0.55	5.0	56	36	43	19	0.55	5.0	29	32	34	19		
0.60	5.0	50	50	47	13	0.60	5.0	17	20	17	13		
0.65	5.0	53	47	46	10	0.65	5.0	7	11	6	10		
0.70	5.0	38	42	36	15	0.70	5.0	5	4	5	9		
0.50	3.5	58	56	45	16	0.50	3.5	15	25	20	16		
0.55	3.5	49	56	39	13	0.55	3.5	6	11	6	11		
0.60	3.5	41	43	29	10	0.60	3.5	5	8	7	5		
0.65	3.5	36	32	28	12	0.65	3.5	2	3	3	6		
0.70	3.5	26	27	15	8	0.70	3.5	1	1	2	2		
0.50	2.0	36	31	21	12	0.50	2.0	3	2	1	1		
0.55	2.0	24	20	17	6	0.55	2.0	2	1	1	1		
0.60	2.0	13	14	13	9	0.60	2.0	2	0	1	3		
0.65	2.0	13	16	7	2	0.65	2.0	1	1	1	0		
0.70	2.0	7	7	6	1	0.70	2.0	0	0	0	0		
0.50	1.0	11	15	3	3	0.50	1.0	0	2	0	0		
0.55	1.0	8	5	5	2	0.55	1.0	1	0	0	1		
0.60	1.0	2	3	1	2	0.60	1.0	0	0	0	1		
0.65	1.0	1	6	1	1	0.65	1.0	0	1	0	0		
0.70	1.0	2	4	0	1	0.70	1.0	0	0	0	0		
0.75	1.0	4	3	0	0	0.75	1.0	1	0	0	0		
0.80	1.0	1	0	1	0	0.80	1.0	0	0	1	0		
0.85	1.0	5	0	0	0	0.85	1.0	0	0	0	0		
0.90	1.0	1	1	0	0	0.90	1.0	1	0	0	0		
0.95	1.0	1	0	0	0	0.95	1.0	1	0	0	0		
0.75	2.0	6	10	2	4	0.75	2.0	1	2	1	1		
0.80	2.0	4	4	3	0	0.80	2.0	0	1	0	0		
0.85	2.0	3	1	3	1	0.85	2.0	0	0	0	0		
0.90	2.0	0	5	0	1	0.90	2.0	0	1	0	0		
0.95	2.0	2	1	3	1	0.95	2.0	1	0	0	0		
0.75	3.5	17	21	10	2	0.75	3.5	0	0	0	1		
0.80	3.5	17	16	12	3	0.80	3.5	1	2	2	0		
0.85	3.5	7	13	8	1	0.85	3.5	0	0	1	0		
0.90	3.5	8	9	8	0	0.90	3.5	0	0	1	0		
0.95	3.5	6	8	5	1	0.95	3.5	0	0	0	0		
0.75	5.0	32	40	26	7	0.75	5.0	1	4	6	1		
0.80	5.0	27	42	25	11	0.80	5.0	1	5	4	3		
0.85	5.0	17	32	11	8	0.85	5.0	1	1	0	1		
0.90	5.0	15	22	13	9	0.90	5.0	4	2	0	1		
0.95	5.0	14	14	11	8	0.95	5.0	0	2	0	1		

Table 19—Continued

total detection efficiency						Bright SHARC detection efficiency					
z	$L_{44}$	1st <sup>a</sup>	2nd <sup>a</sup>	3rd <sup>a</sup>	4th <sup>a</sup>	z	$L_{44}$	1st <sup>a</sup>	2nd <sup>a</sup>	3rd <sup>a</sup>	4th <sup>a</sup>
0.75	7.5	46	38	47	17	0.75	7.5	13	16	17	17
0.80	7.5	49	42	33	17	0.80	7.5	9	7	4	17
0.85	7.5	41	36	35	10	0.85	7.5	3	4	4	6
0.90	7.5	37	44	32	7	0.90	7.5	3	4	2	5
0.95	7.5	38	30	30	15	0.95	7.5	4	2	0	8
0.75	10.0	32	16	26	13	0.75	10.0	46	34	37	9
0.80	10.0	31	18	22	12	0.80	10.0	33	29	23	13
0.85	10.0	37	17	27	9	0.85	10.0	11	22	31	8
0.90	10.0	41	25	30	14	0.90	10.0	8	13	9	13
0.95	10.0	32	26	33	7	0.95	10.0	5	10	6	12

Table 20. Recovered luminosity percentage for the  $c_r=100$  kpc set of parameters

total sample							Bright SHARC sample						
z	$L_{44}$	1st <sup>a</sup>	2nd <sup>a</sup>	3rd <sup>a</sup>	4th <sup>a</sup>	z	$L_{44}$	1st <sup>a</sup>	2nd <sup>a</sup>	3rd <sup>a</sup>	4th <sup>a</sup>		
0.25	1.0	113	104	105	122	0.25	1.0	122	105	114	122		
0.30	1.0	116	108	106	123	0.30	1.0	157	152	142	121		
0.35	1.0	121	103	97	118	0.35	1.0	999	140	164	159		
0.40	1.0	124	97	111	168	0.40	1.0	0	0	0	999		
0.45	1.0	143	143	124	139	0.45	1.0	0	0	0	0		
0.25	2.0	108	103	108	125	0.25	2.0	108	103	108	125		
0.30	2.0	103	98	96	127	0.30	2.0	103	98	96	127		
0.35	2.0	99	94	94	125	0.35	2.0	105	96	98	125		
0.40	2.0	100	99	98	133	0.40	2.0	133	146	131	135		
0.45	2.0	97	97	93	142	0.45	2.0	181	148	142	155		
0.25	3.5	105	103	105	120	0.25	3.5	105	103	105	120		
0.30	3.5	101	98	100	120	0.30	3.5	101	98	100	120		
0.35	3.5	95	92	94	126	0.35	3.5	95	92	94	126		
0.40	3.5	95	93	95	119	0.40	3.5	95	93	95	119		
0.45	3.5	93	94	91	117	0.45	3.5	98	95	93	117		
0.25	5.0	106	102	103	121	0.25	5.0	106	102	103	121		
0.30	5.0	100	97	98	119	0.30	5.0	100	97	98	119		
0.35	5.0	96	93	95	123	0.35	5.0	96	93	95	123		
0.40	5.0	92	92	94	119	0.40	5.0	92	92	94	119		
0.45	5.0	95	93	91	119	0.45	5.0	95	93	91	119		
0.25	7.5	101	101	103	121	0.25	7.5	101	101	103	121		
0.30	7.5	98	97	98	122	0.30	7.5	98	97	98	122		
0.35	7.5	93	94	93	118	0.35	7.5	93	94	93	118		
0.40	7.5	90	93	92	126	0.40	7.5	90	93	92	126		
0.45	7.5	88	91	92	118	0.45	7.5	88	91	92	118		
0.25	10.0	101	101	102	121	0.25	10.0	101	101	102	121		
0.30	10.0	96	97	98	119	0.30	10.0	96	97	98	119		
0.35	10.0	94	94	94	116	0.35	10.0	94	94	94	116		
0.40	10.0	89	91	92	115	0.40	10.0	89	91	92	115		
0.45	10.0	89	88	90	120	0.45	10.0	89	88	90	120		
0.50	10.0	93	88	91	114	0.50	10.0	93	88	91	114		
0.55	10.0	93	91	90	116	0.55	10.0	93	91	90	116		
0.60	10.0	90	89	94	121	0.60	10.0	90	89	94	121		
0.65	10.0	86	90	91	118	0.65	10.0	86	90	91	118		
0.70	10.0	94	91	93	131	0.70	10.0	94	91	93	131		
0.50	7.5	88	96	87	115	0.50	7.5	88	96	87	115		
0.55	7.5	94	89	92	122	0.55	7.5	94	89	92	122		
0.60	7.5	88	95	88	117	0.60	7.5	88	95	88	117		
0.65	7.5	98	91	88	119	0.65	7.5	101	91	89	119		

Table 20—Continued

total sample							Bright SHARC sample						
z	$L_{44}$	1st <sup>a</sup>	2nd <sup>a</sup>	3rd <sup>a</sup>	4th <sup>a</sup>	z	$L_{44}$	1st <sup>a</sup>	2nd <sup>a</sup>	3rd <sup>a</sup>	4th <sup>a</sup>		
0.50	5.0	95	93	91	114	0.50	5.0	95	93	91	114		
0.55	5.0	94	94	91	124	0.55	5.0	102	96	94	124		
0.60	5.0	92	92	91	112	0.60	5.0	104	103	109	112		
0.65	5.0	98	91	89	121	0.65	5.0	161	117	111	121		
0.70	5.0	98	92	91	122	0.70	5.0	148	119	118	132		
0.50	3.5	91	95	91	133	0.50	3.5	104	109	101	133		
0.55	3.5	97	93	96	129	0.55	3.5	134	128	142	132		
0.60	3.5	93	99	108	124	0.60	3.5	130	137	167	131		
0.65	3.5	91	101	103	161	0.65	3.5	172	199	139	193		
0.70	3.5	100	94	105	144	0.70	3.5	999	178	182	157		
0.50	2.0	111	97	97	125	0.50	2.0	150	187	175	999		
0.55	2.0	159	116	111	133	0.55	2.0	999	999	175	156		
0.60	2.0	134	106	119	186	0.60	2.0	190	0	999	999		
0.65	2.0	126	125	147	132	0.65	2.0	999	999	999	0		
0.70	2.0	192	128	158	111	0.70	2.0	0	0	0	0		
0.50	1.0	179	164	135	175	0.50	1.0	0	999	0	0		
0.55	1.0	188	121	144	999	0.55	1.0	999	0	0	999		
0.60	1.0	117	187	121	999	0.60	1.0	0	0	0	0		
0.65	1.0	999	999	999	188	0.65	1.0	0	0	0	0		
0.70	1.0	999	999	0	999	0.70	1.0	0	0	0	0		
0.75	1.0	999	999	0	0	0.75	1.0	999	0	0	0		
0.80	1.0	999	0	999	0	0.80	1.0	0	0	999	0		
0.85	1.0	999	0	0	0	0.85	1.0	0	0	0	0		
0.90	1.0	999	999	0	0	0.90	1.0	999	0	0	0		
0.95	1.0	999	0	0	0	0.95	1.0	999	0	0	0		
0.75	2.0	999	165	999	999	0.75	2.0	999	999	999	999		
0.80	2.0	148	999	999	0	0.80	2.0	0	999	0	0		
0.85	2.0	106	999	999	999	0.85	2.0	0	0	0	0		
0.90	2.0	0	999	0	158	0.90	2.0	0	999	0	0		
0.95	2.0	999	999	999	999	0.95	2.0	999	0	0	0		
0.75	3.5	104	106	122	152	0.75	3.5	0	0	0	0	182	
0.80	3.5	118	119	140	119	0.80	3.5	999	999	999	999	0	
0.85	3.5	104	117	153	141	0.85	3.5	0	0	999	0		
0.90	3.5	108	120	138	0	0.90	3.5	0	0	999	0		
0.95	3.5	145	121	135	179	0.95	3.5	0	0	0	0		
0.75	5.0	94	96	108	124	0.75	5.0	180	133	168	169		
0.80	5.0	102	102	120	145	0.80	5.0	164	188	999	999		
0.85	5.0	101	98	100	136	0.85	5.0	165	174	0	999		
0.90	5.0	139	111	118	156	0.90	5.0	999	169	0	999		
0.95	5.0	127	124	121	174	0.95	5.0	0	999	0	198		

Table 20—Continued

total sample						Bright SHARC sample					
z	$L_{44}$	1st <sup>a</sup>	2nd <sup>a</sup>	3rd <sup>a</sup>	4th <sup>a</sup>	z	$L_{44}$	1st <sup>a</sup>	2nd <sup>a</sup>	3rd <sup>a</sup>	4th <sup>a</sup>
0.75	7.5	98	91	88	121	0.75	7.5	144	104	104	121
0.80	7.5	88	88	91	143	0.80	7.5	128	113	121	143
0.85	7.5	86	90	92	130	0.85	7.5	115	126	126	142
0.90	7.5	87	92	92	120	0.90	7.5	152	131	151	125
0.95	7.5	97	95	92	146	0.95	7.5	152	190	0	168
0.75	10.0	87	92	88	123	0.75	10.0	87	93	88	123
0.80	10.0	92	92	87	139	0.80	10.0	94	93	90	139
0.85	10.0	85	97	92	124	0.85	10.0	107	109	96	124
0.90	10.0	90	88	90	134	0.90	10.0	117	103	115	134
0.95	10.0	87	95	90	139	0.95	10.0	123	125	118	139

Table 21. Detection efficiency percentage for the  $c_r=400$  kpc set of parameters

<i>total detection efficiency</i>						<i>Bright SHARC detection efficiency</i>					
<i>z</i>	$L_{44}$	1st <sup>a</sup>	2nd <sup>a</sup>	3rd <sup>a</sup>	4th <sup>a</sup>	<i>z</i>	$L_{44}$	1st <sup>a</sup>	2nd <sup>a</sup>	3rd <sup>a</sup>	4th <sup>a</sup>
0.25	1.0	13	9	4	5	0.25	1.0	0	3	0	1
0.30	1.0	8	7	3	2	0.30	1.0	0	0	0	0
0.35	1.0	7	4	4	2	0.35	1.0	0	0	0	0
0.40	1.0	2	1	4	3	0.40	1.0	0	0	0	1
0.45	1.0	2	0	2	1	0.45	1.0	0	0	0	0
0.25	2.0	27	32	18	24	0.25	2.0	19	31	14	23
0.30	2.0	35	25	19	13	0.30	2.0	9	12	7	10
0.35	2.0	14	23	14	18	0.35	2.0	3	3	5	11
0.40	2.0	14	17	6	11	0.40	2.0	1	0	1	4
0.45	2.0	8	14	7	8	0.45	2.0	0	0	0	4
0.25	3.5	51	48	40	45	0.25	3.5	50	48	40	45
0.30	3.5	52	52	28	38	0.30	3.5	49	52	28	38
0.35	3.5	37	53	37	27	0.35	3.5	28	50	36	27
0.40	3.5	45	41	27	27	0.40	3.5	20	28	21	26
0.45	3.5	35	35	30	19	0.45	3.5	7	10	12	15
0.25	5.0	49	63	48	51	0.25	5.0	49	63	48	51
0.30	5.0	54	56	52	37	0.30	5.0	54	56	52	37
0.35	5.0	57	58	39	40	0.35	5.0	56	58	39	40
0.40	5.0	54	48	41	43	0.40	5.0	50	47	41	43
0.45	5.0	46	51	35	27	0.45	5.0	31	45	32	27
0.25	7.5	63	68	52	62	0.25	7.5	63	68	52	62
0.30	7.5	60	69	53	59	0.30	7.5	60	69	53	59
0.35	7.5	66	73	60	57	0.35	7.5	65	73	60	57
0.40	7.5	71	68	59	59	0.40	7.5	71	68	59	59
0.45	7.5	59	65	50	45	0.45	7.5	59	65	50	44
0.25	10.0	69	79	64	68	0.25	10.0	69	79	64	68
0.30	10.0	79	74	64	62	0.30	10.0	79	74	64	62
0.35	10.0	71	79	70	75	0.35	10.0	71	79	70	75
0.40	10.0	80	82	66	55	0.40	10.0	80	82	66	55
0.45	10.0	65	72	58	62	0.45	10.0	64	72	58	62
0.50	10.0	69	75	57	57	0.50	10.0	68	75	57	57
0.55	10.0	57	73	56	51	0.55	10.0	55	73	55	51
0.60	10.0	61	63	49	54	0.60	10.0	55	63	49	54
0.65	10.0	60	67	53	37	0.65	10.0	42	63	51	37
0.70	10.0	56	62	36	41	0.70	10.0	27	51	34	41
0.50	7.5	58	60	47	42	0.50	7.5	52	60	47	42
0.55	7.5	45	62	49	35	0.55	7.5	31	59	46	32
0.60	7.5	51	58	41	42	0.60	7.5	26	45	28	41
0.65	7.5	43	42	26	25	0.65	7.5	11	26	9	23

Table 21—Continued

total detection efficiency							Bright SHARC detection efficiency						
z	$L_{44}$	1st <sup>a</sup>	2nd <sup>a</sup>	3rd <sup>a</sup>	4th <sup>a</sup>	z	$L_{44}$	1st <sup>a</sup>	2nd <sup>a</sup>	3rd <sup>a</sup>	4th <sup>a</sup>		
0.50	5.0	37	43	26	29	0.50	5.0	13	24	19	27		
0.55	5.0	35	36	28	27	0.55	5.0	4	10	9	22		
0.60	5.0	32	37	26	27	0.60	5.0	0	2	5	12		
0.65	5.0	25	25	21	19	0.65	5.0	1	2	2	10		
0.70	5.0	19	19	11	7	0.70	5.0	0	0	0	1		
0.50	3.5	28	30	14	28	0.50	3.5	4	4	3	13		
0.55	3.5	22	23	16	9	0.55	3.5	1	0	2	1		
0.60	3.5	13	23	6	6	0.60	3.5	0	1	0	4		
0.65	3.5	11	9	5	7	0.65	3.5	2	0	0	2		
0.70	3.5	9	3	6	3	0.70	3.5	0	0	0	1		
0.50	2.0	5	4	4	6	0.50	2.0	0	0	1	2		
0.55	2.0	1	8	2	1	0.55	2.0	0	1	0	0		
0.60	2.0	6	3	1	2	0.60	2.0	0	0	0	1		
0.65	2.0	3	0	0	1	0.65	2.0	0	0	0	0		
0.70	2.0	2	3	2	0	0.70	2.0	0	1	0	0		
0.50	1.0	1	4	0	0	0.50	1.0	0	0	0	0		
0.55	1.0	1	3	1	1	0.55	1.0	0	0	0	0		
0.60	1.0	6	0	0	0	0.60	1.0	0	0	0	0		
0.65	1.0	0	1	0	0	0.65	1.0	0	0	0	0		
0.70	1.0	0	3	1	0	0.70	1.0	0	0	0	0		
0.75	1.0	4	0	1	0	0.75	1.0	3	0	0	0		
0.80	1.0	2	0	0	0	0.80	1.0	2	0	0	0		
0.85	1.0	0	0	0	1	0.85	1.0	0	0	0	0		
0.90	1.0	1	0	0	0	0.90	1.0	0	0	0	0		
0.95	1.0	0	1	0	0	0.95	1.0	0	0	0	0		
0.75	2.0	2	0	0	0	0.75	2.0	0	0	0	0		
0.80	2.0	0	1	1	0	0.80	2.0	0	0	0	0		
0.85	2.0	2	1	2	0	0.85	2.0	0	0	0	0		
0.90	2.0	1	1	1	0	0.90	2.0	0	0	1	0		
0.95	2.0	0	1	0	0	0.95	2.0	0	0	0	0		
0.75	3.5	7	5	5	2	0.75	3.5	0	0	0	0		
0.80	3.5	2	5	1	3	0.80	3.5	0	0	0	2		
0.85	3.5	3	3	2	1	0.85	3.5	0	1	0	0		
0.90	3.5	0	4	3	0	0.90	3.5	0	0	0	0		
0.95	3.5	2	3	1	1	0.95	3.5	0	0	0	0		
0.75	5.0	14	12	13	4	0.75	5.0	1	0	1	1		
0.80	5.0	11	8	1	6	0.80	5.0	0	1	0	1		
0.85	5.0	5	5	1	0	0.85	5.0	0	0	0	0		
0.90	5.0	7	5	2	2	0.90	5.0	0	0	1	0		
0.95	5.0	4	3	0	1	0.95	5.0	0	0	0	0		

Table 21—Continued

total detection efficiency						Bright SHARC detection efficiency					
z	$L_{44}$	1st <sup>a</sup>	2nd <sup>a</sup>	3rd <sup>a</sup>	4th <sup>a</sup>	z	$L_{44}$	1st <sup>a</sup>	2nd <sup>a</sup>	3rd <sup>a</sup>	4th <sup>a</sup>
0.75	7.5	33	41	25	23	0.75	7.5	1	8	6	18
0.80	7.5	26	24	15	13	0.80	7.5	1	0	2	6
0.85	7.5	19	22	16	18	0.85	7.5	4	2	2	7
0.90	7.5	15	22	9	10	0.90	7.5	0	1	0	2
0.95	7.5	9	15	6	3	0.95	7.5	0	0	0	1
0.75	10.0	46	44	39	32	0.75	10.0	12	26	19	28
0.80	10.0	40	45	39	22	0.80	10.0	5	16	10	18
0.85	10.0	29	47	20	24	0.85	10.0	2	7	3	18
0.90	10.0	37	29	25	18	0.90	10.0	4	2	5	6
0.95	10.0	21	31	18	18	0.95	10.0	4	5	1	9

Table 22. Recovered luminosity percentage for the  $c_r=400$  kpc set of parameters

total sample						Bright SHARC sample					
z	$L_{44}$	1st <sup>a</sup>	2nd <sup>a</sup>	3rd <sup>a</sup>	4th <sup>a</sup>	z	$L_{44}$	1st <sup>a</sup>	2nd <sup>a</sup>	3rd <sup>a</sup>	4th <sup>a</sup>
0.25	1.0	98	101	99	104	0.25	1.0	0	113	0	90
0.30	1.0	115	97	115	105	0.30	1.0	0	0	0	0
0.35	1.0	120	77	113	87	0.35	1.0	0	0	0	0
0.40	1.0	113	85	110	197	0.40	1.0	0	0	0	999
0.45	1.0	99	0	121	192	0.45	1.0	0	0	0	0
0.25	2.0	96	91	93	98	0.25	2.0	94	91	94	99
0.30	2.0	90	83	97	97	0.30	2.0	94	87	123	101
0.35	2.0	87	82	91	114	0.35	2.0	116	110	103	126
0.40	2.0	99	84	85	109	0.40	2.0	193	0	99	123
0.45	2.0	114	84	87	146	0.45	2.0	0	0	0	199
0.25	3.5	94	91	93	99	0.25	3.5	94	91	93	99
0.30	3.5	88	85	89	99	0.30	3.5	88	85	89	99
0.35	3.5	89	81	82	97	0.35	3.5	90	82	82	97
0.40	3.5	85	80	82	104	0.40	3.5	85	84	85	104
0.45	3.5	83	80	79	95	0.45	3.5	95	92	86	98
0.25	5.0	92	90	91	100	0.25	5.0	92	90	91	100
0.30	5.0	88	86	86	100	0.30	5.0	88	86	86	100
0.35	5.0	85	84	83	100	0.35	5.0	85	84	83	100
0.40	5.0	82	79	80	95	0.40	5.0	82	79	80	95
0.45	5.0	80	80	80	106	0.45	5.0	82	82	80	106
0.25	7.5	89	89	90	100	0.25	7.5	89	89	90	100
0.30	7.5	87	85	87	99	0.30	7.5	87	85	87	99
0.35	7.5	84	82	82	99	0.35	7.5	83	82	82	99
0.40	7.5	79	79	80	97	0.40	7.5	79	79	80	97
0.45	7.5	77	80	79	100	0.45	7.5	77	80	79	101
0.25	10.0	89	91	90	100	0.25	10.0	89	91	90	100
0.30	10.0	85	85	85	99	0.30	10.0	85	85	85	99
0.35	10.0	84	83	82	99	0.35	10.0	84	83	82	99
0.40	10.0	79	81	81	99	0.40	10.0	79	81	81	99
0.45	10.0	79	78	78	97	0.45	10.0	79	78	78	97
0.50	10.0	77	77	77	100	0.50	10.0	77	77	77	100
0.55	10.0	77	77	77	97	0.55	10.0	77	77	78	97
0.60	10.0	74	75	75	97	0.60	10.0	75	75	75	97
0.65	10.0	74	75	75	97	0.65	10.0	75	75	75	97
0.70	10.0	75	75	77	99	0.70	10.0	79	77	77	99
0.50	7.5	80	78	77	97	0.50	7.5	80	78	77	97
0.55	7.5	77	77	78	92	0.55	7.5	80	78	78	93
0.60	7.5	76	74	73	98	0.60	7.5	81	76	75	99
0.65	7.5	82	79	75	100	0.65	7.5	107	83	83	102

Table 22—Continued

total sample							Bright SHARC sample						
z	$L_{44}$	1st <sup>a</sup>	2nd <sup>a</sup>	3rd <sup>a</sup>	4th <sup>a</sup>	z	$L_{44}$	1st <sup>a</sup>	2nd <sup>a</sup>	3rd <sup>a</sup>	4th <sup>a</sup>		
0.50	5.0	102	80	87	99	0.50	5.0	102	80	87	99		
0.55	5.0	91	91	91	105	0.55	5.0	91	91	91	105		
0.60	5.0	0	79	93	104	0.60	5.0	0	79	93	104		
0.65	5.0	999	111	113	124	0.65	5.0	999	111	113	124		
0.70	5.0	0	0	0	132	0.70	5.0	0	0	0	132		
0.50	3.5	85	79	80	100	0.50	3.5	121	96	100	111		
0.55	3.5	86	80	88	101	0.55	3.5	170	0	140	130		
0.60	3.5	85	999	88	159	0.60	3.5	0	999	0	187		
0.65	3.5	127	83	100	139	0.65	3.5	999	0	0	999		
0.70	3.5	103	73	97	999	0.70	3.5	0	0	0	999		
0.50	2.0	101	97	106	142	0.50	2.0	0	0	191	999		
0.55	2.0	145	115	122	197	0.55	2.0	0	999	0	0		
0.60	2.0	109	92	119	198	0.60	2.0	0	0	0	999		
0.65	2.0	169	0	0	198	0.65	2.0	0	0	0	0		
0.70	2.0	154	999	122	0	0.70	2.0	0	999	0	0		
0.50	1.0	145	164	0	0	0.50	1.0	0	0	0	0		
0.55	1.0	999	999	115	999	0.55	1.0	0	0	0	0		
0.60	1.0	999	0	0	0	0.60	1.0	0	0	0	0		
0.65	1.0	0	999	0	0	0.65	1.0	0	0	0	0		
0.70	1.0	0	999	999	0	0.70	1.0	0	0	0	0		
0.75	1.0	999	0	999	0	0.75	1.0	999	0	0	0		
0.80	1.0	999	0	0	0	0.80	1.0	999	0	0	0		
0.85	1.0	0	0	0	999	0.85	1.0	0	0	0	0		
0.90	1.0	999	0	0	0	0.90	1.0	0	0	0	0		
0.95	1.0	0	999	0	0	0.95	1.0	0	0	0	0		
0.75	2.0	131	0	0	0	0.75	2.0	0	0	0	0		
0.80	2.0	0	163	189	0	0.80	2.0	0	0	0	0		
0.85	2.0	999	999	999	0	0.85	2.0	0	0	0	0		
0.90	2.0	999	195	999	0	0.90	2.0	0	0	999	0		
0.95	2.0	0	999	0	0	0.95	2.0	0	0	0	0		
0.75	3.5	144	96	141	135	0.75	3.5	0	0	0	0		
0.80	3.5	86	134	105	999	0.80	3.5	0	0	0	999		
0.85	3.5	120	185	138	185	0.85	3.5	0	999	0	0		
0.90	3.5	0	130	77	0	0.90	3.5	0	0	0	0		
0.95	3.5	174	193	999	999	0.95	3.5	0	0	0	0		
0.75	5.0	106	83	104	114	0.75	5.0	999	0	999	150		
0.80	5.0	101	116	97	119	0.80	5.0	0	999	0	172		
0.85	5.0	98	98	100	0	0.85	5.0	0	0	0	0		
0.90	5.0	98	94	145	150	0.90	5.0	0	0	184	0		
0.95	5.0	101	97	0	109	0.95	5.0	0	0	0	0		

Table 22—Continued

total sample						Bright SHARC sample					
z	$L_{44}$	1st <sup>a</sup>	2nd <sup>a</sup>	3rd <sup>a</sup>	4th <sup>a</sup>	z	$L_{44}$	1st <sup>a</sup>	2nd <sup>a</sup>	3rd <sup>a</sup>	4th <sup>a</sup>
0.75	7.5	80	83	84	107	0.75	7.5	118	114	113	111
0.80	7.5	80	77	86	105	0.80	7.5	193	0	151	111
0.85	7.5	106	89	88	103	0.85	7.5	188	140	150	107
0.90	7.5	85	86	78	119	0.90	7.5	0	153	0	182
0.95	7.5	103	84	90	148	0.95	7.5	0	0	0	999
0.75	10.0	78	76	74	97	0.75	10.0	98	82	79	100
0.80	10.0	75	74	72	101	0.80	10.0	83	82	84	106
0.85	10.0	77	78	72	103	0.85	10.0	120	104	84	109
0.90	10.0	77	77	79	93	0.90	10.0	118	113	97	101
0.95	10.0	135	85	78	115	0.95	10.0	999	109	107	136

Table 23. Detection efficiency percentage for the ellipticity equal to 0.01 set of parameters

<i>total detection efficiency</i>						<i>Bright SHARC detection efficiency</i>					
<i>z</i>	<i>L</i> <sub>44</sub>	1st <sup>a</sup>	2nd <sup>a</sup>	3rd <sup>a</sup>	4th <sup>a</sup>	<i>z</i>	<i>L</i> <sub>44</sub>	1st <sup>a</sup>	2nd <sup>a</sup>	3rd <sup>a</sup>	4th <sup>a</sup>
0.25	1.0	39	46	31	29	0.25	1.0	7	10	8	21
0.30	1.0	25	33	17	16	0.30	1.0	2	1	2	3
0.35	1.0	15	20	17	13	0.35	1.0	0	0	0	0
0.40	1.0	6	16	11	5	0.40	1.0	0	1	0	0
0.45	1.0	7	11	5	1	0.45	1.0	0	1	0	0
0.25	2.0	63	74	68	44	0.25	2.0	59	74	68	44
0.30	2.0	67	75	52	46	0.30	2.0	42	66	50	46
0.35	2.0	59	75	42	34	0.35	2.0	9	27	18	29
0.40	2.0	42	42	29	32	0.40	2.0	2	3	5	20
0.45	2.0	26	35	27	17	0.45	2.0	1	2	3	4
0.25	3.5	85	92	82	63	0.25	3.5	85	92	82	63
0.30	3.5	74	91	80	73	0.30	3.5	74	91	80	73
0.35	3.5	74	87	70	55	0.35	3.5	73	86	70	55
0.40	3.5	74	79	65	46	0.40	3.5	59	79	64	46
0.45	3.5	70	66	56	44	0.45	3.5	20	30	26	40
0.25	5.0	95	96	92	65	0.25	5.0	95	96	92	65
0.30	5.0	86	93	93	62	0.30	5.0	86	93	93	62
0.35	5.0	83	94	80	54	0.35	5.0	83	94	80	54
0.40	5.0	87	88	80	63	0.40	5.0	85	88	80	63
0.45	5.0	86	84	76	57	0.45	5.0	80	84	76	56
0.25	7.5	94	99	96	63	0.25	7.5	94	99	96	63
0.30	7.5	96	99	100	64	0.30	7.5	96	99	100	64
0.35	7.5	98	99	97	58	0.35	7.5	98	99	97	58
0.40	7.5	92	95	89	52	0.40	7.5	92	95	89	52
0.45	7.5	94	93	95	54	0.45	7.5	93	93	95	54
0.25	10.0	97	99	98	69	0.25	10.0	97	99	98	69
0.30	10.0	97	100	100	68	0.30	10.0	98	100	100	71
0.35	10.0	99	99	98	64	0.35	10.0	99	100	98	65
0.40	10.0	94	97	93	59	0.40	10.0	94	98	93	60
0.45	10.0	95	94	96	61	0.45	10.0	93	97	96	59
0.50	10.0	92	98	85	63	0.50	10.0	91	97	88	62
0.55	10.0	92	93	92	58	0.55	10.0	93	95	95	54
0.60	10.0	89	92	83	58	0.60	10.0	77	91	84	61
0.65	10.0	85	86	79	55	0.65	10.0	61	79	75	60
0.70	10.0	81	90	73	51	0.70	10.0	61	71	70	60
0.50	7.5	90	96	80	58	0.50	7.5	88	96	80	58
0.55	7.5	90	88	86	48	0.55	7.5	88	88	86	48
0.60	7.5	83	86	77	55	0.60	7.5	66	85	76	54
0.65	7.5	81	82	74	50	0.65	7.5	30	53	46	50

Table 23—Continued

total detection efficiency							Bright SHARC detection efficiency						
z	$L_{44}$	1st <sup>a</sup>	2nd <sup>a</sup>	3rd <sup>a</sup>	4th <sup>a</sup>	z	$L_{44}$	1st <sup>a</sup>	2nd <sup>a</sup>	3rd <sup>a</sup>	4th <sup>a</sup>		
0.50	5.0	74	90	78	56	0.50	5.0	41	79	69	56		
0.55	5.0	73	80	57	39	0.55	5.0	10	36	26	38		
0.60	5.0	58	64	62	34	0.60	5.0	8	15	10	27		
0.65	5.0	43	60	48	31	0.65	5.0	1	5	5	13		
0.70	5.0	40	49	38	19	0.70	5.0	2	3	4	5		
0.50	3.5	56	64	56	41	0.50	3.5	9	12	20	33		
0.55	3.5	44	60	38	31	0.55	3.5	1	3	1	17		
0.60	3.5	44	47	31	20	0.60	3.5	2	3	1	5		
0.65	3.5	32	28	15	16	0.65	3.5	0	1	0	5		
0.70	3.5	26	30	7	13	0.70	3.5	0	0	0	1		
0.50	2.0	22	29	13	10	0.50	2.0	1	3	0	2		
0.55	2.0	14	14	8	5	0.55	2.0	0	0	0	1		
0.60	2.0	8	10	9	2	0.60	2.0	0	0	0	0		
0.65	2.0	7	10	4	2	0.65	2.0	0	0	0	1		
0.70	2.0	6	6	4	5	0.70	2.0	0	0	0	0		
0.50	1.0	3	3	2	1	0.50	1.0	0	0	0	0		
0.55	1.0	1	3	3	0	0.55	1.0	0	0	0	0		
0.60	1.0	1	3	2	0	0.60	1.0	0	0	0	0		
0.65	1.0	1	1	1	0	0.65	1.0	0	0	0	0		
0.70	1.0	1	2	2	1	0.70	1.0	0	0	0	1		
0.75	1.0	1	0	1	0	0.75	1.0	0	0	0	0		
0.80	1.0	0	1	0	0	0.80	1.0	1	0	0	0		
0.85	1.0	0	1	0	0	0.85	1.0	0	0	0	0		
0.90	1.0	1	1	0	0	0.90	1.0	1	0	0	0		
0.95	1.0	1	1	0	0	0.95	1.0	0	1	0	0		
0.75	2.0	3	1	0	0	0.75	2.0	0	0	0	0		
0.80	2.0	3	1	0	0	0.80	2.0	0	0	0	0		
0.85	2.0	0	1	1	0	0.85	2.0	0	0	0	0		
0.90	2.0	0	0	0	2	0.90	2.0	0	0	0	0		
0.95	2.0	0	1	0	0	0.95	2.0	0	0	0	0		
0.75	3.5	12	18	4	5	0.75	3.5	2	0	0	0		
0.80	3.5	19	15	6	8	0.80	3.5	0	0	0	0		
0.85	3.5	10	9	5	3	0.85	3.5	0	0	0	0		
0.90	3.5	12	5	4	0	0.90	3.5	0	0	0	0		
0.95	3.5	3	3	2	2	0.95	3.5	0	0	0	0		
0.75	5.0	36	42	23	19	0.75	5.0	0	1	0	1		
0.80	5.0	28	30	20	16	0.80	5.0	0	0	0	1		
0.85	5.0	25	16	13	6	0.85	5.0	1	0	0	0		
0.90	5.0	16	19	8	8	0.90	5.0	0	2	0	0		
0.95	5.0	10	10	6	4	0.95	5.0	0	0	0	0		

Table 23—Continued

<i>total detection efficiency</i>						<i>Bright SHARC detection efficiency</i>					
z	$L_{44}$	1st <sup>a</sup>	2nd <sup>a</sup>	3rd <sup>a</sup>	4th <sup>a</sup>	z	$L_{44}$	1st <sup>a</sup>	2nd <sup>a</sup>	3rd <sup>a</sup>	4th <sup>a</sup>
0.75	7.5	57	73	55	33	0.75	7.5	1	1	1	1
0.80	7.5	58	56	39	37	0.80	7.5	1	0	2	4
0.85	7.5	48	49	35	25	0.85	7.5	2	0	0	0
0.90	7.5	33	44	30	23	0.90	7.5	1	0	2	0
0.95	7.5	20	37	19	18	0.95	7.5	1	0	0	0
0.75	10.0	67	83	64	43	0.75	10.0	7	13	9	29
0.80	10.0	61	72	59	57	0.80	10.0	4	8	5	28
0.85	10.0	68	69	65	45	0.85	10.0	5	1	3	6
0.90	10.0	33	44	30	23	0.90	10.0	5	1	0	2
0.95	10.0	20	25	20	10	0.95	10.0	1	0	0	5

Table 24. Recovered luminosity percentage for the ellipticity equal to 0.01 set of parameters

total sample						Bright SHARC sample					
z	$L_{44}$	1st <sup>a</sup>	2nd <sup>a</sup>	3rd <sup>a</sup>	4th <sup>a</sup>	z	$L_{44}$	1st <sup>a</sup>	2nd <sup>a</sup>	3rd <sup>a</sup>	4th <sup>a</sup>
0.25	1.0	116	101	104	123	0.25	1.0	133	106	111	128
0.30	1.0	112	99	114	115	0.30	1.0	196	137	176	139
0.35	1.0	132	92	89	120	0.35	1.0	0	0	0	0
0.40	1.0	110	120	122	139	0.40	1.0	0	200	0	0
0.45	1.0	115	161	129	999	0.45	1.0	0	999	0	0
0.25	2.0	110	101	103	114	0.25	2.0	109	101	103	114
0.30	2.0	100	96	97	115	0.30	2.0	97	97	97	115
0.35	2.0	98	91	94	114	0.35	2.0	109	99	101	117
0.40	2.0	95	93	94	112	0.40	2.0	122	155	111	118
0.45	2.0	98	101	94	124	0.45	2.0	148	159	152	147
0.25	3.5	105	102	102	116	0.25	3.5	105	102	102	116
0.30	3.5	96	95	96	115	0.30	3.5	96	95	96	115
0.35	3.5	95	93	95	114	0.35	3.5	95	93	95	114
0.40	3.5	90	90	90	111	0.40	3.5	90	90	90	111
0.45	3.5	91	86	88	110	0.45	3.5	104	92	97	110
0.25	5.0	101	101	101	115	0.25	5.0	101	101	101	115
0.30	5.0	97	96	97	114	0.30	5.0	97	96	97	114
0.35	5.0	93	95	93	113	0.35	5.0	93	95	93	113
0.40	5.0	90	89	90	112	0.40	5.0	90	89	90	112
0.45	5.0	89	88	88	110	0.45	5.0	90	88	88	110
0.25	7.5	103	101	101	112	0.25	7.5	103	101	101	112
0.30	7.5	96	95	96	115	0.30	7.5	96	95	96	115
0.35	7.5	93	93	92	111	0.35	7.5	93	93	92	111
0.40	7.5	90	90	89	111	0.40	7.5	90	90	89	111
0.45	7.5	87	87	87	115	0.45	7.5	87	87	87	115
0.25	10.0	103	101	101	112	0.25	10.0	103	101	101	112
0.30	10.0	96	95	96	115	0.30	10.0	96	95	96	115
0.35	10.0	93	93	92	111	0.35	10.0	93	93	92	111
0.40	10.0	90	90	89	111	0.40	10.0	90	90	89	111
0.45	10.0	87	87	87	115	0.45	10.0	87	87	87	115
0.50	10.0	87	87	85	112	0.50	10.0	87	87	85	112
0.55	10.0	84	87	83	111	0.55	10.0	84	87	83	111
0.60	10.0	84	86	85	117	0.60	10.0	87	86	85	118
0.65	10.0	83	85	83	110	0.65	10.0	91	88	87	110
0.70	10.0	86	82	82	117	0.70	10.0	115	89	89	119
0.50	7.5	87	87	85	112	0.50	7.5	87	87	85	112
0.55	7.5	84	87	83	111	0.55	7.5	84	87	83	111
0.60	7.5	84	86	85	117	0.60	7.5	87	86	85	118
0.65	7.5	83	85	83	110	0.65	7.5	91	88	87	110

Table 24—Continued

total sample							Bright SHARC sample						
z	$L_{44}$	1st <sup>a</sup>	2nd <sup>a</sup>	3rd <sup>a</sup>	4th <sup>a</sup>	z	$L_{44}$	1st <sup>a</sup>	2nd <sup>a</sup>	3rd <sup>a</sup>	4th <sup>a</sup>		
0.50	5.0	87	86	85	115	0.50	5.0	90	87	86	115		
0.55	5.0	83	84	85	115	0.55	5.0	97	91	92	116		
0.60	5.0	86	89	82	115	0.60	5.0	102	111	102	120		
0.65	5.0	85	86	88	117	0.65	5.0	120	119	131	133		
0.70	5.0	90	87	88	114	0.70	5.0	139	156	130	129		
0.50	3.5	89	88	90	114	0.50	3.5	114	106	102	115		
0.55	3.5	85	89	92	120	0.55	3.5	140	120	159	136		
0.60	3.5	96	91	95	109	0.60	3.5	197	150	999	112		
0.65	3.5	89	98	91	137	0.65	3.5	0	177	0	168		
0.70	3.5	103	96	104	119	0.70	3.5	0	0	0	164		
0.50	2.0	189	105	95	130	0.50	2.0	999	165	0	186		
0.55	2.0	122	105	89	169	0.55	2.0	0	0	0	999		
0.60	2.0	119	117	105	110	0.60	2.0	0	0	0	0		
0.65	2.0	128	116	129	999	0.65	2.0	0	0	0	999		
0.70	2.0	148	120	167	176	0.70	2.0	0	0	0	0		
0.50	1.0	185	165	157	999	0.50	1.0	0	0	0	0		
0.55	1.0	999	137	167	0	0.55	1.0	0	0	0	0		
0.60	1.0	999	999	197	0	0.60	1.0	0	0	0	0		
0.65	1.0	121	197	999	0	0.65	1.0	0	0	0	0		
0.70	1.0	999	999	999	999	0.70	1.0	0	0	999	999		
0.75	1.0	999	0	176	0	0.75	1.0	0	0	0	0		
0.80	1.0	0	999	0	0	0.80	1.0	0	0	0	0		
0.85	1.0	0	999	0	0	0.85	1.0	0	0	0	0		
0.90	1.0	999	999	0	0	0.90	1.0	0	0	0	0		
0.95	1.0	999	999	0	0	0.95	1.0	0	0	0	0		
0.75	2.0	999	170	0	0	0.75	2.0	999	0	0	0		
0.80	2.0	999	179	0	0	0.80	2.0	0	0	0	0		
0.85	2.0	0	187	999	0	0.85	2.0	0	0	0	0		
0.90	2.0	0	0	0	999	0.90	2.0	0	0	0	0		
0.95	2.0	0	999	0	0	0.95	2.0	0	0	0	0		
0.75	3.5	122	112	121	154	0.75	3.5	0	999	0	999		
0.80	3.5	115	114	119	144	0.80	3.5	0	0	0	999		
0.85	3.5	178	103	95	159	0.85	3.5	999	0	0	0		
0.90	3.5	119	999	115	0	0.90	3.5	0	999	0	0		
0.95	3.5	110	119	135	167	0.95	3.5	0	0	0	0		
0.75	5.0	91	95	97	112	0.75	5.0	108	999	999	999	134	
0.80	5.0	100	93	135	150	0.80	5.0	999	0	999	999		
0.85	5.0	101	81	99	125	0.85	5.0	999	0	0	0		
0.90	5.0	106	95	179	123	0.90	5.0	999	0	999	0		
0.95	5.0	111	103	125	153	0.95	5.0	195	0	0	0		

Table 24—Continued

total sample							Bright SHARC sample				
z	$L_{44}$	1st <sup>a</sup>	2nd <sup>a</sup>	3rd <sup>a</sup>	4th <sup>a</sup>	z	$L_{44}$	1st <sup>a</sup>	2nd <sup>a</sup>	3rd <sup>a</sup>	4th <sup>a</sup>
0.75	7.5	83	84	82	113	0.75	7.5	103	97	96	115
0.80	7.5	85	90	100	116	0.80	7.5	141	129	999	120
0.85	7.5	93	82	91	124	0.85	7.5	142	96	135	167
0.90	7.5	100	86	84	107	0.90	7.5	193	130	0	121
0.95	7.5	96	87	94	128	0.95	7.5	999	0	0	185
0.75	10.0	83	84	82	113	0.75	10.0	103	97	96	115
0.80	10.0	85	90	100	116	0.80	10.0	141	129	999	120
0.85	10.0	93	82	91	124	0.85	10.0	142	96	135	167
0.90	10.0	100	86	84	107	0.90	10.0	193	130	0	121
0.95	10.0	96	87	94	128	0.95	10.0	999	0	0	185

Table 25. Detection efficiency percentage for the ellipticity equal to 0.30 set of parameters

<i>total detection efficiency</i>						<i>Bright SHARC detection efficiency</i>					
<i>z</i>	<i>L</i> <sub>44</sub>	1st <sup>a</sup>	2nd <sup>a</sup>	3rd <sup>a</sup>	4th <sup>a</sup>	<i>z</i>	<i>L</i> <sub>44</sub>	1st <sup>a</sup>	2nd <sup>a</sup>	3rd <sup>a</sup>	4th <sup>a</sup>
0.25	1.0	34	44	26	28	0.25	1.0	5	12	8	25
0.30	1.0	24	32	20	27	0.30	1.0	4	2	1	12
0.35	1.0	15	14	11	8	0.35	1.0	0	0	0	0
0.40	1.0	9	11	5	3	0.40	1.0	2	0	0	0
0.45	1.0	6	8	5	2	0.45	1.0	1	2	0	0
0.25	2.0	62	66	60	52	0.25	2.0	59	66	60	52
0.30	2.0	63	66	57	48	0.30	2.0	35	62	53	46
0.35	2.0	47	52	39	33	0.35	2.0	8	21	14	29
0.40	2.0	43	49	36	21	0.40	2.0	6	6	3	12
0.45	2.0	31	30	25	17	0.45	2.0	2	1	2	5
0.25	3.5	85	91	73	57	0.25	3.5	85	91	73	57
0.30	3.5	77	84	74	64	0.30	3.5	77	84	74	64
0.35	3.5	73	86	70	59	0.35	3.5	71	86	70	59
0.40	3.5	66	78	65	52	0.40	3.5	45	77	64	51
0.45	3.5	60	74	57	42	0.45	3.5	17	41	35	42
0.25	5.0	89	94	88	68	0.25	5.0	89	94	88	68
0.30	5.0	87	90	87	70	0.30	5.0	87	90	87	70
0.35	5.0	80	87	77	62	0.35	5.0	80	87	77	62
0.40	5.0	84	85	71	59	0.40	5.0	84	85	71	59
0.45	5.0	76	84	82	54	0.45	5.0	69	84	82	54
0.25	7.5	92	100	93	76	0.25	7.5	92	100	93	76
0.30	7.5	91	98	95	76	0.30	7.5	91	98	95	76
0.35	7.5	89	95	94	72	0.35	7.5	89	95	94	72
0.40	7.5	94	97	90	62	0.40	7.5	94	97	90	62
0.45	7.5	91	98	90	65	0.45	7.5	91	98	90	65
0.25	10.0	98	100	99	76	0.25	10.0	98	100	99	76
0.30	10.0	98	98	96	75	0.30	10.0	98	98	96	75
0.35	10.0	96	100	97	63	0.35	10.0	96	100	97	63
0.40	10.0	96	99	93	68	0.40	10.0	96	99	93	68
0.45	10.0	98	96	94	68	0.45	10.0	98	96	94	68
0.50	10.0	96	96	94	58	0.50	10.0	96	96	94	58
0.55	10.0	92	95	88	56	0.55	10.0	92	95	87	56
0.60	10.0	87	93	90	60	0.60	10.0	86	93	90	60
0.65	10.0	88	94	82	54	0.65	10.0	88	94	81	54
0.70	10.0	88	93	80	57	0.70	10.0	72	93	78	57
0.50	7.5	90	86	88	57	0.50	7.5	90	86	88	57
0.55	7.5	85	92	83	52	0.55	7.5	84	92	83	52
0.60	7.5	84	85	70	52	0.60	7.5	66	84	67	52
0.65	7.5	74	81	68	47	0.65	7.5	30	63	51	46

Table 25—Continued

total detection efficiency							Bright SHARC detection efficiency						
z	$L_{44}$	1st <sup>a</sup>	2nd <sup>a</sup>	3rd <sup>a</sup>	4th <sup>a</sup>	z	$L_{44}$	1st <sup>a</sup>	2nd <sup>a</sup>	3rd <sup>a</sup>	4th <sup>a</sup>		
0.50	5.0	83	80	65	49	0.50	5.0	51	74	59	49		
0.55	5.0	71	81	63	38	0.55	5.0	17	45	35	37		
0.60	5.0	57	66	55	41	0.60	5.0	8	13	15	34		
0.65	5.0	50	49	29	29	0.65	5.0	1	7	4	20		
0.70	5.0	37	45	19	20	0.70	5.0	2	5	5	13		
0.50	3.5	62	62	42	36	0.50	3.5	5	24	10	31		
0.55	3.5	39	47	41	25	0.55	3.5	5	8	6	14		
0.60	3.5	26	42	25	15	0.60	3.5	2	7	4	1		
0.65	3.5	24	30	24	8	0.65	3.5	3	3	0	2		
0.70	3.5	13	19	10	4	0.70	3.5	0	1	0	1		
0.50	2.0	18	28	8	8	0.50	2.0	0	1	0	2		
0.55	2.0	15	22	9	6	0.55	2.0	0	1	1	0		
0.60	2.0	12	9	1	7	0.60	2.0	0	0	0	1		
0.65	2.0	4	11	1	8	0.65	2.0	0	1	0	0		
0.70	2.0	5	6	3	1	0.70	2.0	1	0	0	0		
0.50	1.0	3	6	2	1	0.50	1.0	1	0	0	0		
0.55	1.0	3	3	1	1	0.55	1.0	0	0	0	0		
0.60	1.0	1	3	0	0	0.60	1.0	0	0	0	0		
0.65	1.0	4	0	0	0	0.65	1.0	1	0	0	0		
0.70	1.0	2	2	1	0	0.70	1.0	0	0	0	0		
0.75	1.0	1	2	1	1	0.75	1.0	0	0	1	0		
0.80	1.0	0	1	0	1	0.80	1.0	0	0	0	0		
0.85	1.0	0	0	0	0	0.85	1.0	0	0	0	0		
0.90	1.0	1	0	1	0	0.90	1.0	0	0	0	0		
0.95	1.0	0	2	1	0	0.95	1.0	0	0	1	0		
0.75	2.0	3	1	2	0	0.75	2.0	0	1	0	0		
0.80	2.0	5	3	1	1	0.80	2.0	0	0	0	0		
0.85	2.0	2	2	0	1	0.85	2.0	0	0	0	0		
0.90	2.0	1	1	2	0	0.90	2.0	0	0	1	0		
0.95	2.0	2	5	1	0	0.95	2.0	0	0	0	0		
0.75	3.5	13	15	13	7	0.75	3.5	1	1	0	1		
0.80	3.5	3	13	4	6	0.80	3.5	0	0	0	0		
0.85	3.5	6	9	6	6	0.85	3.5	0	0	0	1		
0.90	3.5	8	5	8	4	0.90	3.5	0	0	0	0		
0.95	3.5	10	3	3	1	0.95	3.5	0	0	0	0		
0.75	5.0	23	36	23	7	0.75	5.0	1	1	0	4		
0.80	5.0	19	25	22	6	0.80	5.0	1	1	2	0		
0.85	5.0	15	12	13	6	0.85	5.0	1	0	0	1		
0.90	5.0	7	15	6	3	0.90	5.0	1	0	0	1		
0.95	5.0	11	9	4	4	0.95	5.0	1	0	0	1		

Table 25—Continued

total detection efficiency						Bright SHARC detection efficiency					
z	$L_{44}$	1st <sup>a</sup>	2nd <sup>a</sup>	3rd <sup>a</sup>	4th <sup>a</sup>	z	$L_{44}$	1st <sup>a</sup>	2nd <sup>a</sup>	3rd <sup>a</sup>	4th <sup>a</sup>
0.75	7.5	73	73	44	31	0.75	7.5	10	14	9	26
0.80	7.5	51	59	41	32	0.80	7.5	4	10	6	24
0.85	7.5	39	42	40	25	0.85	7.5	2	2	4	9
0.90	7.5	29	43	23	20	0.90	7.5	0	4	0	5
0.95	7.5	18	32	18	16	0.95	7.5	1	2	0	4
0.75	10.0	82	86	73	54	0.75	10.0	38	66	59	54
0.80	10.0	81	84	77	42	0.80	10.0	22	38	39	41
0.85	10.0	75	77	54	40	0.85	10.0	13	16	11	36
0.90	10.0	72	73	56	37	0.90	10.0	10	13	11	34
0.95	10.0	56	63	49	28	0.95	10.0	4	4	4	18

Table 26. Recovered luminosity percentage for the ellipticity equal to 0.30 set of parameters

total sample						Bright SHARC sample					
z	$L_{44}$	1st <sup>a</sup>	2nd <sup>a</sup>	3rd <sup>a</sup>	4th <sup>a</sup>	z	$L_{44}$	1st <sup>a</sup>	2nd <sup>a</sup>	3rd <sup>a</sup>	4th <sup>a</sup>
0.25	1.0	109	100	106	117	0.25	1.0	127	119	118	119
0.30	1.0	117	102	98	119	0.30	1.0	183	149	125	129
0.35	1.0	115	92	105	120	0.35	1.0	0	0	0	0
0.40	1.0	144	111	126	161	0.40	1.0	999	0	0	0
0.45	1.0	999	177	132	176	0.45	1.0	999	999	0	0
0.25	2.0	106	100	100	114	0.25	2.0	104	100	100	114
0.30	2.0	103	94	95	112	0.30	2.0	105	94	96	113
0.35	2.0	97	92	93	107	0.35	2.0	109	101	101	107
0.40	2.0	98	93	89	113	0.40	2.0	138	111	100	123
0.45	2.0	109	99	98	124	0.45	2.0	153	143	147	149
0.25	3.5	104	101	100	114	0.25	3.5	104	101	100	114
0.30	3.5	99	96	95	113	0.30	3.5	99	96	95	113
0.35	3.5	99	92	92	112	0.35	3.5	99	92	92	112
0.40	3.5	95	89	88	115	0.40	3.5	98	89	88	115
0.45	3.5	95	88	87	114	0.45	3.5	112	93	93	114
0.25	5.0	102	101	101	112	0.25	5.0	102	101	101	112
0.30	5.0	98	96	96	115	0.30	5.0	98	96	96	115
0.35	5.0	96	92	94	112	0.35	5.0	96	92	94	112
0.40	5.0	92	89	89	112	0.40	5.0	92	89	89	112
0.45	5.0	89	89	90	114	0.45	5.0	89	89	90	114
0.25	7.5	101	100	101	113	0.25	7.5	101	100	101	113
0.30	7.5	96	96	96	113	0.30	7.5	96	96	96	113
0.35	7.5	92	91	92	113	0.35	7.5	92	91	92	113
0.40	7.5	89	89	89	112	0.40	7.5	89	89	89	112
0.45	7.5	87	87	89	113	0.45	7.5	87	87	89	113
0.25	10.0	101	101	101	114	0.25	10.0	101	101	101	114
0.30	10.0	94	95	96	113	0.30	10.0	94	95	96	113
0.35	10.0	91	92	91	114	0.35	10.0	91	92	91	114
0.40	10.0	89	88	88	110	0.40	10.0	89	88	88	110
0.45	10.0	88	87	88	110	0.45	10.0	88	87	88	110
0.50	10.0	86	86	84	115	0.50	10.0	86	86	84	115
0.55	10.0	83	85	84	112	0.55	10.0	83	85	85	112
0.60	10.0	84	83	83	112	0.60	10.0	84	83	83	112
0.65	10.0	82	84	82	110	0.65	10.0	82	84	82	110
0.70	10.0	81	83	81	111	0.70	10.0	83	83	82	111
0.50	7.5	87	85	85	113	0.50	7.5	87	85	85	113
0.55	7.5	84	84	85	109	0.55	7.5	84	84	85	109
0.60	7.5	83	83	83	114	0.60	7.5	83	83	83	114
0.65	7.5	79	83	85	110	0.65	7.5	83	85	89	111

Table 26—Continued

total sample							Bright SHARC sample						
z	$L_{44}$	1st <sup>a</sup>	2nd <sup>a</sup>	3rd <sup>a</sup>	4th <sup>a</sup>	z	$L_{44}$	1st <sup>a</sup>	2nd <sup>a</sup>	3rd <sup>a</sup>	4th <sup>a</sup>		
0.50	5.0	89	88	84	115	0.50	5.0	93	89	85	115		
0.55	5.0	87	87	85	117	0.55	5.0	97	92	92	118		
0.60	5.0	84	87	87	110	0.60	5.0	110	99	100	113		
0.65	5.0	81	91	88	119	0.65	5.0	84	124	102	124		
0.70	5.0	89	95	92	129	0.70	5.0	151	152	120	139		
0.50	3.5	87	94	92	116	0.50	3.5	112	111	124	117		
0.55	3.5	89	99	93	121	0.55	3.5	118	150	122	135		
0.60	3.5	99	99	94	111	0.60	3.5	999	153	146	116		
0.65	3.5	99	101	99	114	0.65	3.5	176	194	0	171		
0.70	3.5	98	93	90	119	0.70	3.5	0	190	0	141		
0.50	2.0	113	91	92	144	0.50	2.0	0	176	0	999		
0.55	2.0	130	108	136	124	0.55	2.0	0	999	999	0		
0.60	2.0	124	118	133	178	0.60	2.0	0	0	0	0	999	
0.65	2.0	143	179	100	174	0.65	2.0	0	999	0	0	0	
0.70	2.0	196	163	166	192	0.70	2.0	999	0	0	0	0	
0.50	1.0	156	129	141	108	0.50	1.0	999	0	0	0	0	
0.55	1.0	999	143	179	159	0.55	1.0	0	0	0	0	0	
0.60	1.0	110	999	0	0	0.60	1.0	0	0	0	0	0	
0.65	1.0	999	0	0	0	0.65	1.0	999	0	0	0	0	
0.70	1.0	999	999	153	0	0.70	1.0	0	0	0	0	0	
0.75	1.0	999	999	999	999	0.75	1.0	0	0	0	999	0	
0.80	1.0	0	999	0	999	0.80	1.0	0	0	0	0	0	
0.85	1.0	0	0	0	0	0.85	1.0	0	0	0	0	0	
0.90	1.0	999	0	999	0	0.90	1.0	0	0	0	0	0	
0.95	1.0	0	999	999	0	0.95	1.0	0	0	0	999	0	
0.75	2.0	159	149	111	0	0.75	2.0	0	149	0	0	0	
0.80	2.0	999	180	999	999	0.80	2.0	0	0	0	0	0	
0.85	2.0	999	109	0	162	0.85	2.0	0	0	0	0	0	
0.90	2.0	999	200	999	0	0.90	2.0	0	0	0	999	0	
0.95	2.0	999	999	999	0	0.95	2.0	0	0	0	0	0	
0.75	3.5	114	122	104	133	0.75	3.5	999	999	0	180		
0.80	3.5	88	108	130	127	0.80	3.5	0	0	0	0	0	
0.85	3.5	129	115	99	196	0.85	3.5	0	0	0	0	999	
0.90	3.5	107	104	139	103	0.90	3.5	0	0	0	0	0	
0.95	3.5	179	123	128	152	0.95	3.5	0	0	0	0	0	
0.75	5.0	91	90	92	134	0.75	5.0	150	130	0	153		
0.80	5.0	90	97	101	119	0.80	5.0	178	143	196	0		
0.85	5.0	100	94	96	140	0.85	5.0	191	0	0	177		
0.90	5.0	107	104	87	175	0.90	5.0	999	0	0	999		
0.95	5.0	129	125	124	193	0.95	5.0	999	0	0	999		

Table 26—Continued

total sample						Bright SHARC sample					
z	$L_{44}$	1st <sup>a</sup>	2nd <sup>a</sup>	3rd <sup>a</sup>	4th <sup>a</sup>	z	$L_{44}$	1st <sup>a</sup>	2nd <sup>a</sup>	3rd <sup>a</sup>	4th <sup>a</sup>
0.75	7.5	88	84	85	119	0.75	7.5	124	110	110	122
0.80	7.5	84	84	90	115	0.80	7.5	117	113	135	120
0.85	7.5	85	86	86	111	0.85	7.5	142	151	143	117
0.90	7.5	87	93	80	117	0.90	7.5	0	168	0	135
0.95	7.5	95	97	89	123	0.95	7.5	999	161	0	153
0.75	10.0	82	82	83	110	0.75	10.0	87	84	86	110
0.80	10.0	82	81	85	115	0.80	10.0	96	87	95	116
0.85	10.0	83	84	81	113	0.85	10.0	104	105	99	115
0.90	10.0	82	82	85	112	0.90	10.0	101	110	104	114
0.95	10.0	85	83	85	112	0.95	10.0	122	113	110	117

Table 27. Detection efficiency percentage for the standard set of parameters and the type 2 pointings.

<i>total detection efficiency</i>							<i>Bright SHARC detection efficiency</i>						
<i>z</i>	<i>L</i> <sub>44</sub>	1st <sup>a</sup>	2nd <sup>a</sup>	3rd <sup>a</sup>	4th <sup>a</sup>	<i>z</i>	<i>L</i> <sub>44</sub>	1st <sup>a</sup>	2nd <sup>a</sup>	3rd <sup>a</sup>	4th <sup>a</sup>		
0.25	1.0	34	35	29	25	0.25	1.0	6	11	6	21		
0.30	1.0	16	36	20	13	0.30	1.0	1	4	0	6		
0.35	1.0	10	18	9	16	0.35	1.0	0	1	0	2		
0.40	1.0	7	10	2	4	0.40	1.0	0	1	0	0		
0.45	1.0	3	8	2	2	0.45	1.0	0	0	0	0		
0.25	2.0	69	69	56	52	0.25	2.0	65	69	56	52		
0.30	2.0	63	74	54	49	0.30	2.0	37	68	51	49		
0.35	2.0	63	71	44	38	0.35	2.0	7	14	18	34		
0.40	2.0	43	61	35	22	0.40	2.0	6	7	6	13		
0.45	2.0	24	45	26	15	0.45	2.0	3	2	2	2		
0.25	3.5	87	90	86	58	0.25	3.5	87	90	86	58		
0.30	3.5	73	84	75	56	0.30	3.5	73	84	75	56		
0.35	3.5	73	80	75	55	0.35	3.5	68	80	75	55		
0.40	3.5	75	81	72	59	0.40	3.5	52	81	70	58		
0.45	3.5	69	82	61	47	0.45	3.5	19	33	32	45		
0.25	5.0	94	89	93	68	0.25	5.0	94	89	93	68		
0.30	5.0	93	93	89	58	0.30	5.0	93	93	89	58		
0.35	5.0	93	91	93	60	0.35	5.0	93	91	93	60		
0.40	5.0	90	92	79	60	0.40	5.0	89	92	79	60		
0.45	5.0	85	80	79	53	0.45	5.0	78	80	79	53		
0.25	7.5	97	98	96	62	0.25	7.5	97	98	96	62		
0.30	7.5	99	97	96	69	0.30	7.5	99	97	96	69		
0.35	7.5	96	94	93	59	0.35	7.5	96	94	93	59		
0.40	7.5	96	96	88	53	0.40	7.5	96	96	88	53		
0.45	7.5	90	97	92	44	0.45	7.5	89	97	92	44		
0.25	10.0	93	100	100	67	0.25	10.0	93	100	100	67		
0.30	10.0	98	100	100	58	0.30	10.0	98	100	100	58		
0.35	10.0	99	98	99	54	0.35	10.0	99	98	99	54		
0.40	10.0	99	100	97	61	0.40	10.0	99	100	97	61		
0.45	10.0	93	96	99	56	0.45	10.0	93	96	99	60		
0.50	10.0	96	100	90	60	0.50	10.0	96	100	90	55		
0.55	10.0	91	94	86	51	0.55	10.0	91	94	86	47		
0.60	10.0	96	100	82	56	0.60	10.0	96	100	82	56		
0.65	10.0	97	100	81	55	0.65	10.0	94	100	81	55		
0.70	10.0	74	85	89	50	0.70	10.0	52	82	86	45		
0.50	7.5	91	93	89	52	0.50	7.5	91	93	89	52		
0.55	7.5	87	89	86	46	0.55	7.5	78	89	86	46		
0.60	7.5	85	91	79	47	0.60	7.5	65	89	77	47		

Table 27—Continued

total detection efficiency						Bright SHARC detection efficiency					
z	$L_{44}$	1st <sup>a</sup>	2nd <sup>a</sup>	3rd <sup>a</sup>	4th <sup>a</sup>	z	$L_{44}$	1st <sup>a</sup>	2nd <sup>a</sup>	3rd <sup>a</sup>	4th <sup>a</sup>
0.50	5.0	83	82	73	40	0.50	5.0	44	77	65	40
0.55	5.0	76	77	64	41	0.55	5.0	19	33	29	41
0.60	5.0	66	75	51	40	0.60	5.0	6	17	11	32
0.65	5.0	51	66	36	29	0.65	5.0	3	11	4	18
0.70	5.0	28	44	30	23	0.70	5.0	1	3	3	8
0.50	3.5	57	69	56	30	0.50	3.5	3	16	13	23
0.55	3.5	51	54	40	24	0.55	3.5	6	2	5	8
0.60	3.5	31	47	28	26	0.60	3.5	3	2	2	8
0.65	3.5	25	27	25	17	0.65	3.5	0	3	1	2
0.70	3.5	18	28	20	9	0.70	3.5	0	2	0	0
0.50	2.0	17	29	19	13	0.50	2.0	0	2	0	2
0.55	2.0	12	15	5	6	0.55	2.0	1	1	0	2
0.60	2.0	7	14	5	3	0.60	2.0	0	0	0	0
0.65	2.0	1	5	4	1	0.65	2.0	0	0	0	0
0.70	2.0	2	5	0	0	0.70	2.0	0	0	0	0
0.50	1.0	0	3	3	0	0.50	1.0	0	0	0	0
0.55	1.0	0	2	2	0	0.55	1.0	0	0	0	0
0.60	1.0	0	1	2	0	0.60	1.0	0	0	0	0
0.65	1.0	1	2	0	1	0.65	1.0	0	0	0	1
0.70	1.0	1	2	0	0	0.70	1.0	0	0	0	0

Table 28. Recovered luminosity percentage for the standard set of parameters and the type 2 pointings.

total sample							Bright SHARC sample						
z	$L_{44}$	1st <sup>a</sup>	2nd <sup>a</sup>	3rd <sup>a</sup>	4th <sup>a</sup>	z	$L_{44}$	1st <sup>a</sup>	2nd <sup>a</sup>	3rd <sup>a</sup>	4th <sup>a</sup>		
0.25	1.0	102	108	107	111	0.25	1.0	119	123	123	113		
0.30	1.0	105	104	103	133	0.30	1.0	183	156	0	159		
0.35	1.0	98	104	98	121	0.35	1.0	0	150	0	155		
0.40	1.0	102	122	150	115	0.40	1.0	0	999	0	0		
0.45	1.0	175	132	105	195	0.45	1.0	0	0	0	0		
0.25	2.0	103	104	101	116	0.25	2.0	102	104	101	116		
0.30	2.0	98	95	101	116	0.30	2.0	102	95	101	116		
0.35	2.0	91	93	94	116	0.35	2.0	101	110	102	118		
0.40	2.0	94	94	96	117	0.40	2.0	146	132	122	128		
0.45	2.0	112	92	93	117	0.45	2.0	999	159	141	131		
0.25	3.5	103	100	103	115	0.25	3.5	103	100	103	115		
0.30	3.5	97	97	97	112	0.30	3.5	97	97	97	112		
0.35	3.5	95	93	92	114	0.35	3.5	96	93	92	114		
0.40	3.5	90	93	91	112	0.40	3.5	93	93	91	113		
0.45	3.5	90	88	90	111	0.45	3.5	108	105	96	112		
0.25	5.0	100	101	101	114	0.25	5.0	100	101	101	114		
0.30	5.0	96	96	96	115	0.30	5.0	96	96	96	115		
0.35	5.0	92	94	92	114	0.35	5.0	92	94	92	114		
0.40	5.0	89	89	89	110	0.40	5.0	90	89	89	110		
0.45	5.0	86	88	87	115	0.45	5.0	87	88	87	115		
0.25	7.5	100	102	102	114	0.25	7.5	100	102	102	114		
0.30	7.5	95	96	96	111	0.30	7.5	95	96	96	111		
0.35	7.5	91	93	93	111	0.35	7.5	91	93	93	111		
0.40	7.5	87	91	90	111	0.40	7.5	87	91	90	111		
0.45	7.5	84	89	88	110	0.45	7.5	84	89	88	110		
0.25	10.0	100	101	101	116	0.25	10.0	100	101	101	116		
0.30	10.0	95	96	96	114	0.30	10.0	95	96	96	114		
0.35	10.0	90	92	91	112	0.35	10.0	90	92	91	112		
0.40	10.0	87	89	89	112	0.40	10.0	87	89	89	112		
0.45	10.0	85	87	87	111	0.45	10.0	85	87	87	111		
0.50	10.0	86	88	87	112	0.50	10.0	86	99	87	112		
0.55	10.0	84	85	82	106	0.55	10.0	84	85	82	106		
0.60	10.0	81	85	83	111	0.60	10.0	81	85	83	111		
0.65	10.0	82	84	84	117	0.65	10.0	82	84	84	117		
0.70	10.0	74	82	80	114	0.70	10.0	78	83	81	114		
0.50	7.5	85	86	84	112	0.50	7.5	85	86	84	112		
0.55	7.5	83	85	85	112	0.55	7.5	83	85	85	112		
0.60	7.5	80	85	83	110	0.60	7.5	82	95	83	110		

Table 28—Continued

total sample						Bright SHARC sample					
z	$L_{44}$	1st <sup>a</sup>	2nd <sup>a</sup>	3rd <sup>a</sup>	4th <sup>a</sup>	z	$L_{44}$	1st <sup>a</sup>	2nd <sup>a</sup>	3rd <sup>a</sup>	4th <sup>a</sup>
0.50	5.0	83	88	84	113	0.50	5.0	84	89	85	113
0.55	5.0	84	87	86	115	0.55	5.0	98	93	94	115
0.60	5.0	87	91	85	112	0.60	5.0	128	122	94	115
0.65	5.0	85	90	85	120	0.65	5.0	143	138	115	128
0.70	5.0	88	92	89	117	0.70	5.0	120	172	114	137
0.50	3.5	85	90	85	111	0.50	3.5	119	111	98	115
0.55	3.5	95	86	93	108	0.55	3.5	150	139	135	120
0.60	3.5	91	101	88	117	0.60	3.5	181	143	122	142
0.65	3.5	83	99	88	121	0.65	3.5	0	184	131	143
0.70	3.5	86	101	97	114	0.70	3.5	0	200	0	0
0.50	2.0	102	98	95	141	0.50	2.0	0	134	0	999
0.55	2.0	97	109	139	157	0.55	2.0	155	194	0	999
0.60	2.0	112	106	147	146	0.60	2.0	0	0	0	0
0.65	2.0	999	151	133	168	0.65	2.0	0	0	0	0
0.70	2.0	135	182	0	0	0.70	2.0	0	0	0	0
0.50	1.0	0	180	999	0	0.50	1.0	0	0	0	0
0.55	1.0	0	154	133	0	0.55	1.0	0	0	0	0
0.60	1.0	0	168	999	0	0.60	1.0	0	0	0	0
0.65	1.0	999	999	0	999	0.65	1.0	0	0	0	999
0.70	1.0	188	999	0	0	0.70	1.0	0	0	0	0

Table 29. Detection efficiency percentage for the standard set of parameters and the type 3 pointings.

<i>total detection efficiency</i>							<i>Bright SHARC detection efficiency</i>						
<i>z</i>	<i>L</i> <sub>44</sub>	1st <sup>a</sup>	2nd <sup>a</sup>	3rd <sup>a</sup>	4th <sup>a</sup>	<i>z</i>	<i>L</i> <sub>44</sub>	1st <sup>a</sup>	2nd <sup>a</sup>	3rd <sup>a</sup>	4th <sup>a</sup>		
0.25	1.0	39	49	40	29	0.25	1.0	4	14	12	24		
0.30	1.0	28	32	14	18	0.30	1.0	2	3	2	4		
0.35	1.0	10	22	14	10	0.35	1.0	0	4	0	1		
0.40	1.0	6	10	5	1	0.40	1.0	0	0	0	1		
0.45	1.0	3	4	5	0	0.45	1.0	0	0	0	0		
0.25	2.0	62	71	58	52	0.25	2.0	61	71	58	52		
0.30	2.0	69	67	55	56	0.30	2.0	37	58	50	56		
0.35	2.0	50	53	38	32	0.35	2.0	11	21	13	30		
0.40	2.0	41	48	31	26	0.40	2.0	2	8	8	15		
0.45	2.0	29	29	20	18	0.45	2.0	2	0	1	5		
0.25	3.5	86	90	86	66	0.25	3.5	86	90	86	66		
0.30	3.5	84	92	82	57	0.30	3.5	84	92	82	57		
0.35	3.5	83	86	74	62	0.35	3.5	75	86	74	62		
0.40	3.5	75	80	72	50	0.40	3.5	57	78	71	50		
0.45	3.5	72	79	55	51	0.45	3.5	17	48	38	50		
0.25	5.0	85	92	90	73	0.25	5.0	85	92	90	73		
0.30	5.0	87	92	94	63	0.30	5.0	87	92	94	63		
0.35	5.0	86	91	86	57	0.35	5.0	86	91	86	57		
0.40	5.0	87	86	78	56	0.40	5.0	85	86	78	56		
0.45	5.0	76	86	69	47	0.45	5.0	69	86	69	47		
0.25	7.5	96	99	94	59	0.25	7.5	96	99	94	59		
0.30	7.5	95	92	99	67	0.30	7.5	95	92	99	67		
0.35	7.5	90	99	98	52	0.35	7.5	90	99	98	52		
0.40	7.5	94	95	93	50	0.40	7.5	94	95	93	50		
0.45	7.5	89	95	85	47	0.45	7.5	89	95	85	47		
0.25	10.0	98	99	99	68	0.25	10.0	98	99	99	68		
0.30	10.0	99	98	100	61	0.30	10.0	99	98	100	61		
0.35	10.0	97	99	99	48	0.35	10.0	97	99	99	48		
0.40	10.0	96	97	98	59	0.40	10.0	96	97	98	59		
0.45	10.0	94	98	94	65	0.45	10.0	94	98	94	65		
0.50	10.0	94	94	96	50	0.50	10.0	93	94	96	50		
0.55	10.0	93	97	94	49	0.55	10.0	91	97	94	49		
0.60	10.0	89	86	87	53	0.60	10.0	88	86	87	53		
0.65	10.0	88	89	83	52	0.65	10.0	82	89	83	52		
0.70	10.0	81	90	84	40	0.70	10.0	59	88	80	40		
0.50	7.5	93	97	81	53	0.50	7.5	92	97	81	53		
0.55	7.5	81	93	77	43	0.55	7.5	78	93	76	42		
0.60	7.5	80	89	80	51	0.60	7.5	58	88	77	51		

Table 29—Continued

total detection efficiency						Bright SHARC detection efficiency					
z	$L_{44}$	1st <sup>a</sup>	2nd <sup>a</sup>	3rd <sup>a</sup>	4th <sup>a</sup>	z	$L_{44}$	1st <sup>a</sup>	2nd <sup>a</sup>	3rd <sup>a</sup>	4th <sup>a</sup>
0.50	5.0	79	85	79	36	0.50	5.0	50	80	68	35
0.55	5.0	71	81	63	47	0.55	5.0	24	33	32	43
0.60	5.0	73	68	54	30	0.60	5.0	13	12	16	26
0.65	5.0	60	65	36	37	0.65	5.0	7	12	4	26
0.70	5.0	47	42	30	31	0.70	5.0	3	4	0	12
0.50	3.5	57	76	47	33	0.50	3.5	7	14	10	27
0.55	3.5	42	56	36	23	0.55	3.5	2	9	7	7
0.60	3.5	36	41	26	21	0.60	3.5	1	1	2	4
0.65	3.5	30	34	18	14	0.65	3.5	0	0	0	4
0.70	3.5	17	16	11	6	0.70	3.5	0	1	2	0
0.50	2.0	18	23	12	7	0.50	2.0	0	1	0	1
0.55	2.0	14	16	10	2	0.55	2.0	2	2	1	0
0.60	2.0	7	13	4	1	0.60	2.0	1	1	0	0
0.65	2.0	2	4	0	3	0.65	2.0	0	0	0	0
0.70	2.0	4	4	0	0.70	2.0	0	1	0	0	0
0.50	1.0	2	6	0	0	0.50	1.0	0	1	0	0
0.55	1.0	1	2	1	1	0.55	1.0	0	0	0	0
0.60	1.0	2	4	1	0	0.60	1.0	0	0	0	0
0.65	1.0	1	1	0	1	0.65	1.0	0	0	0	1
0.70	1.0	1	2	1	0	0.70	1.0	0	0	0	0

Table 30. Recovered luminosity percentage for the standard set of parameters and the type 3 pointings.

total sample							Bright SHARC sample						
z	$L_{44}$	1st <sup>a</sup>	2nd <sup>a</sup>	3rd <sup>a</sup>	4th <sup>a</sup>	z	$L_{44}$	1st <sup>a</sup>	2nd <sup>a</sup>	3rd <sup>a</sup>	4th <sup>a</sup>		
0.25	1.0	105	103	107	111	0.25	1.0	121	119	119	114		
0.30	1.0	111	103	109	120	0.30	1.0	999	133	140	142		
0.35	1.0	106	137	117	129	0.35	1.0	0	999	0	166		
0.40	1.0	118	110	128	158	0.40	1.0	0	0	0	0	158	
0.45	1.0	132	134	162	0	0.45	1.0	0	0	0	0	0	
0.25	2.0	105	103	102	112	0.25	2.0	104	103	102	112		
0.30	2.0	94	98	97	115	0.30	2.0	95	99	97	115		
0.35	2.0	96	100	94	117	0.35	2.0	105	111	104	119		
0.40	2.0	95	91	102	115	0.40	2.0	131	112	131	125		
0.45	2.0	109	90	90	118	0.45	2.0	999	0	160	137		
0.25	3.5	105	101	102	115	0.25	3.5	105	101	102	115		
0.30	3.5	96	96	97	118	0.30	3.5	96	96	97	118		
0.35	3.5	95	92	95	113	0.35	3.5	93	92	95	113		
0.40	3.5	90	92	88	114	0.40	3.5	92	93	88	114		
0.45	3.5	89	90	93	110	0.45	3.5	98	95	98	110		
0.25	5.0	102	101	102	116	0.25	5.0	102	101	102	116		
0.30	5.0	97	96	97	112	0.30	5.0	97	96	97	112		
0.35	5.0	95	93	92	115	0.35	5.0	95	93	92	115		
0.40	5.0	92	92	91	110	0.40	5.0	92	92	91	110		
0.45	5.0	88	89	88	114	0.45	5.0	87	89	88	114		
0.25	7.5	101	102	101	115	0.25	7.5	101	102	101	115		
0.30	7.5	95	96	96	113	0.30	7.5	95	96	96	113		
0.35	7.5	92	93	94	114	0.35	7.5	92	93	94	114		
0.40	7.5	89	90	88	113	0.40	7.5	89	90	88	113		
0.45	7.5	87	88	87	112	0.45	7.5	87	88	87	112		
0.25	10.0	101	101	102	114	0.25	10.0	101	101	102	114		
0.30	10.0	96	96	96	114	0.30	10.0	96	96	96	114		
0.35	10.0	91	92	92	113	0.35	10.0	91	92	92	113		
0.40	10.0	88	90	90	112	0.40	10.0	88	90	90	112		
0.45	10.0	86	87	87	111	0.45	10.0	86	87	87	111		
0.50	10.0	87	86	85	110	0.50	10.0	87	86	85	110		
0.55	10.0	85	85	86	113	0.55	10.0	84	85	86	113		
0.60	10.0	84	87	83	112	0.60	10.0	83	87	83	112		
0.65	10.0	84	85	83	112	0.65	10.0	84	85	83	112		
0.70	10.0	81	84	84	116	0.70	10.0	82	84	85	116		
0.50	7.5	84	85	86	112	0.50	7.5	84	85	86	112		
0.55	7.5	82	86	86	115	0.55	7.5	82	86	86	116		
0.60	7.5	83	86	84	116	0.60	7.5	84	87	84	116		

Table 30—Continued

total sample						Bright SHARC sample					
z	$L_{44}$	1st <sup>a</sup>	2nd <sup>a</sup>	3rd <sup>a</sup>	4th <sup>a</sup>	z	$L_{44}$	1st <sup>a</sup>	2nd <sup>a</sup>	3rd <sup>a</sup>	4th <sup>a</sup>
0.50	5.0	88	88	84	109	0.50	5.0	92	89	85	110
0.55	5.0	90	87	88	111	0.55	5.0	100	96	98	114
0.60	5.0	91	87	86	113	0.60	5.0	126	105	97	116
0.65	5.0	92	88	87	120	0.65	5.0	133	111	126	128
0.70	5.0	93	97	87	124	0.70	5.0	184	143	0	151
0.50	3.5	91	88	90	111	0.50	3.5	117	116	121	114
0.55	3.5	85	93	94	114	0.55	3.5	147	146	121	134
0.60	3.5	88	90	102	111	0.60	3.5	162	999	999	135
0.65	3.5	99	93	89	125	0.65	3.5	0	0	0	166
0.70	3.5	103	100	122	118	0.70	3.5	0	171	999	0
0.50	2.0	111	101	103	133	0.50	2.0	0	999	0	197
0.55	2.0	134	121	137	158	0.55	2.0	999	999	999	0
0.60	2.0	133	145	121	114	0.60	2.0	999	999	0	0
0.65	2.0	124	143	0	195	0.65	2.0	0	0	0	0
0.70	2.0	154	999	141	0	0.70	2.0	0	999	0	0
0.50	1.0	154	161	163	188	0.50	1.0	0	999	0	0
0.55	1.0	153	159	164	158	0.55	1.0	0	0	0	0
0.60	1.0	144	155	161	159	0.60	1.0	0	0	0	0
0.65	1.0	124	151	0	0	0.65	1.0	0	0	0	999
0.70	1.0	0	0	0	0	0.70	1.0	0	0	0	0

Table 31. Detection efficiency percentage for the standard set of parameters and the type 6 pointings.

<i>total detection efficiency</i>							<i>Bright SHARC detection efficiency</i>						
<i>z</i>	<i>L</i> <sub>44</sub>	1st <sup>a</sup>	2nd <sup>a</sup>	3rd <sup>a</sup>	4th <sup>a</sup>	<i>z</i>	<i>L</i> <sub>44</sub>	1st <sup>a</sup>	2nd <sup>a</sup>	3rd <sup>a</sup>	4th <sup>a</sup>		
0.25	1.0	35	43	23	28	0.25	1.0	4	17	9	22		
0.30	1.0	31	27	28	14	0.30	1.0	1	2	5	4		
0.35	1.0	12	14	6	7	0.35	1.0	0	5	0	2		
0.40	1.0	6	9	1	4	0.40	1.0	0	0	0	3		
0.45	1.0	4	5	1	2	0.45	1.0	0	4	0	1		
0.25	2.0	58	78	60	55	0.25	2.0	54	78	60	55		
0.30	2.0	66	74	55	47	0.30	2.0	46	65	53	47		
0.35	2.0	60	65	44	34	0.35	2.0	9	24	19	30		
0.40	2.0	40	57	35	28	0.40	2.0	5	6	1	17		
0.45	2.0	19	35	23	15	0.45	2.0	0	0	3	3		
0.25	3.5	85	90	78	68	0.25	3.5	85	90	78	68		
0.30	3.5	80	89	77	73	0.30	3.5	80	89	76	73		
0.35	3.5	70	80	72	52	0.35	3.5	68	80	72	51		
0.40	3.5	73	80	65	52	0.40	3.5	54	80	62	51		
0.45	3.5	62	74	53	47	0.45	3.5	21	38	33	46		
0.25	5.0	87	94	89	65	0.25	5.0	87	94	89	65		
0.30	5.0	95	93	90	60	0.30	5.0	95	93	90	60		
0.35	5.0	82	90	85	63	0.35	5.0	82	90	85	63		
0.40	5.0	83	89	79	65	0.40	5.0	83	89	79	65		
0.45	5.0	83	89	78	56	0.45	5.0	77	88	78	56		
0.25	7.5	95	98	97	63	0.25	7.5	95	98	97	63		
0.30	7.5	94	98	95	73	0.30	7.5	94	98	95	73		
0.35	7.5	94	98	94	52	0.35	7.5	94	98	94	52		
0.40	7.5	89	98	90	67	0.40	7.5	89	98	90	67		
0.45	7.5	83	96	87	50	0.45	7.5	83	96	87	50		
0.25	10.0	98	100	97	65	0.25	10.0	98	100	97	65		
0.30	10.0	96	99	95	57	0.30	10.0	96	99	95	57		
0.35	10.0	100	99	96	60	0.35	10.0	100	99	96	60		
0.40	10.0	95	98	96	58	0.40	10.0	95	98	96	58		
0.45	10.0	97	94	95	58	0.45	10.0	97	94	95	58		
0.50	10.0	87	97	94	52	0.50	10.0	87	97	94	52		
0.55	10.0	89	94	91	44	0.55	10.0	89	94	91	44		
0.60	10.0	85	99	85	56	0.60	10.0	84	99	85	56		
0.65	10.0	86	94	84	55	0.65	10.0	82	94	84	55		
0.70	10.0	80	90	87	43	0.70	10.0	65	89	82	43		
0.50	7.5	88	94	83	52	0.50	7.5	88	94	83	52		
0.55	7.5	84	91	89	43	0.55	7.5	82	91	89	43		
0.60	7.5	78	91	85	49	0.60	7.5	64	91	81	49		

Table 31—Continued

total detection efficiency						Bright SHARC detection efficiency					
z	$L_{44}$	1st <sup>a</sup>	2nd <sup>a</sup>	3rd <sup>a</sup>	4th <sup>a</sup>	z	$L_{44}$	1st <sup>a</sup>	2nd <sup>a</sup>	3rd <sup>a</sup>	4th <sup>a</sup>
0.50	5.0	67	85	79	62	0.50	5.0	43	76	74	60
0.55	5.0	70	84	63	40	0.55	5.0	19	33	27	39
0.60	5.0	69	70	56	43	0.60	5.0	11	10	14	38
0.65	5.0	50	67	42	27	0.65	5.0	5	8	7	13
0.70	5.0	31	48	30	22	0.70	5.0	2	6	1	9
0.50	3.5	52	60	50	31	0.50	3.5	6	16	11	25
0.55	3.5	43	51	34	34	0.55	3.5	5	7	2	15
0.60	3.5	27	41	25	24	0.60	3.5	2	3	2	8
0.65	3.5	24	29	18	10	0.65	3.5	0	3	1	1
0.70	3.5	17	20	16	8	0.70	3.5	1	1	1	1
0.50	2.0	14	17	10	6	0.50	2.0	3	1	2	1
0.55	2.0	7	12	6	8	0.55	2.0	1	0	1	0
0.60	2.0	7	9	4	3	0.60	2.0	0	2	0	1
0.65	2.0	3	5	3	0	0.65	2.0	0	0	0	0
0.70	2.0	4	5	2	1	0.70	2.0	0	0	0	0
0.50	1.0	1	2	1	0	0.50	1.0	0	0	1	0
0.55	1.0	0	1	0	1	0.55	1.0	0	0	0	0
0.60	1.0	1	2	1	1	0.60	1.0	0	0	0	0
0.65	1.0	0	2	1	0	0.65	1.0	0	0	1	0
0.70	1.0	0	2	0	0	0.70	1.0	0	0	0	0

Table 32. Recovered luminosity percentage for the standard set of parameters and the type 6 pointings.

total sample							Bright SHARC sample						
z	$L_{44}$	1st <sup>a</sup>	2nd <sup>a</sup>	3rd <sup>a</sup>	4th <sup>a</sup>	z	$L_{44}$	1st <sup>a</sup>	2nd <sup>a</sup>	3rd <sup>a</sup>	4th <sup>a</sup>		
0.25	1.0	116	103	96	123	0.25	1.0	121	111	105	127		
0.30	1.0	124	102	105	117	0.30	1.0	192	999	120	153		
0.35	1.0	129	113	95	148	0.35	1.0	0	146	0	182		
0.40	1.0	127	110	148	999	0.40	1.0	0	0	0	999		
0.45	1.0	999	999	101	999	0.45	1.0	0	999	0	999		
0.25	2.0	105	102	103	116	0.25	2.0	105	102	103	116		
0.30	2.0	108	94	95	111	0.30	2.0	110	94	96	111		
0.35	2.0	101	93	100	123	0.35	2.0	120	100	115	125		
0.40	2.0	102	91	90	127	0.40	2.0	128	115	93	146		
0.45	2.0	98	95	104	116	0.45	2.0	0	0	148	133		
0.25	3.5	106	100	100	115	0.25	3.5	106	100	100	115		
0.30	3.5	101	96	98	113	0.30	3.5	101	96	98	113		
0.35	3.5	95	93	93	112	0.35	3.5	96	93	93	113		
0.40	3.5	93	91	91	112	0.40	3.5	96	91	92	113		
0.45	3.5	96	89	90	115	0.45	3.5	111	94	95	115		
0.25	5.0	103	101	102	116	0.25	5.0	103	101	102	116		
0.30	5.0	99	95	97	113	0.30	5.0	99	95	97	113		
0.35	5.0	97	92	92	113	0.35	5.0	97	92	92	113		
0.40	5.0	92	91	89	112	0.40	5.0	92	91	89	112		
0.45	5.0	92	86	86	108	0.45	5.0	92	87	86	108		
0.25	7.5	103	101	101	115	0.25	7.5	103	101	101	115		
0.30	7.5	99	95	96	113	0.30	7.5	99	95	96	113		
0.35	7.5	95	91	93	113	0.35	7.5	95	91	93	113		
0.40	7.5	92	88	89	112	0.40	7.5	92	88	89	112		
0.45	7.5	91	86	88	112	0.45	7.5	91	86	88	112		
0.25	10.0	102	101	102	115	0.25	10.0	102	101	102	115		
0.30	10.0	97	96	96	114	0.30	10.0	97	96	96	114		
0.35	10.0	94	91	93	114	0.35	10.0	94	91	93	114		
0.40	10.0	90	88	90	112	0.40	10.0	90	88	90	112		
0.45	10.0	89	86	87	112	0.45	10.0	89	86	87	112		
0.50	10.0	86	86	86	113	0.50	10.0	86	86	86	113		
0.55	10.0	85	85	85	112	0.55	10.0	85	85	85	112		
0.60	10.0	84	84	84	111	0.60	10.0	84	84	84	111		
0.65	10.0	83	82	81	111	0.65	10.0	83	82	81	111		
0.70	10.0	81	83	81	111	0.70	10.0	84	83	82	111		
0.50	7.5	87	85	85	112	0.50	7.5	87	85	85	112		
0.55	7.5	87	87	85	115	0.55	7.5	87	87	85	115		
0.60	7.5	85	85	85	112	0.60	7.5	85	85	85	112		

Table 32—Continued

total sample						Bright SHARC sample					
z	$L_{44}$	1st <sup>a</sup>	2nd <sup>a</sup>	3rd <sup>a</sup>	4th <sup>a</sup>	z	$L_{44}$	1st <sup>a</sup>	2nd <sup>a</sup>	3rd <sup>a</sup>	4th <sup>a</sup>
0.50	5.0	92	86	87	110	0.50	5.0	96	87	88	110
0.55	5.0	91	86	86	113	0.55	5.0	107	95	93	113
0.60	5.0	91	84	89	111	0.60	5.0	124	104	110	113
0.65	5.0	95	88	86	111	0.65	5.0	159	136	111	117
0.70	5.0	97	94	90	126	0.70	5.0	999	143	154	144
0.50	3.5	94	85	87	112	0.50	3.5	114	102	105	115
0.55	3.5	104	90	90	115	0.55	3.5	154	119	120	127
0.60	3.5	100	92	90	125	0.60	3.5	160	193	149	144
0.65	3.5	93	94	98	123	0.65	3.5	0	147	128	172
0.70	3.5	106	96	113	136	0.70	3.5	999	139	154	999
0.50	2.0	140	102	117	126	0.50	2.0	187	999	999	156
0.55	2.0	154	96	137	126	0.55	2.0	999	0	999	0
0.60	2.0	147	162	132	999	0.60	2.0	0	999	0	999
0.65	2.0	127	137	135	0	0.65	2.0	0	0	0	0
0.70	2.0	184	121	999	141	0.70	2.0	0	0	0	0
0.50	1.0	999	193	999	0	0.50	1.0	0	0	999	0
0.55	1.0	0	999	0	999	0.55	1.0	0	0	0	0
0.60	1.0	999	999	195	999	0.60	1.0	0	0	0	0
0.65	1.0	0	999	999	0	0.65	1.0	0	0	999	0
0.70	1.0	0	999	0	0	0.70	1.0	0	0	0	0

Table 33. Detection efficiency percentage for the standard set of parameters and the type 7 pointings.

<i>total detection efficiency</i>							<i>Bright SHARC detection efficiency</i>						
<i>z</i>	<i>L</i> <sub>44</sub>	1st <sup>a</sup>	2nd <sup>a</sup>	3rd <sup>a</sup>	4th <sup>a</sup>	<i>z</i>	<i>L</i> <sub>44</sub>	1st <sup>a</sup>	2nd <sup>a</sup>	3rd <sup>a</sup>	4th <sup>a</sup>		
0.25	1.0	36	39	24	19	0.25	1.0	5	11	5	16		
0.30	1.0	26	29	14	17	0.30	1.0	4	4	5	5		
0.35	1.0	6	16	4	7	0.35	1.0	0	0	1	3		
0.40	1.0	6	4	4	1	0.40	1.0	0	0	1	0		
0.45	1.0	5	1	1	0	0.45	1.0	0	0	0	0		
0.25	2.0	71	71	61	47	0.25	2.0	67	71	61	47		
0.30	2.0	71	68	57	42	0.30	2.0	45	58	52	42		
0.35	2.0	59	50	40	35	0.35	2.0	10	17	15	33		
0.40	2.0	37	45	33	24	0.40	2.0	4	3	7	15		
0.45	2.0	24	32	20	18	0.45	2.0	1	0	1	6		
0.25	3.5	86	86	78	55	0.25	3.5	85	86	78	55		
0.30	3.5	92	90	72	62	0.30	3.5	92	90	71	62		
0.35	3.5	83	87	63	56	0.35	3.5	76	87	63	56		
0.40	3.5	82	80	74	49	0.40	3.5	53	77	67	49		
0.45	3.5	62	74	55	44	0.45	3.5	11	49	26	42		
0.25	5.0	90	93	88	63	0.25	5.0	90	93	88	63		
0.30	5.0	89	91	94	67	0.30	5.0	89	91	94	67		
0.35	5.0	88	92	82	60	0.35	5.0	87	92	82	60		
0.40	5.0	78	89	77	58	0.40	5.0	76	89	77	58		
0.45	5.0	74	85	69	49	0.45	5.0	64	85	69	49		
0.25	7.5	97	96	96	65	0.25	7.5	97	96	96	65		
0.30	7.5	97	99	92	54	0.30	7.5	97	99	92	54		
0.35	7.5	91	96	95	58	0.35	7.5	91	96	95	58		
0.40	7.5	93	95	92	52	0.40	7.5	93	95	92	52		
0.45	7.5	91	94	86	51	0.45	7.5	91	94	86	51		
0.25	10.0	96	100	100	70	0.25	10.0	96	100	100	70		
0.30	10.0	98	98	97	71	0.30	10.0	98	98	97	71		
0.35	10.0	96	99	99	61	0.35	10.0	96	99	99	61		
0.40	10.0	95	99	98	73	0.40	10.0	95	99	98	73		
0.45	10.0	97	96	96	45	0.45	10.0	97	96	96	45		
0.50	10.0	96	96	91	47	0.50	10.0	96	96	91	47		
0.55	10.0	94	98	92	48	0.55	10.0	93	98	92	48		
0.60	10.0	90	90	88	55	0.60	10.0	88	90	88	55		
0.65	10.0	88	90	84	41	0.65	10.0	80	90	83	41		
0.70	10.0	88	85	81	39	0.70	10.0	73	82	81	39		
0.50	7.5	93	92	79	58	0.50	7.5	92	92	79	58		
0.55	7.5	88	91	78	43	0.55	7.5	80	91	78	43		
0.60	7.5	77	87	76	35	0.60	7.5	49	85	75	35		

Table 33—Continued

total detection efficiency						Bright SHARC detection efficiency					
z	$L_{44}$	1st <sup>a</sup>	2nd <sup>a</sup>	3rd <sup>a</sup>	4th <sup>a</sup>	z	$L_{44}$	1st <sup>a</sup>	2nd <sup>a</sup>	3rd <sup>a</sup>	4th <sup>a</sup>
0.50	5.0	77	85	72	47	0.50	5.0	43	78	68	47
0.55	5.0	69	72	57	42	0.55	5.0	11	35	33	40
0.60	5.0	57	62	44	29	0.60	5.0	11	15	8	26
0.65	5.0	42	54	39	21	0.65	5.0	4	5	4	13
0.70	5.0	35	48	23	13	0.70	5.0	3	4	4	6
0.50	3.5	53	62	42	31	0.50	3.5	13	13	16	29
0.55	3.5	36	54	29	23	0.55	3.5	2	7	4	12
0.60	3.5	30	34	17	17	0.60	3.5	0	4	5	8
0.65	3.5	29	26	20	10	0.65	3.5	2	1	1	3
0.70	3.5	18	19	7	9	0.70	3.5	0	2	1	3
0.50	2.0	15	21	6	4	0.50	2.0	0	0	2	2
0.55	2.0	5	3	5	1	0.55	2.0	0	0	0	0
0.60	2.0	4	4	2	2	0.60	2.0	0	0	0	1
0.65	2.0	4	2	1	2	0.65	2.0	0	1	0	2
0.70	2.0	2	1	3	2	0.70	2.0	0	0	0	0
0.50	1.0	3	2	1	1	0.50	1.0	1	0	0	0
0.55	1.0	1	1	1	0	0.55	1.0	1	0	0	0
0.60	1.0	1	0	0	0	0.60	1.0	0	0	0	0
0.65	1.0	1	1	2	0	0.65	1.0	1	0	1	0
0.70	1.0	0	0	0	0	0.70	1.0	0	0	0	0

Table 34. Recovered luminosity percentage for the standard set of parameters and the type 7 pointings.

total sample							Bright SHARC sample						
z	$L_{44}$	1st <sup>a</sup>	2nd <sup>a</sup>	3rd <sup>a</sup>	4th <sup>a</sup>	z	$L_{44}$	1st <sup>a</sup>	2nd <sup>a</sup>	3rd <sup>a</sup>	4th <sup>a</sup>		
0.25	1.0	115	100	104	120	0.25	1.0	145	112	119	121		
0.30	1.0	129	99	115	126	0.30	1.0	181	114	148	160		
0.35	1.0	170	102	102	145	0.35	1.0	0	0	166	186		
0.40	1.0	123	144	167	148	0.40	1.0	0	0	999	0		
0.45	1.0	999	116	144	0	0.45	1.0	0	0	0	0		
0.25	2.0	106	99	101	116	0.25	2.0	105	99	101	116		
0.30	2.0	103	94	97	112	0.30	2.0	102	95	97	112		
0.35	2.0	98	92	93	120	0.35	2.0	116	104	98	121		
0.40	2.0	104	88	91	127	0.40	2.0	136	116	118	141		
0.45	2.0	102	89	88	119	0.45	2.0	100	0	141	123		
0.25	3.5	104	100	102	114	0.25	3.5	104	100	102	114		
0.30	3.5	100	96	99	114	0.30	3.5	100	96	99	114		
0.35	3.5	98	89	93	115	0.35	3.5	96	89	93	115		
0.40	3.5	91	89	90	114	0.40	3.5	93	90	91	114		
0.45	3.5	90	89	88	113	0.45	3.5	101	92	94	114		
0.25	5.0	103	101	102	113	0.25	5.0	103	101	102	113		
0.30	5.0	98	95	97	113	0.30	5.0	98	95	97	113		
0.35	5.0	95	92	94	112	0.35	5.0	94	92	94	112		
0.40	5.0	88	89	94	115	0.40	5.0	88	89	94	115		
0.45	5.0	88	87	87	110	0.45	5.0	89	87	87	110		
0.25	7.5	102	101	102	116	0.25	7.5	102	101	102	116		
0.30	7.5	97	96	96	113	0.30	7.5	97	96	96	113		
0.35	7.5	93	93	93	112	0.35	7.5	93	93	93	112		
0.40	7.5	90	90	90	112	0.40	7.5	90	90	90	112		
0.45	7.5	89	88	86	113	0.45	7.5	89	88	86	113		
0.25	10.0	102	101	101	114	0.25	10.0	102	101	101	114		
0.30	10.0	96	95	97	113	0.30	10.0	96	95	97	113		
0.35	10.0	93	91	93	112	0.35	10.0	93	91	93	112		
0.40	10.0	91	88	89	115	0.40	10.0	91	88	89	115		
0.45	10.0	89	87	88	112	0.45	10.0	89	87	88	112		
0.50	10.0	86	86	86	111	0.50	10.0	86	86	86	111		
0.55	10.0	84	84	84	111	0.55	10.0	84	84	84	111		
0.60	10.0	83	83	83	109	0.60	10.0	82	83	83	109		
0.65	10.0	82	82	82	113	0.65	10.0	82	82	82	113		
0.70	10.0	85	82	82	111	0.70	10.0	85	82	82	111		
0.50	7.5	88	86	87	112	0.50	7.5	87	86	87	112		
0.55	7.5	86	85	84	114	0.55	7.5	85	85	84	114		
0.60	7.5	81	83	86	111	0.60	7.5	82	83	86	111		

Table 34—Continued

total sample						Bright SHARC sample					
z	$L_{44}$	1st <sup>a</sup>	2nd <sup>a</sup>	3rd <sup>a</sup>	4th <sup>a</sup>	z	$L_{44}$	1st <sup>a</sup>	2nd <sup>a</sup>	3rd <sup>a</sup>	4th <sup>a</sup>
0.50	5.0	89	86	87	112	0.50	5.0	94	87	87	112
0.55	5.0	86	84	87	114	0.55	5.0	98	91	94	115
0.60	5.0	88	87	85	112	0.60	5.0	114	99	101	114
0.65	5.0	90	88	86	115	0.65	5.0	130	119	118	123
0.70	5.0	91	88	94	121	0.70	5.0	123	132	136	134
0.50	3.5	93	87	90	127	0.50	3.5	121	105	105	129
0.55	3.5	87	90	91	115	0.55	3.5	134	114	130	129
0.60	3.5	96	94	104	137	0.60	3.5	0	141	145	170
0.65	3.5	104	102	106	136	0.65	3.5	156	143	183	170
0.70	3.5	107	123	123	131	0.70	3.5	0	187	172	168
0.50	2.0	98	97	127	139	0.50	2.0	0	0	171	152
0.55	2.0	132	85	127	150	0.55	2.0	0	0	0	0
0.60	2.0	137	107	99	176	0.60	2.0	0	0	0	999
0.65	2.0	171	195	999	999	0.65	2.0	0	999	0	999
0.70	2.0	143	138	175	999	0.70	2.0	0	0	0	0
0.50	1.0	189	999	999	999	0.50	1.0	999	0	0	0
0.55	1.0	999	999	158	0	0.55	1.0	999	0	0	0
0.60	1.0	999	0	0	0	0.60	1.0	0	0	0	0
0.65	1.0	999	999	999	0	0.65	1.0	999	0	999	0
0.70	1.0	0	0	0	0	0.70	1.0	0	0	0	0

Table 35. Detection efficiency percentage for the standard set of parameters and the type 8 pointings.

<i>total detection efficiency</i>						<i>Bright SHARC detection efficiency</i>					
<i>z</i>	<i>L</i> <sub>44</sub>	1st <sup>a</sup>	2nd <sup>a</sup>	3rd <sup>a</sup>	4th <sup>a</sup>	<i>z</i>	<i>L</i> <sub>44</sub>	1st <sup>a</sup>	2nd <sup>a</sup>	3rd <sup>a</sup>	4th <sup>a</sup>
0.25	1.0	34	47	33	31	0.25	1.0	5	14	8	24
0.30	1.0	22	31	24	17	0.30	1.0	3	2	0	4
0.35	1.0	10	16	9	9	0.35	1.0	0	2	0	2
0.40	1.0	5	13	3	1	0.40	1.0	0	0	0	0
0.45	1.0	6	4	2	2	0.45	1.0	0	0	0	0
0.25	2.0	56	81	54	51	0.25	2.0	54	80	54	51
0.30	2.0	58	80	65	54	0.30	2.0	45	75	61	53
0.35	2.0	57	57	55	52	0.35	2.0	17	12	25	46
0.40	2.0	47	52	32	25	0.40	2.0	5	7	4	15
0.45	2.0	29	48	25	15	0.45	2.0	6	2	1	7
0.25	3.5	81	89	74	65	0.25	3.5	81	89	74	65
0.30	3.5	74	93	80	69	0.30	3.5	74	93	80	69
0.35	3.5	84	87	71	63	0.35	3.5	84	86	71	63
0.40	3.5	76	84	72	54	0.40	3.5	61	80	68	52
0.45	3.5	68	69	59	44	0.45	3.5	26	36	27	43
0.25	5.0	90	99	89	71	0.25	5.0	90	99	89	71
0.30	5.0	89	91	83	63	0.30	5.0	89	91	83	63
0.35	5.0	93	94	82	67	0.35	5.0	93	94	82	67
0.40	5.0	93	90	82	69	0.40	5.0	93	90	82	69
0.45	5.0	75	92	75	48	0.45	5.0	74	92	74	48
0.25	7.5	95	98	94	65	0.25	7.5	95	98	94	65
0.30	7.5	91	99	98	63	0.30	7.5	91	99	98	63
0.35	7.5	95	98	93	58	0.35	7.5	95	98	93	58
0.40	7.5	92	97	88	59	0.40	7.5	92	97	88	59
0.45	7.5	90	95	91	57	0.45	7.5	90	94	91	57
0.25	10.0	99	99	97	72	0.25	10.0	99	99	97	72
0.30	10.0	94	100	98	62	0.30	10.0	94	100	98	62
0.35	10.0	97	96	98	51	0.35	10.0	97	96	98	51
0.40	10.0	92	97	98	50	0.40	10.0	92	97	98	50
0.45	10.0	93	95	95	58	0.45	10.0	93	95	95	58
0.50	10.0	93	100	94	57	0.50	10.0	93	100	94	57
0.55	10.0	91	97	90	49	0.55	10.0	91	97	90	49
0.60	10.0	87	92	86	60	0.60	10.0	87	92	86	60
0.65	10.0	83	94	87	42	0.65	10.0	83	94	87	42
0.70	10.0	83	90	81	50	0.70	10.0	76	88	78	50
0.50	7.5	88	96	88	51	0.50	7.5	88	96	88	51
0.55	7.5	90	93	79	46	0.55	7.5	89	93	79	46
0.60	7.5	86	84	74	54	0.60	7.5	70	83	72	54

Table 35—Continued

total detection efficiency						Bright SHARC detection efficiency					
z	$L_{44}$	1st <sup>a</sup>	2nd <sup>a</sup>	3rd <sup>a</sup>	4th <sup>a</sup>	z	$L_{44}$	1st <sup>a</sup>	2nd <sup>a</sup>	3rd <sup>a</sup>	4th <sup>a</sup>
0.50	5.0	73	78	74	48	0.50	5.0	48	72	62	47
0.55	5.0	74	83	61	48	0.55	5.0	23	36	22	45
0.60	5.0	54	70	65	37	0.60	5.0	11	9	17	35
0.65	5.0	49	65	43	37	0.65	5.0	6	7	4	23
0.70	5.0	35	53	35	24	0.70	5.0	2	5	4	10
0.50	3.5	54	66	55	43	0.50	3.5	8	15	9	39
0.55	3.5	33	66	39	31	0.55	3.5	5	7	8	13
0.60	3.5	29	41	21	30	0.60	3.5	2	1	1	7
0.65	3.5	20	33	18	10	0.65	3.5	1	5	1	2
0.70	3.5	12	24	7	6	0.70	3.5	0	0	0	1
0.50	2.0	19	27	5	17	0.50	2.0	0	0	0	3
0.55	2.0	12	12	5	6	0.55	2.0	0	2	0	2
0.60	2.0	7	6	6	6	0.60	2.0	0	1	0	2
0.65	2.0	4	5	1	4	0.65	2.0	0	0	0	0
0.70	2.0	3	2	0	0	0.70	2.0	0	1	0	0
0.50	1.0	2	3	3	0	0.50	1.0	1	0	0	0
0.55	1.0	1	1	1	0	0.55	1.0	0	0	0	0
0.60	1.0	0	0	0	0	0.60	1.0	0	0	0	0
0.65	1.0	3	1	0	0	0.65	1.0	1	0	0	0
0.70	1.0	0	1	1	0	0.70	1.0	0	0	0	0

Table 36. Recovered luminosity percentage for the standard set of parameters and the type 8 pointings.

total sample							Bright SHARC sample						
z	$L_{44}$	1st <sup>a</sup>	2nd <sup>a</sup>	3rd <sup>a</sup>	4th <sup>a</sup>	z	$L_{44}$	1st <sup>a</sup>	2nd <sup>a</sup>	3rd <sup>a</sup>	4th <sup>a</sup>		
0.25	1.0	145	101	102	117	0.25	1.0	999	112	119	120		
0.30	1.0	120	103	97	112	0.30	1.0	173	135	0	121		
0.35	1.0	114	108	97	152	0.35	1.0	0	191	0	999		
0.40	1.0	118	118	112	116	0.40	1.0	0	0	0	0		
0.45	1.0	150	105	166	117	0.45	1.0	0	0	0	0		
0.25	2.0	107	101	104	115	0.25	2.0	106	101	104	115		
0.30	2.0	102	98	95	113	0.30	2.0	102	99	96	114		
0.35	2.0	101	95	90	114	0.35	2.0	107	116	98	115		
0.40	2.0	98	97	82	115	0.40	2.0	145	137	101	124		
0.45	2.0	120	91	100	114	0.45	2.0	184	134	140	128		
0.25	3.5	111	101	101	117	0.25	3.5	111	101	101	117		
0.30	3.5	101	98	97	115	0.30	3.5	101	98	97	115		
0.35	3.5	103	90	93	113	0.35	3.5	103	90	93	113		
0.40	3.5	101	90	91	112	0.40	3.5	102	91	92	113		
0.45	3.5	93	92	87	109	0.45	3.5	108	100	96	109		
0.25	5.0	104	101	101	116	0.25	5.0	104	101	101	116		
0.30	5.0	97	96	97	113	0.30	5.0	97	96	97	113		
0.35	5.0	94	95	91	113	0.35	5.0	94	95	91	113		
0.40	5.0	94	88	90	116	0.40	5.0	94	88	90	116		
0.45	5.0	92	90	90	114	0.45	5.0	91	90	90	114		
0.25	7.5	102	100	101	114	0.25	7.5	102	100	101	114		
0.30	7.5	97	95	96	114	0.30	7.5	97	95	96	114		
0.35	7.5	97	93	92	114	0.35	7.5	97	93	92	114		
0.40	7.5	91	90	89	112	0.40	7.5	91	90	89	112		
0.45	7.5	93	88	88	113	0.45	7.5	93	88	88	113		
0.25	10.0	102	101	101	115	0.25	10.0	102	101	101	115		
0.30	10.0	97	95	96	113	0.30	10.0	97	95	96	113		
0.35	10.0	93	92	92	112	0.35	10.0	93	92	92	112		
0.40	10.0	90	89	89	115	0.40	10.0	90	89	89	115		
0.45	10.0	88	88	86	113	0.45	10.0	88	88	86	113		
0.50	10.0	86	85	85	111	0.50	10.0	86	85	85	111		
0.55	10.0	83	85	84	113	0.55	10.0	83	85	84	113		
0.60	10.0	83	83	84	109	0.60	10.0	83	83	84	109		
0.65	10.0	83	85	81	114	0.65	10.0	83	85	81	114		
0.70	10.0	90	86	82	111	0.70	10.0	91	86	82	111		
0.50	7.5	92	87	88	112	0.50	7.5	92	87	88	112		
0.55	7.5	86	86	84	115	0.55	7.5	86	86	84	115		
0.60	7.5	93	88	83	114	0.60	7.5	96	88	83	114		

Table 36—Continued

total sample						Bright SHARC sample					
z	$L_{44}$	1st <sup>a</sup>	2nd <sup>a</sup>	3rd <sup>a</sup>	4th <sup>a</sup>	z	$L_{44}$	1st <sup>a</sup>	2nd <sup>a</sup>	3rd <sup>a</sup>	4th <sup>a</sup>
0.50	5.0	98	85	85	113	0.50	5.0	106	86	86	114
0.55	5.0	105	86	84	112	0.55	5.0	152	95	93	112
0.60	5.0	94	85	85	115	0.60	5.0	126	109	101	116
0.65	5.0	92	85	87	116	0.65	5.0	153	107	104	123
0.70	5.0	122	92	91	118	0.70	5.0	999	136	124	138
0.50	3.5	92	90	86	113	0.50	3.5	113	114	100	113
0.55	3.5	94	88	93	115	0.55	3.5	146	114	119	131
0.60	3.5	93	88	91	115	0.60	3.5	125	98	135	141
0.65	3.5	100	128	107	131	0.65	3.5	130	999	181	162
0.70	3.5	105	95	93	132	0.70	3.5	0	0	0	999
0.50	2.0	92	94	85	134	0.50	2.0	0	0	0	196
0.55	2.0	100	126	118	176	0.55	2.0	0	999	0	999
0.60	2.0	139	127	137	199	0.60	2.0	0	999	0	999
0.65	2.0	178	142	152	194	0.65	2.0	0	0	0	0
0.70	2.0	153	999	0	0	0.70	2.0	0	999	0	0
0.50	1.0	999	123	143	0	0.50	1.0	999	0	0	0
0.55	1.0	999	999	999	0	0.55	1.0	0	0	0	0
0.60	1.0	0	0	0	0	0.60	1.0	0	0	0	0
0.65	1.0	999	999	0	0	0.65	1.0	999	0	0	0
0.70	1.0	0	999	999	0	0.70	1.0	0	0	0	0

Table 37. Detection efficiency percentage for the standard set of parameters and the type 9 pointings.

<i>total detection efficiency</i>							<i>Bright SHARC detection efficiency</i>						
<i>z</i>	<i>L</i> <sub>44</sub>	1st <sup>a</sup>	2nd <sup>a</sup>	3rd <sup>a</sup>	4th <sup>a</sup>	<i>z</i>	<i>L</i> <sub>44</sub>	1st <sup>a</sup>	2nd <sup>a</sup>	3rd <sup>a</sup>	4th <sup>a</sup>		
0.25	1.0	45	47	37	32	0.25	1.0	14	20	17	28		
0.30	1.0	32	36	28	15	0.30	1.0	0	4	4	9		
0.35	1.0	14	22	14	8	0.35	1.0	1	4	0	2		
0.40	1.0	15	19	8	6	0.40	1.0	0	1	0	3		
0.45	1.0	7	10	7	6	0.45	1.0	0	0	1	2		
0.25	2.0	86	91	77	57	0.25	2.0	86	91	77	57		
0.30	2.0	86	85	78	46	0.30	2.0	79	83	78	46		
0.35	2.0	78	86	64	47	0.35	2.0	27	33	26	44		
0.40	2.0	70	67	56	26	0.40	2.0	6	7	11	19		
0.45	2.0	57	55	43	25	0.45	2.0	2	3	2	9		
0.25	3.5	95	99	92	62	0.25	3.5	95	99	92	62		
0.30	3.5	96	96	97	54	0.30	3.5	96	96	97	54		
0.35	3.5	95	92	92	40	0.35	3.5	95	92	92	40		
0.40	3.5	86	93	90	45	0.40	3.5	82	93	90	45		
0.45	3.5	84	90	85	27	0.45	3.5	41	64	62	27		
0.25	5.0	97	99	99	55	0.25	5.0	97	99	99	55		
0.30	5.0	98	98	99	57	0.30	5.0	98	98	99	57		
0.35	5.0	96	100	94	50	0.35	5.0	96	100	94	50		
0.40	5.0	97	99	98	44	0.40	5.0	97	99	98	44		
0.45	5.0	94	95	94	36	0.45	5.0	94	95	94	36		
0.25	7.5	97	100	98	63	0.25	7.5	97	100	98	63		
0.30	7.5	97	100	100	52	0.30	7.5	97	100	100	52		
0.35	7.5	99	98	98	52	0.35	7.5	99	98	98	52		
0.40	7.5	97	98	98	42	0.40	7.5	97	98	98	42		
0.45	7.5	95	97	98	29	0.45	7.5	95	97	98	29		
0.25	10.0	99	100	100	63	0.25	10.0	99	100	100	63		
0.30	10.0	98	100	99	45	0.30	10.0	98	100	99	45		
0.35	10.0	100	100	98	46	0.35	10.0	100	100	98	46		
0.40	10.0	98	100	98	47	0.40	10.0	98	100	98	47		
0.45	10.0	98	99	98	38	0.45	10.0	98	99	98	38		
0.50	10.0	98	98	97	29	0.50	10.0	98	98	97	29		
0.55	10.0	95	100	93	29	0.55	10.0	95	100	93	29		
0.60	10.0	95	98	86	24	0.60	10.0	95	98	86	24		
0.65	10.0	92	97	78	29	0.65	10.0	92	97	78	29		
0.70	10.0	88	84	77	36	0.70	10.0	86	84	76	36		
0.50	7.5	97	99	91	29	0.50	7.5	97	99	91	29		
0.55	7.5	97	97	89	25	0.55	7.5	97	97	89	25		
0.60	7.5	90	96	83	21	0.60	7.5	89	96	83	21		

Table 37—Continued

total detection efficiency						Bright SHARC detection efficiency					
z	$L_{44}$	1st <sup>a</sup>	2nd <sup>a</sup>	3rd <sup>a</sup>	4th <sup>a</sup>	z	$L_{44}$	1st <sup>a</sup>	2nd <sup>a</sup>	3rd <sup>a</sup>	4th <sup>a</sup>
0.50	5.0	98	95	92	37	0.50	5.0	92	95	89	37
0.55	5.0	85	89	78	30	0.55	5.0	24	56	44	29
0.60	5.0	80	80	62	20	0.60	5.0	7	15	14	19
0.65	5.0	67	68	57	30	0.65	5.0	6	3	7	25
0.70	5.0	58	67	41	17	0.70	5.0	4	3	4	10
0.50	3.5	73	82	60	29	0.50	3.5	13	22	18	29
0.55	3.5	56	65	49	26	0.55	3.5	6	6	6	16
0.60	3.5	50	62	40	15	0.60	3.5	5	7	7	5
0.65	3.5	36	47	24	12	0.65	3.5	2	3	0	2
0.70	3.5	40	31	23	8	0.70	3.5	2	1	3	0
0.50	2.0	33	49	23	9	0.50	2.0	0	1	3	2
0.55	2.0	29	29	22	7	0.55	2.0	1	0	1	1
0.60	2.0	20	20	11	5	0.60	2.0	0	0	0	0
0.65	2.0	15	11	7	3	0.65	2.0	0	1	2	0
0.70	2.0	11	7	8	0	0.70	2.0	0	0	0	0
0.50	1.0	12	9	5	4	0.50	1.0	0	0	0	1
0.55	1.0	6	5	4	4	0.55	1.0	0	0	0	0
0.60	1.0	4	7	2	1	0.60	1.0	0	1	0	0
0.65	1.0	3	5	3	1	0.65	1.0	0	0	0	0
0.70	1.0	3	5	3	0	0.70	1.0	0	0	1	0

Table 38. Recovered luminosity percentage for the standard set of parameters and the type 9 pointings.

total sample							Bright SHARC sample						
z	$L_{44}$	1st <sup>a</sup>	2nd <sup>a</sup>	3rd <sup>a</sup>	4th <sup>a</sup>	z	$L_{44}$	1st <sup>a</sup>	2nd <sup>a</sup>	3rd <sup>a</sup>	4th <sup>a</sup>		
0.25	1.0	109	105	106	130	0.25	1.0	116	120	112	132		
0.30	1.0	98	103	110	119	0.30	1.0	0	136	176	136		
0.35	1.0	106	125	117	153	0.35	1.0	191	999	0	999		
0.40	1.0	117	113	128	186	0.40	1.0	0	999	0	999		
0.45	1.0	124	109	999	184	0.45	1.0	0	0	999	999		
0.25	2.0	103	105	104	122	0.25	2.0	103	105	104	122		
0.30	2.0	98	100	98	115	0.30	2.0	99	100	98	115		
0.35	2.0	94	97	97	120	0.35	2.0	101	108	111	121		
0.40	2.0	92	94	96	116	0.40	2.0	127	117	117	119		
0.45	2.0	92	93	101	127	0.45	2.0	144	135	182	155		
0.25	3.5	103	103	104	117	0.25	3.5	103	103	104	117		
0.30	3.5	99	98	98	120	0.30	3.5	99	98	98	120		
0.35	3.5	96	93	95	119	0.35	3.5	96	93	95	119		
0.40	3.5	92	93	90	116	0.40	3.5	92	93	90	116		
0.45	3.5	90	91	93	121	0.45	3.5	99	93	95	121		
0.25	5.0	102	103	103	118	0.25	5.0	102	103	103	118		
0.30	5.0	97	98	97	116	0.30	5.0	97	98	97	116		
0.35	5.0	93	94	94	118	0.35	5.0	93	94	94	118		
0.40	5.0	90	92	92	118	0.40	5.0	90	92	92	118		
0.45	5.0	89	91	88	114	0.45	5.0	89	91	88	114		
0.25	7.5	100	101	101	117	0.25	7.5	100	101	101	117		
0.30	7.5	96	97	98	119	0.30	7.5	96	97	98	119		
0.35	7.5	92	94	94	118	0.35	7.5	92	94	94	118		
0.40	7.5	88	90	93	117	0.40	7.5	88	90	93	117		
0.45	7.5	86	88	88	116	0.45	7.5	86	88	88	116		
0.25	10.0	97	98	100	115	0.25	10.0	97	98	100	115		
0.30	10.0	93	93	98	117	0.30	10.0	93	93	98	117		
0.35	10.0	92	93	93	117	0.35	10.0	92	93	93	117		
0.40	10.0	90	90	90	117	0.40	10.0	90	90	90	117		
0.45	10.0	86	89	88	114	0.45	10.0	86	89	88	114		
0.50	10.0	84	87	87	114	0.50	10.0	84	87	87	114		
0.55	10.0	83	86	88	118	0.55	10.0	83	86	88	118		
0.60	10.0	82	85	86	120	0.60	10.0	82	85	86	120		
0.65	10.0	85	84	84	115	0.65	10.0	85	84	84	115		
0.70	10.0	78	85	84	121	0.70	10.0	79	85	84	121		
0.50	7.5	86	87	87	116	0.50	7.5	86	87	87	116		
0.55	7.5	85	86	87	122	0.55	7.5	85	86	87	122		
0.60	7.5	84	87	87	117	0.60	7.5	84	87	87	117		

Table 38—Continued

total sample						Bright SHARC sample					
z	$L_{44}$	1st <sup>a</sup>	2nd <sup>a</sup>	3rd <sup>a</sup>	4th <sup>a</sup>	z	$L_{44}$	1st <sup>a</sup>	2nd <sup>a</sup>	3rd <sup>a</sup>	4th <sup>a</sup>
0.50	5.0	87	89	88	116	0.50	5.0	87	89	88	116
0.55	5.0	84	88	88	115	0.55	5.0	93	92	92	115
0.60	5.0	83	86	87	118	0.60	5.0	102	105	108	117
0.65	5.0	88	85	87	114	0.65	5.0	127	116	118	115
0.70	5.0	87	88	84	123	0.70	5.0	136	143	129	128
0.50	3.5	88	90	93	124	0.50	3.5	107	102	110	124
0.55	3.5	93	88	91	122	0.55	3.5	145	119	122	133
0.60	3.5	92	94	98	126	0.60	3.5	145	150	146	154
0.65	3.5	88	100	94	115	0.65	3.5	155	194	0	126
0.70	3.5	97	94	117	129	0.70	3.5	179	152	200	0
0.50	2.0	91	93	105	126	0.50	2.0	0	161	182	175
0.55	2.0	105	99	185	142	0.55	2.0	999	0	999	999
0.60	2.0	104	109	105	134	0.60	2.0	0	0	0	0
0.65	2.0	105	132	153	129	0.65	2.0	0	999	999	0
0.70	2.0	125	122	130	0	0.70	2.0	0	0	0	0
0.50	1.0	139	111	181	999	0.50	1.0	0	0	0	999
0.55	1.0	140	117	999	999	0.55	1.0	0	0	0	0
0.60	1.0	163	178	118	146	0.60	1.0	0	999	0	0
0.65	1.0	122	144	187	999	0.65	1.0	0	0	0	0
0.70	1.0	999	166	999	0	0.70	1.0	0	0	999	0

Table 39. Detection efficiency percentage for the standard set of parameters and the pointings with point sources.

<i>total detection efficiency</i>						<i>Bright SHARC detection efficiency</i>					
z	$L_{44}$	1st <sup>a</sup>	2nd <sup>a</sup>	3rd <sup>a</sup>	4th <sup>a</sup>	z	$L_{44}$	1st <sup>a</sup>	2nd <sup>a</sup>	3rd <sup>a</sup>	4th <sup>a</sup>
0.25	1.0	40	43	28	31	0.25	1.0	5	13	5	17
0.30	1.0	36	34	21	15	0.30	1.0	0	3	1	3
0.35	1.0	15	21	16	8	0.35	1.0	0	0	2	2
0.40	1.0	3	15	6	3	0.40	1.0	0	0	1	0
0.45	1.0	4	9	4	2	0.45	1.0	0	0	1	0
0.25	2.0	73	74	48	51	0.25	2.0	72	74	48	51
0.30	2.0	72	64	60	53	0.30	2.0	49	60	55	52
0.35	2.0	62	67	61	43	0.35	2.0	12	24	30	41
0.40	2.0	40	54	33	31	0.40	2.0	1	7	2	19
0.45	2.0	33	41	29	14	0.45	2.0	0	2	0	1
0.25	3.5	81	93	83	54	0.25	3.5	81	93	83	54
0.30	3.5	83	90	75	64	0.30	3.5	83	90	75	64
0.35	3.5	84	92	76	60	0.35	3.5	76	92	76	60
0.40	3.5	73	84	70	48	0.40	3.5	51	83	67	46
0.45	3.5	72	78	57	44	0.45	3.5	20	40	25	42
0.25	5.0	94	95	91	65	0.25	5.0	94	95	91	65
0.30	5.0	92	97	87	68	0.30	5.0	92	97	87	68
0.35	5.0	92	92	83	64	0.35	5.0	92	92	83	64
0.40	5.0	89	90	83	60	0.40	5.0	89	90	82	60
0.45	5.0	80	85	71	46	0.45	5.0	69	85	70	46
0.25	7.5	99	99	98	67	0.25	7.5	99	99	98	67
0.30	7.5	96	97	97	70	0.30	7.5	96	97	97	70
0.35	7.5	93	100	96	67	0.35	7.5	93	100	96	67
0.40	7.5	96	95	95	59	0.40	7.5	96	95	95	59
0.45	7.5	94	97	83	59	0.45	7.5	93	97	83	59
0.25	10.0	100	99	96	63	0.25	10.0	100	99	96	63
0.30	10.0	97	99	98	67	0.30	10.0	97	99	98	67
0.35	10.0	97	99	96	61	0.35	10.0	97	99	96	61
0.40	10.0	99	97	94	61	0.40	10.0	99	97	94	61
0.45	10.0	97	99	90	52	0.45	10.0	97	99	90	52
0.50	10.0	94	99	92	61	0.50	10.0	94	99	92	61
0.55	10.0	93	97	92	62	0.55	10.0	93	97	92	62
0.60	10.0	93	97	84	58	0.60	10.0	92	97	84	58
0.65	10.0	89	90	86	56	0.65	10.0	85	90	86	56
0.70	10.0	89	94	80	46	0.70	10.0	64	94	75	46
0.50	7.5	90	95	87	58	0.50	7.5	86	95	87	58
0.55	7.5	82	91	89	56	0.55	7.5	78	91	89	56
0.60	7.5	90	88	83	51	0.60	7.5	65	87	79	51

Table 39—Continued

total detection efficiency						Bright SHARC detection efficiency					
z	$L_{44}$	1st <sup>a</sup>	2nd <sup>a</sup>	3rd <sup>a</sup>	4th <sup>a</sup>	z	$L_{44}$	1st <sup>a</sup>	2nd <sup>a</sup>	3rd <sup>a</sup>	4th <sup>a</sup>
0.50	5.0	73	76	71	50	0.50	5.0	40	70	67	50
0.55	5.0	69	81	68	47	0.55	5.0	18	39	25	46
0.60	5.0	65	74	51	40	0.60	5.0	3	21	13	37
0.65	5.0	51	62	40	29	0.65	5.0	2	7	4	18
0.70	5.0	31	47	29	18	0.70	5.0	0	3	4	5
0.50	3.5	66	63	48	39	0.50	3.5	9	7	10	34
0.55	3.5	50	55	40	25	0.55	3.5	1	2	8	15
0.60	3.5	40	47	21	15	0.60	3.5	4	1	0	2
0.65	3.5	26	38	25	14	0.65	3.5	0	3	0	3
0.70	3.5	22	30	17	17	0.70	3.5	0	2	0	2
0.50	2.0	14	25	13	9	0.50	2.0	1	0	1	0
0.55	2.0	9	13	10	9	0.55	2.0	0	0	1	0
0.60	2.0	8	11	7	2	0.60	2.0	0	1	1	0
0.65	2.0	2	3	3	1	0.65	2.0	0	0	0	0
0.70	2.0	2	4	0	2	0.70	2.0	0	0	0	2
0.50	1.0	3	1	3	1	0.50	1.0	0	0	0	1
0.55	1.0	1	3	1	0	0.55	1.0	0	0	0	0
0.60	1.0	2	0	0	2	0.60	1.0	0	0	0	0
0.65	1.0	0	2	1	1	0.65	1.0	0	1	0	0
0.70	1.0	2	0	0	3	0.70	1.0	0	0	0	3

Table 40. Recovered luminosity percentage for the standard set of parameters and the pointings with point sources.

total sample							Bright SHARC sample						
z	$L_{44}$	1st <sup>a</sup>	2nd <sup>a</sup>	3rd <sup>a</sup>	4th <sup>a</sup>	z	$L_{44}$	1st <sup>a</sup>	2nd <sup>a</sup>	3rd <sup>a</sup>	4th <sup>a</sup>		
0.25	1.0	104	103	97	111	0.25	1.0	118	114	111	121		
0.30	1.0	105	104	98	107	0.30	1.0	0	147	180	98		
0.35	1.0	96	101	124	127	0.35	1.0	0	0	185	160		
0.40	1.0	79	106	111	143	0.40	1.0	0	0	999	0		
0.45	1.0	155	136	178	999	0.45	1.0	0	0	999	0		
0.25	2.0	101	102	102	115	0.25	2.0	101	102	102	115		
0.30	2.0	96	97	100	116	0.30	2.0	98	98	102	116		
0.35	2.0	93	96	101	113	0.35	2.0	105	110	114	114		
0.40	2.0	90	92	93	117	0.40	2.0	113	127	101	127		
0.45	2.0	95	95	98	116	0.45	2.0	0	166	0	135		
0.25	3.5	102	102	101	113	0.25	3.5	102	102	101	113		
0.30	3.5	96	95	96	114	0.30	3.5	96	95	96	114		
0.35	3.5	91	95	92	111	0.35	3.5	92	95	92	111		
0.40	3.5	88	92	89	113	0.40	3.5	89	92	89	114		
0.45	3.5	88	90	88	112	0.45	3.5	97	97	96	113		
0.25	5.0	101	101	101	114	0.25	5.0	101	101	101	114		
0.30	5.0	95	96	97	114	0.30	5.0	95	96	97	114		
0.35	5.0	92	93	92	117	0.35	5.0	92	93	92	117		
0.40	5.0	90	91	89	113	0.40	5.0	90	91	89	113		
0.45	5.0	86	88	88	110	0.45	5.0	87	88	88	110		
0.25	7.5	101	101	102	116	0.25	7.5	101	101	102	116		
0.30	7.5	95	97	97	116	0.30	7.5	95	97	97	116		
0.35	7.5	92	92	93	114	0.35	7.5	92	92	93	114		
0.40	7.5	89	89	89	111	0.40	7.5	89	89	89	111		
0.45	7.5	87	89	86	114	0.45	7.5	87	89	86	114		
0.25	10.0	97	99	102	115	0.25	10.0	97	99	102	115		
0.30	10.0	95	96	96	114	0.30	10.0	95	96	96	114		
0.35	10.0	90	93	92	114	0.35	10.0	90	93	92	114		
0.40	10.0	87	89	89	111	0.40	10.0	87	89	89	111		
0.45	10.0	85	88	87	111	0.45	10.0	85	88	87	111		
0.50	10.0	85	86	85	111	0.50	10.0	85	86	85	111		
0.55	10.0	84	85	85	111	0.55	10.0	84	85	85	111		
0.60	10.0	83	83	85	111	0.60	10.0	83	83	85	111		
0.65	10.0	79	83	83	113	0.65	10.0	79	83	83	113		
0.70	10.0	80	83	83	113	0.70	10.0	82	83	84	113		
0.50	7.5	86	86	84	113	0.50	7.5	85	86	84	113		
0.55	7.5	83	86	85	111	0.55	7.5	83	86	85	111		
0.60	7.5	80	84	86	113	0.60	7.5	80	84	86	113		

Table 40—Continued

total sample						Bright SHARC sample					
z	$L_{44}$	1st <sup>a</sup>	2nd <sup>a</sup>	3rd <sup>a</sup>	4th <sup>a</sup>	z	$L_{44}$	1st <sup>a</sup>	2nd <sup>a</sup>	3rd <sup>a</sup>	4th <sup>a</sup>
0.50	5.0	87	88	84	111	0.50	5.0	90	88	85	111
0.55	5.0	87	117	84	112	0.55	5.0	101	155	90	112
0.60	5.0	82	88	86	113	0.60	5.0	93	102	101	113
0.65	5.0	84	87	87	118	0.65	5.0	999	114	112	127
0.70	5.0	85	92	88	121	0.70	5.0	0	169	123	153
0.50	3.5	90	84	86	118	0.50	3.5	123	96	110	121
0.55	3.5	82	88	90	120	0.55	3.5	115	150	126	129
0.60	3.5	94	89	78	115	0.60	3.5	164	173	0	174
0.65	3.5	94	103	89	120	0.65	3.5	0	999	0	156
0.70	3.5	92	100	97	128	0.70	3.5	0	166	0	121
0.50	2.0	98	92	104	119	0.50	2.0	188	0	199	0
0.55	2.0	103	105	126	118	0.55	2.0	0	0	171	0
0.60	2.0	96	127	172	122	0.60	2.0	0	999	999	0
0.65	2.0	103	115	105	161	0.65	2.0	0	0	0	0
0.70	2.0	104	117	0	999	0.70	2.0	0	0	0	999
0.50	1.0	115	159	92	999	0.50	1.0	0	0	0	999
0.55	1.0	999	999	999	0	0.55	1.0	0	0	0	0
0.60	1.0	999	0	0	999	0.60	1.0	0	0	0	0
0.65	1.0	0	999	999	999	0.65	1.0	0	999	0	0
0.70	1.0	999	0	0	999	0.70	1.0	0	0	0	999

Table 41. Detection efficiency percentage for the standard set of parameters and the pointings with extended X-ray sources.

<i>total detection efficiency</i>						<i>Bright SHARC detection efficiency</i>					
z	$L_{44}$	1st <sup>a</sup>	2nd <sup>a</sup>	3rd <sup>a</sup>	4th <sup>a</sup>	z	$L_{44}$	1st <sup>a</sup>	2nd <sup>a</sup>	3rd <sup>a</sup>	4th <sup>a</sup>
0.25	1.0	38	40	26	32	0.25	1.0	4	14	4	15
0.30	1.0	37	36	24	13	0.30	1.0	1	2	2	2
0.35	1.0	17	22	15	4	0.35	1.0	0	0	2	4
0.40	1.0	4	15	6	5	0.40	1.0	1	1	1	0
0.45	1.0	4	8	5	6	0.45	1.0	0	0	0	1
0.25	2.0	76	74	46	57	0.25	2.0	72	74	49	54
0.30	2.0	70	62	65	53	0.30	2.0	44	65	53	52
0.35	2.0	60	66	68	45	0.35	2.0	12	23	32	45
0.40	2.0	43	58	36	33	0.40	2.0	2	4	1	17
0.45	2.0	37	44	24	14	0.45	2.0	0	2	0	3
0.25	3.5	78	97	87	53	0.25	3.5	83	92	85	55
0.30	3.5	80	93	76	66	0.30	3.5	85	91	74	66
0.35	3.5	81	97	75	67	0.35	3.5	75	94	73	63
0.40	3.5	76	83	73	43	0.40	3.5	56	85	69	45
0.45	3.5	69	72	56	42	0.45	3.5	23	41	22	46
0.25	5.0	93	98	95	65	0.25	5.0	94	97	93	64
0.30	5.0	92	95	83	67	0.30	5.0	95	99	87	63
0.35	5.0	89	93	83	64	0.35	5.0	96	93	84	66
0.40	5.0	88	91	86	63	0.40	5.0	84	91	83	63
0.45	5.0	83	85	74	46	0.45	5.0	63	86	72	47
0.25	7.5	98	99	96	67	0.25	7.5	91	99	99	69
0.30	7.5	96	97	97	74	0.30	7.5	93	98	95	72
0.35	7.5	93	100	96	63	0.35	7.5	94	100	97	68
0.40	7.5	98	96	96	57	0.40	7.5	95	96	94	57
0.45	7.5	93	92	85	59	0.45	7.5	97	98	87	54
0.25	10.0	100	94	98	64	0.25	10.0	100	99	97	62
0.30	10.0	98	95	96	62	0.30	10.0	97	100	98	68
0.35	10.0	95	99	94	65	0.35	10.0	98	98	95	61
0.40	10.0	96	98	95	67	0.40	10.0	99	99	93	62
0.45	10.0	98	96	93	55	0.45	10.0	96	98	92	54
0.50	10.0	95	98	94	63	0.50	10.0	95	98	93	64
0.55	10.0	93	96	96	62	0.55	10.0	94	98	91	60
0.60	10.0	89	95	85	55	0.60	10.0	93	97	85	59
0.65	10.0	87	93	84	57	0.65	10.0	85	92	86	54
0.70	10.0	87	95	86	48	0.70	10.0	65	93	73	44
0.50	7.5	91	96	84	54	0.50	7.5	83	96	87	57
0.55	7.5	83	92	87	52	0.55	7.5	72	92	87	59
0.60	7.5	90	83	83	54	0.60	7.5	67	88	78	52

Table 41—Continued

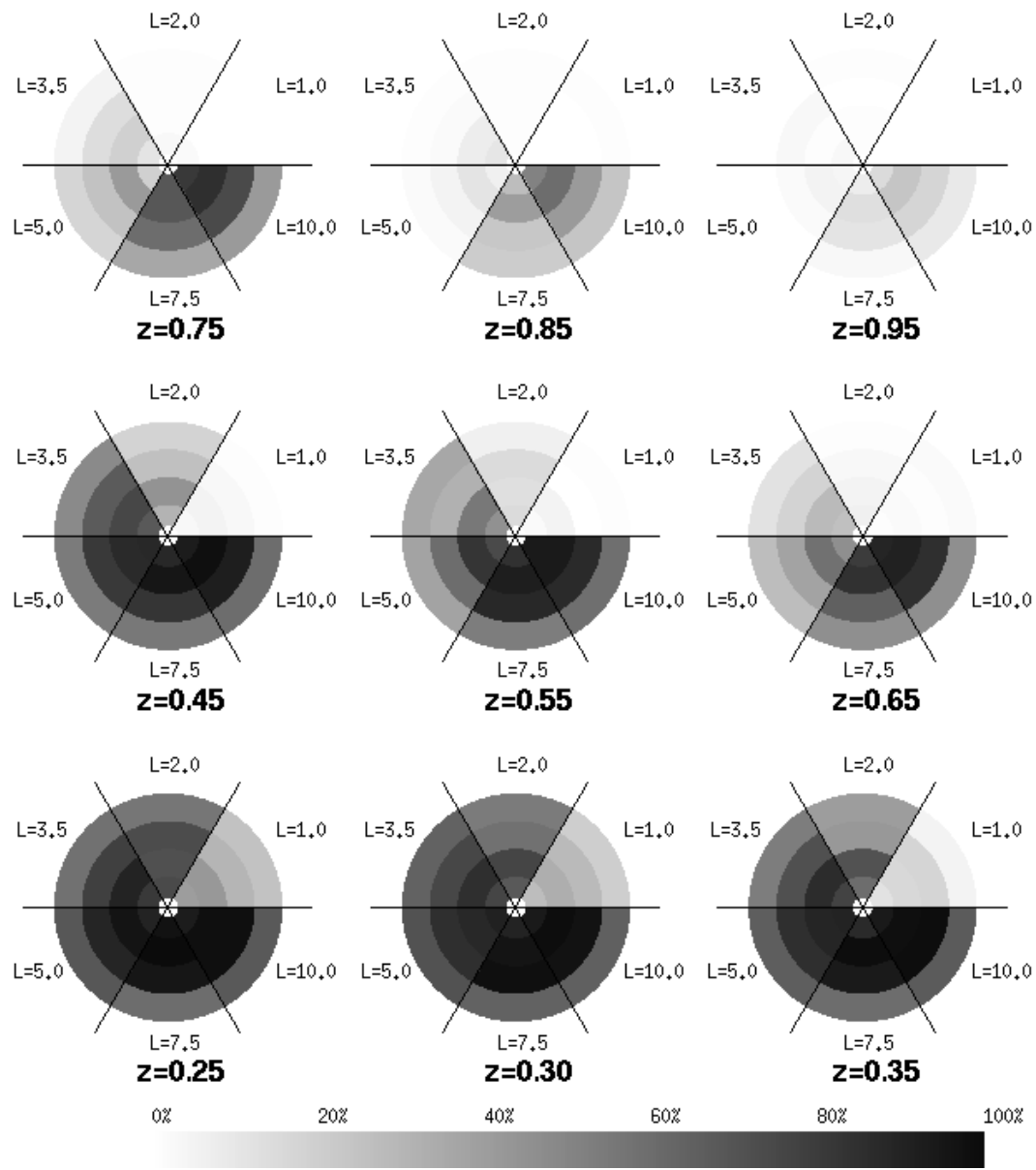
total detection efficiency						Bright SHARC detection efficiency					
z	$L_{44}$	1st <sup>a</sup>	2nd <sup>a</sup>	3rd <sup>a</sup>	4th <sup>a</sup>	z	$L_{44}$	1st <sup>a</sup>	2nd <sup>a</sup>	3rd <sup>a</sup>	4th <sup>a</sup>
0.50	5.0	73	74	74	56	0.50	5.0	43	77	68	53
0.55	5.0	70	83	67	43	0.55	5.0	16	42	25	48
0.60	5.0	63	75	54	46	0.60	5.0	2	22	12	36
0.65	5.0	47	63	47	27	0.65	5.0	3	8	3	19
0.70	5.0	28	47	26	15	0.70	5.0	0	4	5	5
0.50	3.5	69	64	45	34	0.50	3.5	11	8	11	36
0.55	3.5	48	55	44	23	0.55	3.5	2	2	9	14
0.60	3.5	40	43	23	14	0.60	3.5	3	2	0	1
0.65	3.5	29	36	25	16	0.65	3.5	1	3	1	3
0.70	3.5	19	34	15	16	0.70	3.5	0	1	0	4
0.50	2.0	11	23	12	7	0.50	2.0	1	0	1	0
0.55	2.0	10	16	13	8	0.55	2.0	1	1	2	1
0.60	2.0	7	14	4	5	0.60	2.0	0	2	1	0
0.65	2.0	3	4	3	2	0.65	2.0	0	0	0	0
0.70	2.0	1	3	4	3	0.70	2.0	1	0	1	1
0.50	1.0	4	5	5	1	0.50	1.0	0	1	0	1
0.55	1.0	1	3	1	0	0.55	1.0	0	0	1	0
0.60	1.0	3	2	0	4	0.60	1.0	0	1	0	1
0.65	1.0	1	4	1	3	0.65	1.0	1	1	1	0
0.70	1.0	3	0	0	3	0.70	1.0	0	1	0	4

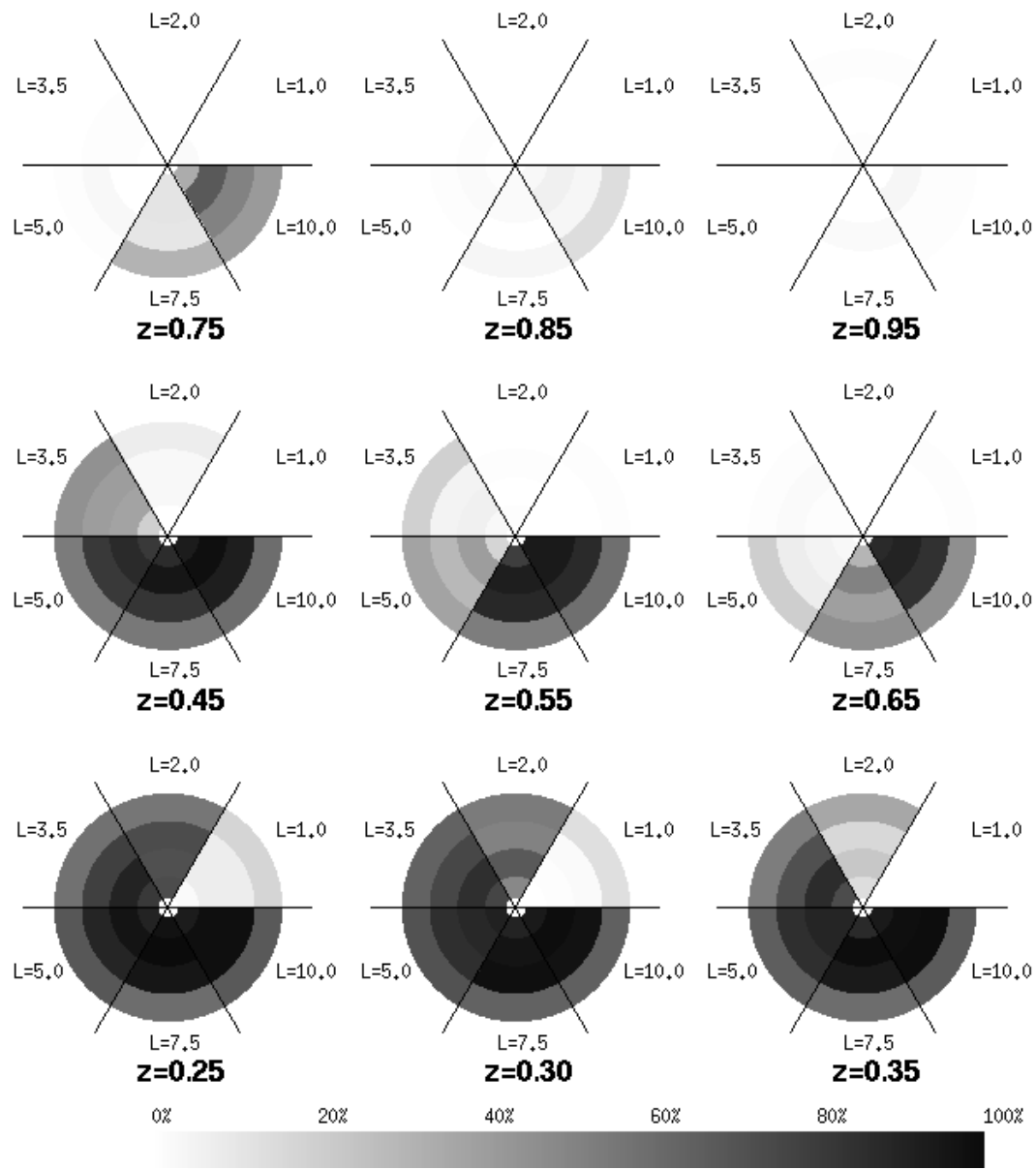
Table 42. Recovered luminosity percentage for the standard set of parameters and the pointings with extended X-ray sources.

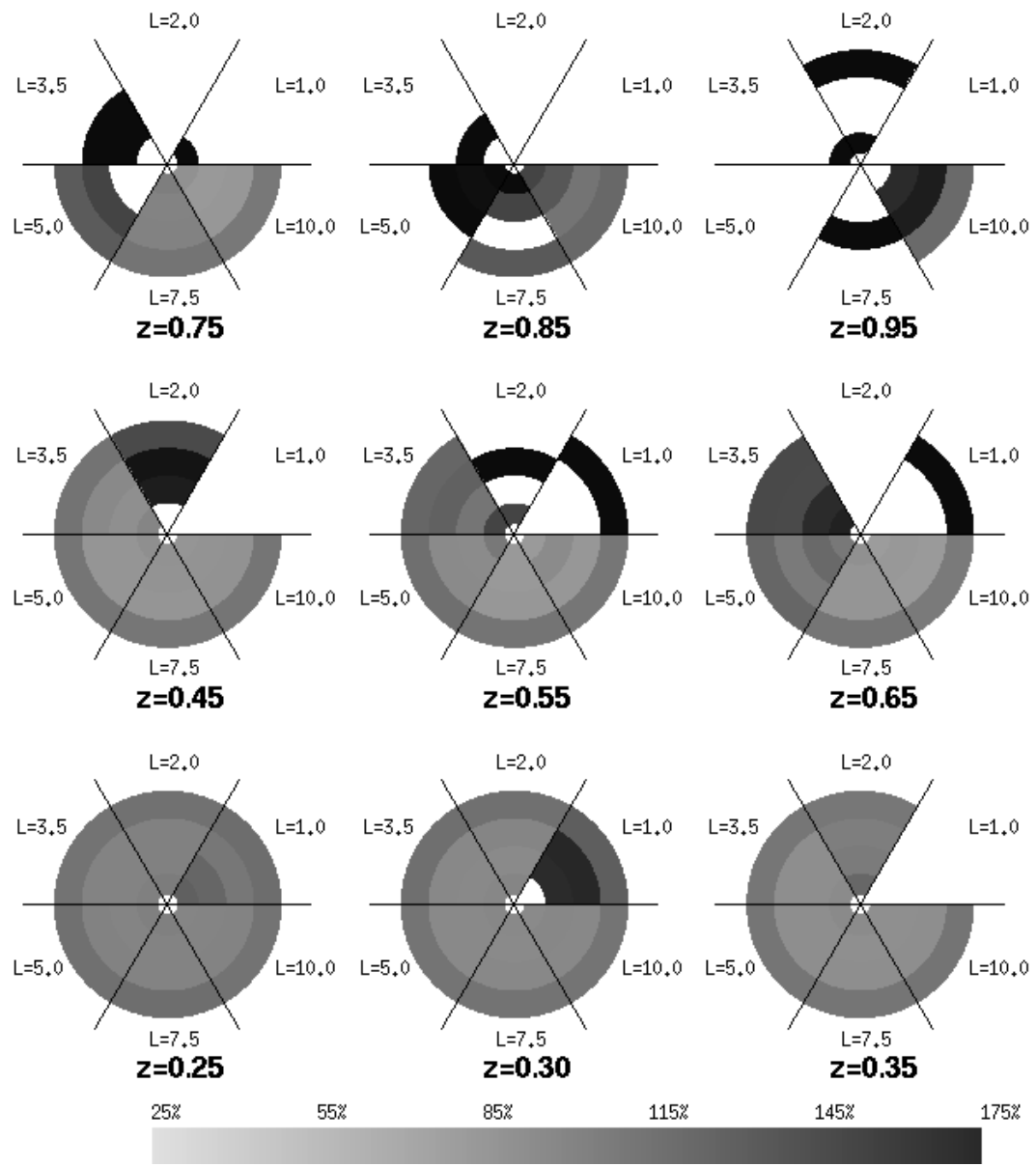
total sample							Bright SHARC sample						
z	$L_{44}$	1st <sup>a</sup>	2nd <sup>a</sup>	3rd <sup>a</sup>	4th <sup>a</sup>	z	$L_{44}$	1st <sup>a</sup>	2nd <sup>a</sup>	3rd <sup>a</sup>	4th <sup>a</sup>		
0.25	1.0	102	107	97	113	0.25	1.0	111	116	110	125		
0.30	1.0	108	106	95	104	0.30	1.0	0	145	182	94		
0.35	1.0	95	104	127	126	0.35	1.0	0	0	184	166		
0.40	1.0	74	103	114	147	0.40	1.0	0	0	999	0		
0.45	1.0	156	137	173	999	0.45	1.0	0	0	999	0		
0.25	2.0	108	108	104	116	0.25	2.0	100	107	105	117		
0.30	2.0	94	95	105	117	0.30	2.0	94	98	107	118		
0.35	2.0	93	97	107	115	0.35	2.0	106	119	115	119		
0.40	2.0	96	98	95	114	0.40	2.0	117	125	104	125		
0.45	2.0	98	96	93	113	0.45	2.0	0	164	0	136		
0.25	3.5	103	103	106	115	0.25	3.5	108	100	102	113		
0.30	3.5	96	95	96	117	0.30	3.5	96	98	95	118		
0.35	3.5	98	98	97	118	0.35	3.5	95	97	96	104		
0.40	3.5	85	99	85	115	0.40	3.5	84	98	88	115		
0.45	3.5	83	97	84	114	0.45	3.5	93	99	97	116		
0.25	5.0	108	104	108	114	0.25	5.0	104	103	103	113		
0.30	5.0	95	93	96	115	0.30	5.0	96	93	95	112		
0.35	5.0	96	98	98	117	0.35	5.0	97	96	96	115		
0.40	5.0	97	99	85	116	0.40	5.0	98	98	89	113		
0.45	5.0	88	85	85	112	0.45	5.0	80	89	88	115		
0.25	7.5	103	107	103	114	0.25	7.5	106	103	104	117		
0.30	7.5	95	94	95	113	0.30	7.5	92	99	93	115		
0.35	7.5	94	93	93	115	0.35	7.5	95	98	94	114		
0.40	7.5	87	86	87	116	0.40	7.5	86	85	86	116		
0.45	7.5	88	88	88	117	0.45	7.5	87	87	87	117		
0.25	10.0	94	96	103	114	0.25	10.0	94	98	104	113		
0.30	10.0	93	94	94	117	0.30	10.0	96	96	96	114		
0.35	10.0	95	93	99	115	0.35	10.0	98	95	97	113		
0.40	10.0	86	84	89	114	0.40	10.0	88	88	88	110		
0.45	10.0	88	88	88	111	0.45	10.0	85	87	89	111		
0.50	10.0	85	89	87	114	0.50	10.0	84	86	80	110		
0.55	10.0	87	87	89	113	0.55	10.0	86	85	88	111		
0.60	10.0	88	86	86	110	0.60	10.0	87	88	86	113		
0.65	10.0	75	88	85	113	0.65	10.0	74	84	88	111		
0.70	10.0	84	87	83	110	0.70	10.0	83	85	89	110		
0.50	7.5	83	85	89	113	0.50	7.5	86	87	86	113		
0.55	7.5	88	87	87	110	0.55	7.5	89	87	87	110		
0.60	7.5	80	89	86	114	0.60	7.5	88	85	88	113		

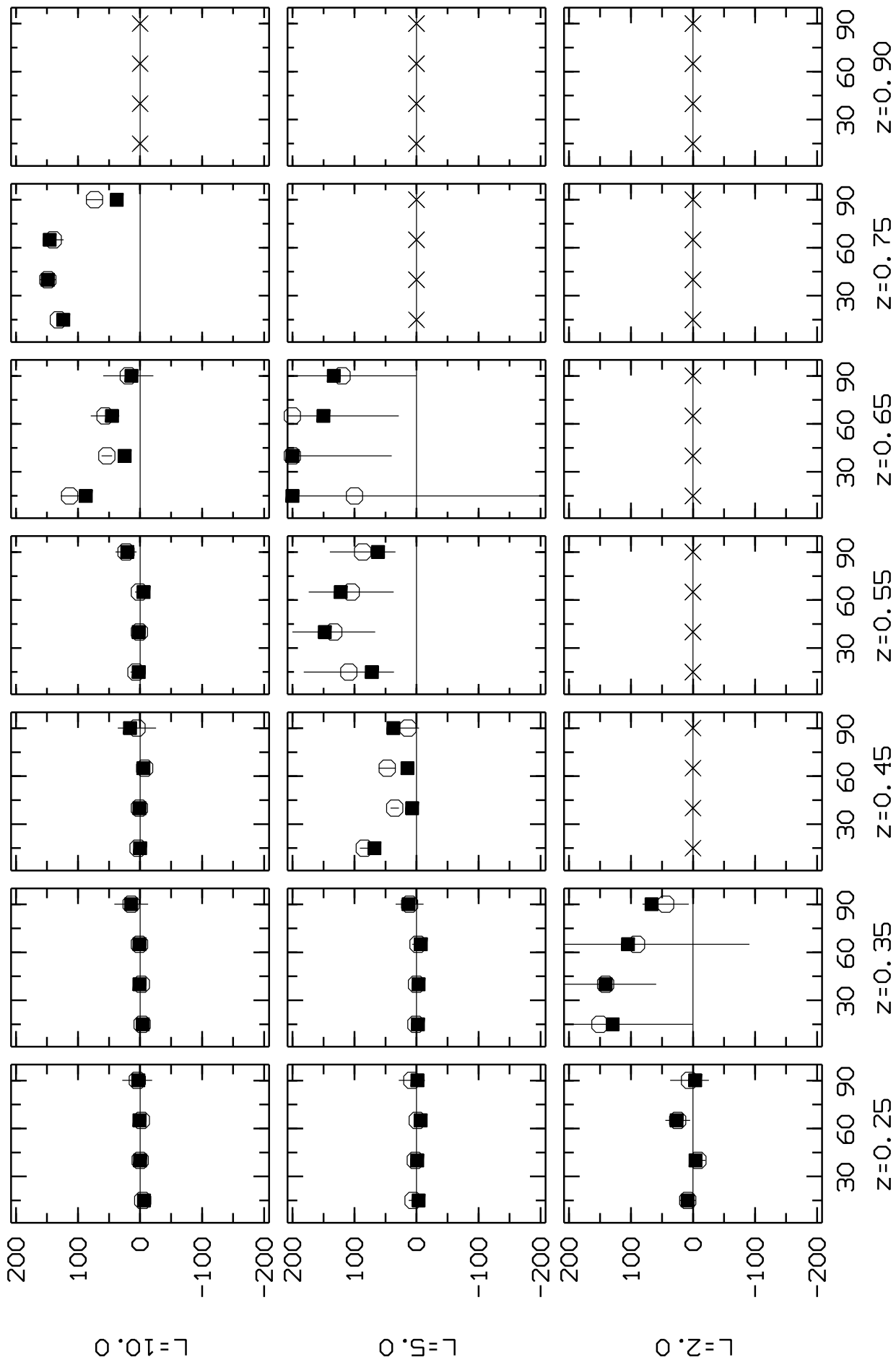
Table 42—Continued

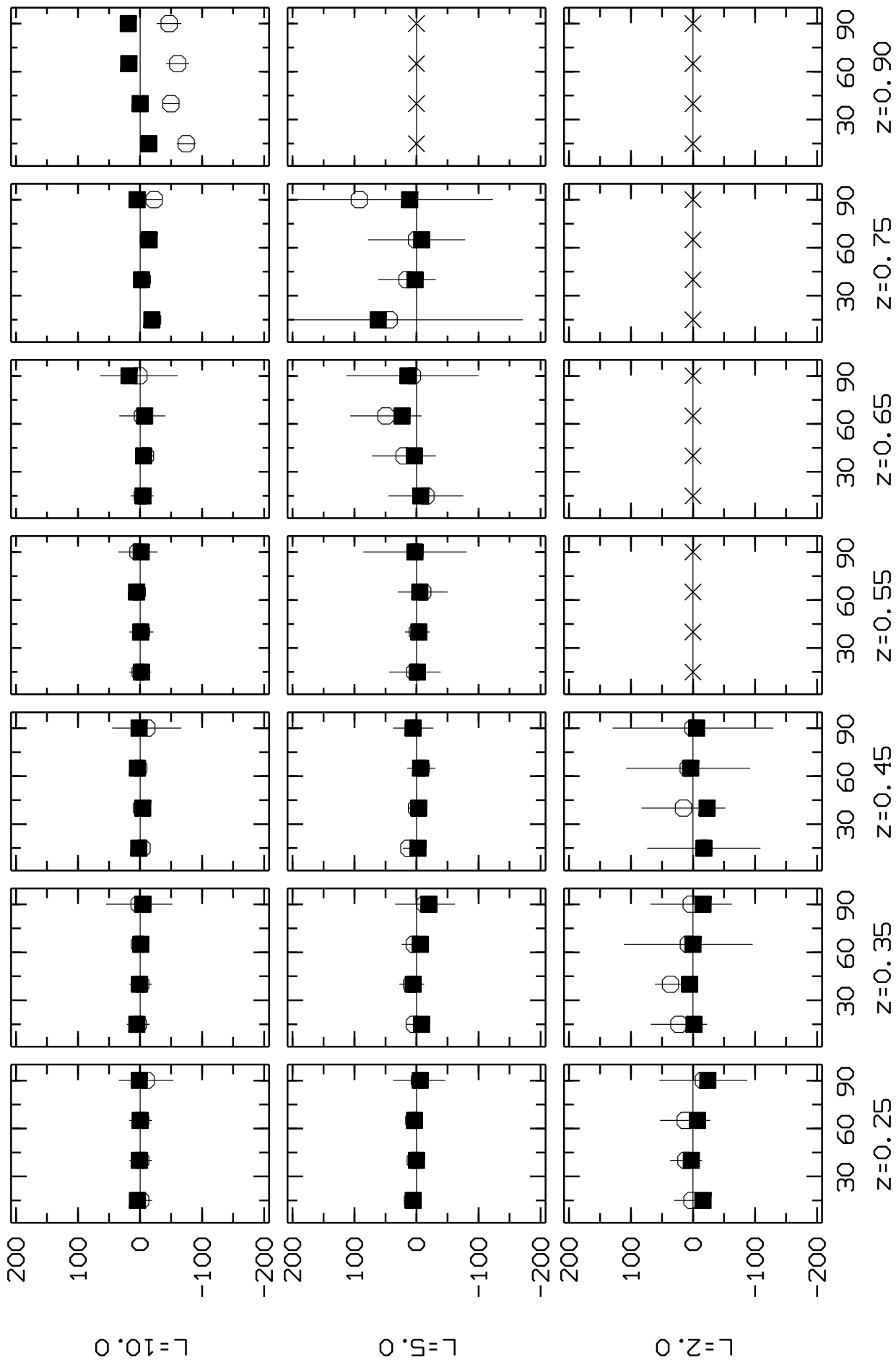
total sample						Bright SHARC sample					
z	$L_{44}$	1st <sup>a</sup>	2nd <sup>a</sup>	3rd <sup>a</sup>	4th <sup>a</sup>	z	$L_{44}$	1st <sup>a</sup>	2nd <sup>a</sup>	3rd <sup>a</sup>	4th <sup>a</sup>
0.50	5.0	88	86	86	111	0.50	5.0	96	89	85	112
0.55	5.0	87	114	88	111	0.55	5.0	107	150	93	113
0.60	5.0	84	85	89	113	0.60	5.0	95	101	103	114
0.65	5.0	83	87	87	115	0.65	5.0	999	111	112	127
0.70	5.0	86	99	86	126	0.70	5.0	0	169	125	153
0.50	3.5	93	84	86	119	0.50	3.5	123	99	116	125
0.55	3.5	87	89	95	121	0.55	3.5	116	151	122	125
0.60	3.5	94	86	77	118	0.60	3.5	167	175	0	176
0.65	3.5	96	104	88	121	0.65	3.5	0	999	0	152
0.70	3.5	94	102	99	122	0.70	3.5	0	161	0	120
0.50	2.0	92	96	103	120	0.50	2.0	183	0	197	0
0.55	2.0	101	107	125	122	0.55	2.0	0	0	170	0
0.60	2.0	98	124	176	112	0.60	2.0	0	999	999	0
0.65	2.0	109	115	107	160	0.65	2.0	0	0	0	0
0.70	2.0	105	114	4	999	0.70	2.0	0	0	0	999
0.50	1.0	113	156	99	999	0.50	1.0	0	0	0	999
0.55	1.0	999	999	999	0	0.55	1.0	0	0	0	0
0.60	1.0	999	0	0	999	0.60	1.0	0	0	0	0
0.65	1.0	0	999	999	999	0.65	1.0	0	999	0	0
0.70	1.0	999	0	0	999	0.70	1.0	0	0	0	999

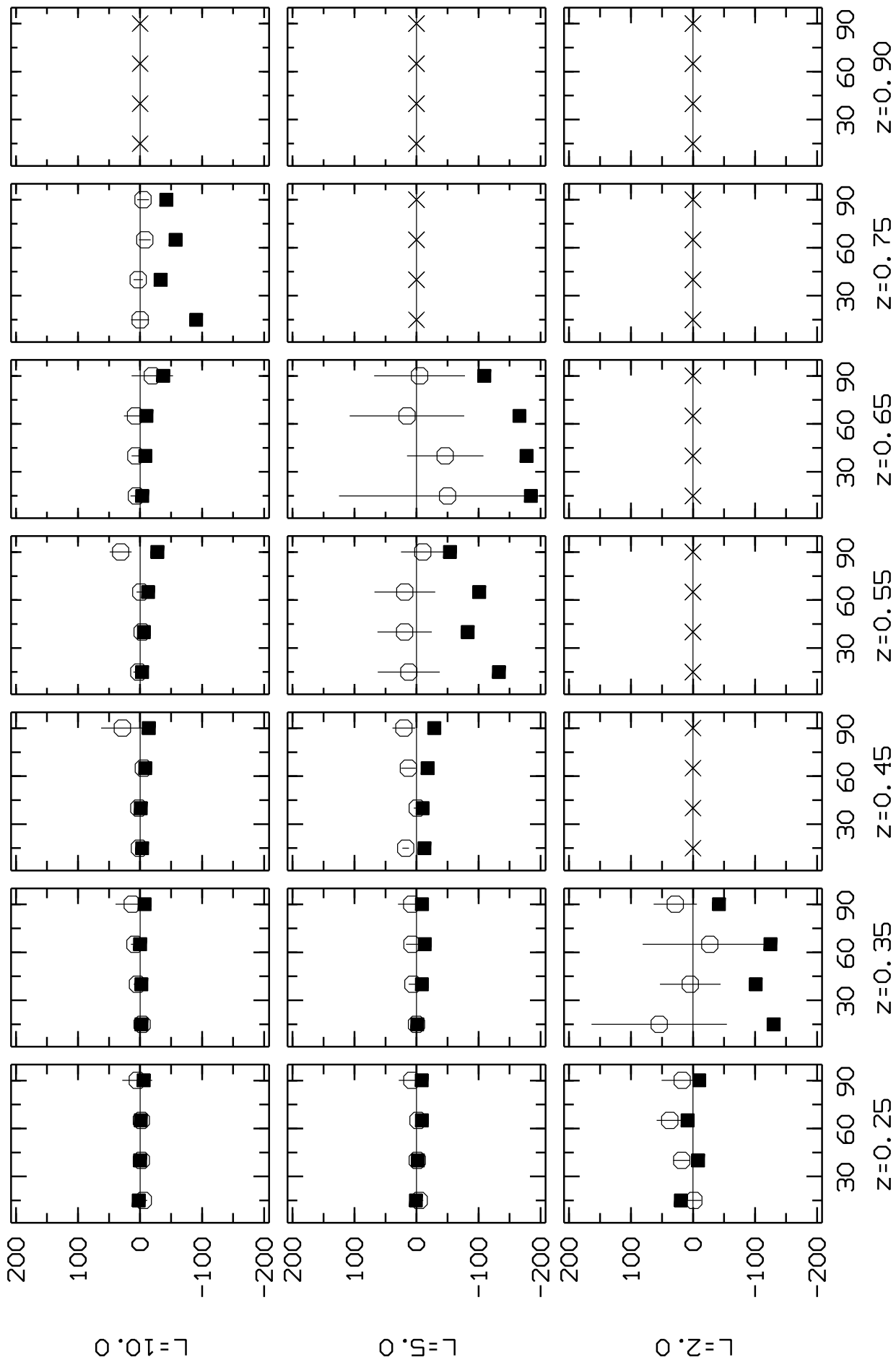


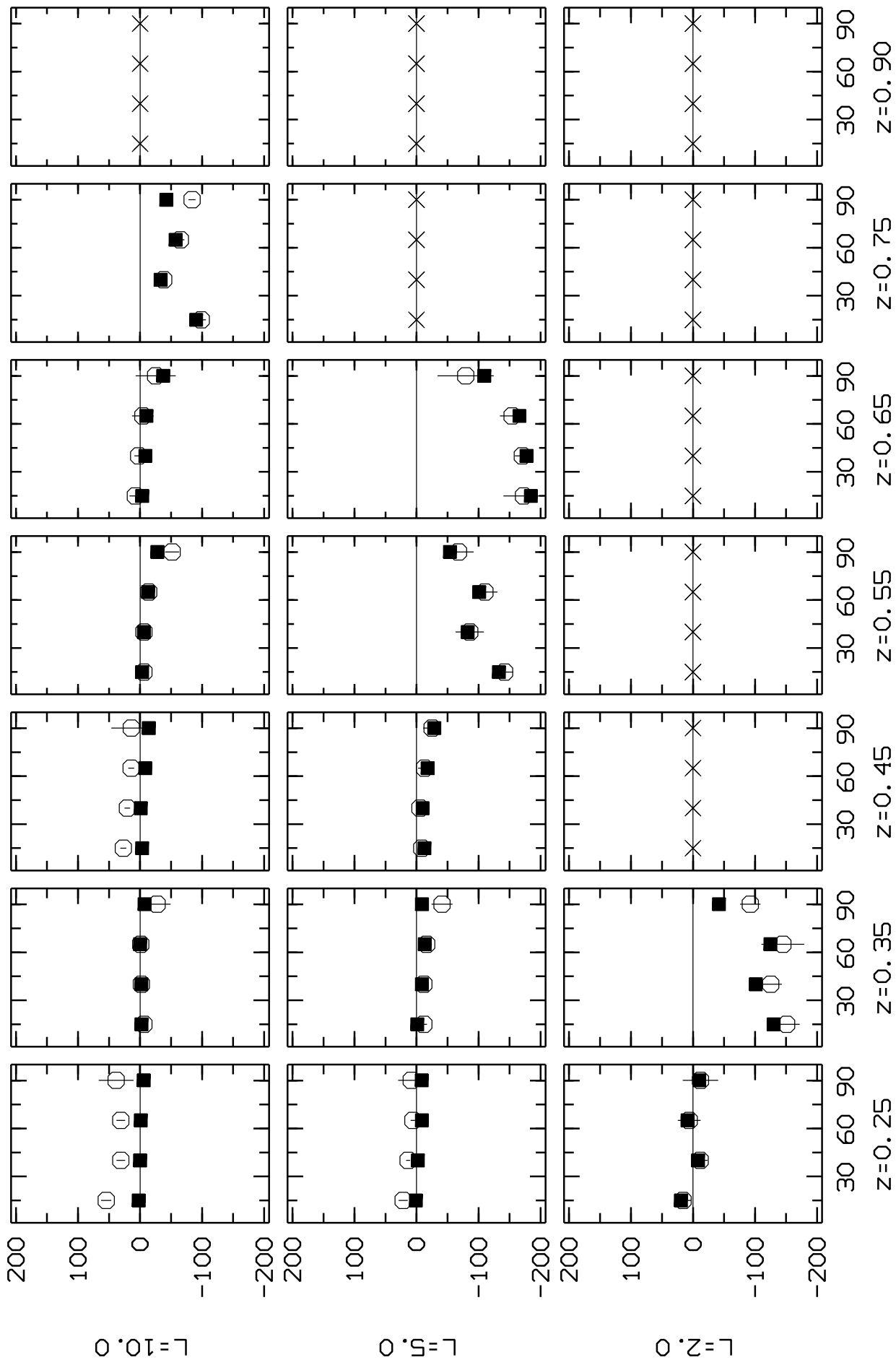


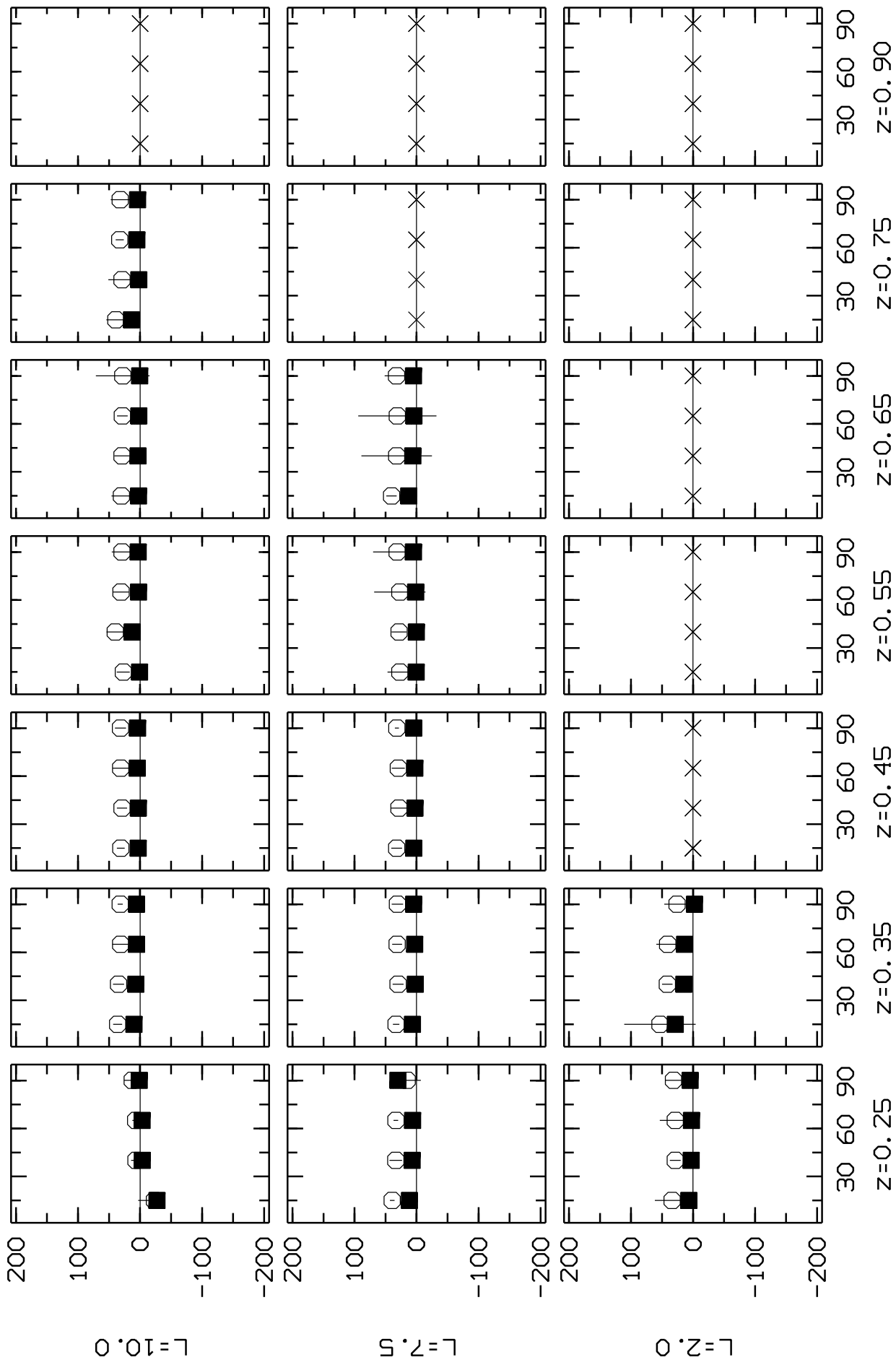


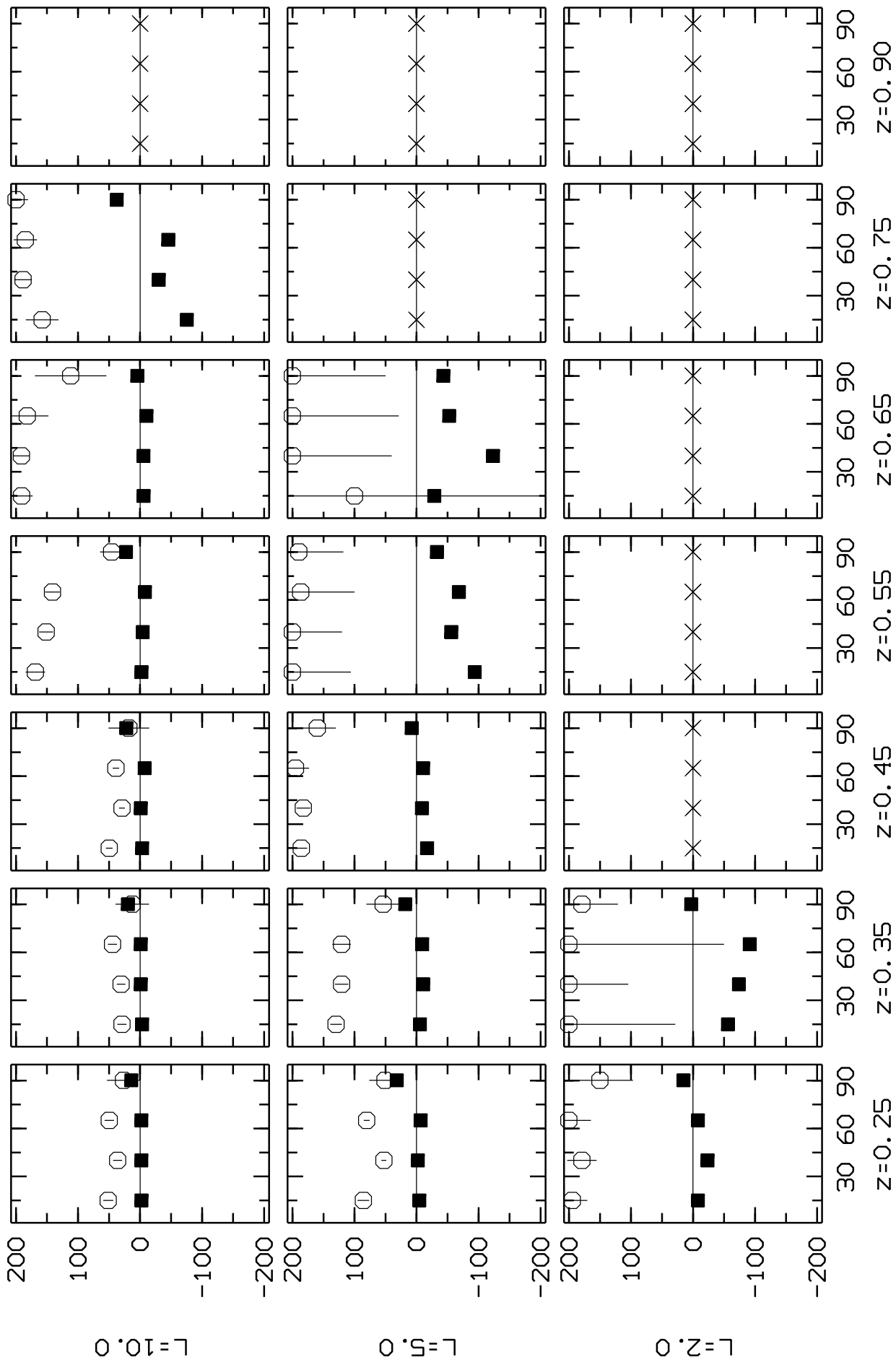


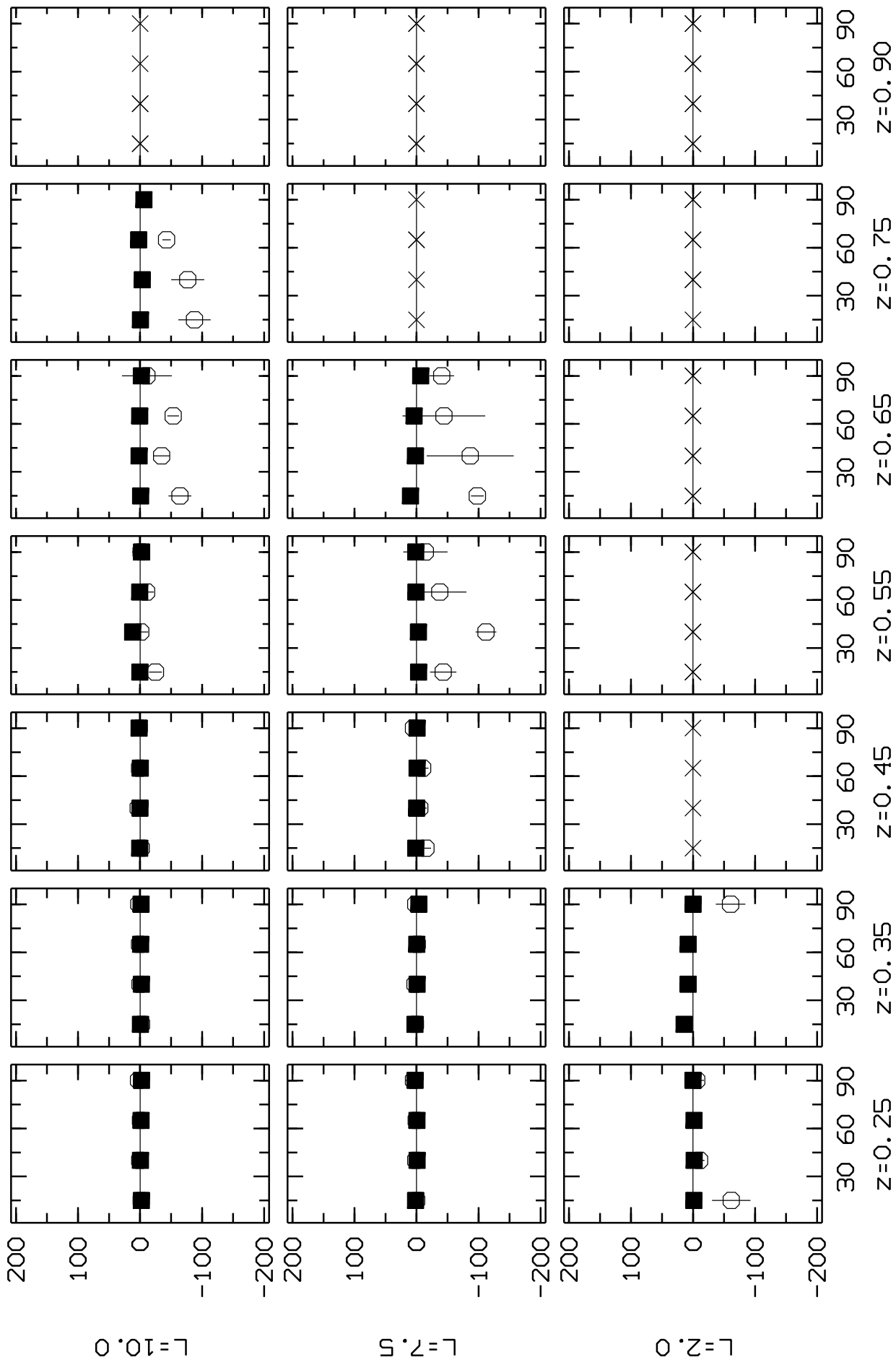


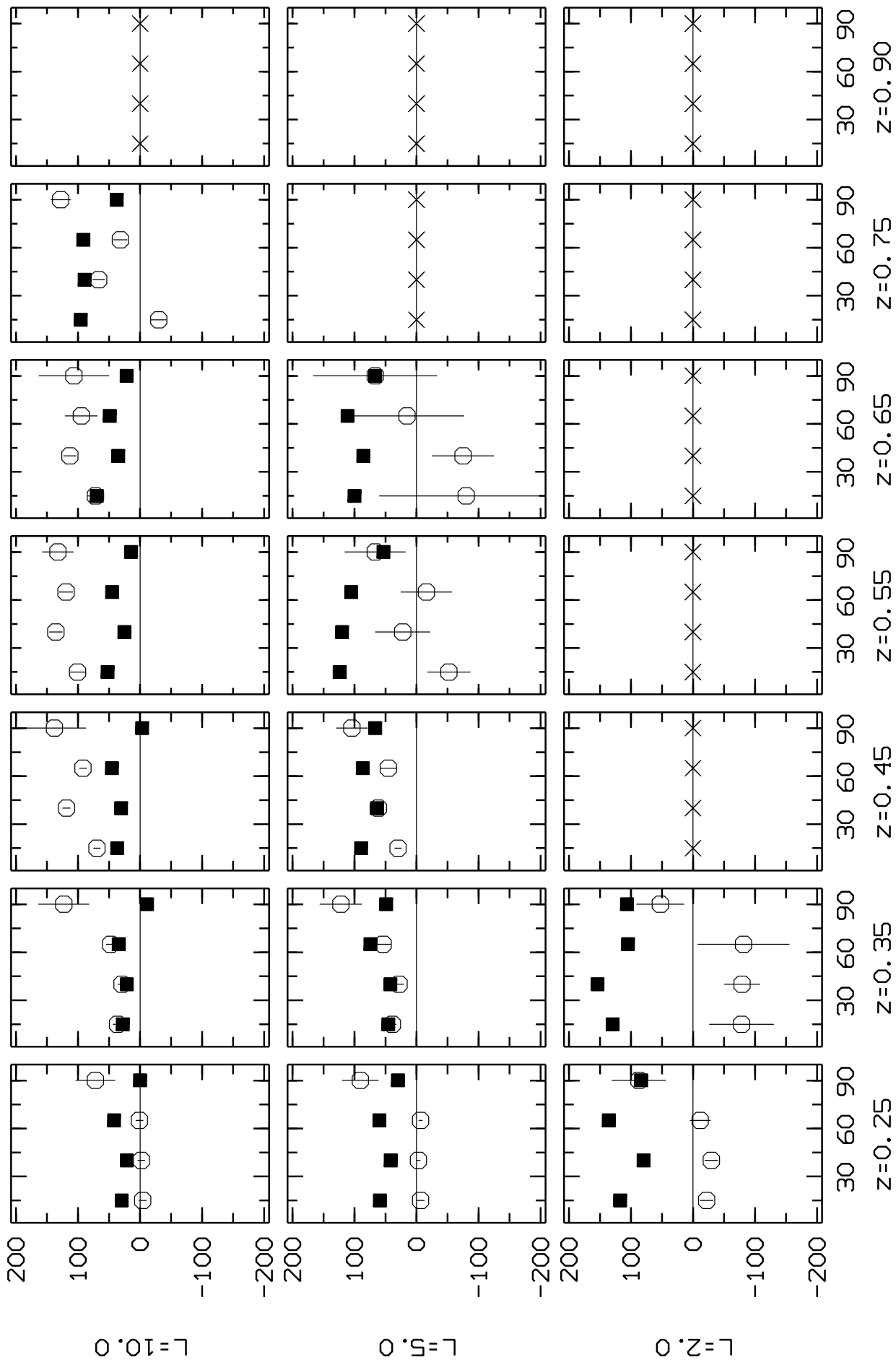


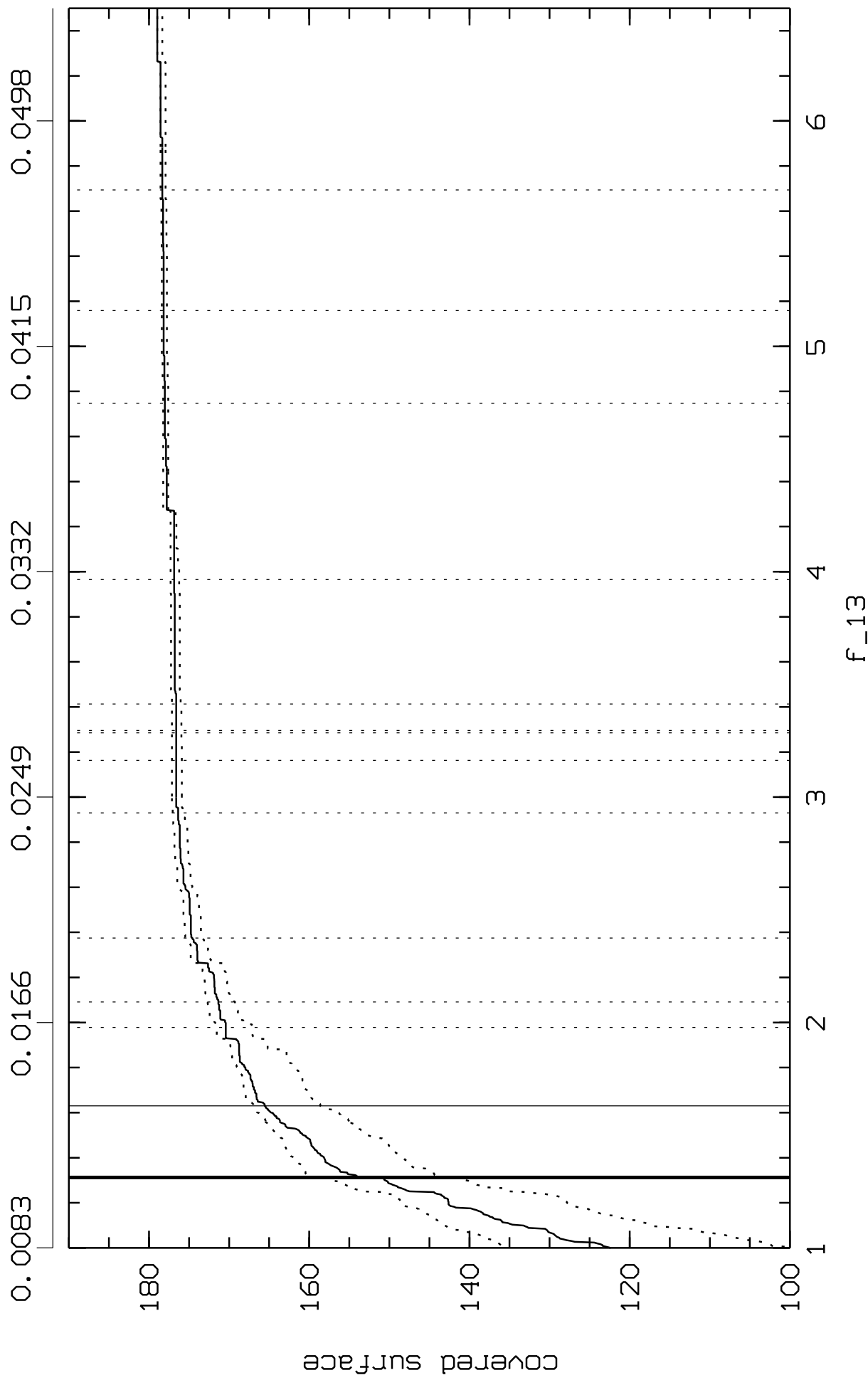




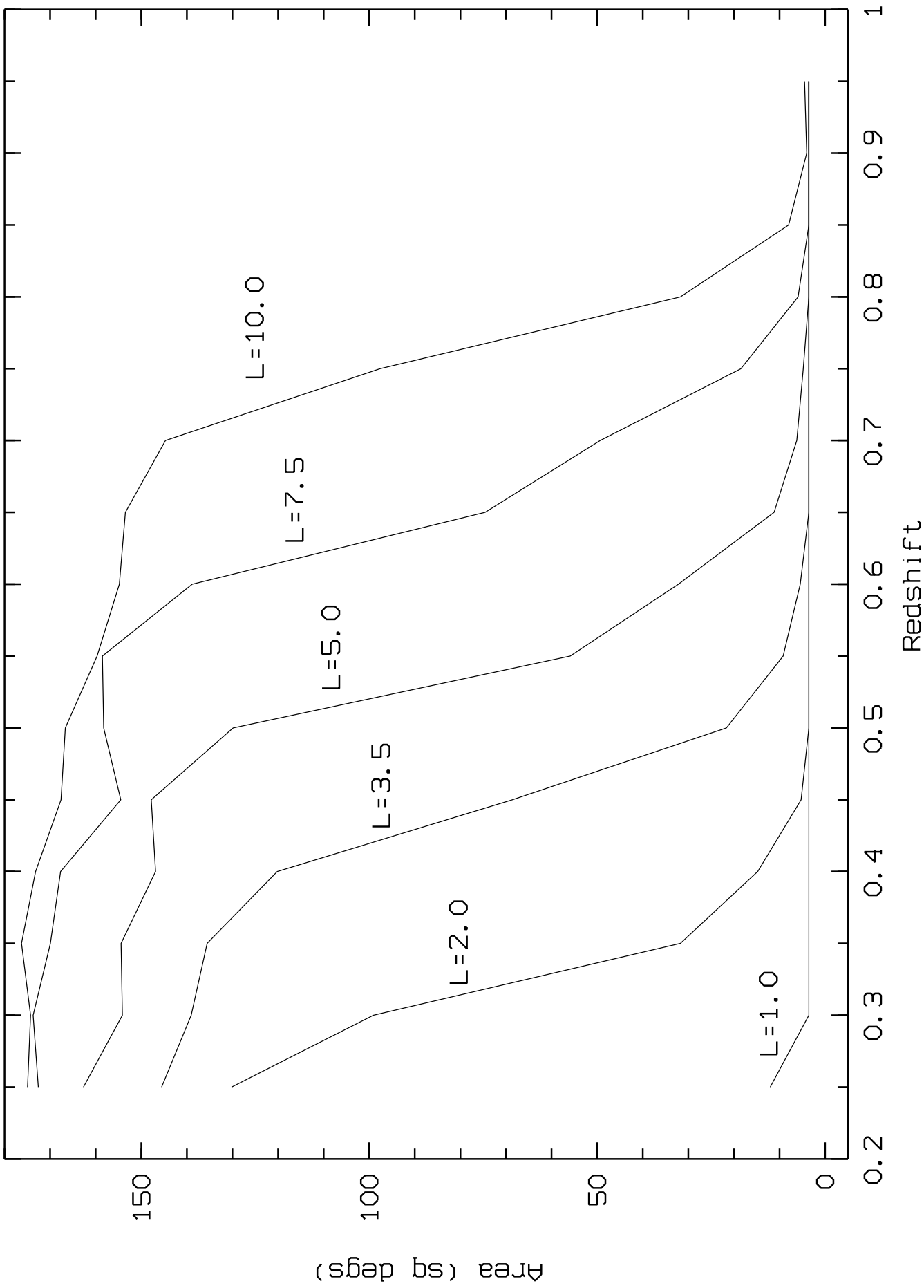


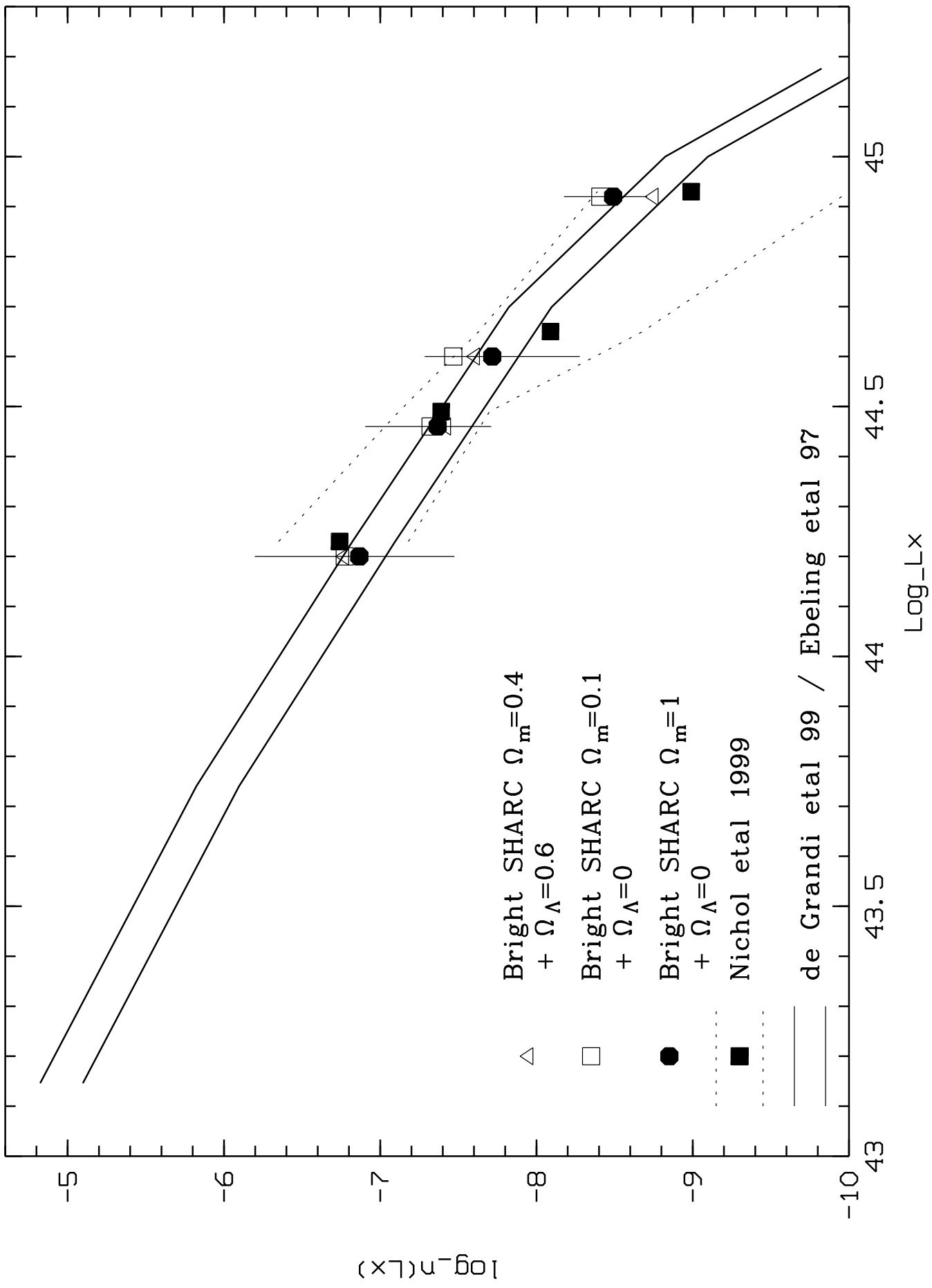


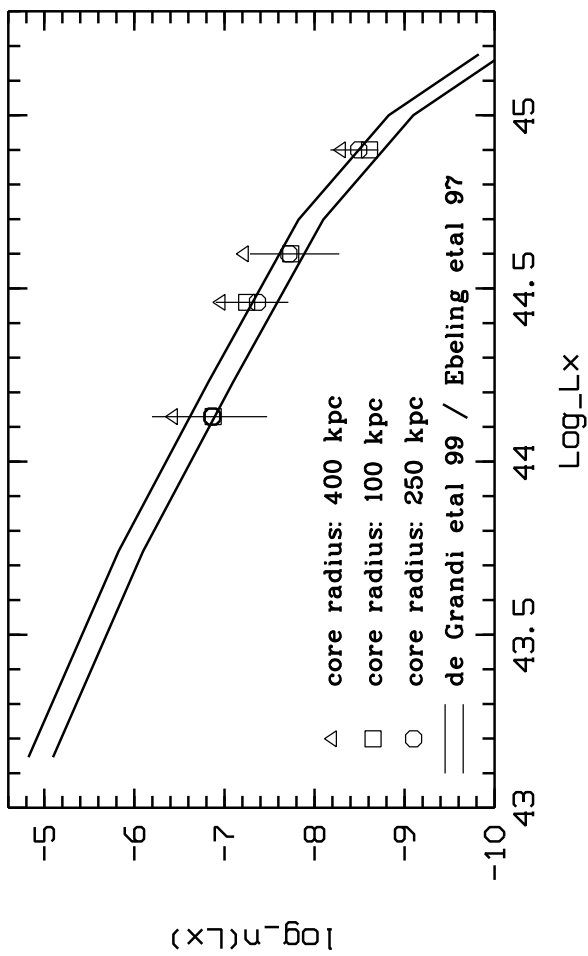
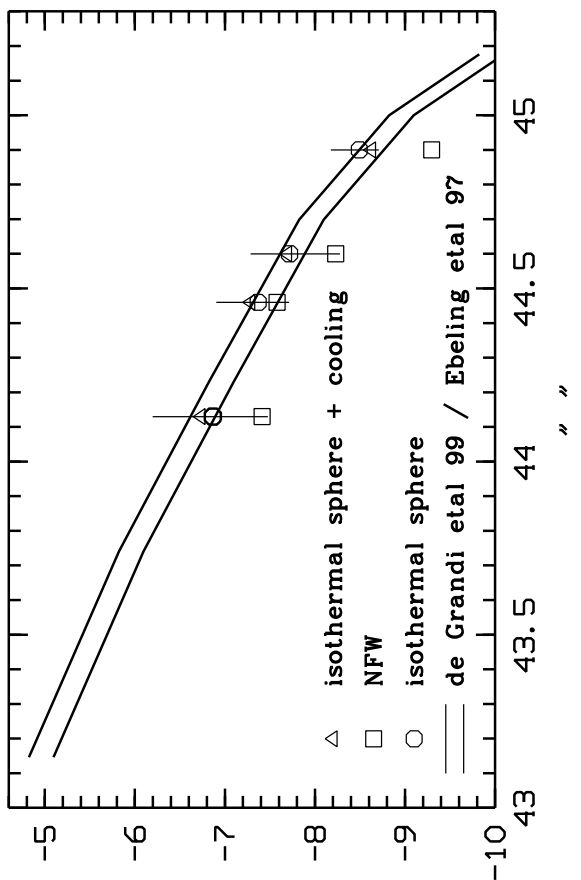




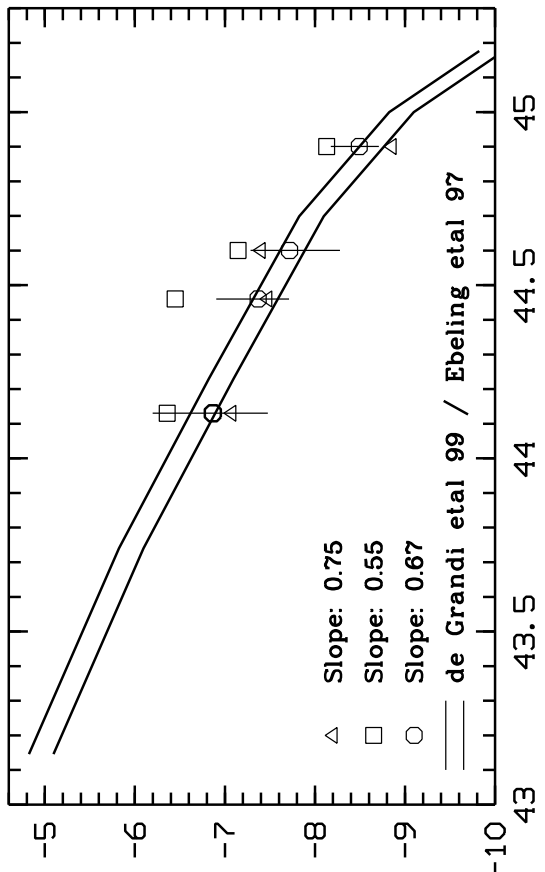
covered surface



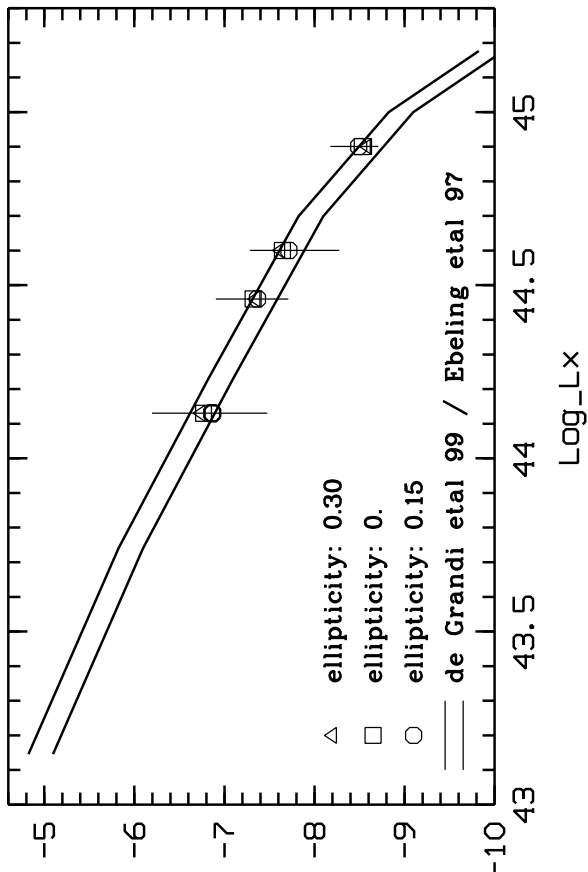




$\log_n(Lx)$



$\log_n(Lx)$



$\log_n(Lx)$